

AD-A225 609

CDRL A004 - G230-JJS-89

MULTI-SENSOR APPROACH TO COUNTERMINE DETECTION

JAMES J. STAMBONI AND JAMES H. ANAPOL
TEXTRON DEFENSE SYSTEMS
201 Lowell Street
Wilmington, MA 01887

15 SEPTEMBER 1989

FINAL REPORT FOR THE PERIOD
22 JULY 1988 - 22 AUGUST 1989
CONTRACT NUMBER DAAK70-88-C-0029

UNCLASSIFIED

Prepared for

DEFENSE ADVANCED RESEARCH PROJECTS AGENCY
1400 Wilson Boulevard
Arlington, VA 22209

BELVOIR RESEARCH AND DEVELOPMENT CENTER
Belvoir Procurement Division
Fort Belvoir, Virginia 22060-5606

DTIC
ELECTE
AUG 09 1990

6 E

D

DISTRIBUTION STATEMENT A

Approved for public release;
Distribution Unlimited

Unclassified

SECURITY CLASSIFICATION OF THIS PAGE

REPORT DOCUMENTATION PAGE

1. REPORT SECURITY CLASSIFICATION Unclassified		10. STRICTIVE MARKINGS None	
2a. SECURITY CLASSIFICATION AUTHORITY N/A		3. DISTRIBUTION/AVAILABILITY OF REPORT Unclassified/Unlimited	
7b. DECLASSIFICATION/DOWNGRADING SCHEDULE N/A			
4. PERFORMING ORGANIZATION REPORT NUMBER(S) CDRL-A004 G230-JJS-89		5. MONITORING ORGANIZATION REPORT NUMBER(S)	
6a. NAME OF PERFORMING ORGANIZATION Textron Defense Systems	6b. OFFICE SYMBOL (if applicable)	7a. NAME OF MONITORING ORGANIZATION BRDEC	
6c. ADDRESS (City, State and ZIP Code) 201 Lowell Street Wilmington, MA 01887		7b. ADDRESS (City, State and ZIP Code) Belvoir Procurement Division Fort Belvoir, VA 22060-5606	
8a. NAME OF FUNDING SPONSORING ORGANIZATION DARPA	8b. OFFICE SYMBOL (if applicable)	9. PROCUREMENT INSTRUMENT IDENTIFICATION NUMBER DAAK70-88-C-0029	
8c. ADDRESS (City, State and ZIP Code) 1400 Wilson Blvd. Arlington, VA 22209		10. SOURCE OF FUNDING NOS.	
		PROGRAM ELEMENT NO	PROJECT NO
		TASK NO	WORK UNIT NO
11. TITLE (Include Security Classification) Multi-Sensor Approach to Countermine Detection (U)			
12. PERSONAL AUTHOR(S) Stamboni, James J. and Anapol, James H.			
13a. TYPE OF REPORT Final	13b. TIME COVERED FROM 88/7/22 TO 89/8/22	14. DATE OF REPORT 1989 September, 15	15. PAGE COUNT 208
16. SUPPLEMENTARY NOTATION			
17. COSATI CODES		18. SUBJECT TERMS (Continue on reverse if necessary and identify by block number)	
FIELD	GROUP	SUB-GR	
15	06	06	Multi-Sensor, Data Fusion, Neural Transforms, Real Time Processing
17	05	01.02	
19. ABSTRACT (Continue on reverse if necessary and identify by block number) X <i>micron</i> This report documents the application of Multi-Sensor Data Fusion to Mine Detection, in an effort to improve Detection/False Alarm performance. A survey of Mine Sensing techniques is summarized. Multi-Sensor (Passive IR (3-5 μ m and 8-12 μ m), Passive Visible, Active IR), coincident data is presented from both a Ground Base Platform and an Airborne (Helicopter) Platform. Neural transform technology is applied to individual mine detection as well as minefield detection. Real Time Implementation is addressed and demonstrated. <i>micron</i> <i>RH4</i>			
20. DISTRIBUTION/AVAILABILITY OF ABSTRACT UNCLASSIFIED/UNLIMITED X SAME AS RPT = DTIC USERS =		21. ABSTRACT SECURITY CLASSIFICATION Unclassified	
22a. NAME OF RESPONSIBLE INDIVIDUAL James J. Stamboni		22b. TELEPHONE NUMBER (include area code) 508-657-6917	22c. OFFICE SYMBOL

CDRL A004 - G230-JJS-89

MULTI-SENSOR APPROACH TO COUNTERMINE DETECTION

JAMES J. STAMBONI AND JAMES H. ANAPOL
TEXTRON DEFENSE SYSTEMS
201 Lowell Street
Wilmington, MA 01887

15 SEPTEMBER 1989

FINAL REPORT FOR THE PERIOD
22 JULY 1988 - 22 AUGUST 1989
CONTRACT NUMBER DAAK70-88-C-0029

UNCLASSIFIED

Accession For	
NTIS GRA&I	<input checked="checked" type="checkbox"/>
DTIC TAB	<input type="checkbox"/>
Unannounced	<input type="checkbox"/>
Justification	
By	
Distribution/	
Availability Codes	
Dist	Avail and/or Special
A-1	

Prepared for

DEFENSE ADVANCED RESEARCH PROJECTS AGENCY
1400 Wilson Boulevard
Arlington, VA 22209

BELVOIR RESEARCH AND DEVELOPMENT CENTER
Belvoir Procurement Division
Fort Belvoir, Virginia 22060-5606

EXTERNAL DISTRIBUTION

STRBE-JM	3
DTIC	12
AMSTR/PVAC	2
DARPA/TTO	3

TABLE OF CONTENTS

	<u>PAGE</u>
1.0 INTRODUCTION	1
1.1 Project Objective	2
1.2 Technical Approach	3
1.3 Summary of Accomplishments	5
1.4 Recommendations	13
2.0 CANDIDATE SENSOR (P) EVALUATION	16
2.1 Objective	16
2.2 Approach	16
2.3 Results and Conclusions	17
3.0 SYSTEM CONCEPT DEFINITION	24
3.1 Objective	24
3.2 Technical Approach	24
3.3 Results and Conclusions	24
3.4 System Analysis	30
3.5 Countermeasure System Parameters	38
4.0 MULTI-SENSOR DATA COLLECTION	44
4.1 Objective	44
4.2 Technical Approach	44
4.3 Data Collection I	45
4.4 Data Collection II	48
5.0 ALGORITHM DEVELOPMENT	53
5.1 Objective	54
5.2 Approach	54
5.3 Results	55
5.3.1 AMIDARS Data	55
5.3.2 Mine Detection	59

TABLE OF CONTENTS (CONT'D)

	<u>PAGE</u>
5.3.2.1 Data Collection 1	59
5.3.2.2 Data Collection 2	72
5.3.3 Minefield Detection	85
5.3.3.1 Minefield Detection Algorithm	85
5.3.3.2 System Cues for Detecting the Location of Minefields	102
5.4 Conclusions	105
5.4.1 Mine Detection	105
5.4.2 Minefield Detection	106
6.0 REAL TIME PROCESSING HARDWARE/SOFTWARE DEVELOPMENT	109

LIST OF FIGURES

<u>FIGURE #</u>	<u>TITLE</u>	<u>PAGE</u>
1.1	Multi-Sensor Testbed for Data Collection 1	8
1.2	Airborne Multi-Sensor Testbed for Data Collection	9
1.3	Ground Controlled Airborne Platform Concept	11
1.4	Airborne Platform Concept	12
2.1	35 GHZ FMCW Radar Performance	22
3.1	Ground Controlled Airborne Platform Concept	25
3.2	Airborne Platform Concept	28
3.3	Implementation of Airborne Platform Concept	29
3.4	Effective Forward Velocity of Movement	31
3.5	Delay Distance Versus False Alarm Rate	33
3.6	Probability of Minefield Detection Versus Threshold	35
3.7	Probability of Minefield False Alarm Versus Threshold	36
3.8	Mine Clearing Produced Delay	37
3.9	Scan Rate Versus Number of Detectors	39
3.10	Data Rate Versus Number of Detectors	40
4.1	Multi-Sensor Testbed for Data Collection 1	46
4.2	Cherry Picker Platform Used in Data Collection 1	47
4.3	Mines in Typical Clutter for Data Collection 1	49
4.4	Airborne Testbed Mounted on Helicopter for Data Collection 2	50
4.5	Close-Up of Airborne Multi-Sensor Testbed	51
5.1	Typical AMIDARS Data	56
5.2	Amplitude Threshold Determination by Nitrogen Analysis	57
5.3	Detections Resulting From Amplitude Thresholding	58
5.4	Set-Up for Data Collection 1	60
5.5	Typical Data From Data Collection 1 (IR, Visible)	61
5.6	Gradient Processing of Visible Imagery Data	62
5.7	Single Sensor (High Level) Feature Fusion	64
5.8	Results of Single Source (High Level) Feature Fusion	65
5.9	Multi-Sensor Decision Level Fusion (High Level Features)	66
5.10	Results of Multi-Sensor Decision Level Fusion	67
5.11	Multi-Sensor (High Level), Feature Fusion	68

LIST OF FIGURES

<u>FIGURE #</u>	<u>TITLE</u>	<u>PAGE</u>
5.12	Results of Multi-Sensor (High Level) Feature Fusion	69
5.13	Single Sensor Raw Data Fusion	70
5.14	Results of Single Sensor Raw Data Fusion	71
5.15	Multi-Sensor Data Fusion	73
5.16	Results of Multi-Sensor Data Fusion	74
5.17	2-DFFT of Simple Solid Mine Models	75
5.18	2-DFFT of Simple Edge Models of Mines	76
5.19	Single Sensor (Low Level) Feature Fusion	77
5.20	Results of Single Sensor (Low Level) Feature Fusion	78
5.21	Multi-Sensor (Low Level) Feature Fusion	79
5.22	Results of Multi-Sensor (Low Level) Feature Fusion	80
5.23	Airborne Multi-Sensor Testbed	81
5.24	12 Inch Square Plastic Mine (Training)	82
5.25	12 Inch Circular Metal Mine (Training)	83
5.26	12 Inch Circular Plastic Mine (Training)	84
5.27	12 Inch Square Plastic Mine (Test)	86
5.28	12 Inch Square Plastic Mine (Test)	87
5.29	12 Inch Circular Metal Mine (Test)	88
5.30	12 Inch Circular Metal Mine (Test)	89
5.31	12 Inch Circular Metal Mine (Test)	90
5.32	12 Inch Square Plastic Mine (Test)	91
5.33	12 Inch Square Plastic Mine (Test)	92
5.34	Sample Minefield and False Alarm Distributions	93
5.35	Histograms of Spatial Distributions of Mine-Like Detections	95
5.36	Minefield Detection Versus Mine Scattering	96
5.37	Composite Minefield/False Alarm Synthetic Image (3M-10)	97
5.38	Composite Minefield/False Alarm Synthetic Image (5M-10)	98
5.39	Composite Minefield/False Alarm Synthetic Image (10M-10)	99
5.40	Composite Minefield/False Alarm Synthetic Image (20M-10)	100
5.41	Sample False Alarm Spatial Distributions	101

LIST OF FIGURES

<u>FIGURE #</u>	<u>TITLE</u>	<u>PAGE</u>
5.42	Probability of Minefield Detection and False Alarm Detection (20 FA/Search Area Train)	103
5.43	Probability of Minefield, Detection and False Alarm Rejection (10 FA/Search Area - Train)	104
5.44	Automatic Terrain Classification	106
6.1	Strawman System Timing/Throughput Sizing	110
6.2	Scanning Laser Sensor Test Bed (Housing)	111
6.3	Scanning Laser Sensor Testbed (Optics)	112
6.4	Real Time Processor/Display System	113
6.5	8S Fort Tower at Camp Edwards, MA	114
6.6	Laydown of Mine Simulants for Real Time Processor Demo	116
6.7	Real Time Display of Raw & Processed Data	117
6.8	Echo Strength Versus Range as a Function of Mine Color	118
6.9	Effect of Absorption on Range Management	119
6.10	Processor Analysis	121
6.11	Processor Chip Cost Trends	123
6.12	Processing System Architecture	124

LIST OF TABLES

<u>TABLE #</u> <u>NUMBER</u>	<u>TITLE</u>	<u>PAGE</u>
1.1	Data Collection Summary	7
2.1	Candidate COUNTERMINE Sensors Trade-Off	18
2.2	"Core" Sensor Suite For Data Fusion	20
3.1	TDS Countermines System Parameters (Preliminary)	42

List of Appendix

Appendix A

Bibliography of Revelant Literature

Appendix B1

Sensor Suite Description for Data Collection 1

Appendix B2

Coincident Data From Data Collection 1

Appendix C

Airborne Multi-Sensor Test Bed

Appendix D

System Cues for Detecting the Location of Mines

Appendix E

KBVision Systems

1.0 INTRODUCTION

Existing mine detection, location, neutralization, and marking systems are severely limited by the following shortcomings:

- Mine Clearing process is too slow with too small search areas.
- Remote sensing capability is limited (standoff).
- False Alarms are unacceptably high.
- Systems are burdensome to the user (size, etc.)
- Detection performance against covered and buried mines is low.

Current systems have exhibited difficulty in detecting conventional anti-armor, anti-vehicular and anti-personnel mines (whose kill radius is within 1 to 2 meters of the mine) with acceptable false alarm rates, whether they be scatterable or hand/vehicle emplaced. They do not address the mine threat of the future (mid to late 1990's), the smart wide area mine, whose kill radius typically extends beyond 100 meters.

Textron Defense Systems (TDS) is currently developing three different smart wide area mine-type weapon systems: Wide Area Mines (WAM), Anti-Helicopter Mine (AHM), and Autonomous Robotics Weapon System (AROWS). WAM, a mine system that attacks both armor and soft vehicles as well as personnel, is an ARDEC program that will be entering FSD in late CY89. The AHM is a weapon system being developed to deny nap-of the earth navigation tactics to enemy helicopters. This is a joint DARPA/ARDEC program that is entering the proof of principle demonstration phase. AROWS is a TDS discretionary funded program to address the technologies required for the next generation (after WAM and AHM) of mine-like weapon systems. The TDS program is being supplemented by a DARPA/ARDEC contract to demonstrate integration of some of these key technologies (acoustic sensing, intermine communication, and platform mobility).

Our efforts on these programs has given us invaluable expertise in the tactics of mine warfare and the technologies required for mine development: sensors, signal processing, fuzing systems, S&A's, explosives, and lethal mechanisms. Because of this commitment to smart wide area mines, TDS is very interested and involved in all aspects of the countermine problem. We believe that a thorough understanding of the

vulnerability of mines to remote detection, location, neutralization, and marking is a key requirement in mine-like weapon systems development.

During this phase of the Countermine Detection Program, TDS has concentrated on the problem of individual mine and minefield detection using its expertise in sensors, signal processing, and multi-sensor data fusion, along with our understanding of minefield deployment and tactics, to successfully demonstrate a multi-tiered software architecture that has the potential for significant improvements in mine/minefield detection and false alarm rejection performance (relative to existing techniques) in a real time, on-board processor. We are pleased to present our findings in this final report.

1.1 Project Objective

TDS' objective during this phase of the Countermine Detection Program was to demonstrate a multi-sensor mine detection approach that could reduce the current limitations in mine detection systems. The attributes of that approach would therefore include:

1. High detection probability against metallic and non-metallic mines that are surface layed, covered (eg. by foliage or brush); or buried
2. Low false alarm rates against man-made and non man-made clutter, as well as internal sensor noise.
3. Day/night, all-weather, and all-terrain operation.
4. Immunity to countermeasures.
5. Large search area.
6. Rapid rate of forward advancement.
7. Real-time on-board processing for mine detection, location, neutralization, and marking.
8. Compact, lightweight, modular design adaptable for hand-held, vehicle mounted, and airborne applications.
9. Cost effective

1.2 Technical Approach

Our technical approach to the mine detection problem incorporated multi-spectral sensing and advanced processing techniques into a three-tiered architecture that autonomously accomplishes:

- Detection and location of individual mines-(Level 1)
- Detection of minefield characteristics to improve confidence in individual mine detection process (Level 2)
- Interpretation of terrain and man-made structures (roads, bridges) for clues to enhance the confidence levels on the individual mine and minefield detection process-(Level 3)

TDS conducted a thorough investigation of the available literature for the components of a sensor suite that had the most applicability to the mine detection problem and were consistent with the objectives set forth in Section 1.1. This was complemented with analysis of TDS' in-house sensor technologies, namely: active and passive IR, visible/low high level TV (LLLTV), active MMW, acoustics, and ultrasonics. From this activity a sensor suite was selected for each application: hand-held, vehicle mounted, and airborne. A sensor suite potentially common to all applications was defined. This core suite consisted of active IR (range, amplitude and polarization), multi-spectral passive IR (intensity, absolute thermal, and 2-D spatial), and low-light level visible (intensity and high resolution 2-D spatial). As the program progressed we continually factored in the sensor work being accomplished by other contractors on this DARPA/BRDEC program, as that information became available through the tri-mester review meetings.

Readily available sensors were then identified and evaluated for their suitability to the core sensor suite. TDS owned sensors and rentable/leasable off-the-shelf sensors were considered. Though the available sensors selected for the temporal and spatial coincident data collection exercise did not exhibit all the desired characteristics, we were able to acquire data in the active IR (range only), passive IR (3-5 um and 8-12 um), and visible (two fields-of-view).

TDS collected coincident multi-sensor data during two different time periods, late fall/winter, (November 1988-March 1989) and late spring (June). The first exercise was conducted on the grounds of TDS'

Wilmington, MA. facility using a cherry picker platform, and the second test was conducted in Stockbridge, NY using TDS' multi-sensor airborne testbed. The passive IR and visible sensor data were recorded on video tapes, and the active IR range data was digitized and recorded on floppy disk.

After each data collection activity, the video tapes were reviewed and two sets of data were extracted and digitized for algorithm development; one set for algorithm training and the other set for algorithm performance evaluation. The digitized data was signal conditioned by amplitude normalization, spatial filtering, and sensor artifact removal prior to use in the algorithm development activities.

As stated earlier, TDS' processing approach utilized three levels of decision making and confidence enhancement. The individual mine detection and location task was accomplished using low-level features extracted from the multi-sensor suite and input to a neural transform processor. TDS considered and analyzed fusion at all levels: raw data, low level features, high level features and sensor decision outputs, and determined that the low-level features from each sensor were the most appropriate. We also considered three different neural transform paradigms:

- Backward Propagation
- Restricted Coulomb Energy
- Adaptive Resonance Theory

We analyzed two different techniques for minefield detection given a distribution of individual mine and false mine detections. The first technique utilized a Hough transform for colinearity assessment and a Fourier transform for intermine periodicity estimate, coupled with associated decision logic. This technique proved successful for the "well-behaved" linear minefield, however, was not extendable to the more general two dimensional scatterable mine field distribution problem. The second technique used neural transforms of the mine/false mine field distribution in two dimensional Fourier space to estimate minefield characteristics such as orientation, aspect ratio, density, and periodicity. This technique proved very effective against both one and two dimensional distributions of mines.

The technical approach that was taken by TDS for the third and highest level processing---the interpretation of terrain and man-made structures, included the interview of a human minefield detection "expert" for the scene context that would indicate or clue the presence or likelihood of a minefield and development of techniques for automatically extracting these clues. The adaptive resonance neural transform was applied in an unsupervised learning mode to provide the scene interpretation function. Rules were "extracted" from the expert for incorporation into acknowledge based processor workstation, the KB Vision System developed by Amerinex Artificial Intelligence, a spin-off company of University of Massachusetts researchers, including Professor Ed Riseman.

1.3 Summary of Accomplishments

During this phase of the Countermine Detection Program, TDS has achieved substantial and at times dramatic accomplishments in all task areas: Candidate sensors evaluation, multi-sensor data collection, algorithm development, real time processor development, and mine detection system concept definition. Those accomplishments are briefly highlighted here. The details of the achievements are discussed in the appropriate sections of this report.

Sensor suites were selected for airborne, vehicle mounted, and hand-held mine detection applications. These selections were based on extensive review of previous work documented in the literature as well as progress made during this phase of the program by other contractors. A sensor suite potentially common to all applications was defined as :

- multi-spectral passive IR
- passive low light level visible (or UV)
- pulsed active IR (profile, echo strength and polarization)

Initially ground penetrating radar (GPR) was also included in the sensor suite for its ability to detect buried mines. The GPR approaches were compatible with hand-held and vehicle mounted mine detection systems but did not exhibit much potential for the large stand-off ranges required for airborne systems. Several promising multi-spectral passive near IR and IR approaches were revealed during the course of the program that exhibited good potential for detecting partially covered and buried

mines at long stand-off ranges as well as for the shorter hand-held and vehicle mounted ranges. Lawrence Livermore National Labs (LLNL), BETAC Corporation, and Monroe Company all described approaches that claimed (and in some cases showed data!) to work against the partially covered and/or buried mine. Although data from these sensor systems is presently limited, TDS believes that there is some promise in each technique and will continue to monitor and analyze the progress of their activities with potential working relationships for the next phase of this program. Based on available data, TDS believes that LLNL's 2-color IR approach should perform equivalently to GPR and also provide substantially longer stand-off range. The potential of these passive near-IR and IR techniques that would work at all required stand-offs, coupled with the demonstrated and documented capability that already exists to independently detect clues to buried mine locations (perturbed earth assessment using passive and active IR sensing techniques) enabled us to remove the GPR approach from our sensor suite.

In our proposal we also committed to evaluating 35 GHZ MMW radar as a possible sensor for the TDS sensor suite. We considered an FM-CW system with one-foot range gate resolution and 6 inch aperture antennas. Our analysis showed that even the largest (12" diameter) mines could be detected only at very short ranges (<30 feet), and even then with great difficulty, due to self-jam noise limits. This analysis was supported with data taken during our June data collection effort.

TDS conducted coincident multi-sensor mine and clutter data collection during 2 test periods. The conditions are summarized in Table 1.1. Figure 1.2 shows TDS's airborne multi-sensor testbed, a 3 million dollars capital investment that was used for the second data collection effort.

During this program, TDS' multi-sensor, multi-feature, multi level software architecture has demonstrated potential improvement in mine detection and false target reduction performance compared to more conventional systems. The specific accomplishments include:

Level 1 - Individual mine detection (Low Level)

- Low level feature fusion of 2-color passive IR (3-5um and 8-12um) and visible thru neural transforms shows dramatic reduction in false target detections (eliminated

TDS COUNTERMINE DETECTION PROGRAM

DATA COLLECTION/SUMMARY

TEST #1

- WINTER (LATE NOVEMBER THRU MID MARCH)
 - TDS WILMINGTON, MA., FACILITY (TYPICAL N.E FIELDS AND WOODS)
 - COINCIDENT PASSIVE IR, VISIBLE AND ACTIVE IR (RANGE ONLY) SENSORS (FIGURE 1.1)
 - 50 FOOT RANGE, 60 DEGREE DEPRESSION ANGLE, CHERRY PICKER PLATFORM
 - BRDEC PROVIDED PLASTIC (3) AND METALLIC (3) TRAINING MINES
 - 20 SETS OF DATA EXTRACTED AND DIGITIZED, MORE POSSIBLE

TEST #2

- LATE SPRING (JUNE)
 - STOCKBRIDGE, NY TEST SITE (EMULATES EUROPEAN COUNTRY-SIDE)
 - TDS COINCIDENT MULTI-SENSOR AIRBORNE TEST BED PROVIDED: (FIGURE 1.2)
 - NFOV AND WFOV VISIBLE (IMAGING)
 - 3-5UM AND 8-12UM PASSIVE IR (IMAGING)
 - 35 GHZ FM-CW RADAR (REAL BEAM)
 - 50 FOOT RANGE, 60 DEGREE DEPRESSION ANGLE
 - INEL PROVIDED NEW PLASTIC MINES (3) PLUS ABOVE TRAINING MINES
 - 16 SETS OF DATA EXTRACTED AND DIGITIZED, MORE POSSIBLE
 - PARALLEL EFFORT COLLECTED ACTIVE IR DATA FROM TOWER FOR REAL TIME DEMO

7/19/89JS
6

TEXTRON

DEFENSE SYSTEMS

TABLE 1.1
DATA COLLECTION SUMMARY

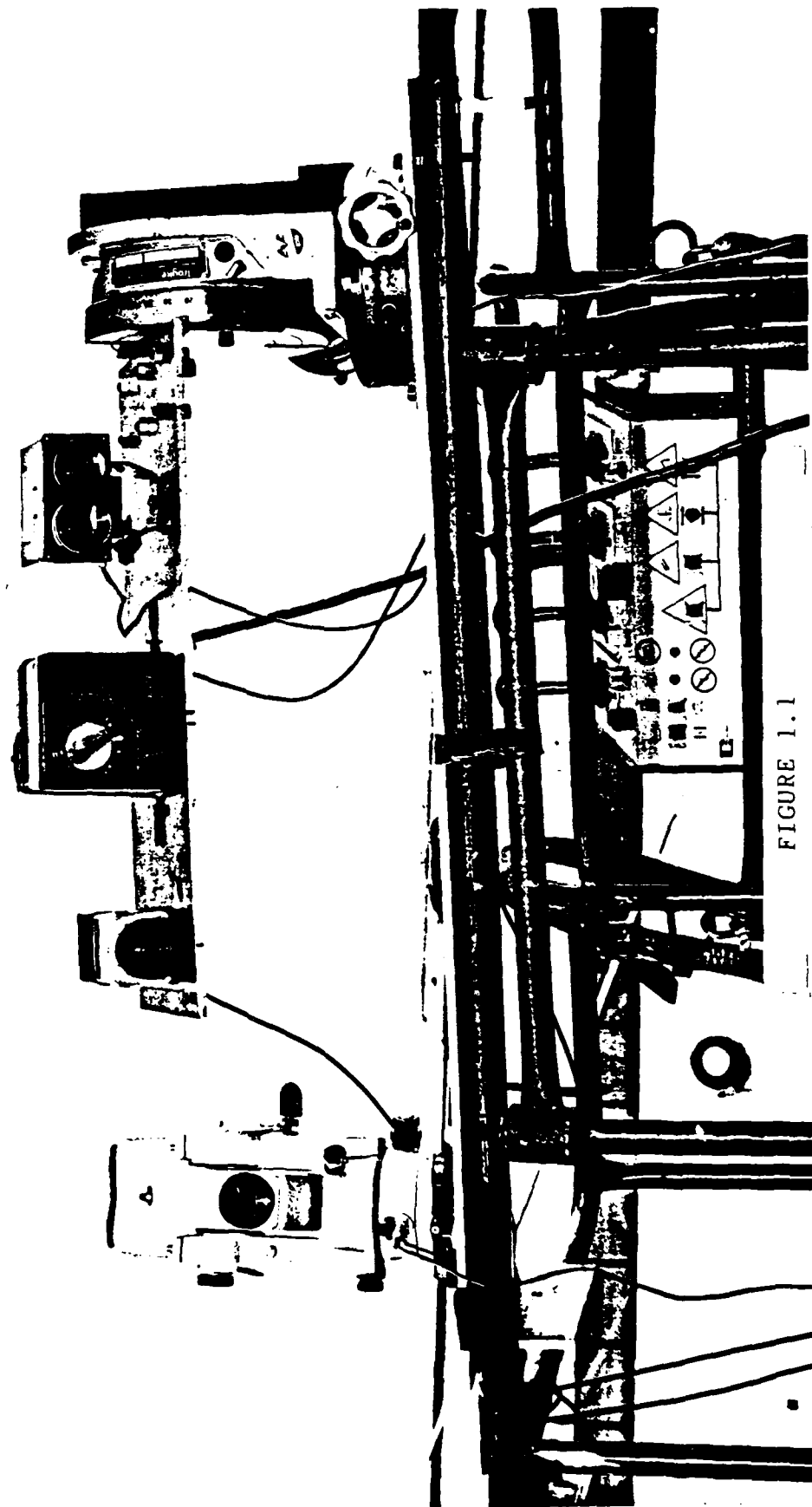


FIGURE 1.1
Multi-Sensor Test Bed for Data Collection 1

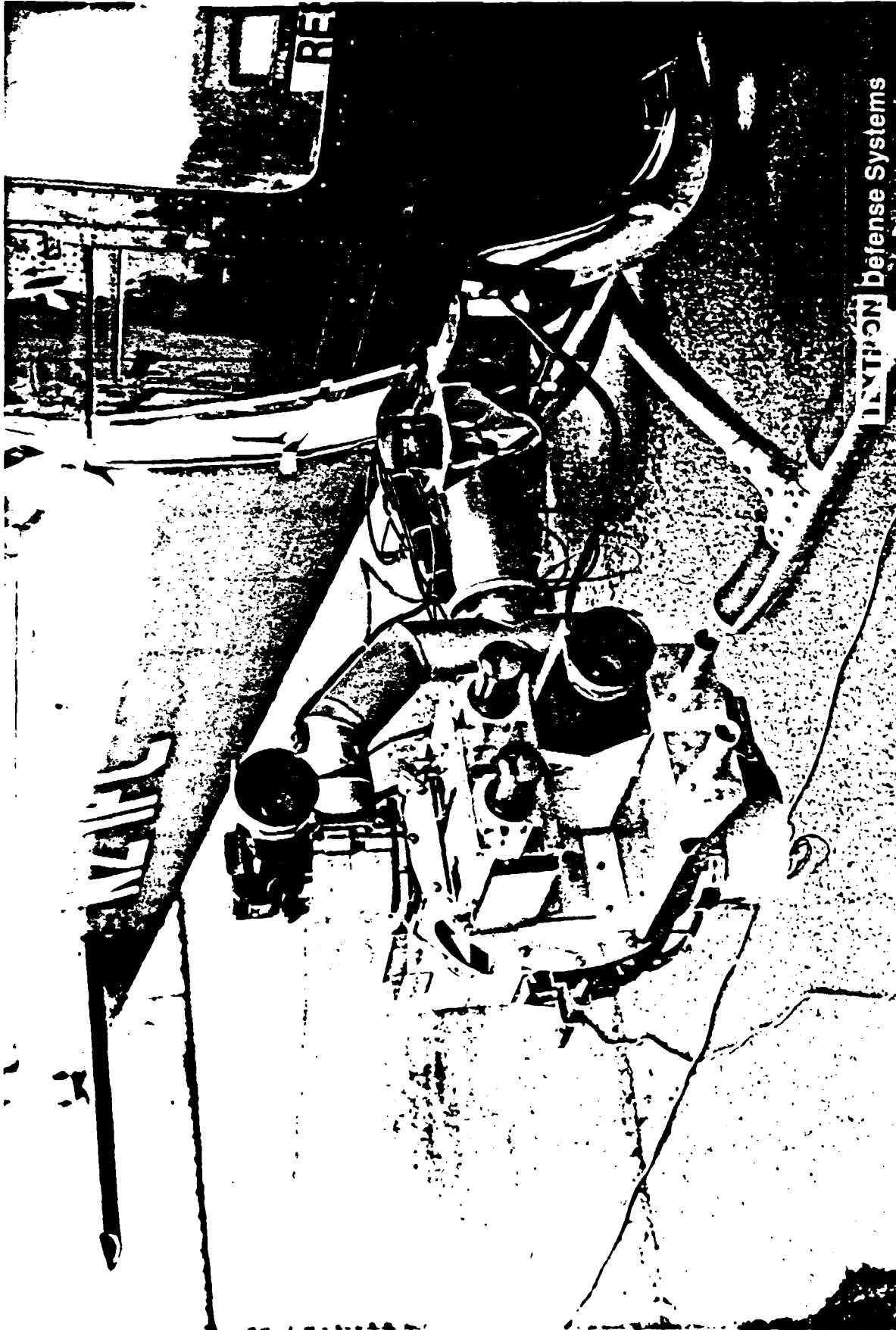


FIGURE 1.2
Airborne Multi-Sensor Test Bed for Data Collection

all false alarms for the limited data collected a relative to a single sensor performance

- Demonstrated real time neural transform processing for

Level 2 -Minefield Detection (Mid Level)

- Combined Hough/Fourier transform technique measuring co-linearity and periodicity significantly reduced false target detections for 1-D minefield distributions
- Neural transform technique was successfully applied to detect both 1-D and 2-D minefield distributions imbedded in severe false alarm scenarios

Level 3 -Syntactic Inferencing (High Level)

- Expertise extracted to determine rule base for minefield presence
- Neural transforms successfully used to classify environment (Forest, Meadow, Treeline)

TDS defined two notional system concepts that offered the potential for meeting the key mine detection system requirements of acceptable individual mine detection and false alarm performance, rapid rate of forward advancement and wide search area coverage. The first concept, a ground based, ground controlled airborne platform (GCAP) is shown in Figure 1.3. It is characterized by relatively short range operation (~100 feet) and short reach with respect to carrier platform, small/cheap sensors, expendable platform and a two-way communications link to the carrier ground platform. The second concept (Figure 1. 4), an autonomous airborne platform (helicopter) offers more reach, higher speed, longer stand-off and longer duty time than the GCAP approach, however, at a higher cost, requiring larger, more complex, and costly sensors. Additional systems considerations such as mine neutralization and marking integrated with sensor suite requirements will ultimately determine the actual design for the notional concepts developed during this program.

TDS COUNTERMINE DETECTION PROGRAM

GROUND CONTROLLED AIRBORNE PLATFORM CONCEPT

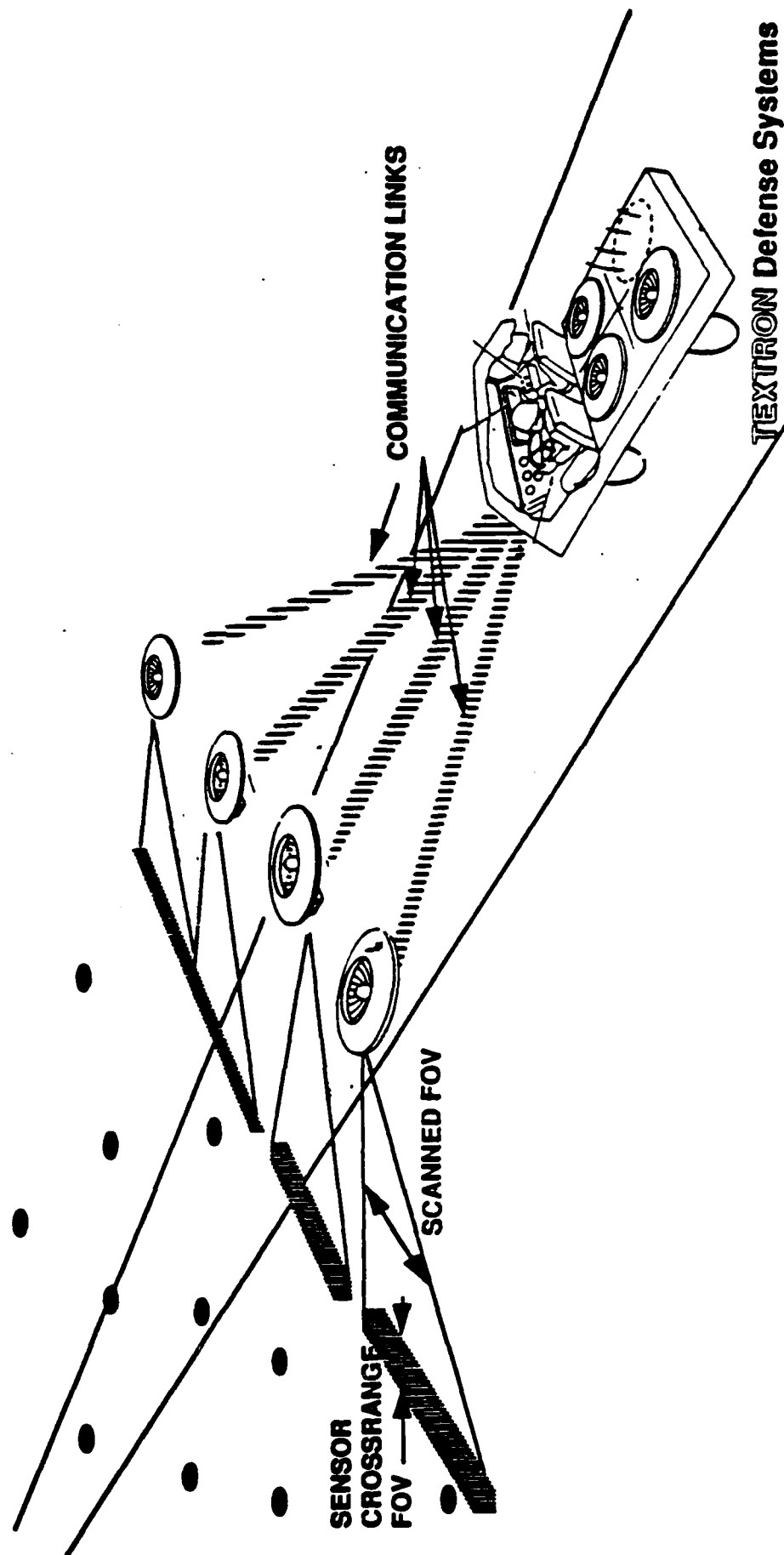
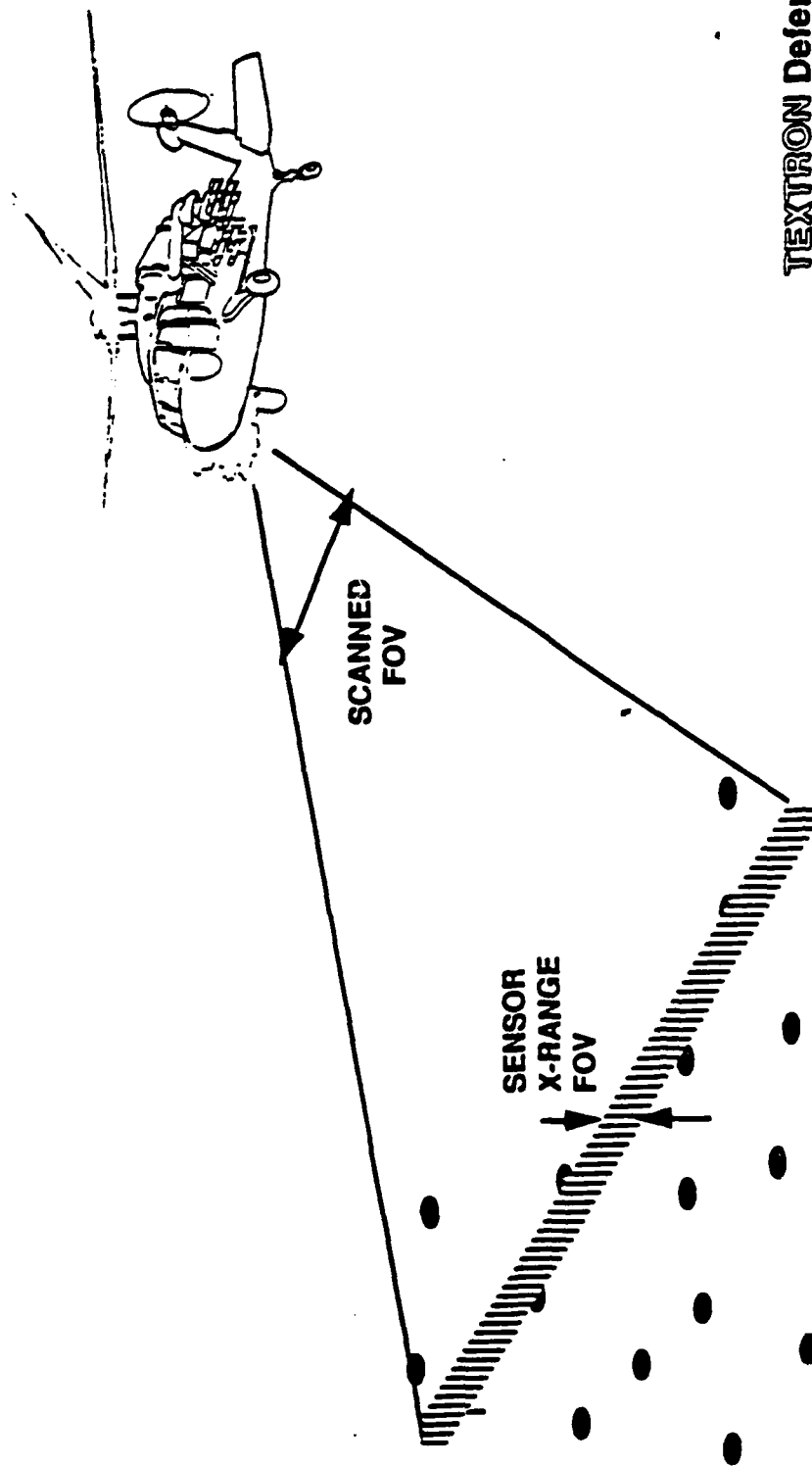


FIGURE 1.3

Ground Controlled Airborne Platform Concept

TDS COUNTERMINE DETECTION PROGRAM

AIRBORNE PLATFORM CONCEPT



TEXTRON Defense Systems

FIGURE 1.4
Airborne Platform Concept

1.4 Recommendations

The next phase of the mine detection program should emphasize sensor suite optimization, data collection, algorithm development, and real time brassboard system development. Based on the results of this Phase 1 study, TDS recommends using: 1) an active IR sensor with fine range resolution ($\leq 1\text{cm}$) as well as echo strength and polarization measurements and beam divergence consistent with less than 4 cm IFOV at the stand-off range; 2) SAIC's UV camera along with a TDS high resolution video camera (operating with a low light level capability); 3) multi-spectral passive IR imaging radiometers capable of making both wideband and narrowband measurements simultaneously so that the technical approaches of LLNL, BETAC, and Monroe can be evaluated side by side. One of the promising close range buried mine detection sensors (SAIC's nuclear approach, TITAN's nuclear approach, or SRS's 2 color X-ray system) should also be incorporated into the sensor suite for performance comparison.

The spatially and temporally coincident multi-sensor data collection activities should take place at several locations during the different seasons of the year. Locations emulating the soils and vegetation of Central/Eastern Europe, the Mideast, and Southeast Asia should be used. Grayling, Michigan, Stockbridge, NY, Yuma, Arizona, and Nellis AFB, Nevada are regions that have been used to simulate some of these locations. Winter and spring are probably the two seasons of principle interest because of soil moisture variations, vegetation, and the effects of snow and rain on mine signatures. The measurement program should treat both stand-off range and sensor depression angle as independent variables with slant range between 50 and 500 feet and depression angle between 30 and 60 degrees(with respect to horizontal). The data collection should include metallic and non-metallic mines or mine simulants of representatives shapes and sizes. Surface, partially covered, and buried mines of varying depths should be included. Representative minefield spatial distributions for typical hand, truck, and airborne deployment systems should be simulated.

Future algorithm development and evaluation efforts must be continued at the individual mine detection, minefield detection and high level scene context cueing levels, with quantification of individual mine

and minefield detection and false alarm statistics the key result. The data base described in the previous paragraph should provide representative training and testing sets for this activity. The performance of our minefield detection algorithm as a function of mine deployment technique and measured false alarm spatial distributions needs to be quantified. The use of the output of the minefield detection algorithm to increase the confidence level on individual mine detections and to further reduce false alarms should be demonstrated.

The scene understanding level of our overall software architecture must be implemented and evaluated. At present we are looking at two different approaches to the processing. Our original approach was to combine our automatic scene classification capability with a knowledge base of minefield cues gathered from extensive interviewing with TDS's inhouse expert, Dr. Raymond Macedonia. The knowledge based processing would be implemented and evaluated on our Knowledge Based Vision System. Recently, Dr. R. Sickler, of the Engineering School, Ft. Leonard Wood, also informed TDS of the existence of a software package, developed by the Army and coded in LISP, that took digitized topographical maps as input and automatically determined the likelihood of minefield presence over the various regions of the maps. TDS recommends evaluation of this software and comparison against our original approach and a determination of how to integrate the selected approach into the demonstration system during the next phase of the program.

The issues of real time processing have been partially addressed with limited real time implementation of an active laser sensor/processor, and analysis has shown that this can be readily extended to multi-sensor, multi-feature processing with available processor chip technology. The actual hardware/software architecture and design should be completed, brassboarded, and demonstrated during the next phase of the program.

Our final recommendations for follow-on efforts are in the area of system concept definition and system design. Several systems issues should be resolved during the next phase of the program. Do we need both airborne and ground based systems working together to accomplish the job or is one enough? What are the requirements? How do the mine neutralization and marking functions integrate with the mine detection

system? These systems design questions should be addressed and at least partially answered during the next phase of the program.

2.0 CANDIDATE SENSORS EVALUATION

2.1 Objective

The objective of this task was to assess the sensor technologies that could be applied to the mine detection problem and to select the most promising sensor suites for hand held, vehicle mounted, and airborne mine detection systems. Off-the-shelf devices, state-of-the-art sensors, and advanced, next generation sensors were to be considered in the evaluation. The resultant sensor suite had to offer the potential for detecting metallic and non-metallic mines, surface laid, partially covered, and totally buried with a very high confidence level while exhibiting very low false alarm probability .

2.2 Approach

The approach taken for the candidate sensors' evaluation was to research the available literature on mine detection sensors and to assess each sensor in terms of real time processing, day/night and all weather operation, buried mine detection, non-metallic mine detection, minefield detection capability and stand-off potential. Appendix A contains a bibliography of the relevant literature that was surveyed in this evaluation process. The most promising sensor suite was then identified for each application: hand-held, vehicle mounted, and airborne.

In addition to the literature search activity, TDS also gained insight into promising mine detection sensor technologies during each of the trimester reviews on the Countermine Detection Program. The open symposium style of presentations permitted excellent exchanges of ideas, concepts, and technologies.

The final avenue for input to the candidate sensors' evaluation analysis was technical and programmatic discussions directly with other sensor technology developers who were not funded under the current program. Those firms included BETAC Corporation and The Monroe Company.

2.3 Results and Conclusions

Table 2.1 contains a summary of the qualitative comparison of the different technologies that either have been or could be applied to the mine detection problem. Analysis of this table applied to the three different platforms: hand-held, vehicle mounted, and airborne, led TDS initially to conclude that a common "core" sensor suite could be applied to all three type systems. This "core" suite could be augmented by sensors unique to the each application, if required, from Pd, Pfa considerations. Table 2.2 summarizes the sensors and their attributes that comprise TDS' core sensor suite. While we felt strongly that the ground penetrating radar techniques could be applied to hand-held and vehicle borne applications, we believe that it would be quite limited in stand-off, and of questionable utility for the airborne platform applications.

In addition to the qualitative preliminary analysis summarized above, TDS had in-depth technical discussions with many sensor technology developers, including:

- Lawrence Livermore: multi -spectral IR
- SAIC: UV
- Optech : active laser
- GSSI: ground penetrating radar
- MA/COM: ground penetrating radar and passive MMW radiometer
- BETAC multi-spectral near IR
- Monroe Company: multi spectral near IR

At this time Lawrence Livermore's work with TEMPS (Temperature Evaluated Mine Position Survey), and both BETAC's and Monroe's work on Passive Reflectance Spectroscopy, appear to offer the most additional performance potential. LLNL's approach has demonstrated the ability to find buried mines, while the second approach also appears to have capability against obscured (masked, blocked, brush covered) targets. These techniques are of great interest to TDS (in conjunction with our multi-feature, multi-sensor data fusion processing approach) because they offer the potential for detecting buried and/or obscured mines at the highest vehicle speeds and longest stand-offs with "off the shelf"

TDS COUNTERMINE DETECTION PROGRAM

CANDIDATE COUNTERMINE SENSORS VS. TACTICAL OPERATIONAL CAPABILITIES (QUALITATIVE)

SENSOR CLASS	TYPE	DAY/		BURIED MINE		BURIED		MINEFIELD DETECTION	STAND-OFF CAPABILITY
		NIGHT	ALL- WEATHER	DIRECT DETECTION	NON-METALLIC MINE DETECTION	?			
ULTRAVIOLET VISUAL (PLUS NEAR-IR)	PHOTOCATHODE	N	N	N				Y	Y
	LOW-LIGHT-LEVEL TV	Y	N	N	N			Y	Y
	PHOTOGRAPHIC FILM	N	N	N	N			Y	Y
INFRARED	BROADBAND RADIOMETER	N	N	N	N			Y	Y
	MULTI-NARROW BAND RADIOMETER	Y	N	N	N			Y	Y
	LASER PROFILOMETER/ REFLECTOMETER	Y	N	N	N			Y	Y
	NEAR-FIELD RADAR	Y	Y	Y	Y			N	N
ELECTROMAGNETIC	SYNTHETIC APERTURE RADAR	Y	Y	N	N			Y	Y
	REAL APERTURE RADAR	Y	Y	N	N			Y	Y
	GROUND-PENETRATING RADAR	Y	Y	Y	Y			Y	Y

TEXTRON Defense Systems

TABLE 2.1

Candidate Countermine Sensors Trade-Off

TDS COUNTERMINE DETECTION PROGRAM

CANDIDATE COUNTERMINE SENSORS VS. TACTICAL OPERATIONAL CAPABILITIES (QUALITATIVE)

CLASS	SENSOR	TYPE	REAL- TIME	DAY/ NIGHT	ALL- WEATHER	BURIED MINE		NON-METALLIC MINE DETECTION	MINEFIELD DETECTION	STAND-OFF CAPABILITY
						DIRECT DETECTION	BURIED			
ELECTROMAGNETIC (CONT'D)	HARMONIC RADAR		Y	Y	Y	N	N	N	N	N
	HARMONIC		Y	Y	Y	Y	Y	?	?	/
	MICROWAVE RADIOMETER		Y	Y	?	Y	?	?	?	Y
	HIGH-POWER MICROWAVE		Y	Y	?	Y	?	?	?	?
BIOSENSORS			N	Y	N	Y	Y	N	N	N
MAGNETIC	FLUXGATE MAGNETOMETER/ GRADIOMETER		Y	Y	Y	Y	Y	N	N	N
	INDUCTANCE BRIDGE		Y	Y	Y	Y	Y	N	N	N
ACOUSTIC/SEISMIC	LASER VIBROMETER		Y	Y	N	Y	Y	N	N	N
NUCLEAR	2 COLOR X-RAY BACK- SCATTER		N	Y	N	Y	Y	N	N	N
TRACE GAS			N	Y	N	Y	Y	N	N	N

THE X-11 RION Defense Systems

Table 2.1 (Continued)

TDS COUNTERMINE DETECTION PROGRAM

"CORE" SENSOR SUITE FOR DATA FUSION

- LOW-LIGHT-LEVEL, HIGH RESOLUTION TELEVISION-(OR UV)
PASSIVE MODE, HIGH SPATIAL RESOLUTION/VISIBLE TEXTURE,
LARGE AREA COVERAGE, REAL-TIME, MATURE TECHNOLOGY, LOW
COST, COMPACT
- MULTI-BAND, HIGH-RESOLUTION INFRARED RADIOMETER-
PASSIVE, HIGH SPATIAL RESOLUTION, THERMAL PROFILE (BOTH
RELATIVE AND ABSOLUTE TEMPERATURE), LARGE AREA
COVERAGE, REAL-TIME, MATURE TECHNOLOGY, DAY/NIGHT
- HIGH-RESOLUTION, INFRARED LASER PROFILOMETER/REFLECTO-METER
HIGH SPATIAL RESOLUTION, RANGE, POLARIZATION, AND
REFLECTIVITY, PROFILES, LARGE AREA COVERAGE, REAL-TIME,
MATURE TECHNOLOGY, DAY/NIGHT
- GROUND PENETRATING RADAR-
SUBSURFACE, NON-METALLIC MINE DETECTION, ALL-WEATHER

8/22/89

TABLE 2.2

"Core" Sensor Suite for Data Fusion

TEXTRON

DEFENSE SYSTEMS

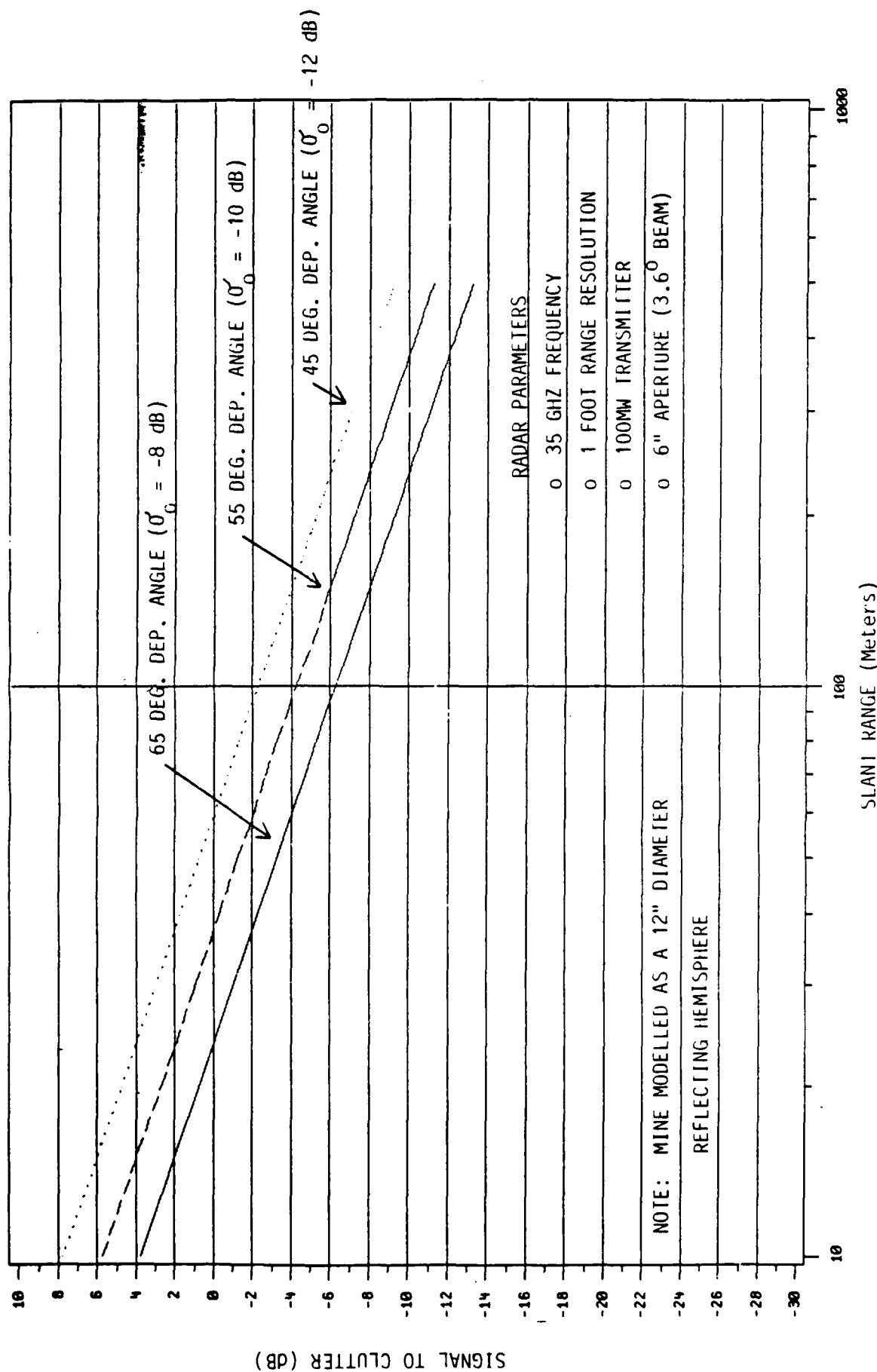
hardware that we believe will be smaller in size, lower in power, lower in cost, and better suited for long standoff mine detection than other approaches such as the Harmonic SAR (HSAR) technique. Also since they both rely on spectral measurements rather than spatial measurements partial covering should not prove to be difficult to deal with. Another potential advantage of the TDS sensor suite is that it could be compatible with some already existing helicopter avionics systems, at least in terms of some of the sensors (visible, passive IR). It is TDS' assessment that the HSAR approach is the only other potentially viable airborne stand-off detection system for buried mines.

TDS has also had continuing dialog with SAIC on their imaging UV detection technique. It is not clear to us at this time that there is phenomenology in the UV that would make it more suitable than the visible or IR bands already being investigated by TDS, however, we believe that only simultaneous and coincident data collection will answer this question.

TDS is currently working with the organizations cited above to define a multi-sensor airborne data collection effort for the follow-on phase to this program. TDS has developed an airborne (helicopter) multi-sensor testbed that incorporates registered, coincident IR (3-5 μm and 8-12 μm), visible (narrow and wide FOV), and MMW (35 GHZ, FM-CW dual circular polarization, 1 foot range resolution) sensors on a stabilized gimbal platform with 2 degrees of freedom motion. The design of the testbed is modular so that additional sensors such as the active IR or UV may be added or substituted in the existing sensor suite.

The effective use of visible, passive IR, and active IR sensors for mine detection has been well documented. The application of active MMW sensing to the mine detection problem, on the other hand, has been very limited. TDS has developed a 35 GHZ MMW radar for anti-armor submunition applications. This instrumentation quality sensor utilizes an FM-CW waveform, dual circular polarization, and one foot range gate resolution for its target discrimination capability. Its six inch aperture antennas result in a 3.6 degree beam width at 35 GHZ. Figure 2.1 shows analytical curves of signal to clutter (S/C) ratio versus slant range for this radar at various depression angles (45, 55, 65° with respect to horizontal). Typical radars require better than 15 dB for high confidence

35 GHZ FMCW RADAR PERFORMANCE VERY MARGINAL IN AN RCS MODE



target detection (>0.95) and acceptable false alarm rate ($<10^{-5}$). More sophisticated signal processing approaches allow the S/C to degrade to about 6dB, while still maintaining acceptable performance. From Figure 2.1 it is seen that this would constrain the operating range of our radar to less than 15 meters. This very limited stand-off does not make MMW radar an attractive candidate for an airborne mine detection system, however, it may have some utility for hand-held and vehicle mounted applications. These calculations were confirmed with measurements made using TDS's multi-sensor airborne testbed during our second data collection exercise under this program. That effort will be discussed in Section 4.

3.0 SYSTEM CONCEPT DEFINITION

3.1 Objective

The objective of this effort was to develop a preliminary mine detection system concept including definition of system attributes, performance goals and limitations, physical and functional descriptions, and size, weight, power and cost estimates.

3.2 Technical Approach

The core sensor suite recommended in the candidate sensors' evaluation could be applied equally well to hand-held, vehicle mounted, and airborne mine detection systems. TDS focussed on forward rate of advancement and large search area as driving requirements in our system concept definition. The large search area requirement implied wide field of view coverage. From our experience in smart wide area mines programs (ERAM, WAM, AHM), with their immense lethal zones (>100 meters in radius from the mine) we believe that stand-off is also a key requirement for mine detection platform survivability. These considerations led us to concepts for both the ground based and airborne mine detection systems that had the sensor suite elevated on an aerial platform.

3.3 Results and Conclusions

TDS has defined two notional concepts for a mine detection system:

- Ground Controlled Airborne Platform (GCAP)
- Autonomous airborne platform (AAP)

Figure 3.1 depicts our concept for GCAP. In this concept the multi-sensor suite is integrated into an unmanned aerial vehicle (UAV) such as the ducted fan gas powered "aerobot" currently under development by Moller Industries (shown in the system sketch). Moller has a 20HP model that is 16.5 inches in diameter, has a duty time of 45 minutes, a maximum range of 60 miles, and a maximum speed of 75 mph for a 30 pound payload. Weight versus speed, range, and duty time trade-offs must be made in future development efforts. The azimuthal scan of the field of view can be accomplished by platform rotational motion, thereby potentially eliminating the need for a gimbal subsystem. The aerobots are dispensed

TDS COUNTERMINE DETECTION PROGRAM

GROUND CONTROLLED AIRBORNE PLATFORM CONCEPT

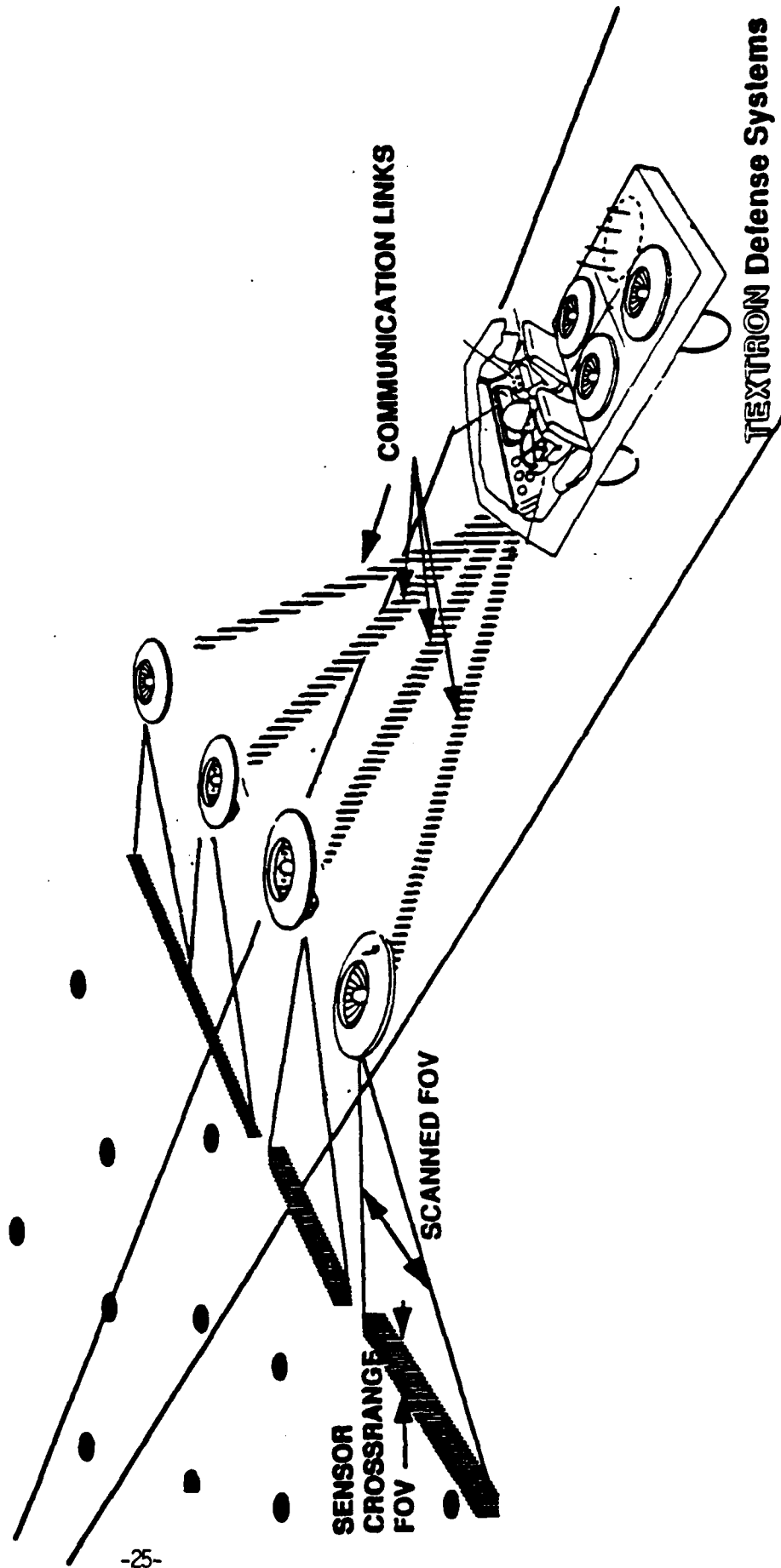


FIGURE 3.1

Ground Controlled Airborne Platform Concept

from a ground vehicle such as that shown in Figure 3.1. A two-way link (either fiber optic or secure RF) provides communications between aerobot and ground vehicle. TDS is currently under contract to DARPA/ARDEC for the development of short range secure communications which could be applied to this system.

The communications from vehicle to aerobot include mode commands (sensor stare, sensor scan, aerobot hover, aerobot advance) and motion commands (increase altitude, decrease altitude, rate of forward advance). The data that is linked back to the ground vehicle from the aerobot can consist of raw or processed sensor data, or both. The actual partitioning of the real time processing function between aerobot and ground vehicle must be done in a subsequent phase. In addition, aerobot position relative to ground vehicle and sensor pointing direction relative to aerobot flight path will be provided using the appropriate on-board (the airborne platform) instrumentation. This will be used to map mine detection locations on a stored digitized topographical map within the ground vehicle. This will produce a real time display as well as a permanently stored/marked map.

In its systems operation the GCAP will typically search from altitudes between 50 and 300 feet with the sensor suite looking down at a 60 degree depression angle. The search width will be nominally 100 feet. This ground based vehicle approach offers significantly better speed and search area coverage than other ground based systems (that include nuclear, X-ray, GPR, or vapor detection sensors) by virtue of the core sensor suite selected. The inherent sensitivity of the detectors used in TDS's multi-sensor approach requires significantly less integration time (and hence faster system operation) for achieving acceptable signal to noise compared to the competing sensors.

The GCAP concept has the potential for better P_d , P_f a performance per dollar cost compared to longer stand-off systems such as the autonomous airborne platform (helicopter) because its lower altitude operation enables simpler, smaller, cheaper sensors. The GCAP platform (aerobot) is both more expendable (lower cost) and more survivable (smaller size) than conventional AAP approaches. Although the specific operation of the GCAP must still be determined during the subsequent phases, the concept has the flexibility to accomplish both large area

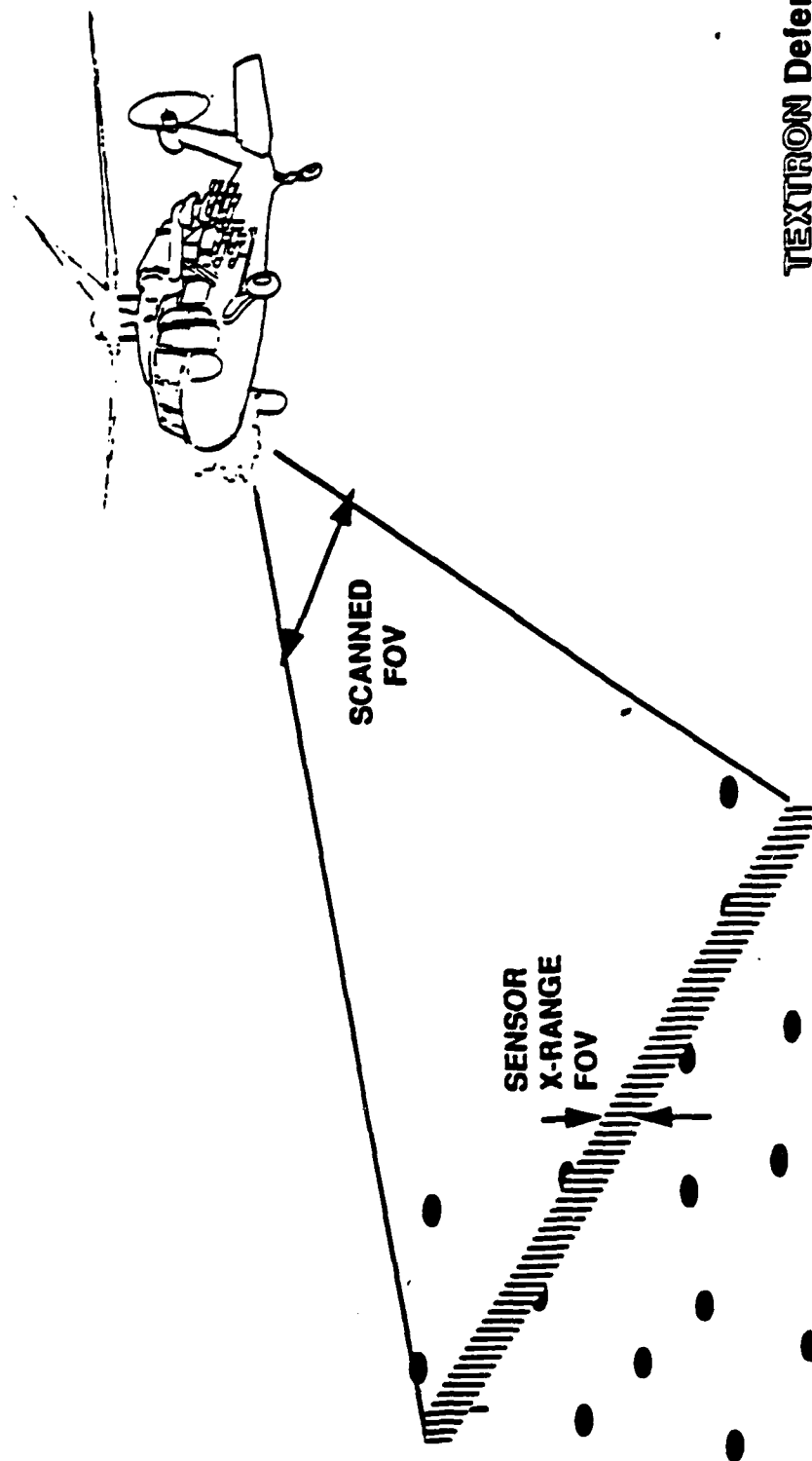
(higher altitude) mine/minefield cueing functions and lower altitude individual mine detection, using altitude and velocity commands to the aerobot by the ground control vehicle.

Figure 3.2 depicts our concept for the more conventional autonomous airborne platform (AAP), a manned helicopter. In this approach the sensor suite is mounted on a stabilized platform attached to the helicopter that is gimbaled to accomplish the required azimuthal scan. TDS has developed (under a 3 million dollar, 2 year capital investment) a multi-sensor airborne testbed that integrates with a UH-1B helicopter. That testbed, shown in Figure 3.3 exemplifies one potential configuration for this system concept. Appendix C describes the TDS airborne multi-sensor test bed in detail.

As discussed previously, the AAP would operate at substantially higher altitude (>1000 feet) and longer stand-off ranges than the GCAP resulting in a larger search area coverage, with a larger, more expensive sensor suite. The AAP approach also offers more reach, higher speed, and longer duty time than the GCAP concept. Another advantage of the AAP Concept includes the fact that the OH-58D scout helicopters have already been assigned to the mission of mine detection and location, so that the platform is defined, unlike the GCAP where both the aerobot and dispenser vehicle must be defined and developed. Finally, existing helicopter avionics sensor suites may be adaptable or retrofitted for real-time mine detection, thus again reducing the cost of system development and the logistics of incorporation into the inventory.

TDS COUNTERMINE DETECTION PROGRAM

AIRBORNE PLATFORM CONCEPT



TEXTRON Defense Systems

FIGURE 3.2

Airborne Platform Concept

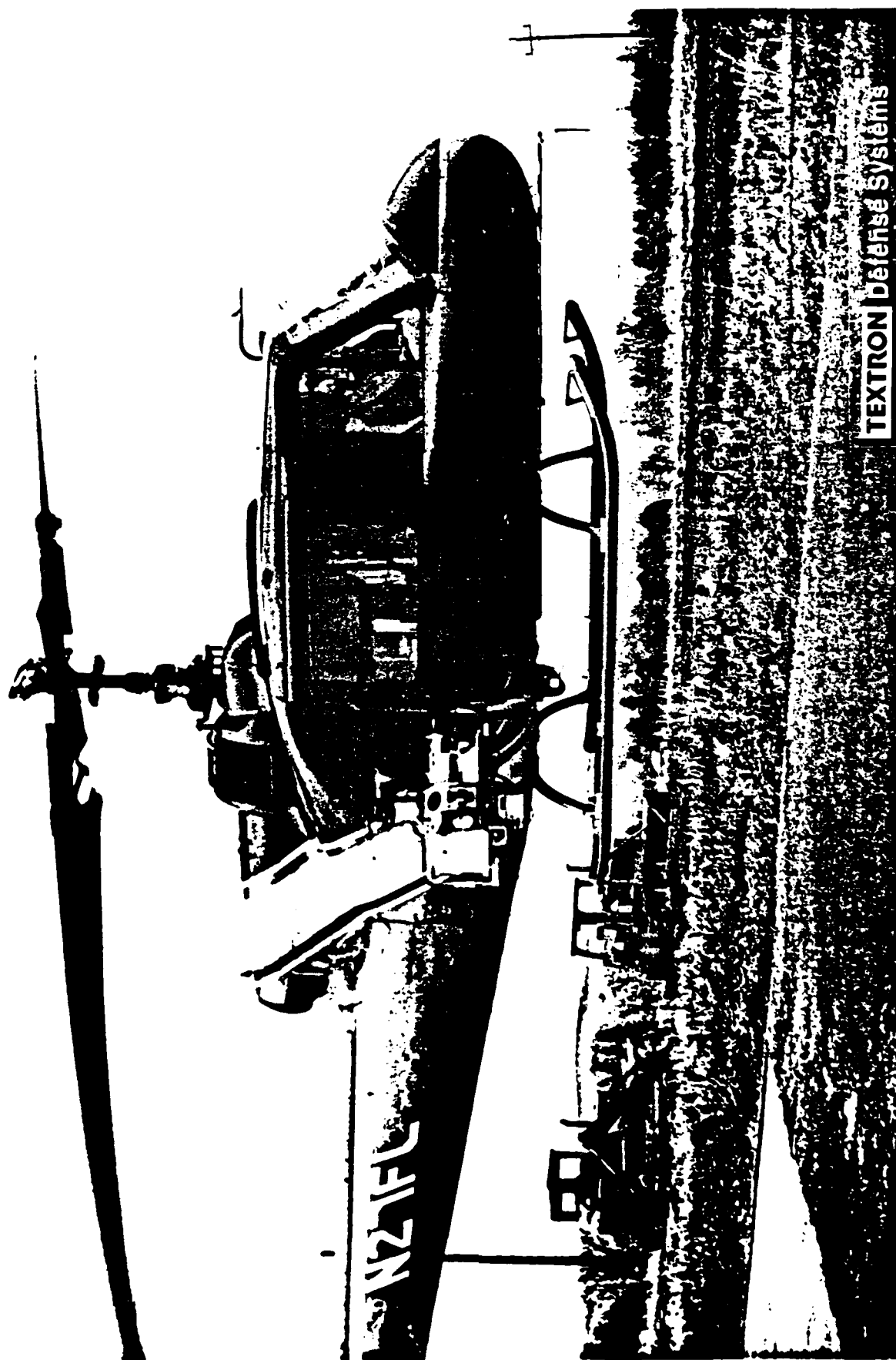


FIGURE 3.3
Implementation of Airborne Platform Concept

3.4 System Analysis

The notional concepts described in the previous section were analyzed to determine preliminary performance goals and sensor design parameters. The preliminary performance goals included:

- P_m : Probability of individual mine detection
- P_{fa} : Probability of individual mine-like false alarm
(combined effects due to sensor internal system noise as well as clutter/background induced false alarms)
- P_{mf} : Probability of detecting the minefield
- P_{fam} : Probability of minefield-like false alarm (i.e. probability of saying a minefield is present, when in fact no minefield is present)

The key sensor design parameters that were analyzed included:

- sensor instantaneous field of view (spatial resolution)
- sensor total field of view
 - downrange (in terms of number of parallel detectors)
 - crossrange (in terms of azimuthal scanning requirements)
- scan rate and data thruput

For this analysis, the following assumptions were made:

- The downrange (in direction of platform forward motion) extent of the search coverage is 200 meters.
- The crossrange (in direction perpendicular to platform forward motion) extent of the search coverage is 30 meters (± 15 meters off the forward velocity direction).
- The required platform forward velocity is 25 mph but the desire is for greater than 35 mph.

The first calculation relates the individual mine-like false alarm probability, P_{fa} , to the troop delay or reduction in forward rate of advancement due to false alarms. For this analysis the forward velocity of the column was 35 mph prior to entering the minefield. Every time a false alarm was registered, the column came to rest for a period of three minutes (believed to be very optimistic) while the absence of a real mine was confirmed. Figure 3.4 shows the "effective" rate of forward advancement as a function of the log (P_{fa}). Independent decisions on the

TDS COUNTERMINE DETECTION PROGRAM

EFFECTIVE FORWARD VELOCITY OF MOVEMENT

VD = 35 M.P.H.

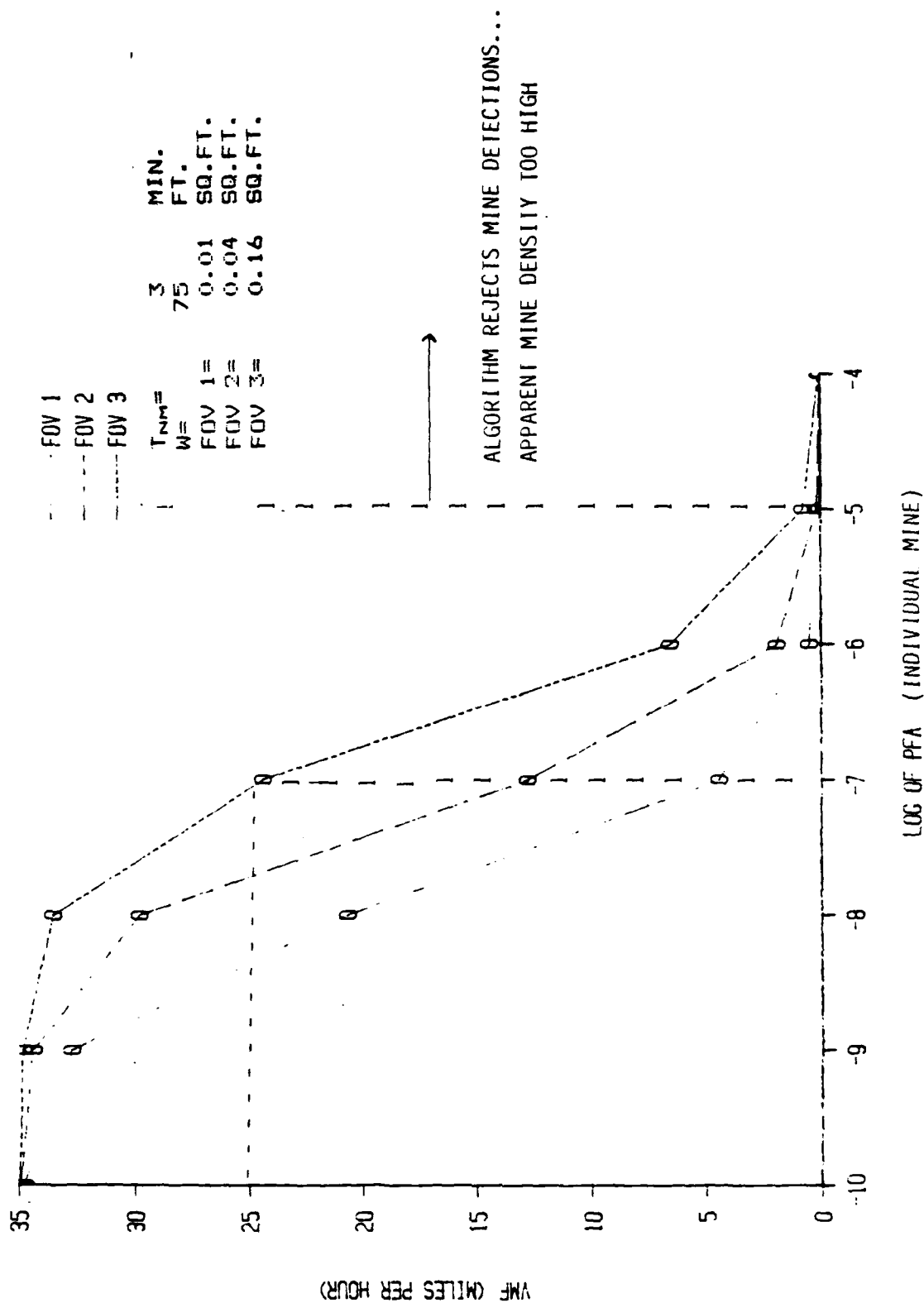


FIGURE 3.4
Effective Forward Velocity of Movement

presence or absence of a mine were made on either every $.1 \times .1 = .01$ sq. ft. (FOV 1), $.2 \times .2 = .04$ sq. ft. (FOV 2), or $.4 \times .4 = .16$ sq. ft. (FOV 3) within the designated search area. Since the mines sizes considered were between 3 inches and 12 inches in diameter, we selected the .4ft (5") x .4ft (5") field of view as the independent measurement area. From the figure we see that in order to retain an effective velocity of greater than 25mph we must maintain an individual mine-like false alarm probability, $P_{fa} \leq 10^{-7}$.

Figure 3.5 presents another perspective on quantifying the effects of individual mine-like false alarms. The identical parameters were used as in the previous calculation, however here we are evaluating the delay distance between the mine clearing apparatus and the front line of the forward moving troops that need to traverse through the minefield. The assumption in this calculation was that the troops would not enter the minefield until a 30 meter wide path is cleared through the 200 meter depth of the field. Given that it is desirable to have the minefield clearing function in close proximity to the troops traversing the field, this figure supports the requirement to maintain $P_{fa} \leq 10^{-7}$.

Sensor system requirements were further analyzed to determine the relationships between individual mine detection/false alarm probabilities and minefield detection/false alarm probabilities. The analysis quantified the following trades:

- Probability of detecting the minefield as a function of the probability of detecting individual mines (where the minefield detection criteria is the detection of at least "N" individual mines, N being varied parametrically).
- Probability of falsely detecting a minefield as a function of the per look probability of false alarm, using the same minefield detection criteria as above
- Delay associated with falsely detecting a minefield as a function of the expected probability of detecting an individual mine.

The parameters used in the analysis included:

- 30m (wide) x 200m (long) search area
- 30 mines distributed over the search area (1 per 200m²)
- sensor takes an independent look at the ground every

TDS COUNTERMINE DETECTION PROGRAM

DELAY DISTANCE BETWEEN MINE CLEARING APPARATUS
AND FRONT LINE OF FORWARD MOVING TROOPS

FOR $L = 656.16$ FT. AND $VD = 35$ M.P.H.

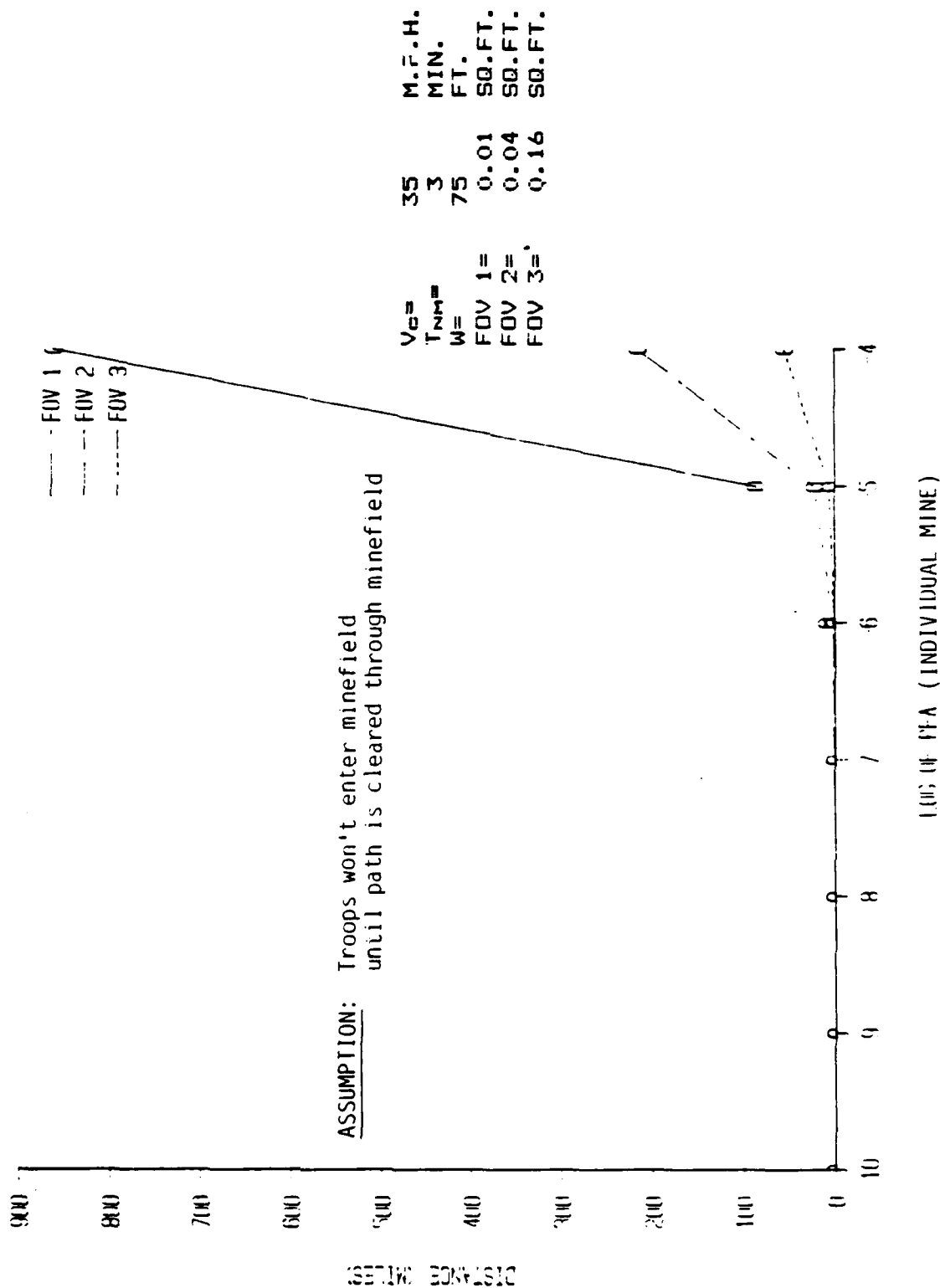


FIGURE 3.5

Delay Distance Versus False Alarm Rate

TEXTION Defense Systems

$$0.4 \times 0.4 = 0.16 \text{ sq. ft.}$$

- mines can be cleared/neutralized at a rate of 27m^2 per man-hour
- The delay produced by a false minefield detection is estimated by the ground area searched during the neutralization/clearing process to assure that the probability of detecting at least 1 mine, if any were present, is ≥ 0.999 .

The mine density of 1 per 200m^2 was derived from unclassified documentation on Soviet minefield deployment where 3 rows of mines are seeded, with an interrow spacing of between 10 and 40 meters. The intermine spacing along any row is between 3 and 5 meters. Consideration of the various encounter geometries of the troops approaching minefield resulted in a range of densities from 1 per 300m^2 to 1 per 30m^2 . The density of 1 per 200m^2 was selected as typical. The mine clearing/neutralization rate of 27m^2 per man-hour was extracted directly from the Army's field handbook, FM5-34.

Figure 3.6 plots the probability of minefield detection versus the mine quantity detection threshold for an individual mine detection probability, P_m , of 0.8. To achieve a minefield detection probability, P_{fam} , greater than 0.95, the mine threshold should be set at ≤ 18 . This means that the system must detect between 1 and 18 of the 30 mines (over the 6000m^2 area) in order to declare a minefield detection with greater than 0.95 probability. Figure 3.7 shows the probability of minefield-like false alarm, P_{fam} , as a function of the same mine threshold for a single look false alarm probability, P_{fa} , of 10^{-4} . From this figure it can be concluded that a mine detection threshold greater than 18 will yield a $P_{fam} \leq 0.05$. For an individual mine detection probability of 0.8, and an individual mine-like false alarm probability of 10^{-4} , with a minefield detection criteria of 18 individual mine detections, the probability of falsely classifying a 6000m^2 area as a minefield is less than 0.05. Figure 3.8 plots man-hours of delay resulting from a false minefield detection as a function of the probability of individual mine detection. The curve indicates that for an individual mine detection probability, P_m , of 0.8 (from above), the delay will be less than 3 man hours, but more importantly this point falls on the flat part of the

$P_m = 0.8$

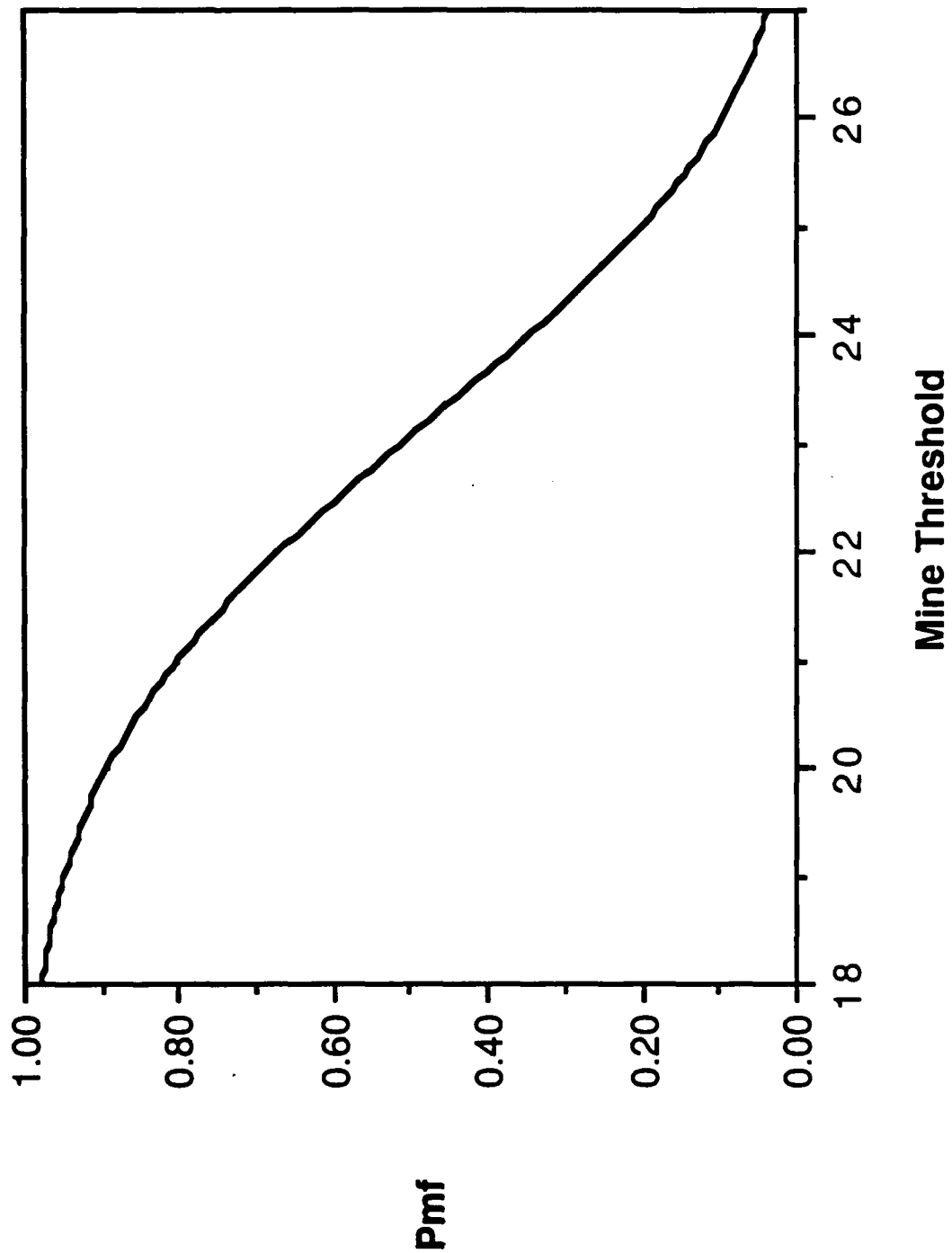


FIGURE 3.6
Probability of Minefield Detection VS Threshold

Pfa = .0001

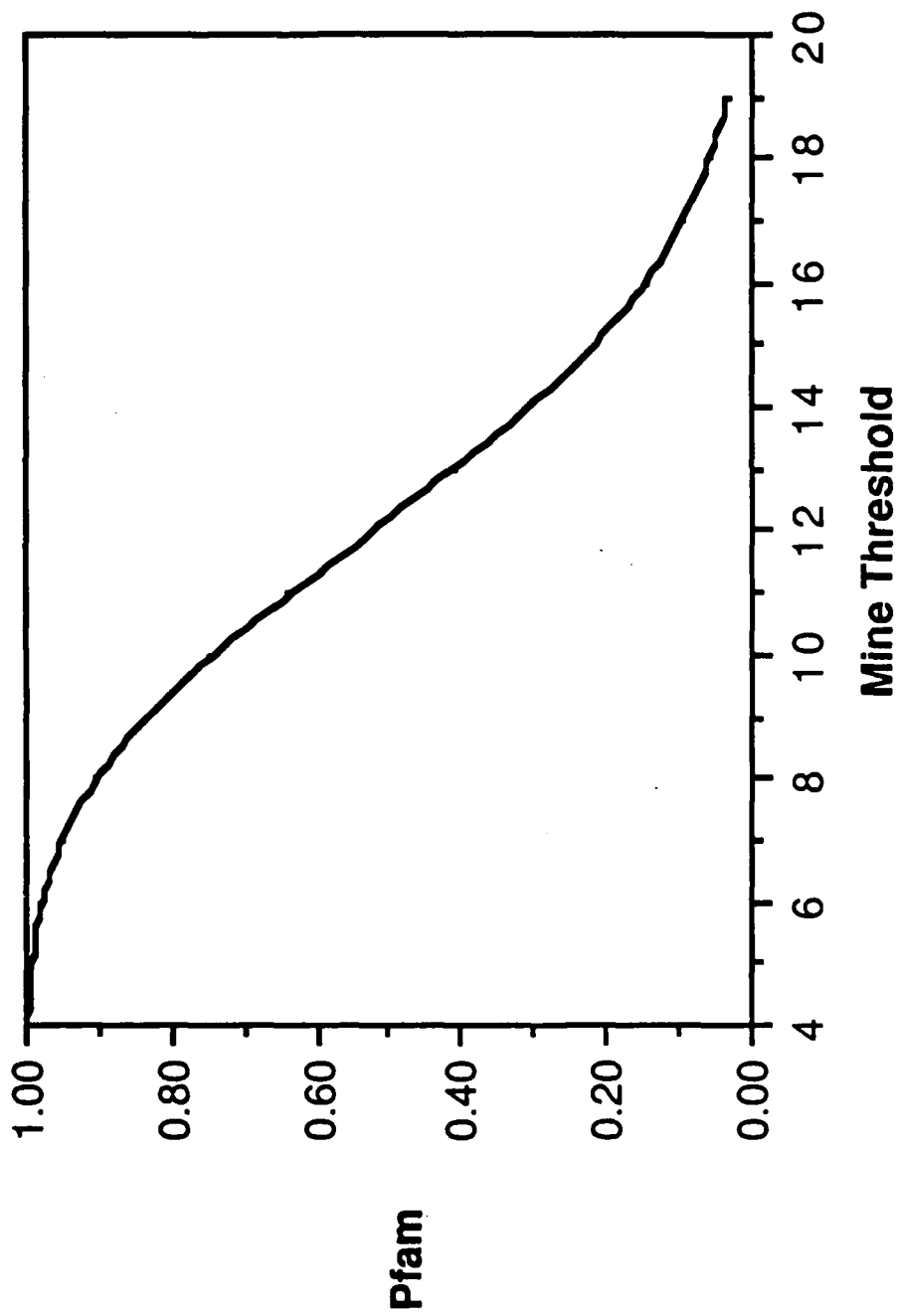
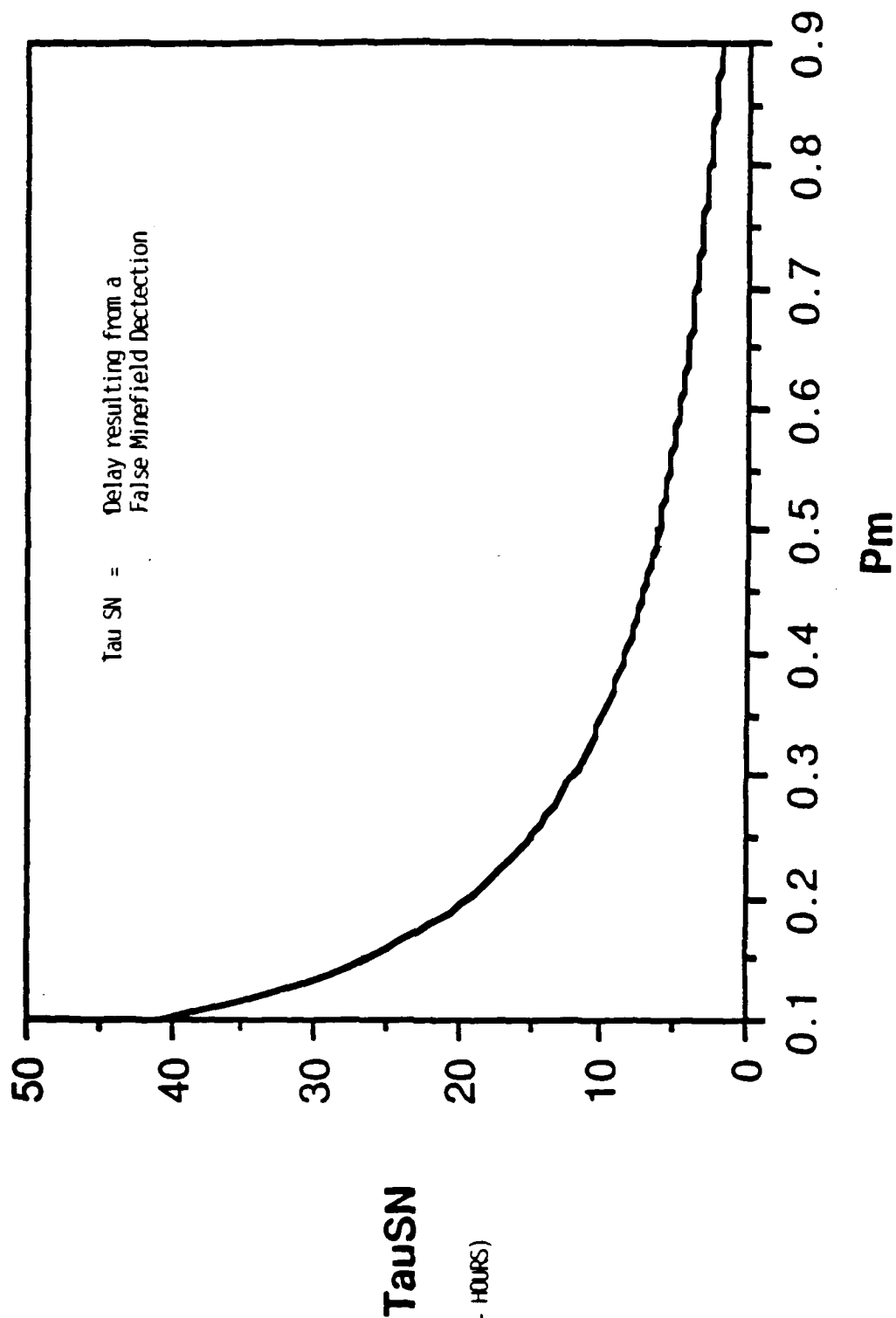


FIGURE 3.7
Probability of Minefield False Alarm VS Threshold

TauSN vs Pm



PROBABILITY OF DETECTING A SINGLE MINE

FIGURE 3.8

Mine Clearing Produced Delay

man hour curve, where delay is quite insensitive to individual mine detection probability.

Figure 3.9 and 3.10 contain plots of sensor scan rate versus number of parallel detectors and data rate versus number of parallel detectors for a 1" x 1" IFOV at NADIR. This IFOV is a preliminary sensor design parameter based on mine dimensions of 3", 6", and 12" diameter. The analysis was completed for a platform forward velocity of 35mph and a ± 30 degree azimuth scan. The calculation required contiguous IFOVs at NADIR so that there would be no holes in the ground coverage search pattern. These curves suggest that both the requirements for detector array size and data thrupt are well within the state of the art of the respective sensor and electronics processing technologies. The thrupt analysis is carried through in detail in Section 6 on real time operation.

3.5 Countermine System Parameters

Table 3.1 summarizes the preliminary TDS countermine system parameters. Note that many of the performance parameters are called out as goals or TBDs, since insufficient data exists at this time to support final commitments. Also, note that the range of values in the system size, weight, and cost parameters is to accommodate both GCAP and AAP notional system concepts.

SENSOR TRADE: SCAN RATE VS NUMBER DETECTORS
CONCLUSION: REASONABLE ARRAYS YIELD REASONABLE SCAN RATES

- PLATFORM VELOCITY = 35 MPH
- SCANNED FOV (AZ) = ± 30 DEG
- SENSOR IFOV (RADIR) = $1'' \times 1''$
- CONTIGUOUS IFOVS AT RADIR

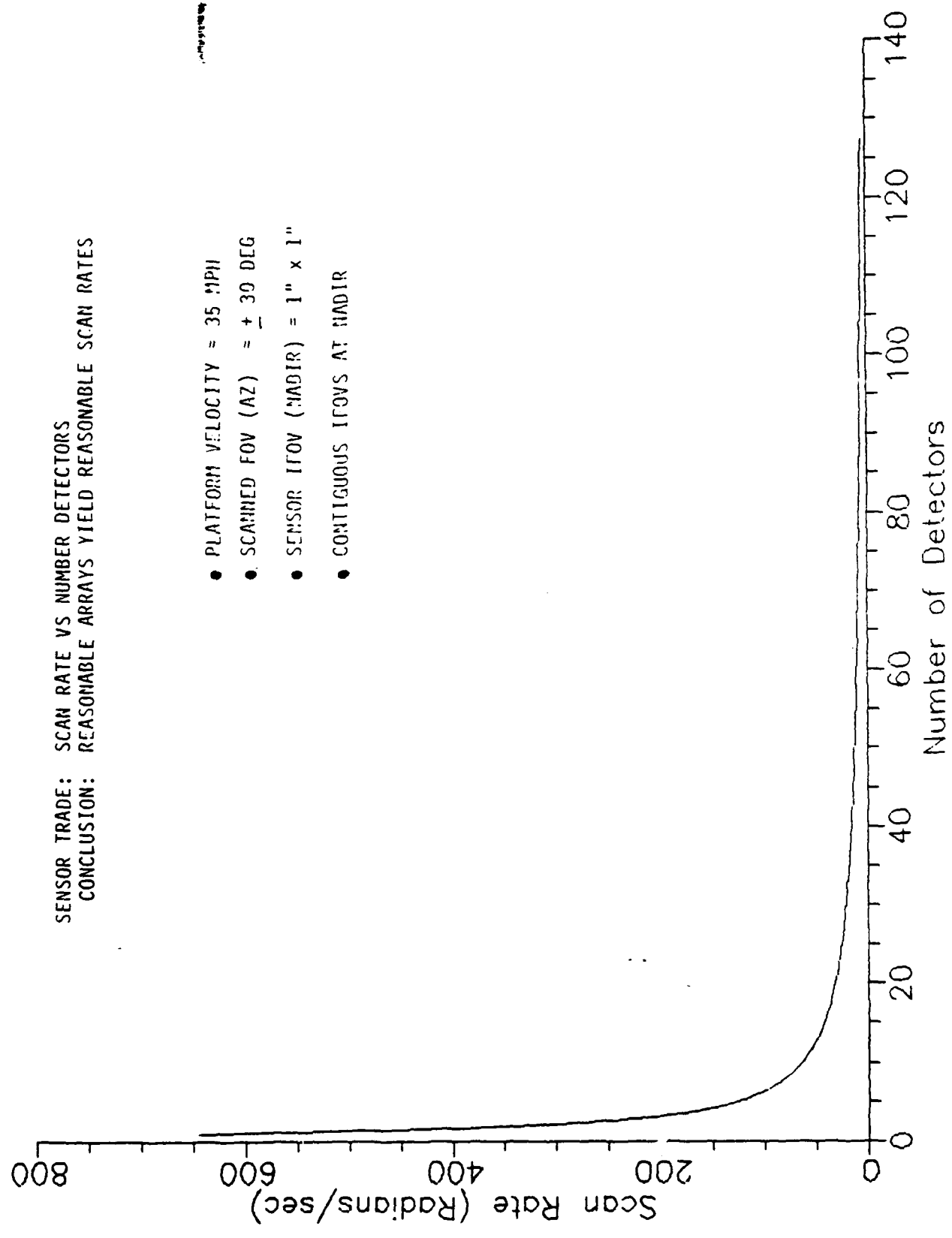
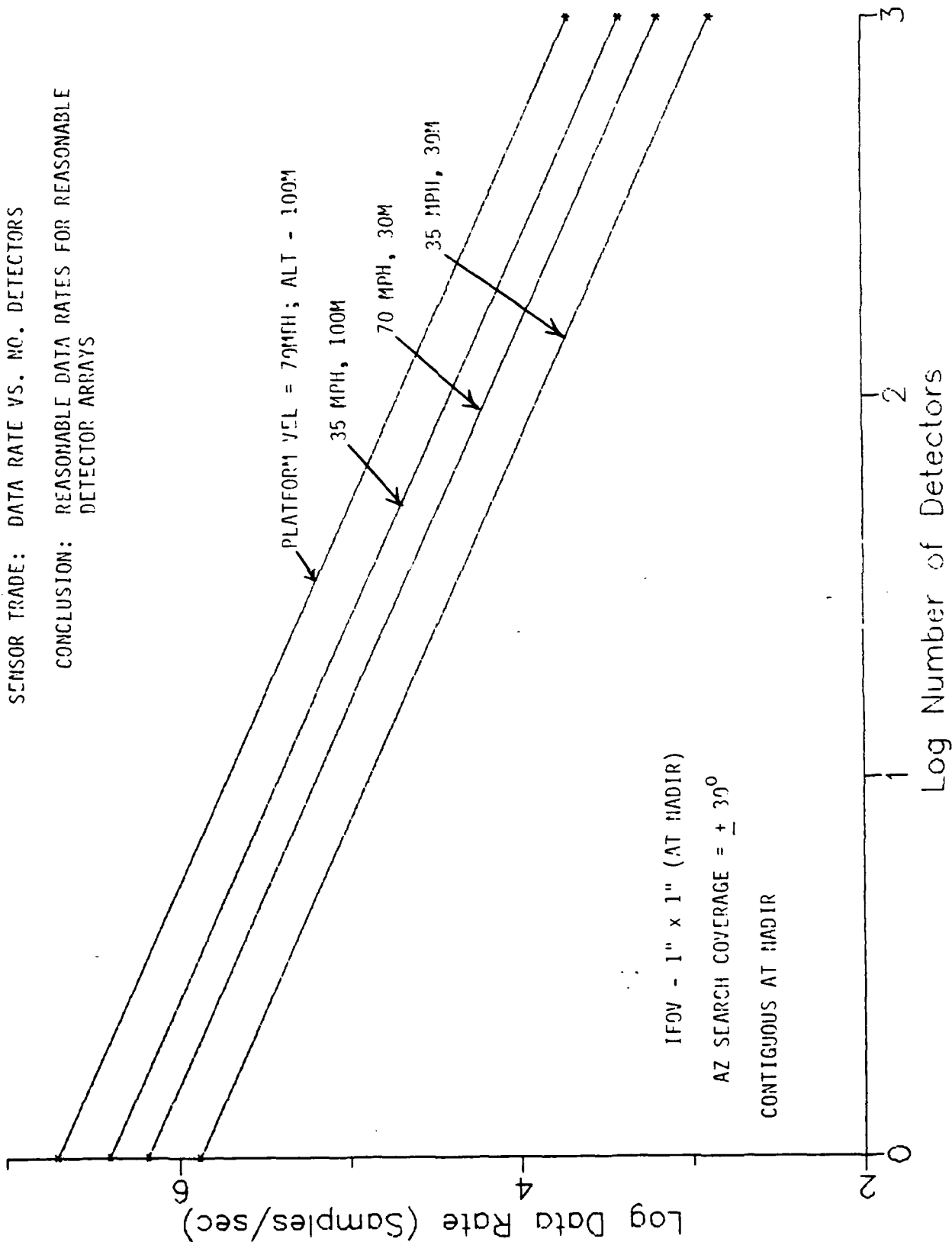


FIGURE 3.9
Scan Rate Versus Number of Detectors

TDS COUNTERMINE DETECTION PROGRAM

SENSOR TRADE: DATA RATE VS. NO. DETECTORS

CONCLUSION: REASONABLE DATA RATES FOR REASONABLE DETECTOR ARRAYS



DEFENSE SYSTEMS

FIGURE 3.10
Data Rate Versus Number of Detectors

TDS COUNTERMINE DETECTION PROGRAM

TDS COUNTERMINE SYSTEM PARAMETERS (PRELIMINARY)

NAME OF SYSTEM:

MULTI-SENSOR MINE DETECTION SYSTEM
BASELINE: MULTI-SPECTRAL PASSIVE IR,
LLTV (OR UV), ACTIVE IR

1. MINE TYPES DETECTED:

METALLIC, NON-METALLIC, ANTI-ARMOR,
ANTI-VEHICULAR, ANTI-PERSONNEL (TBD)

2. MAXIMUM BURIAL DEPTH FOR $P_D > 0.9$:

4-6 INCHES (TBD)

3. PERFORMANCE FOR SURFACE MINES IN MODERATE CLUTTER:

- MIN. SCAN AREA: 30M (WIDE) X 200M (LONG)
- RATE OF FORWARD MOVEMENT: 35 MPH
- INDIVIDUAL MINE DETECTION
 - P_D (MINE) > 0.95 (GOAL)
 - P_{FA} (MINE) $< 10^{-8}$ (GOAL) PER LOOK
- MINEFIELD DETECTION
 - P_D (FIELD) > 0.99 (GOAL) • P_D (MINE) > 0.8 (GOAL)
 - P_{FA} (FIELD) < 0.05 (GOAL) • P_{FA} (MINE) $< 10^{-4}$ (GOAL)

FFF TDS COUNTERMINE DETECTION PROGRAM

TDS COUNTERMINE SYSTEM PARAMETERS (PRELIMINARY) - CONTINUED

- | | | |
|----|------------------------------------|---|
| 4. | ENVIRONMENTAL/TERRAIN CONSTRAINTS: | ENVIRONMENTAL: SOME DEGRADATION IN HEAVY RAIN
AND FOG

TERRAIN: NONE |
| 5. | EXPECTED FALSE ALARM GENERATORS | DEBRIS FROM MAN-MADE PRODUCTS AND DISCRETE
NATURAL CLUTTER (I.E., ROCKS) |
| 6. | COUNTERMEASURES: | HEAVY OBSCURANT SMOKES AND HIGH FIDELITY
DECOYS |
| 7. | SYSTEM SIZE; | 750 - 1500 IN ³ (APPLICATION RANGE DEPENDENT) |
| 8. | SYSTEM WEIGHT: | 50 - 150 LBS (APPLICATION RANGE DEPENDENT) |
| 9. | MAXIMUM RANGE OF OPERATION: | > 100 FT |

7/19/88JS
9

TEXTRON

DEFENSE SYSTEMS

TDS COUNTERMINE DETECTION PROGRAM

TDS COUNTERMINE SYSTEM PARAMETERS

(PRELIMINARY) CONTINUED

10. SYSTEM COST:

75 - 150K WITHOUT PLATFORM (APPLICATION RANGE DEPENDENT)

11. SAFETY HAZARDS:

POTENTIAL EYE DAMAGE DUE TO LASER SENSOR

12. AREAS OF TECHNICAL RISK:

- P_D, P_{FA} AND POSITION LOCATION PERFORMANCE ON INDIVIDUAL MINES
- BURIED MINE PERFORMANCE AT STAND-OFF RANGES

13. OVERALL RISK ASSESSMENT:

LOW TO MEDIUM

14. OTHER SYSTEM USES:

DETECTION, CLASSIFICATION, POSITION LOCATION FOR SURVEILLANCE OF OTHER GROUND TARGET TYPES (EX. TANKS, TRUCKS, SSM SITE ELEMENTS, SAM SITE ELEMENTS, AIRFIELDS, RAILROADS)

7/19/89JS
10

TEXTRON

DEFENSE SYSTEMS

program. Neither the sensor suite nor the individual sensor performance parameters were "optimized" for the mine detection problem. Once again, the objective of this phase of TDS's program was to demonstrate the performance improvement potential of multi-sensor systems using advanced processing techniques over single sensor systems.

TDS was unable to obtain any REMIDS or MERADOR data over the course of this program. We did receive AMIDARS data in December, however, it was of limited use because of its single sensor (one color passive IR) design and unavailability of ground truth data to locate the mines. This data is a single 8k pixel by 8k pixel image containing at least four minefields, each consisting of two parallel rows of about 25 mines each. The mines themselves are barely resolved covering approximately 2x2 pixels. There are also paved and dirt roads, farm trucks, truck activity, farm buildings, farm machinery, areas of random rock outcrops, a stream and a variety of vegetation in this image. This image also has some fairly severe sensor artifact signatures. Fortunately, the artifacts do not appear to be in the areas of the minefields. No other Government data base on mine and/or minefields could be identified by TDS.

Because of the urgent need for multi-sensor data in order to initiate algorithm development, TDS decided to accelerate its schedule for the first data collection effort as much as possible. This would then be followed by additional data collection during the next significant seasonal change. Summaries of each data collection effort are contained on the following pages.

4.3 Data Collection I

The first TDS multi-sensor data collection activity was conducted at TDS' Wilmington facility during the winter months. The sensors consisted of a high resolution visible TV camera, an 8-12 um passive IR imaging radiometer, and an active gallium arsenide laser range finder (Figure 4.1) all boresighted together on a common mounting plate that was then attached to a Cherry-Picker platform (Figure 4.2) that was elevated to approximately 40 feet and oriented at a depression angle of 60 degrees (with respect to horizontal), resulting in a 50 foot slant range. The detailed description of this test hardware is contained in Appendix B. The simulated mines used for this first data gathering exercise were plastic

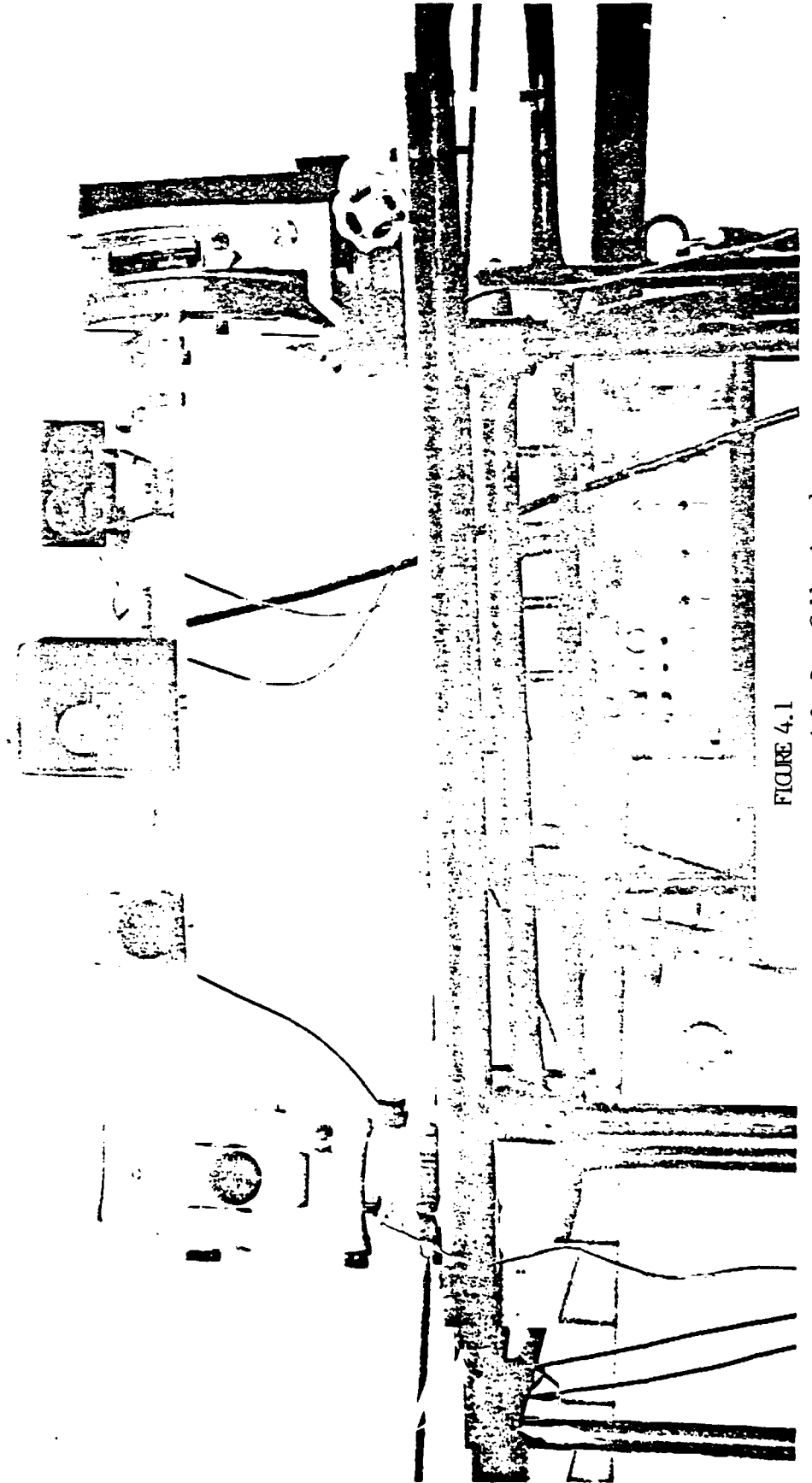


FIGURE 4.1
Multi-Sensor Test Bed for Data Collections 1

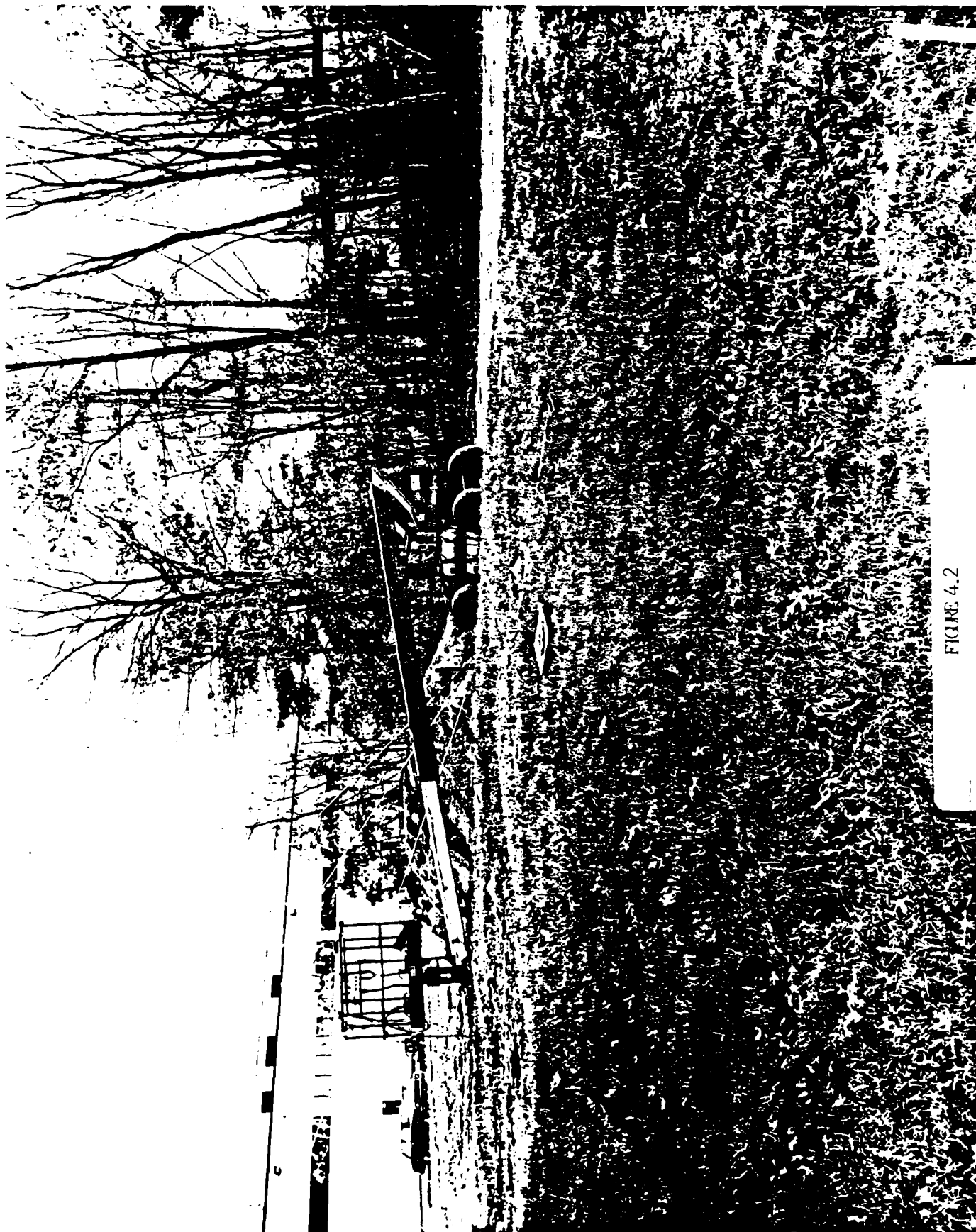


FIGURE 4.2

Cherry Picker Platform Used in Data Collection I

and metallic training mines provided by BRDEC. Theses were approximately 12 inches in diameter by 3 inches high. The metallic simulates were round in shape while the plastic ones were square. Figure 4.3 shows the plastic and metallic mines in a typical New England grassy background in the November-December time frame. Appendix B presents of the data extracted and digitized from this initial data collection. The remainder of this data is presented in Section 5 of this report, Algorithm Development.

In general the quality of the data was fair. The visible data was good. The active laser range data was also good, however, the amount of information in the data that would allow one to discriminate between mines and clutter in a range-only mode is still questionable. There were problems encountered in the recording of the passive IR data that rendered some of this data as unusable. The problems were associated with inappropriate gain settings, 60 Hz "pick-up" noise, and poor TV synch. This resulted in some of the data being "washed out" and non-compatible with frame grabber/data digitizing hardware and software.

In summary, useful data was collected for 6 different mine conditions and 25 different clutter regions in this first data collection exercise.

4.4 Data collection II

A second multi-sensor data collection activity took place at Stockbridge, New York in early June using TDS's 3 million dollar capital asset, our airborne multi-sensor testbed. (Figure 4.4) This helicopter-borne platform includes boresighted 3-5 μ m, 8-12 μ m, high resolution visible and 35 GHZ MMW sensors mounted on a two-axis actively stabilized gimbal. (Figure 4.5). Appendix C contains a detailed description of the TDS testbed sensors and stabilized platform characteristics. The helicopter was flown at a 40 foot altitude and 60 degree depression angle (yielding a 50 foot slant range) over a linear laydown of mine simulants.

The simulants included the 3", 6", and 12" circular plastic mine simulants provided by INEL, as well as the 6-12" mine simulants (3 plastic square, 3 metallic round) originally provided by BRDEC. The intermine spacing was approximately 30 feet. Four of the mines were located out in the open in a mowed grass runway area, one was on the



FIGURE 4.3
Mires in Typical Clutter for Data Collection 1

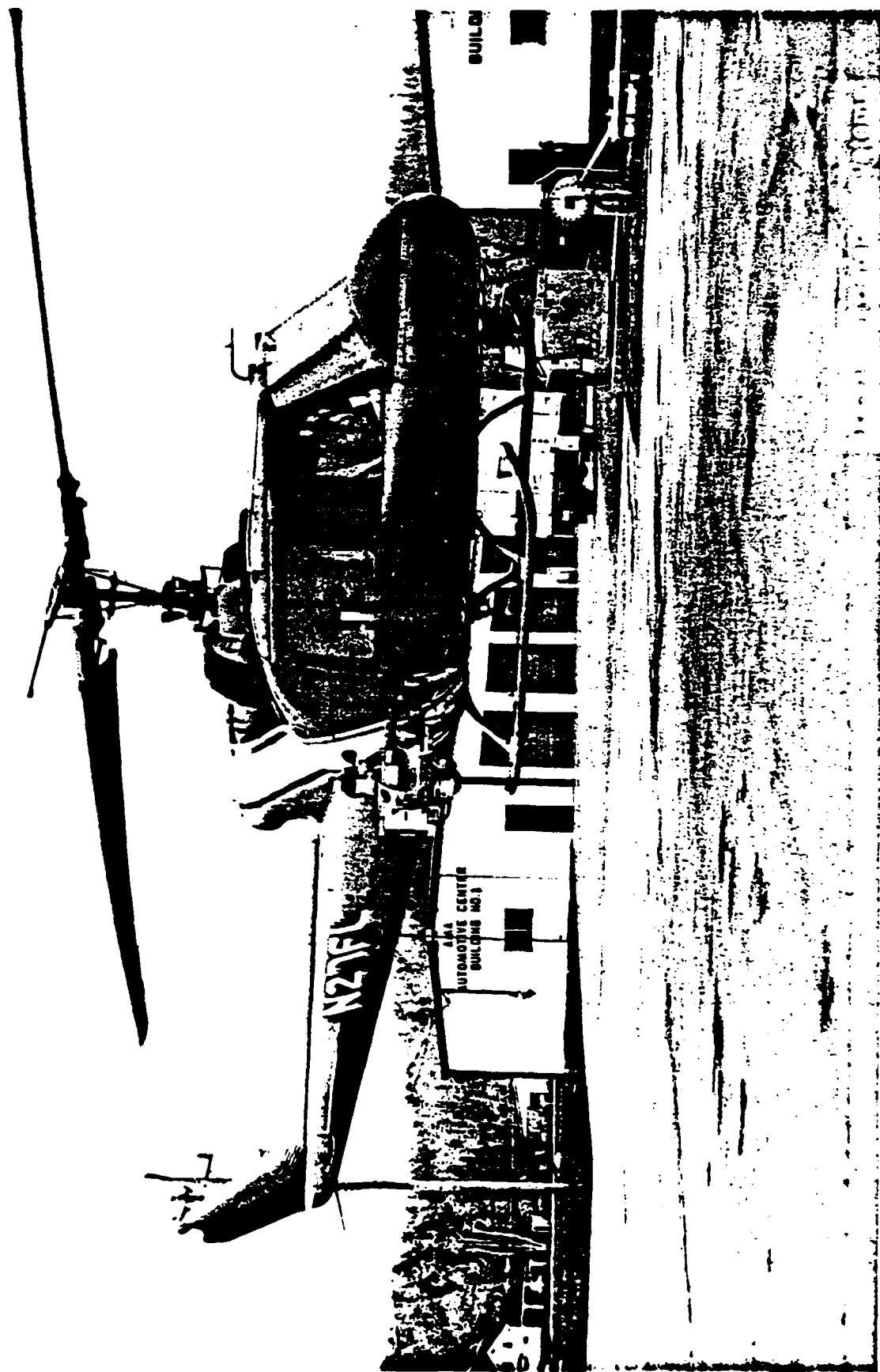


FIGURE 4.4 Collection 2
Airborne Tested Mounted on Helicopter for Data

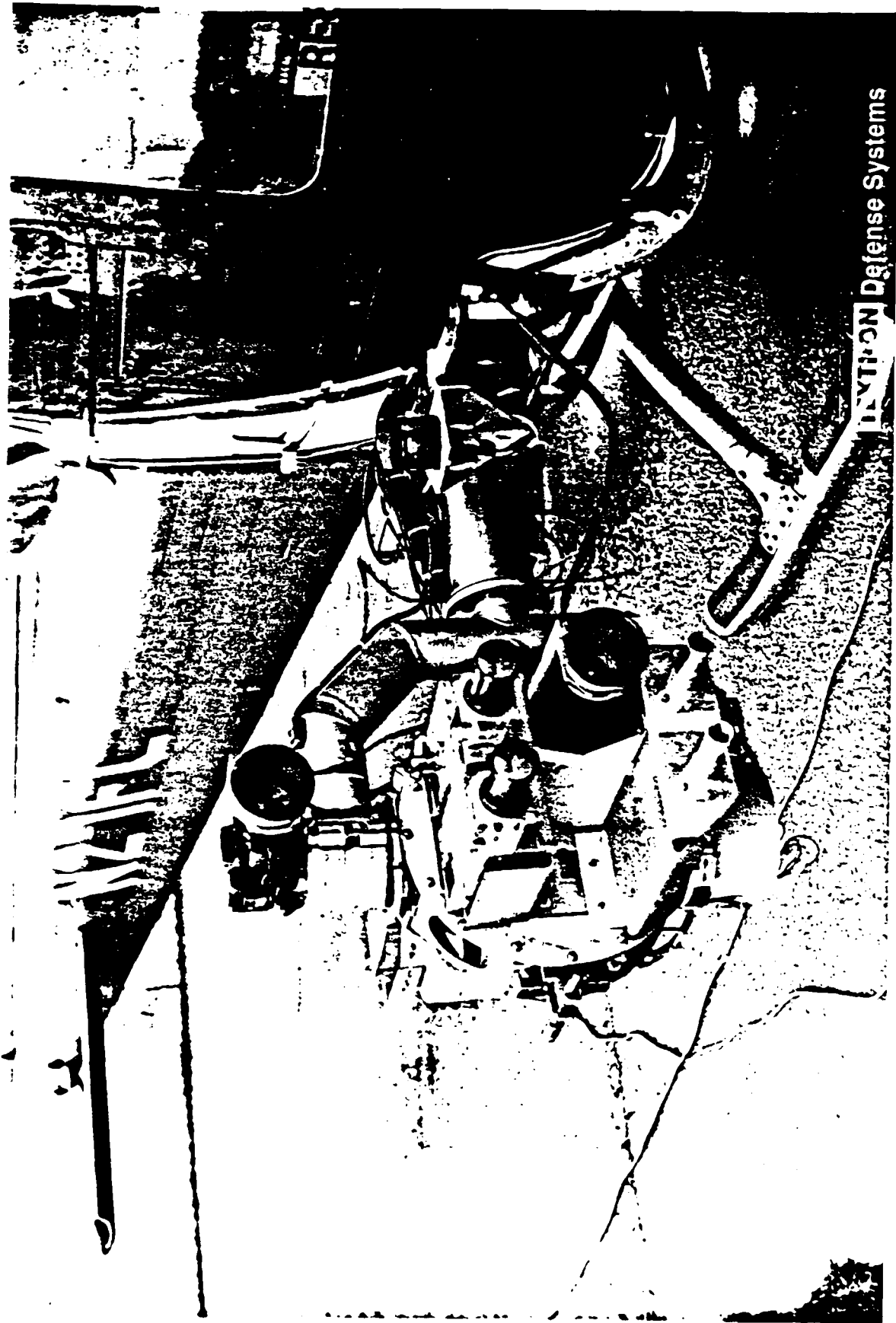


FIGURE 4.5

Close-Up of Airborne Multi-Sensor Test Bed
Single Sensor (High Level) Feature Fusion

border between the mowed area and a tall grassy region, and the remaining four were emplaced in the tall grassy areas. The data collected during this activity is presented and discussed in the following section (Section 5, Algorithm Development).

In a separate activity TDS's active laser rangefinder was used to collect additional mine and background signature data against the same 9 mine simulates as above. The tests were conducted from an 85 foot tower at TDS's Ballistic Test Facility on Cape Cod, MA and used to demonstrate the real time implementation of our neural transform signal processing approach. Schedule and cost constraints prevented the integration of this sensor onto the multi-sensor airborne testbed during this phase of the program, however, this effort is recommended for a follow-on program. This data will be discussed and presented in Section 6 of this report- Real Time Processor Development.

5.0 ALGORITHM DEVELOPMENT

The algorithm development task was divided into two sub-tasks: the detection of mines themselves and the detection of groups of mines comprising a minefield. The final determinant of whether an observed set of mine detections is or is not a minefield rests upon how well the detections fits a set of such criteria considered to be representative of a minefield.

Mine detection focuses upon both extracting information from the various modes of sensor data, either singly or in combination, and combining such information in a manner to optimally determine the potential existence of mines. That is, fusion may occur both at the data level prior to information extraction and at the information level after such extraction. In addition, any other available pertinent information may be applied to adapt the processing in ways appropriate to specific conditions. Such auxiliary information may be supplied from external sources or derived from other processes within the system.

Minefields are of two general types: hand/machine emplaced and scattered. Hand or machine emplaced minefields are laid down in regular patterns both for the sake of maximum complete coverage and to be better able to retrieve the mines. The patterns are a matter of doctrine and may sometimes be predefined according to specially supplied tape measures. Such a minefield may, for example, consist of several segments of two rows of approximately 50 mines each spaced about 15 feet apart. Anti-vehicle minefields may have associated anti-personnel minefields to prevent removal by opposing forces.

Never scattered minefields are deliverable by dropping from any of several airborne platforms. Hence they will exhibit a reasonably random distribution of mines. They may nevertheless be detectable on the basis of appearing in denser clusters than is typical of false alarms, being comprised of a very specific number of mines and/or exhibiting a detectable overall shape or orientation. In combination, such features may suffice to discriminate scattered minefields from naturally scattered false alarms.

5.1 Objective

The objective of the algorithm development effort for the Mine and Minefield Detection program is to apply multi-sensor data fusion to:

- 1) Improve individual mine detection
- 2) Reduce individual false alarms
- 3) Improve minefield detection
- 4) Reduce minefield false alarms

Single sensor systems, with dominant sensor features, are sensitive to the availability of those features over all conditions as well as the probability of those features being observed from non-mines (i.e. false alarms). Combining multiple single sensors (each with dominant features) and decision logic reduces false alarms. However, detection remains sensitive to the availability of individual dominant sensor features.

Multi-sensor data fusion appears to be less sensitive to dominant individual features and also reduces false alarms.

5.2 Approach

There are four questions that were considered in designing the mine detection system :

- 1) What physical measurements can be taken that will determine that a mine is present ?

These measurements, including size, shape, spectrum, texture, contrast, symmetry, absorption, reflection, structure, chemical content etc have been considered for mine detection by TDS and/or other program contractors during the course of this program.

- 2) What sensors can be used to obtain these physical measurements?

Under this program, a number of sensors that can measure these features have been identified including passive infra-red detectors, ultra-violet detectors, laser, radar, nuclear detectors, pulse induction, magnetometers, acoustic vibrometers and others

- 3) How are these measurements represented in terms of features, preferably invariant ?

3) How are these measurements represented in terms of features, preferably invariant ?

Under this program, TDS has investigated several ways of representing this data as defined by three major feature categories:

- 1) High Level Processed Features
- 2) Low Level Processed Features
- 3) Unprocessed Features (i.e.raw data)

These categories are defined in detail in the following sections.

4) What processing architecture should be used to implement an algorithm for real time detection based on these features ?

TDS investigated the application of Neural Network technology combined with elements of more conventional statistical signal and image processing to determine a processing architecture.

5.3 Results

5.3.1 AMIDARS Data

Figures 5.1 shows examples of AMIDARS data (single color, passive infra-red) for adjacent frames. There is a string of mines in this data as well as a road going through the area. It is not obvious where the mines are located from these frames. Figure 5.2 shows the results of amplitude threshold processing of this data. As indicated in Figure 5.2, a histogram of the frame is generated and a threshold was set based on this histogram. Because the detected mines (i.e. above the threshold) are hard to see, Figure 5.3 displays the detections without the background. Note the large number of individual mine-like false alarms. The minefield is located at the top center of Figure 5.3. The detected mines appear along a straight line with approximately equal separation between mines (except where mines are not detected). However, a deterministic pattern may not always exist (i.e scatterable mines). This data reinforces the objectives for reduced false alarms and improved minefield detection. Under this program, TDS developed a multi-sensor technique to reduce individual false alarms and a minefield detection technique which is not dependent on specific lay-down patterns and can handle a large number of false alarms.

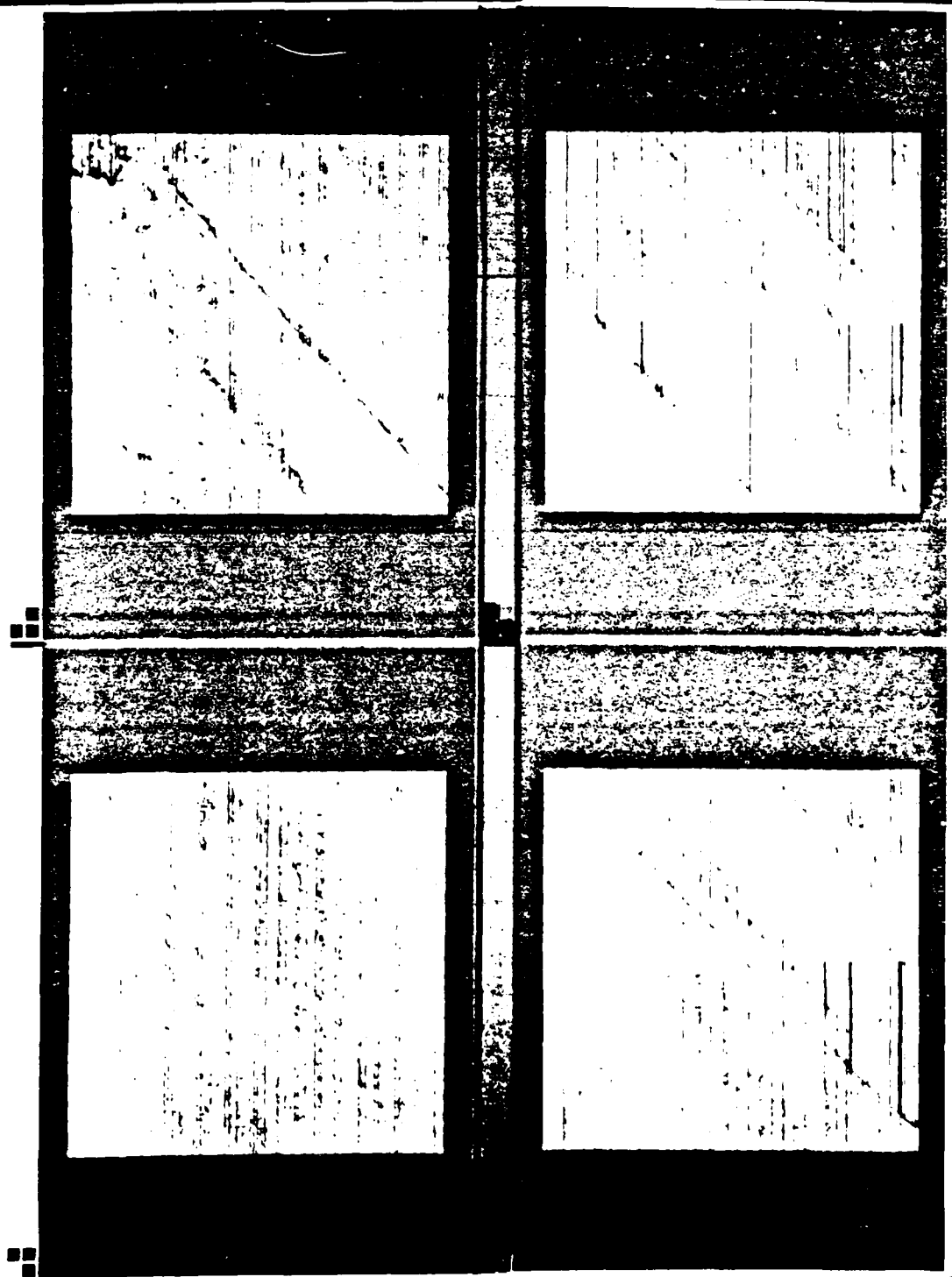


FIGURE 5.1
Typical Wallows Data

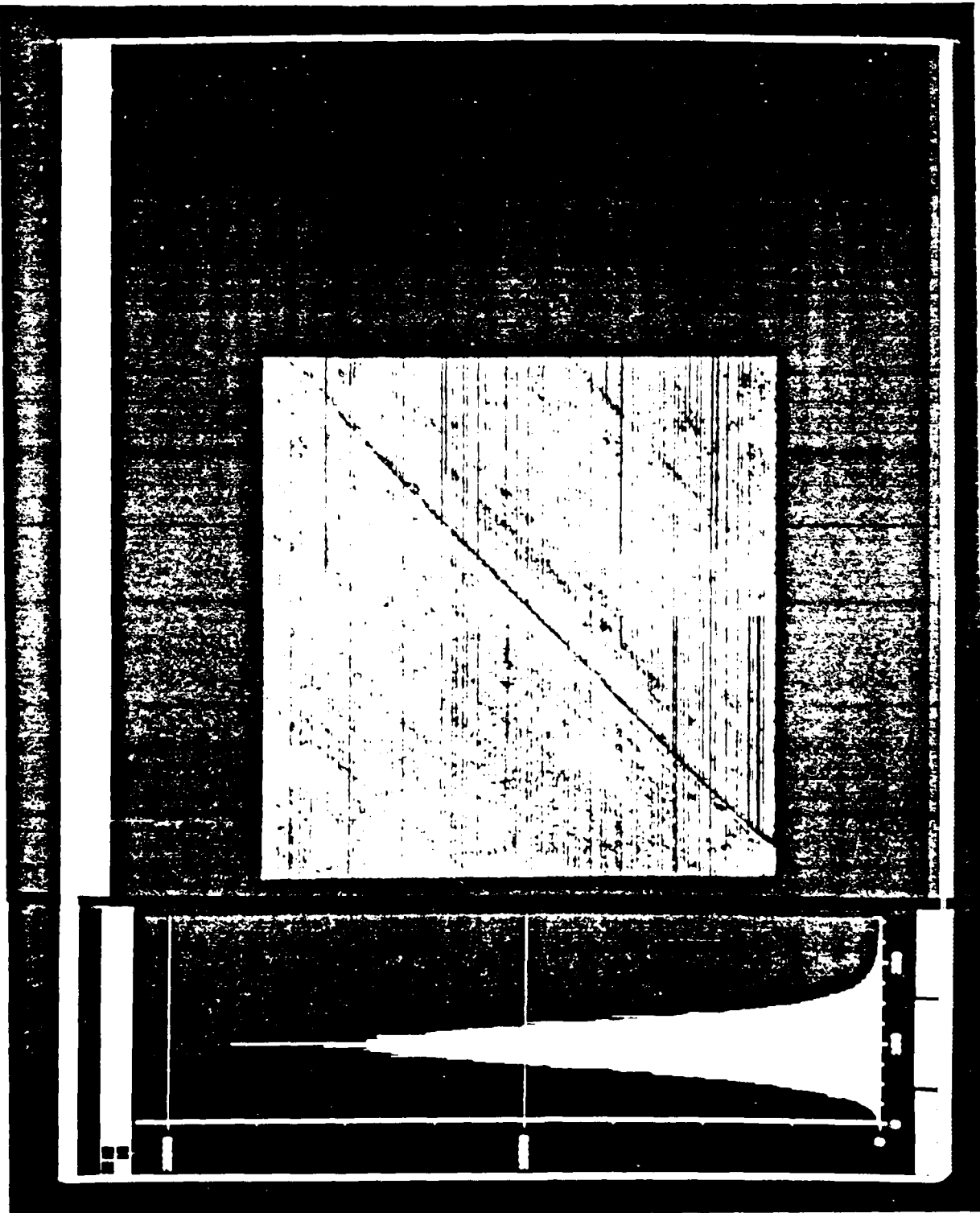


FIGURE 5.2
Amplitude Threshold Determination by Nitrogen Anal

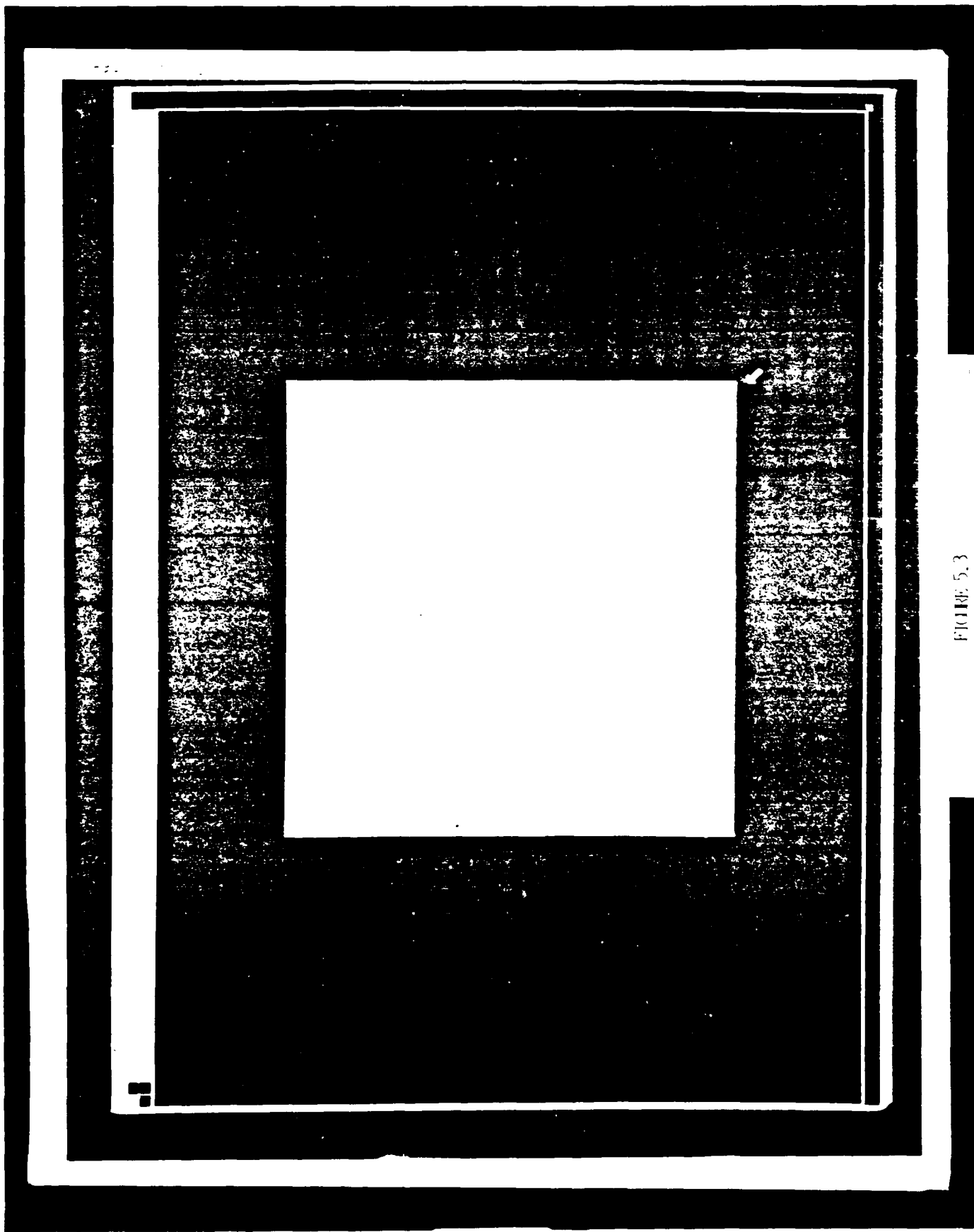


FIGURE 5.3
Detections Resulting From Amplitude Inversion

5.3.2 Mine Detection

As discussed previously, two sets of data collection were performed during this program. The first data collection used a sensor suite deployed on a cherry picker (figure 5.4). The cherry picker was deployed at a height of about 40 feet looking down at the mines at an angle of approximately 60 degrees. Visible and 8-12 micron passive IR data was obtained with two mines in the field-of-view (figure 5.5). The second data collection used the TDS multi-sensor airborne testbed described in the previous section.

5.3.2.1 Data Collection # 1

Data from the first first data collection activity was initially processed using High Level processed features. Various statistical, edge detection and segmentation routines were applied to the collected data. The statistics included: mean and maximum brightness within a mine sized region. standard deviation, kurtosis, and entropy. Another measure was auto correlation which measures the rotational symmetry within a region. Gradient , Sobel edge enhancement, and Burns edge detection techniques were applied.

The results of these investigations showed that the best discriminants were mean and maximum brightness and symmetry. Therefore moments of the intensity and gradient probability distributions were further investigated. By thresholding the passive IR imagery, it was determined that intensity was a reasonable IR feature to use. Moments (maximum, mean, and standard deviation) were generated from intensity histograms based on 12 x 12 pixel windows (1 foot x 1 foot) of the image. These windows overlapped by 75 % in both the horizontal and vertical directions. Based on thresholding, it was determined that intensity was not a good feature for the visible image. For the visible image, the gradient of the intensity (Figure 5.6) was determined to be a better feature than the raw intensity. Corresponding histograms and moments of the visible intensity gradient were therefore also generated .

A neural network was trained by giving samples of the moment features of mines and backgrounds from both the visible and passive IR

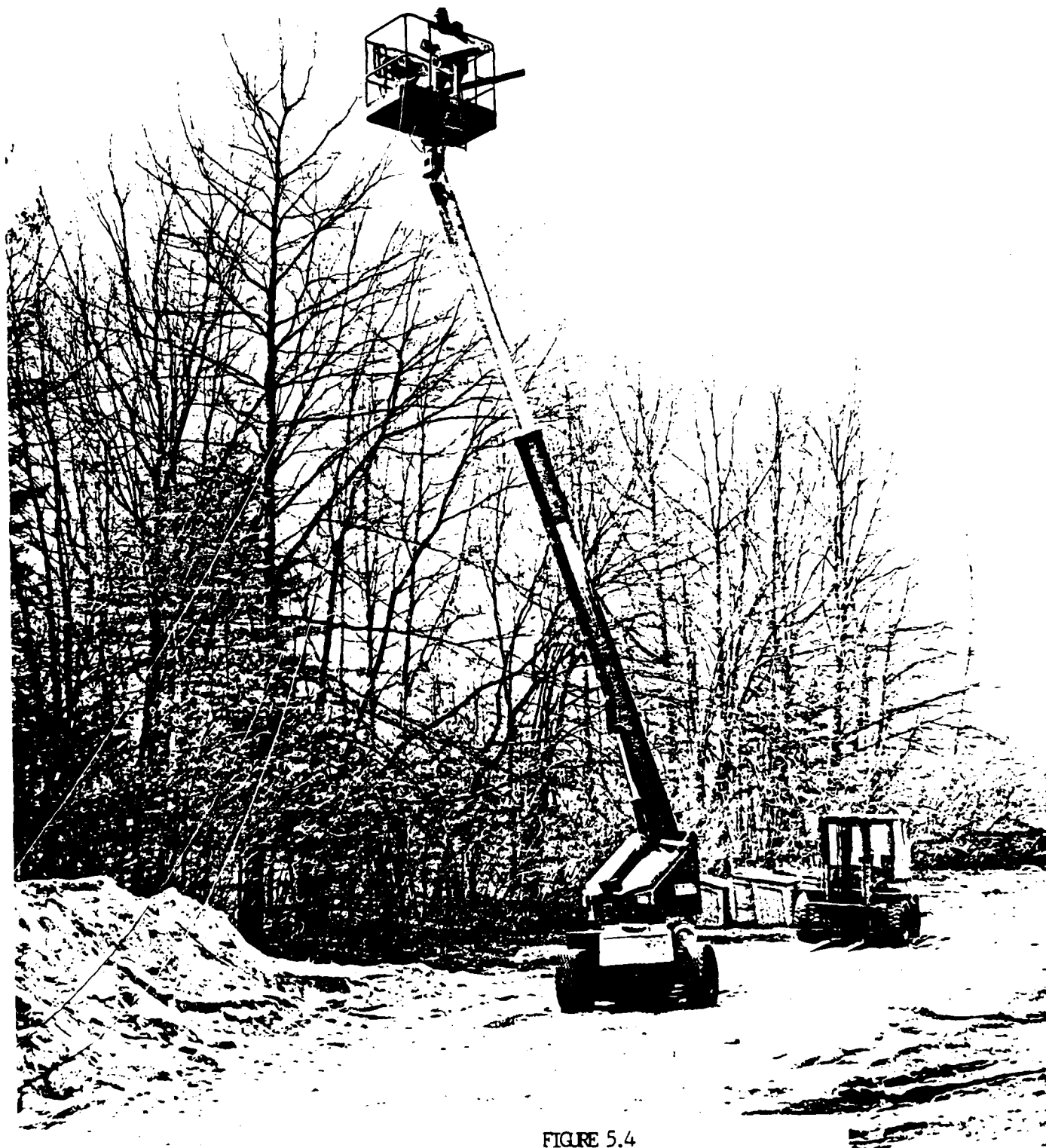
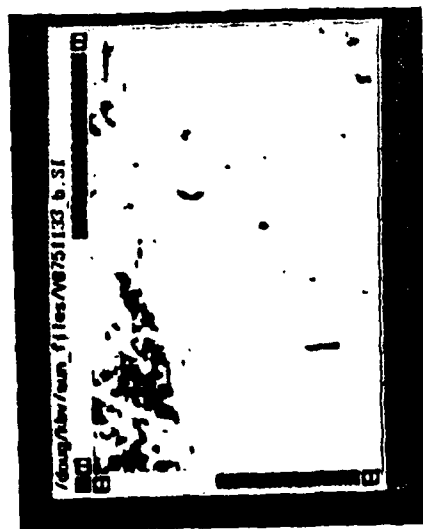


FIGURE 5.4
Set-Up for Data Collection 1

TEST # 1 - DATA FRAME # 1133 (WARM MINES)

VISIBLE



IR
(8 - 12)

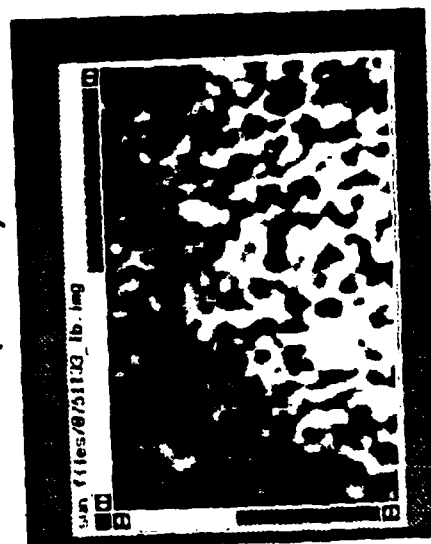


FIGURE 5.5

Typical Data from Data Collection 1 (IR Visible)

TEST # 1 - DATA FRAME # 1133 (WARM MINES)

VISIBLE

VISIBLE
GRADIENT

IR
(8 - 12)

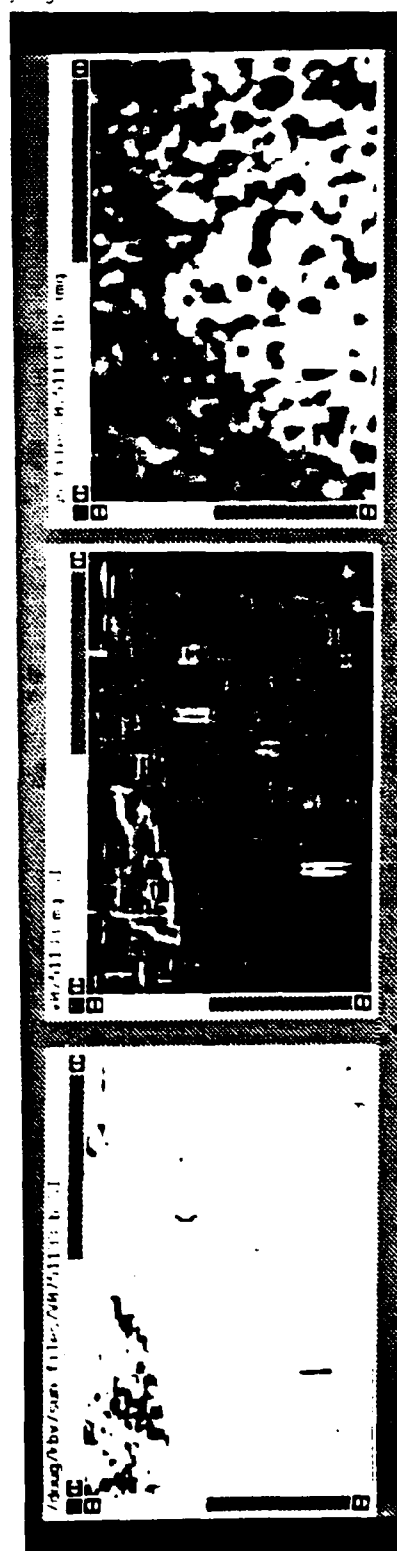


FIGURE 5.6
Gradient Processing of Visible Imagery Data

imagery (Figure 5.7). The neural network was trained with one set of data and then tested on another set of data. In the test set, a 12 x 12 window was moved from left to right over the image. Figure 5.8 shows the results of using these high level features with a trained neural network to detect mines using a single sensor. Both mines were detected by the visible sensor with a number of spatially different false alarms. Only one mine was detected by the passive IR sensor which also had a number of false alarms. The detection output from each sensor was then combined with decision logic based on the detection from each sensor and its associated confidence (Figure 5.9 - sensor/decision level fusion). By using a high confidence threshold in the decision logic, the first mine was detected; no false alarms were generated. By lowering the confidence threshold, the second mine was also detected still without any false alarms being generated (Figure 5.10). A second test case, where the mines were much cooler, generated the same results. The limitation of this approach is that voting relies on at least one of the two sensors to having dominant features which result in a mine detection a high confidence.

Under many conditions (high clutter, high atmospheric attenuation due to weather or battlefield obscurants, partial occlusion of the target signature, etc.) the dominant features from a given sensor may be greatly eroded. Therefore, a number of sensors/features may be needed, each providing a piece of information, however, none providing a high confidence detection by itself. To fuse this data, fusion would have to occur at a lower level than the decision level example above. Several approaches for feature fusion were considered with the goal of obtaining the same level (or better) of performance (i.e. detect both mines with no false alarms) as the decision level fusion. In the first approach, the same moment data was input as a single vector to train the neural net (Figure 5.11). The results, using the same data as above, were that the first mine was detected with no false alarms, and when the threshold was lowered, the second mine was detected, however, there were also some false alarms (Figure 5.12) . The next approach considered used the raw pixel data directly (scaled to the minimum and maximum values) to train the neural network (Figure 5.13). Again, the same data was used as a baseline. In this case, when each sensor was run separately, both mines were detected but with substantial false alarms (Figure 5.14). By fusing the

SINGLE SENSOR FEATURE FUSION (HIGH LEVEL)

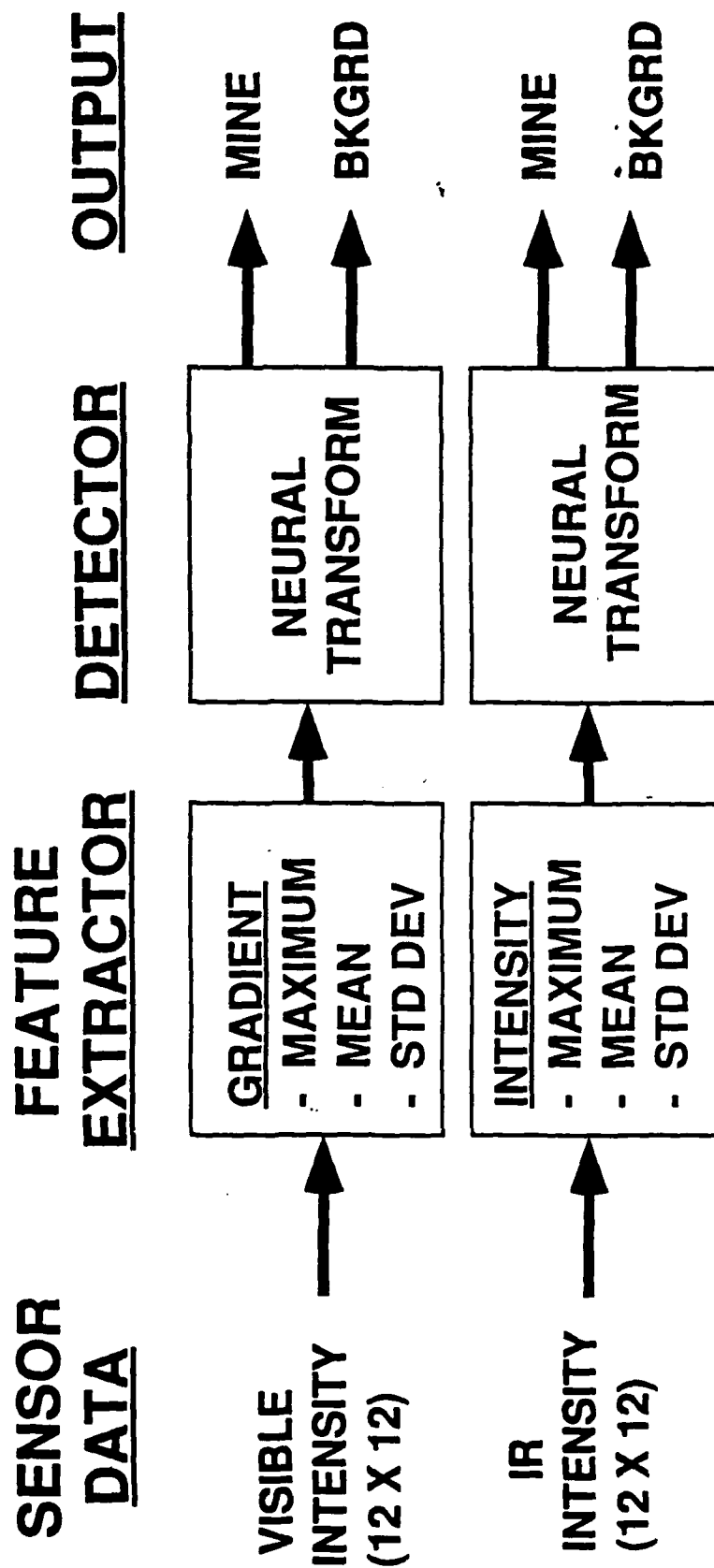


FIGURE 5.7

Single Sensor (High Level) Feature Fusion

TEST #1

SINGLE SENSOR DETECTION FEATURE FUSION (HIGH LEVEL)

FRAME # 1133

VISIBLE

IR
(8 - 12)

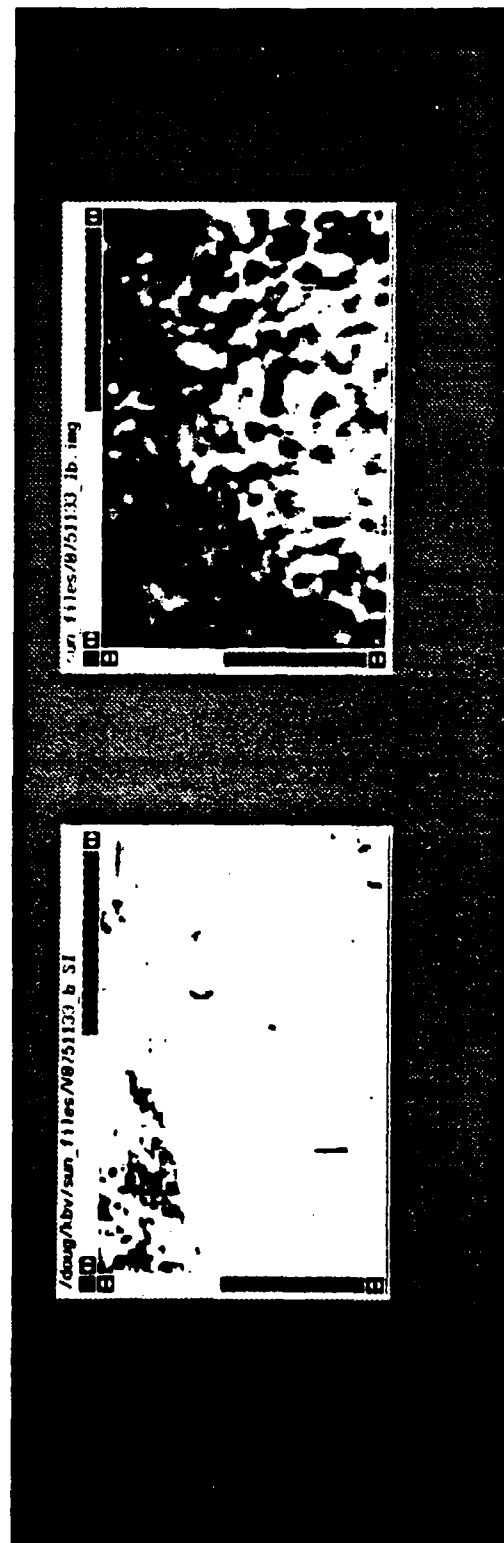


FIGURE 5.8
Results of Single Sensor (High Level) Feature Fus.

MULTI-SENSOR DECISION LEVEL FUSION (HIGH LEVEL FEATURES)

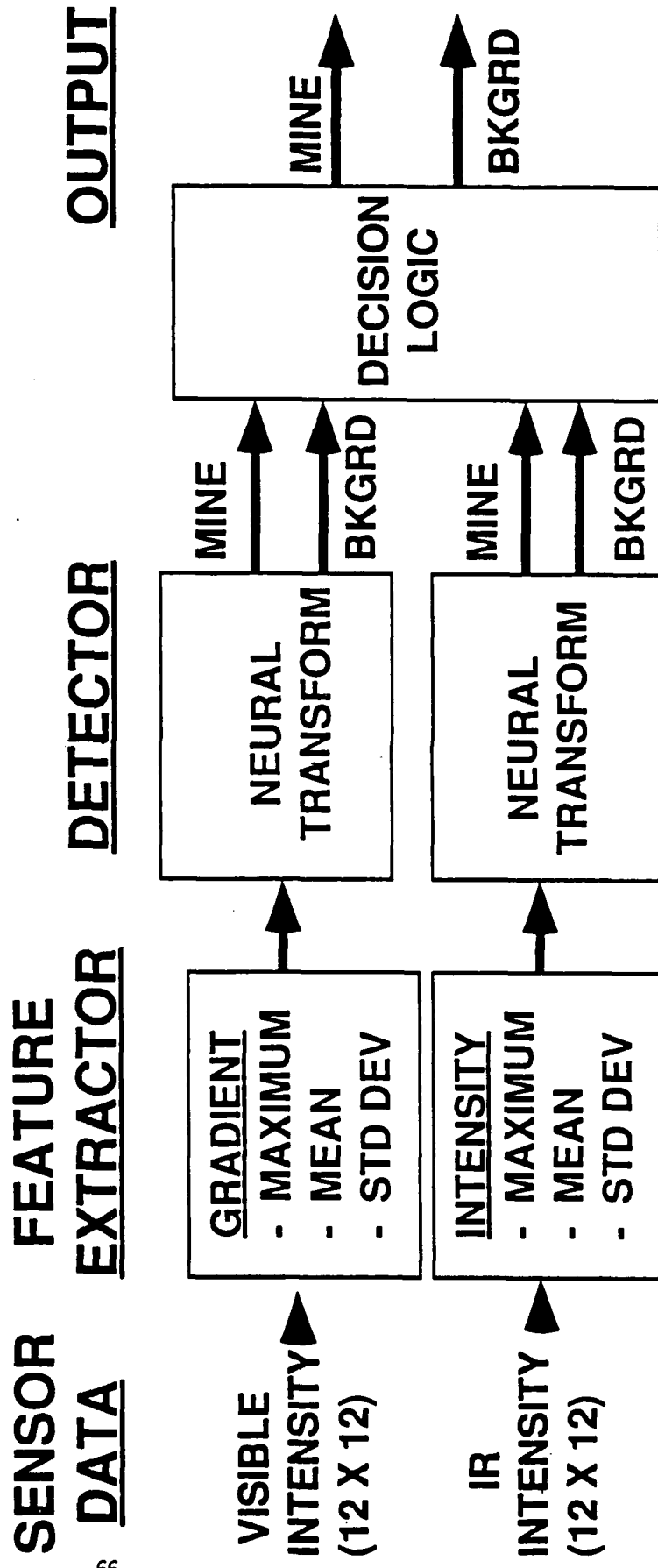


FIGURE 5.9

Multi-Sensor Decision Level Fusion (High Level Features)

TEST #1

MULTI-SENSOR DETECTION DECISION LEVEL FUSION

FRAME # 1133

THRESHOLD
HIGH

THRESHOLD
LOWER

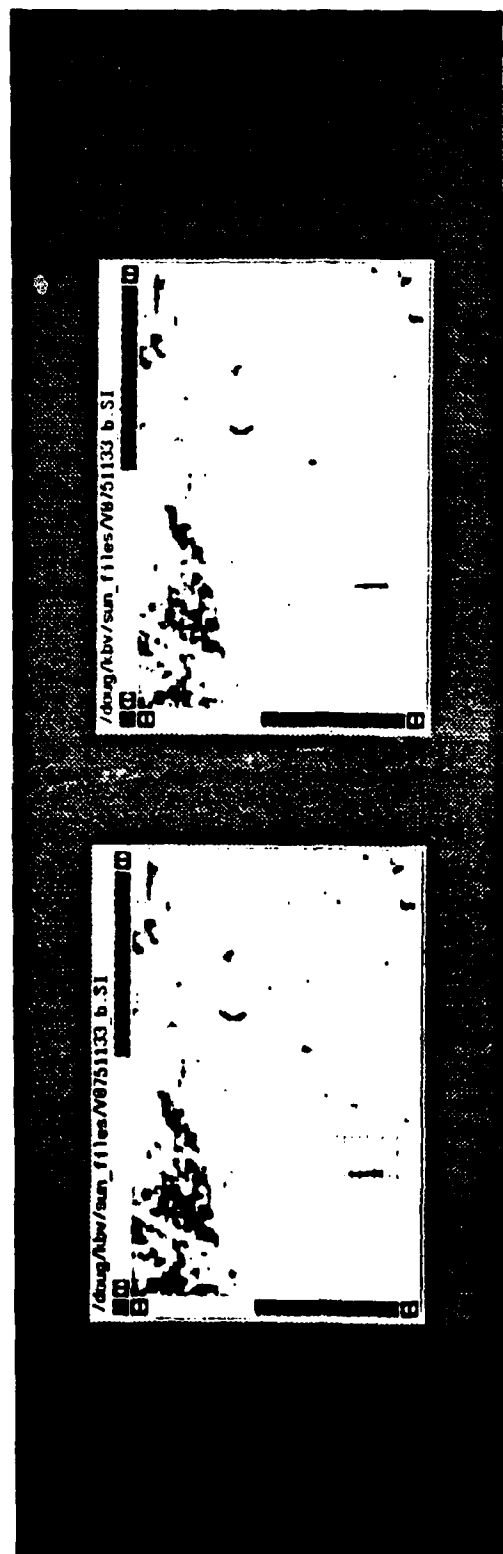


FIGURE 5.10

Results of Multi-Sensor Decision Level Fusion

MULTI - SENSOR FEATURE FUSION (HIGH LEVEL)

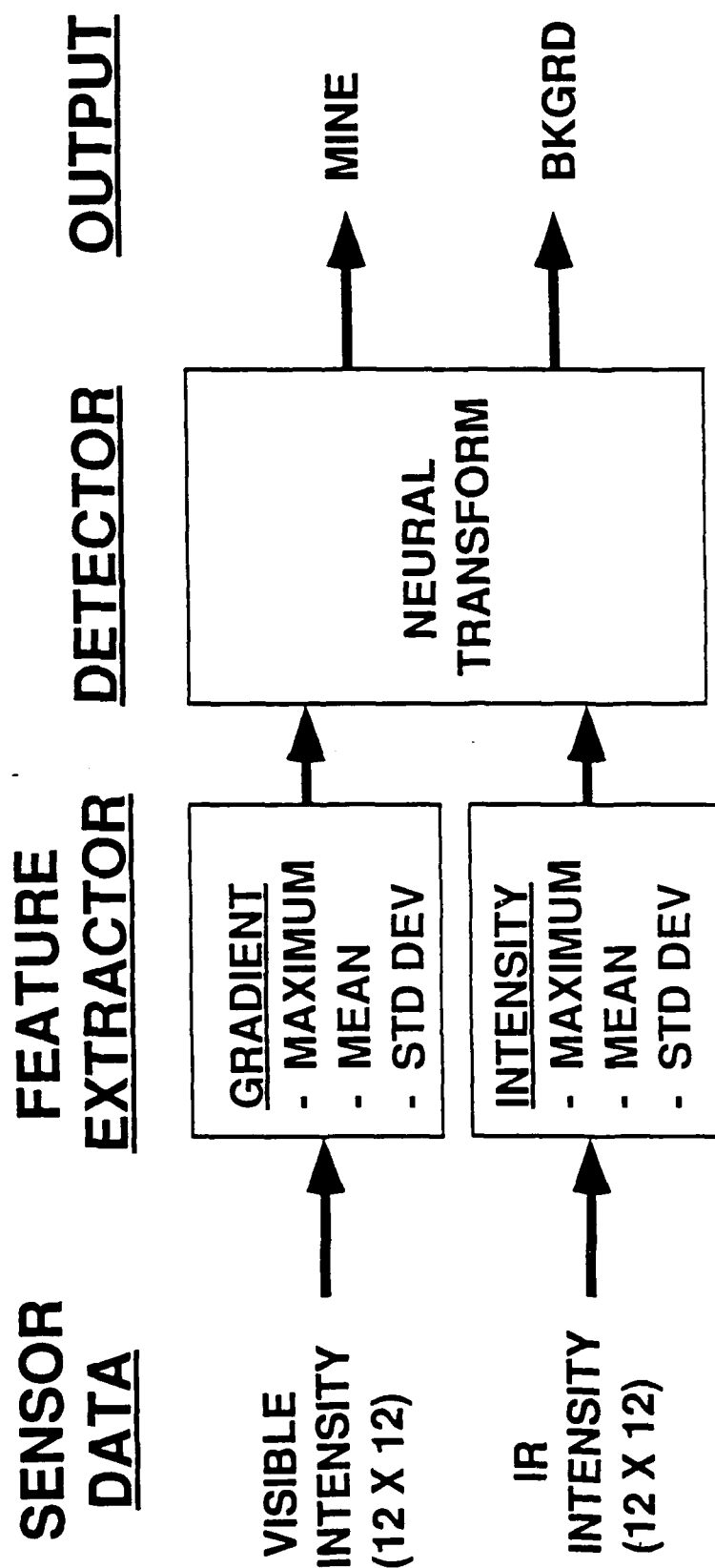


FIGURE 5.11

Multi-Sensor (High Level) Feature Fusion

TEST #1

MULTI-SENSOR DETECTION FEATURE FUSION (HIGH LEVEL)

FRAME # 1133

THRESHOLD
HIGH

THRESHOLD
LOWER

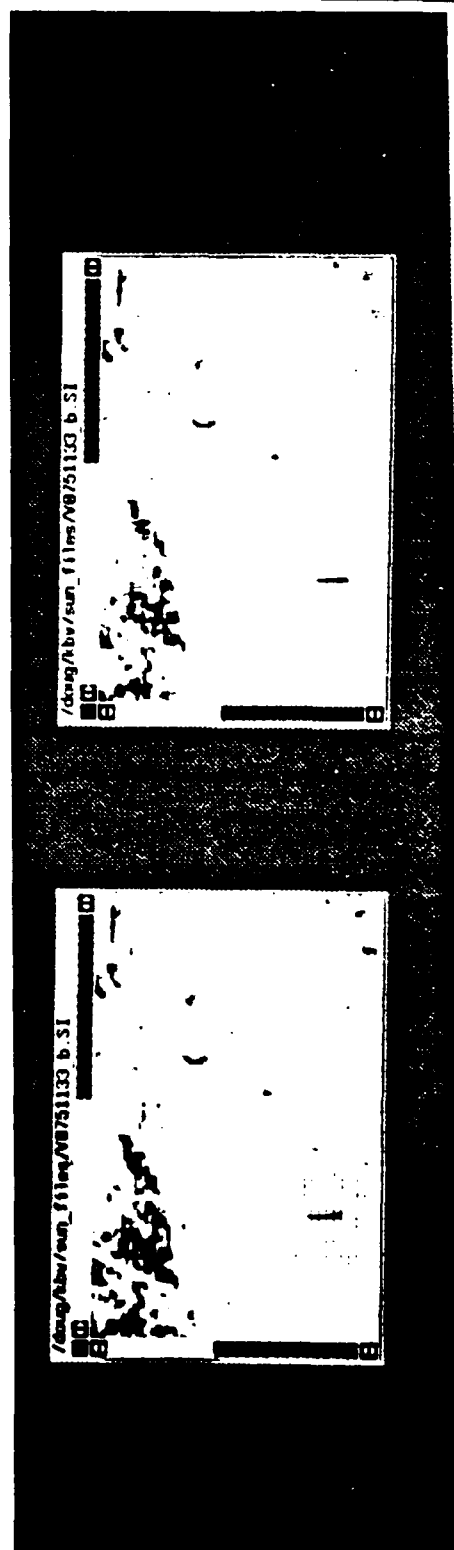


FIGURE 5.12

Results of Multi-Sensor (High Level) Feature Fus.

SINGLE SENSOR DATA FUSION

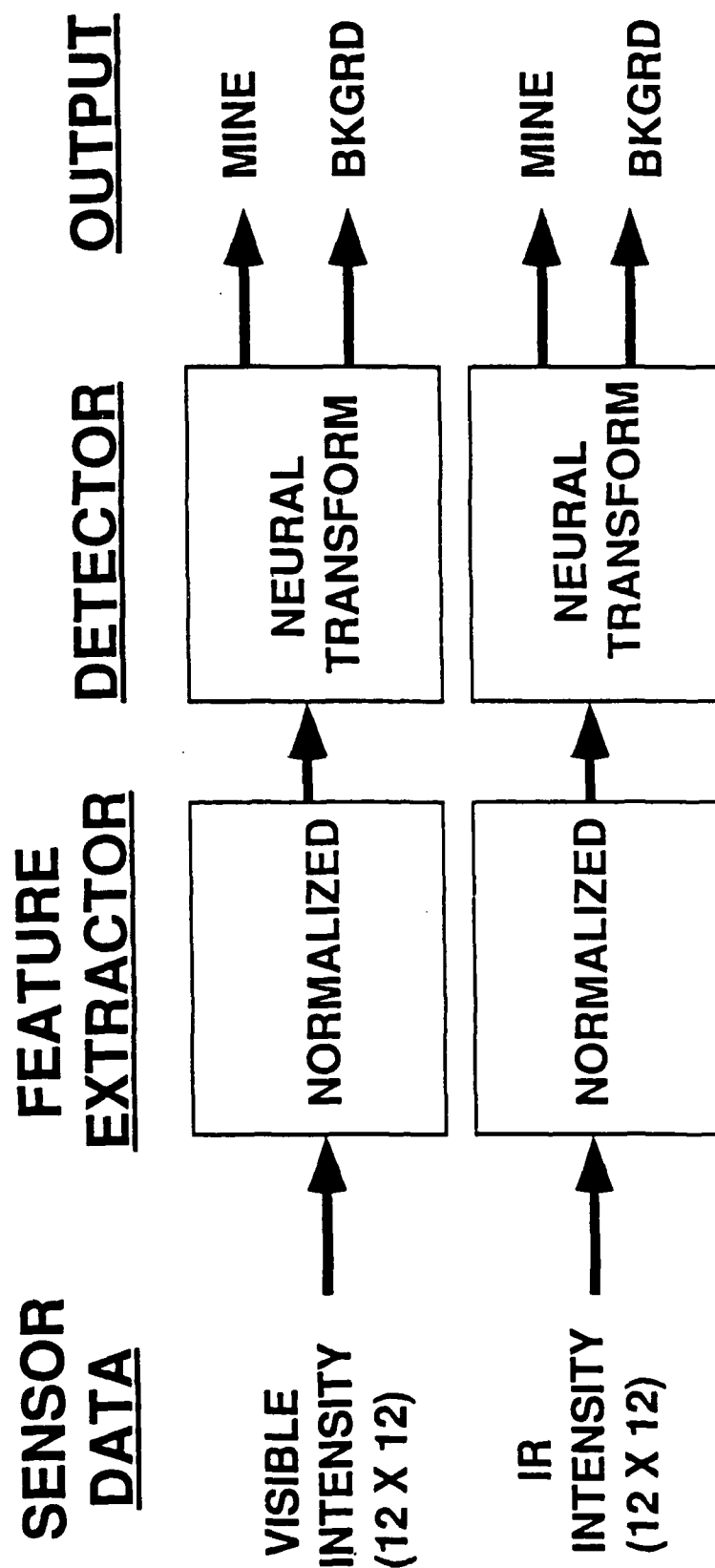


FIGURE 5.13

Single Sensor Data Fusion

TEST #1

SINGLE SENSOR DETECTION

NORMALIZED DATA

FRAME # 1133

VISIBLE

IR
(8 - 12)

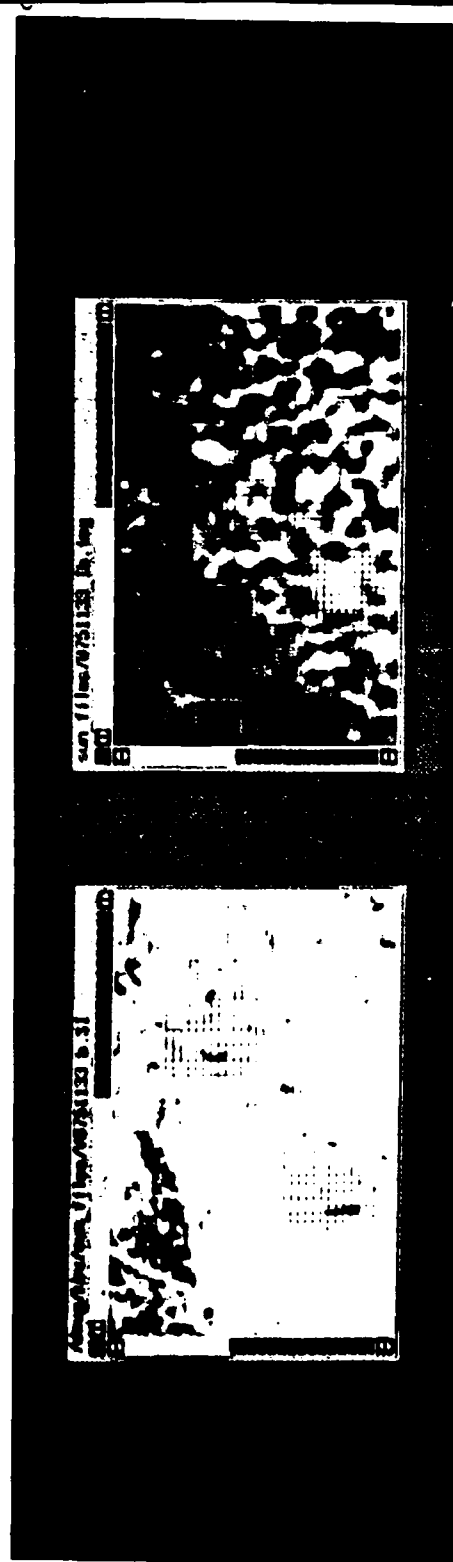


FIGURE 5.14
Results of Single Sensor Raw Data Fusion

raw data (Figure 5.15), both mines were still detected and the number of false alarms were greatly reduced (Figure 5.16). However, the performance was not as good as with the decision logic (i.e. no false alarms).

The third approach used the raw histograms of the IR intensity and the visible gradient to train the neural network. The results were similar to using the raw data directly. Both mines were detected and the number of false alarms were reduced, however, the performance was still not as good as with the decision logic. The fourth approach applied a two dimensional FFT to the IR and visible data window and integrated over spatial frequency bands and over spatial orientations, using ring and wedge integration techniques, to maintain the spatial relationships that were lost using the histograms. Simulated examples of the two dimensional FFT for a square and round mine are illustrated in Figures 5.17 and 5.18. For the single sensor case (Figure 5.19), the visible sensor detected both mines with no false alarms and the passive IR sensor detected both mines with few false alarms (Figure 5.20). When the data is fused (Figure 5.21), both mines are detected with no false alarms (Figure 5.22). Thus, the performance using the two dimensional FFT with ring and wedge integrators is equivalent to the performance using decision logic. TDS believes that this level of data fusion is less sensitive to high confidence detections by a single sensor, however, more statistical data is required to prove this point.

5.3.2.2 Data Collection # 2

The next set of mine detection/false alarm tests (Data Collection #2) were run using the TDS multi-sensor airborne testbed (ABTB). As discussed in the previous section and illustrated in Figure 5.23, the ABTB consists of two IR imaging radiometers (3-5 micron and 8-12 micron), a 35 GHz FMCW millimeter wave radar, and wide and narrow field of view digital CCD video cameras. The platform is motion compensated and there is a Mini-Ranger to determine position. Figures 5.24 - 5.26 show examples of the data from the sensors on the ABTB for a 12 inch square plastic mine, a twelve inch circular metal mine and a twelve inch circular plastic mine respectively. All three mines were in the open and were used as training data for the neural network. The two dimensional FFT with ring

MULTI - SENSOR DATA FUSION

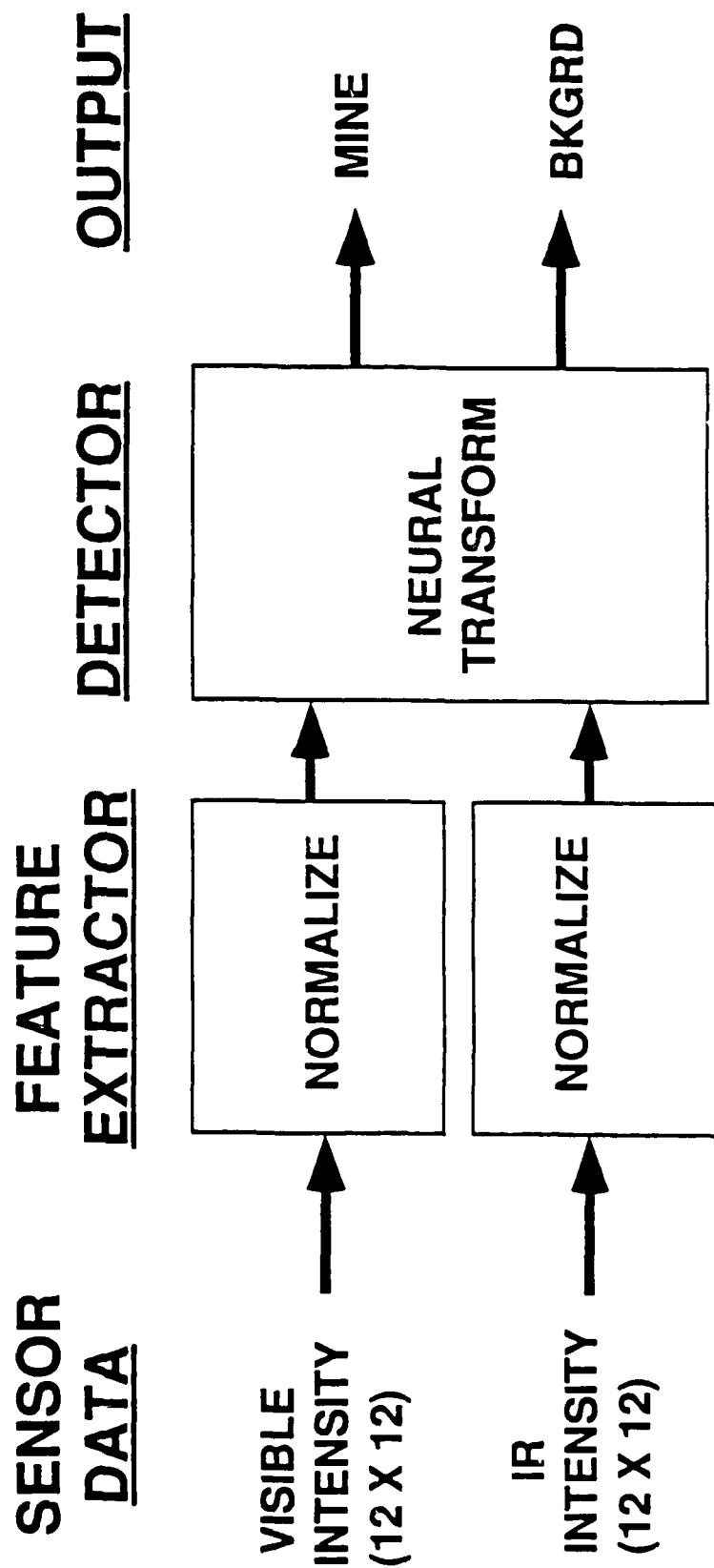


FIGURE 5.15

Multi-Sensor Data Fusion

TEST #1

MULTI-SENSOR DETECTION

DATA FUSION

FRAME # 1133

VISIBLE

IR
(8 - 12)

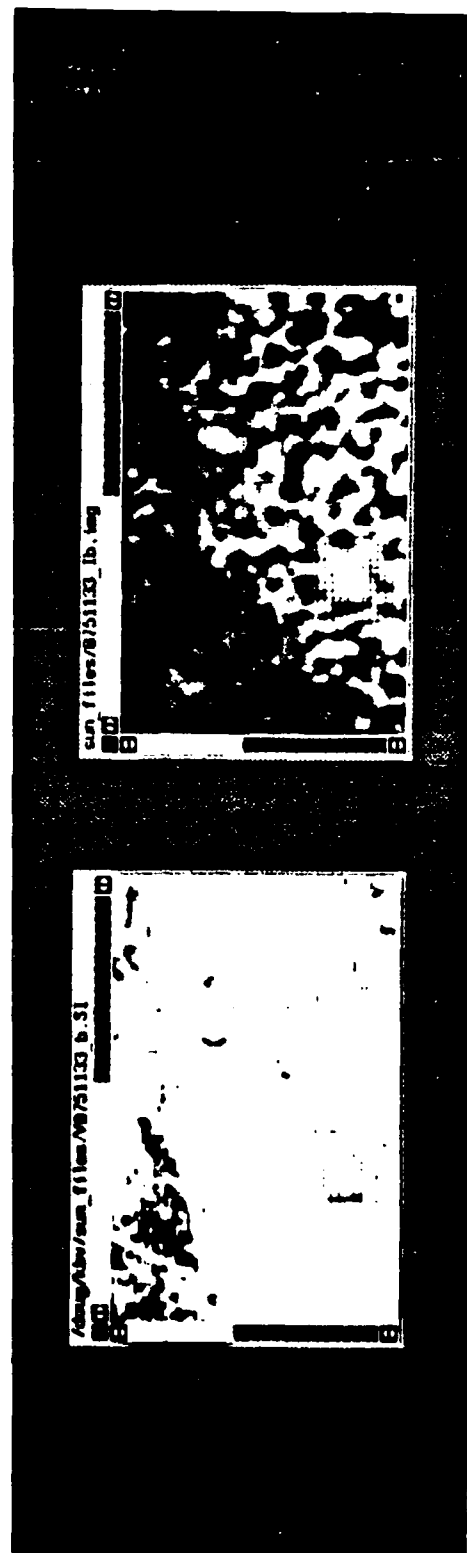


FIGURE 5.16
Results of Multi-Sensor Data Fusion

2-D FFT MODEL DATA

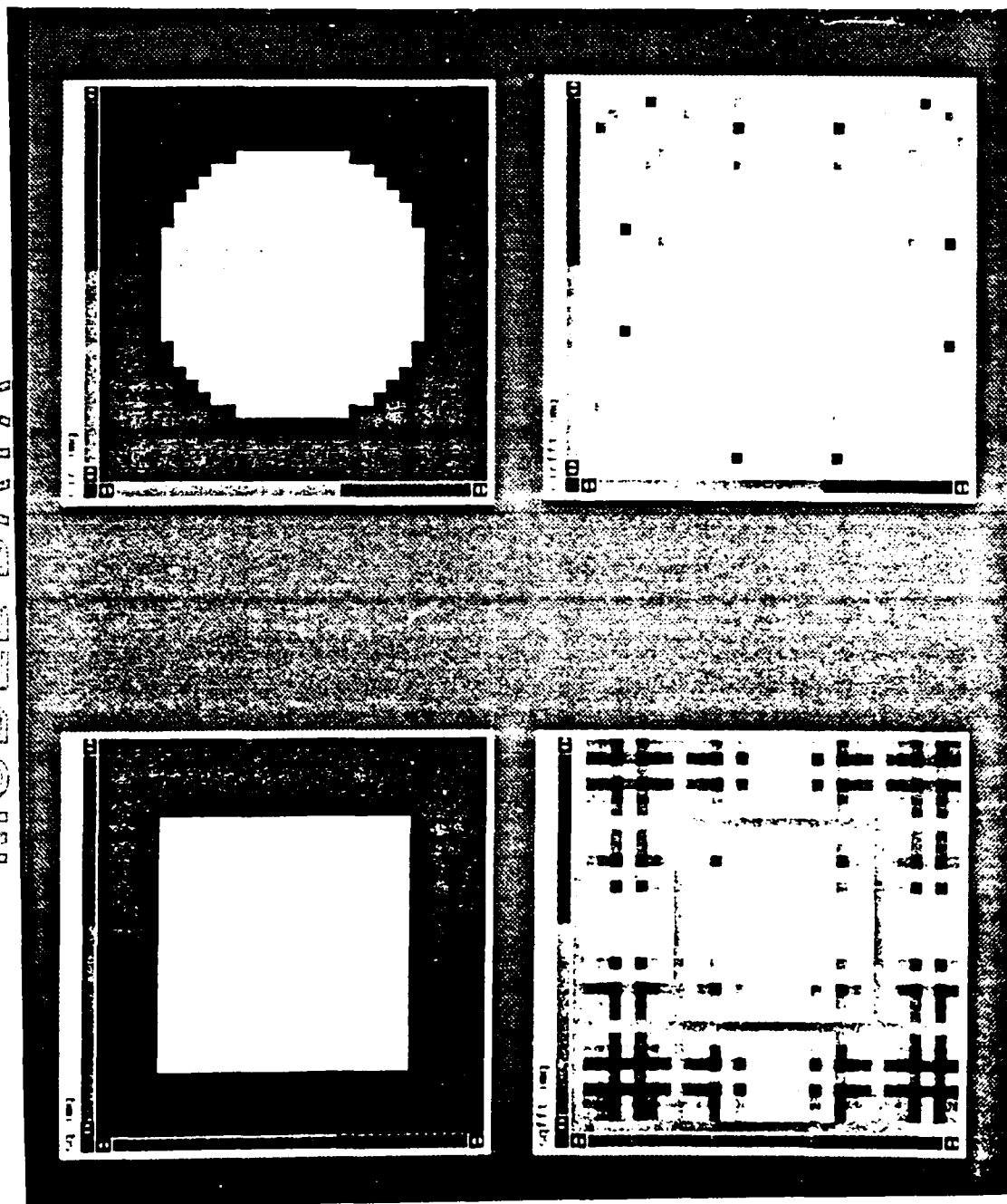


FIGURE 5.17
2-D FFT of Simple Solid Mine Models

2-D FFT MODEL DATA

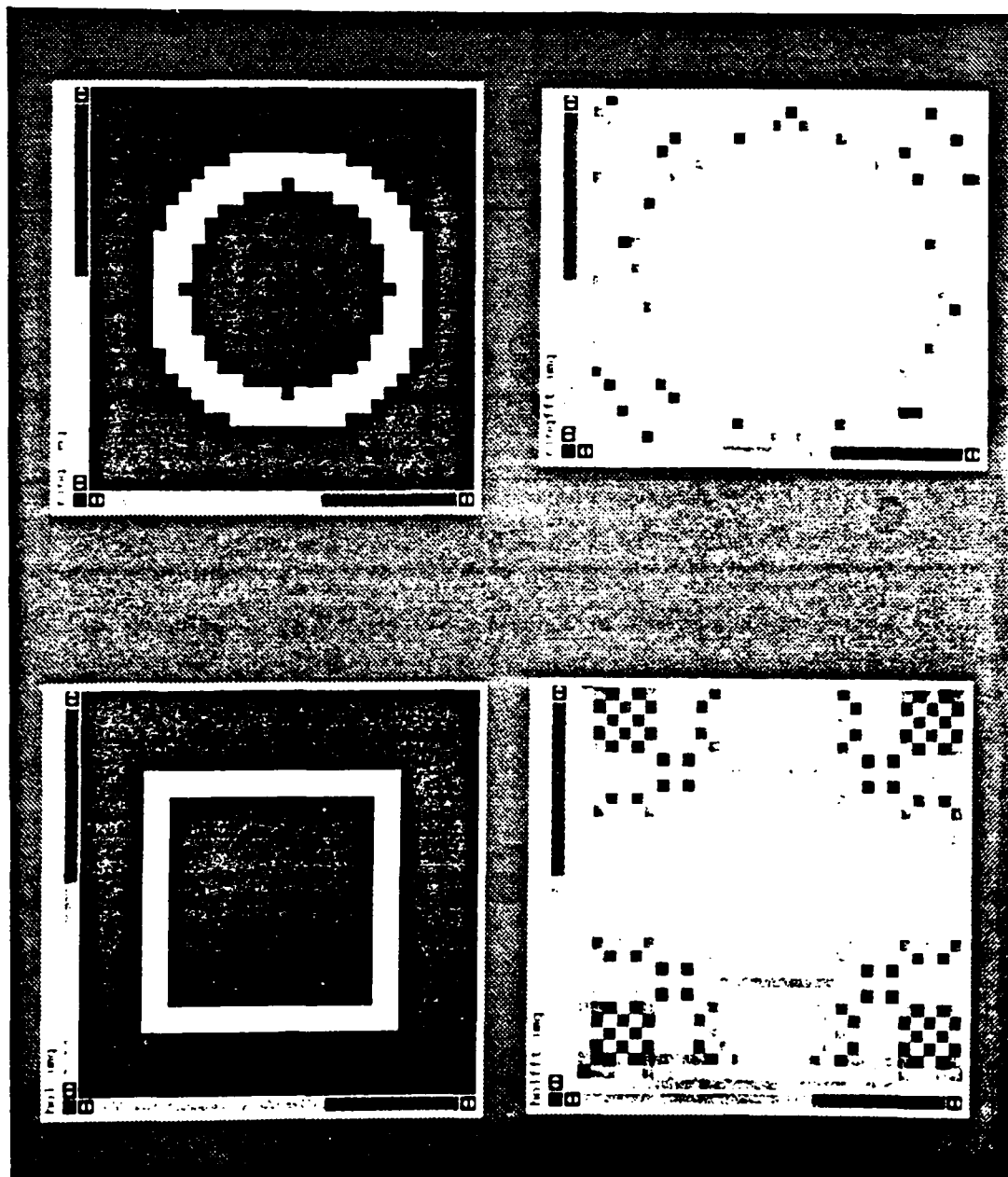


FIGURE 5.18
2-D FFT of Simple Edge Models of Mines

SINGLE SENSOR FEATURE FUSION (LOW LEVEL)

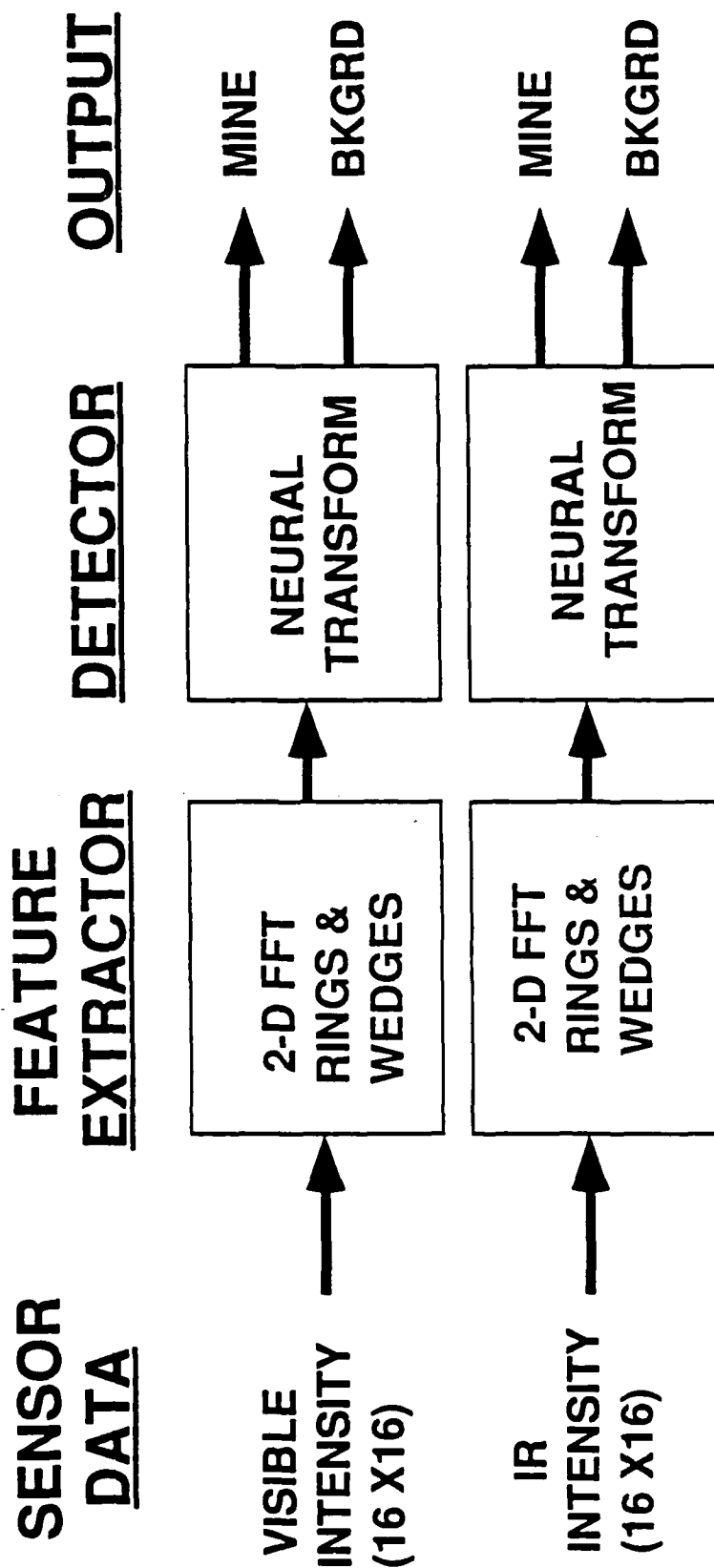


FIGURE 5.19
Single Sensor (Low Level) Feature Fusion

TEST # 1

SINGLE SENSOR DETECTION FEATURE FUSION (LOW LEVEL)

FRAME # 1133

VISIBLE

IR
(8 - 12)

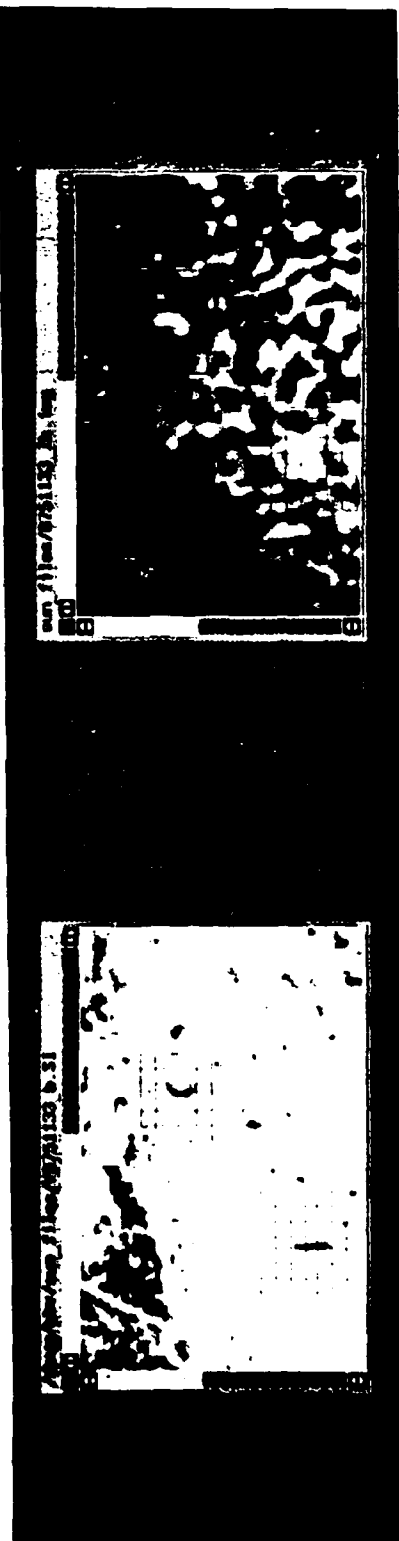


FIGURE 5.20

Results of Single Sensor (Low Level) Feature Fusion

MULTI - SENSOR FEATURE FUSION (LOW LEVEL)

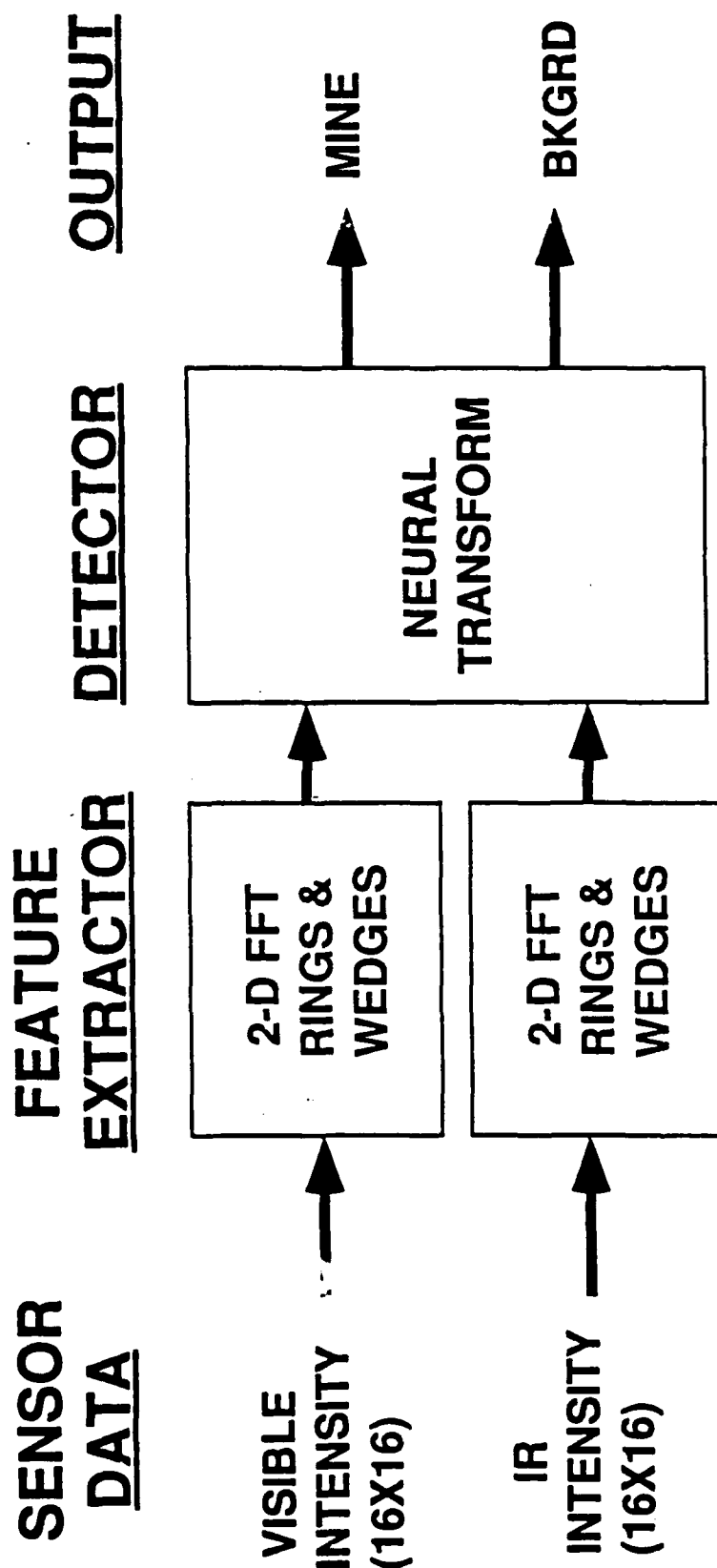


FIGURE 5.21

Multi-Sensor (Low Level) Feature Fusion

TEST #1
MULTI-SENSOR DETECTION
FEATURE FUSION (LOW LEVEL)
FRAME # 1133

VISIBLE

IR
(8 - 12)

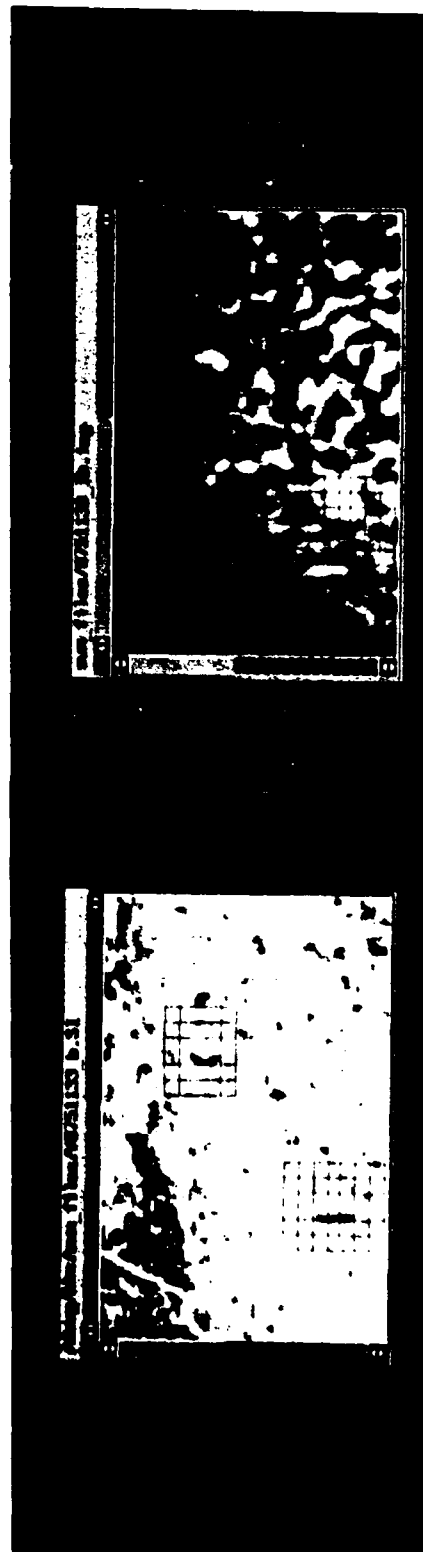
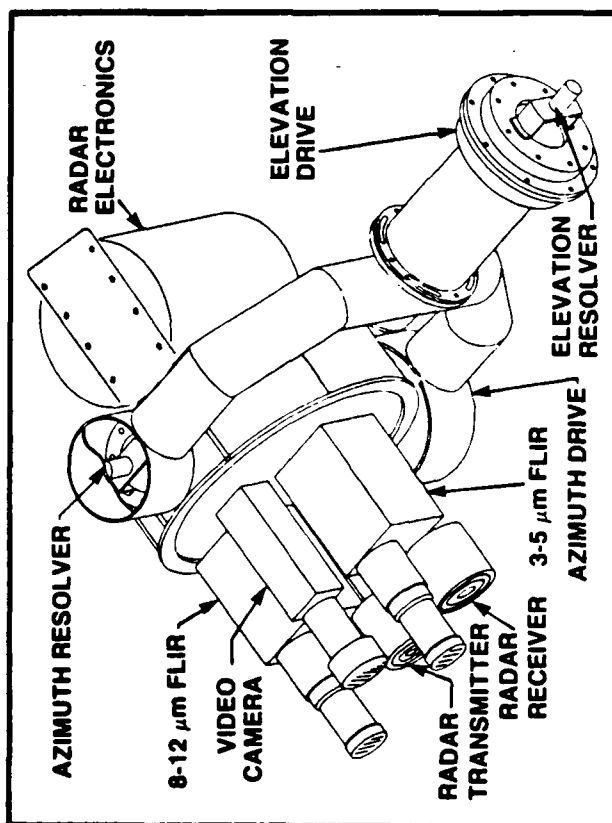


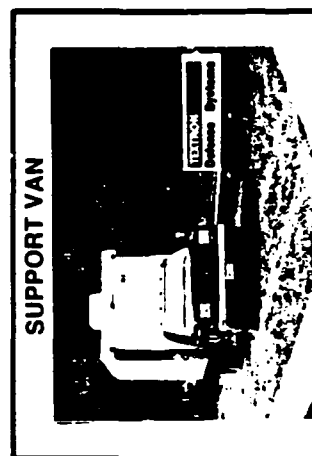
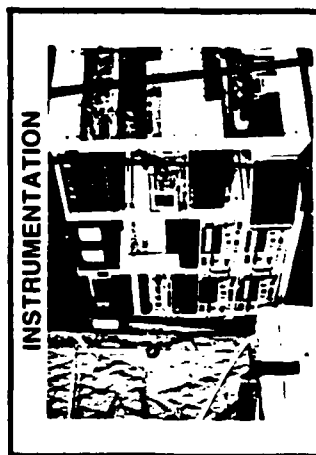
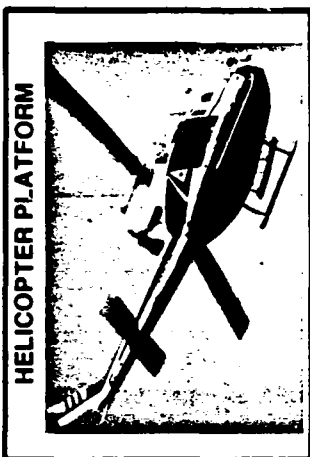
FIGURE 5.22
Results of Multi-Sensor (Low Level) Feature Fusion

AIRBORNE MULTISENSOR TEST BED

STABILIZED SENSOR SUITE



- 35 GHz MMW, FULLY COHERENT RADAR
- 3-5 μm , 8-12 μm IMAGING IR
- VISIBLE TV
- GROWTH TO INCLUDE:
 - 94 GHz MMW
 - ACTIVE IR
 - LADAR



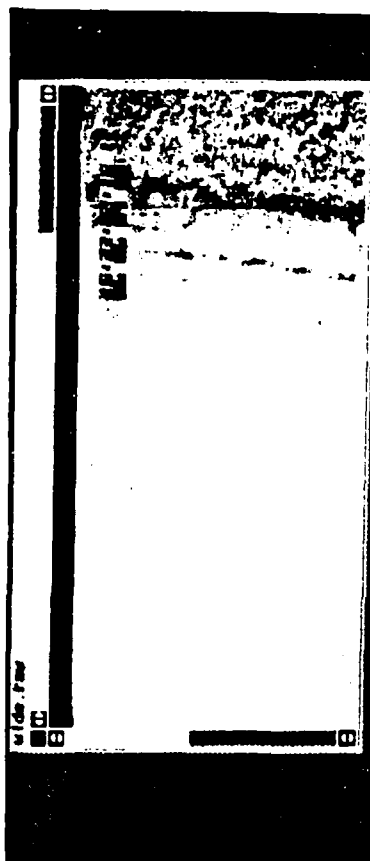
TEXTRON Defense Systems

46-2325N

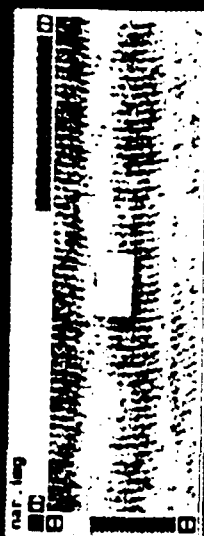
FIGURE 5.23
Airborne Multi-Sensor Test Bed

ATB TEST - 12 INCH SQ PLASTIC MINE (TRAIN)

VISIBLE
WIDE FOV



VISIBLE
NARROW FOV



IR (8 - 12)



IR (3 - 5)

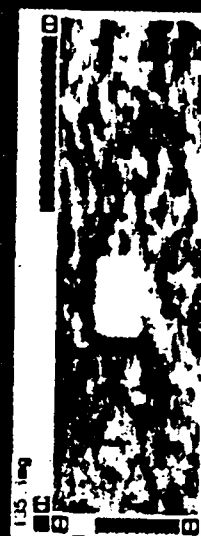
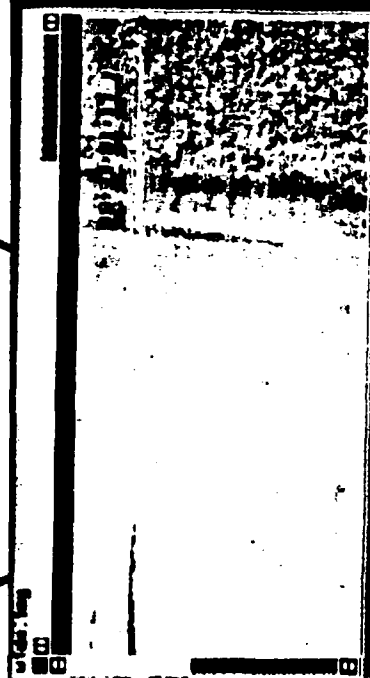


FIGURE 5.24
12 Inch Square Plastic Mine (Training)

ATB TEST - 12 INCH CIRC METAL MINE (TRAIN)

VISIBLE
WIDE FOV



VISIBLE
NARROW FOV



IR (8 - 12)



IR (3 - 5)



FIGURE 5.25

12 Inch Circular Metal Mine (Training)

ATB TEST - 12 INCH CIRC PLASTIC MINE (TRAIN)

VISIBLE
WIDE FOV

VISIBLE
NARROW FOV

IR (8 - 12)

IR (3 - 5)



FIGURE 5.26
12 Inch Circular Plastic Mine (Training)

and wedge integrators, discussed previously, were used for feature extraction. Data on smaller circular plastic (6 inch and 3 inch) mines was also generated, however, this analysis concentrates on the larger mines since some of those were also hidden or occluded in the high grass.

Figure 5.27 and 5.28 show the results of running the trained neural network against a test set of mine data in the open. A window was run with 75% overlap in both the x and y directions. Several detections were made on each mine without any false alarms. In addition, it was not necessary to see the whole mine in a window in order to make a detection. Figures 5.29 - 5.33 show the twelve inch circular metal mines in the high grass (Figure 5.29- 5.31) and the twelve inch square plastic mine in the high grass (Figure 5.32 and 5.33). In these cases the mines are fairly well hidden, however, the mines are each detected several times in all cases. A single false alarm was generated in two cases (figures 5.29 and 5.32). Applying logic requiring more than one adjacent detection on a mine eliminates single hit false alarms. With such logic, the results of this limited test data is a $P_d = 1$ and $P_{fa} = 0$.

5.3.3 Minefield Detection

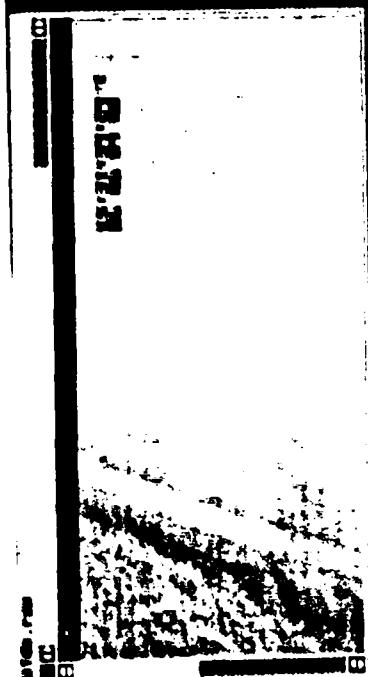
In order to evaluate algorithms for minefield detection and false alarm, a minefield deployment simulation was used whose variable were orientation of the deployment vector and distribution of the mines orthogonal to the deployment vector. Assuming that all scatterable minefield have a preferred orientation and a dominant intermine spacing, each test case (i.e. minefield laydown) consisted of an orientation drawn from a uniform random distribution over 360 degrees of rotation and intermine spacings which were normally distributed orthogonal to the deployment vector with values of standard variation from 0 to 20 meters. False alarms were generated with a uniform random distribution over the search area. Figure 5.34 illustrates examples of minefield distributions with zero meters and ten meters standard deviation as well as a typical sample of a false alarm distribution.

5.3.3.1 Minefield Detection Algorithm

A neural network was used to develop the minefield detection algorithm. The first feature set used were the values of the distribution of range of

ATB TEST - 12 INCH SQ PLASTIC MINE (IN OPEN)

VISIBLE
WIDE FOV



VISIBLE
NARROW FOV



IR (8 - 12)



IR (3 - 5)

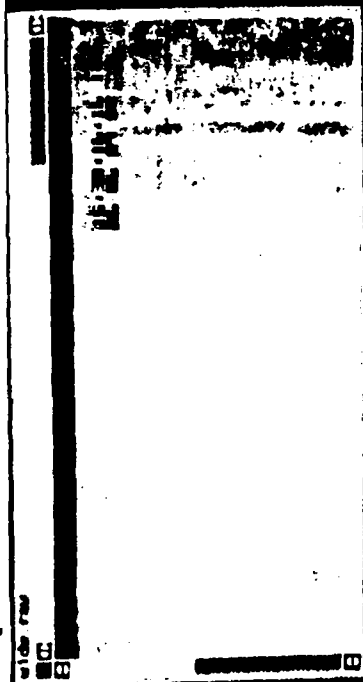


FIGURE 5.27

12 Inch Square Plastic Mine (Test)

ATB TEST - 12 INCH SQ PLASTIC MINE (IN OPEN)

VISIBLE
WIDE FOV



VISIBLE
NARROW FOV



IR (8 - 12)



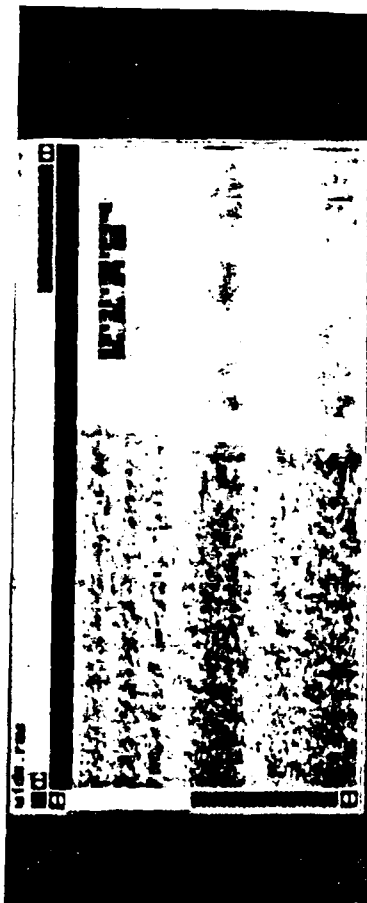
IR (3 - 5)



FIGURE 5.28
12 Inch Square Plastic Mine (Test)

ATB TEST - 12 INCH CIRC METAL MINE (IN HIGH GRASS)

VISIBLE
WIDE FOV



VISIBLE
NARROW FOV



IR (8 - 12)



IR (3 - 5)

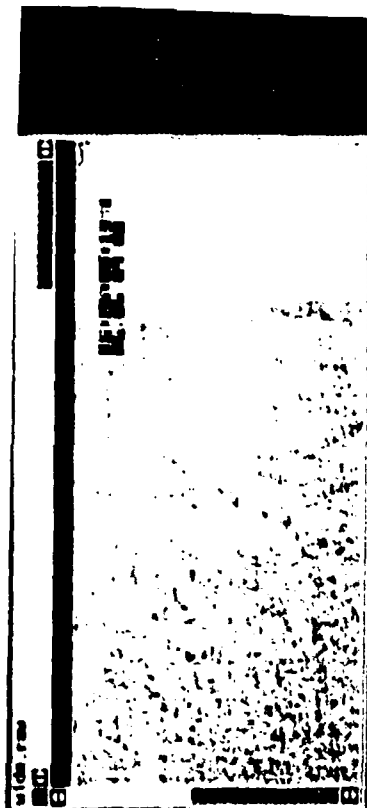


FIGURE 5.29

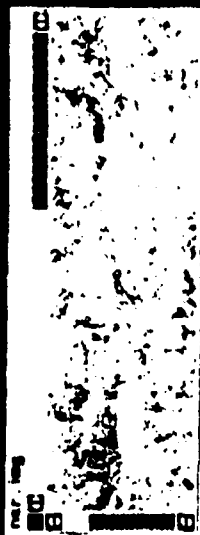
12 Inch Circular Metal Mine (Test)

ATB TEST - 12 INCH CIRC METAL MINE (IN HIGH GRASS)

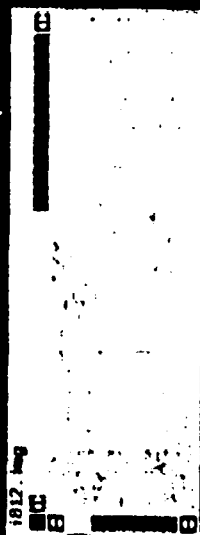
VISIBLE
WIDE FOV



VISIBLE
NARROW FOV



IR (8 - 12)



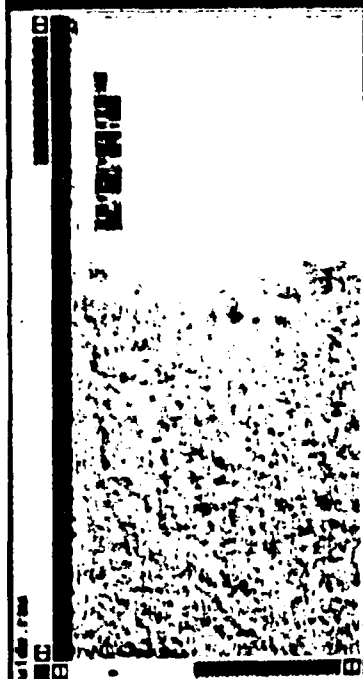
IR (3 - 5)



FIGURE 5.30
12 Inch Circular Metal Mine (Test)

ATB TEST - 12 INCH CIRC METAL MINE (IN HIGH GRASS)

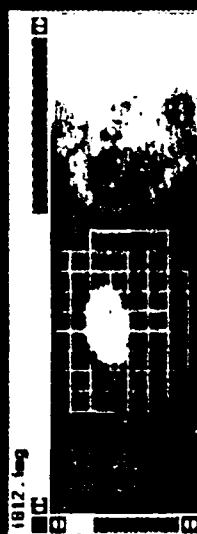
VISIBLE
WIDE FOV



VISIBLE
NARROW FOV



IR (8 - 12)



IR (3 - 5)

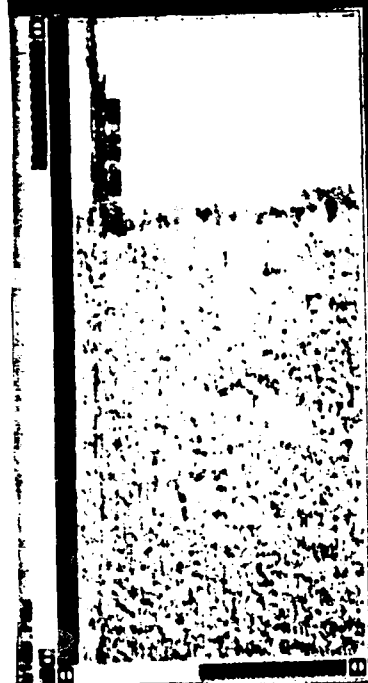


FIGURE 5.31

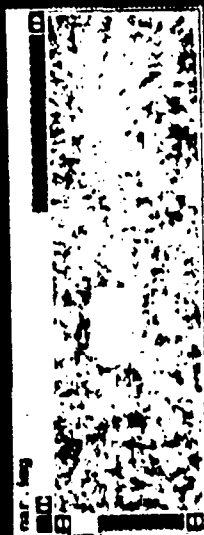
12 Inch Circular Metal Mine (Test)

ATB TEST - 12 INCH SQ PLASTIC MINE (IN HIGH GRASS)

VISIBLE
WIDE FOV



VISIBLE
NARROW FOV



IR (8 - 12)



IR (3 - 5)



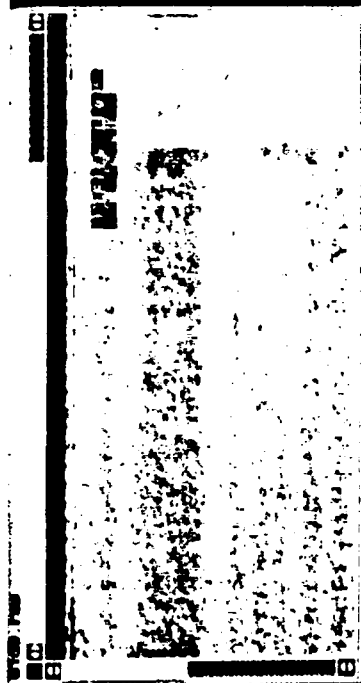
0413

FIGURE 5.32

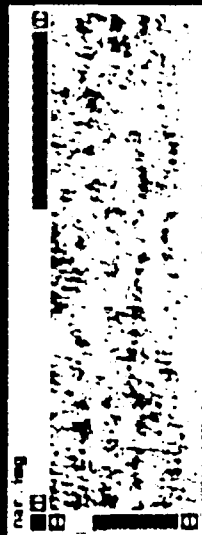
12 Inch Square Plastic Mine (Test)

ATB TEST - 12 INCH SQ PLASTIC MINE (IN HIGH GRASS)

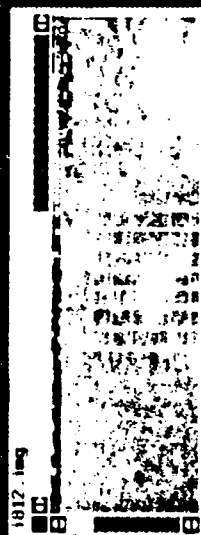
VISIBLE
WIDE FOV



VISIBLE
NARROW FOV



IR (8 - 12)



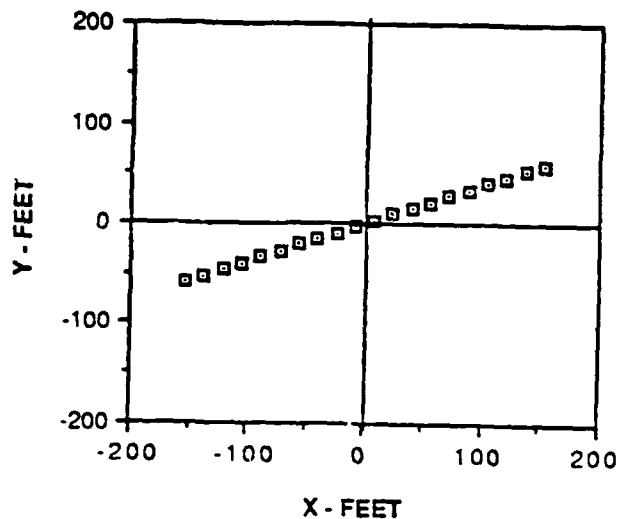
IR (3 - 5)



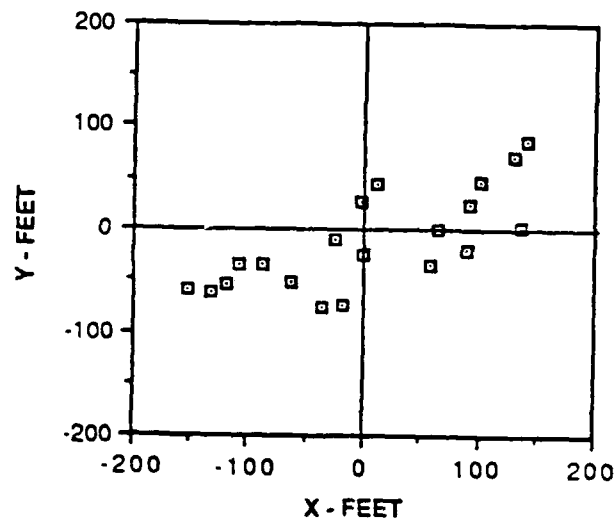
FIGURE 5.33

12 Inch Square Plastic Mine (Test)

1-D DISTRIBUTION



2-D DISTRIBUTION (10M SIGMA)



FALSE ALARM DISTRIBUTION

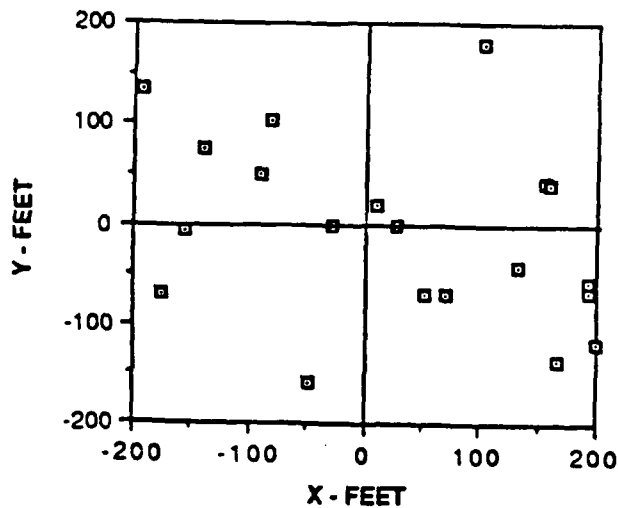


FIGURE 5.34

Sample Minefield & False Alarm Distributions

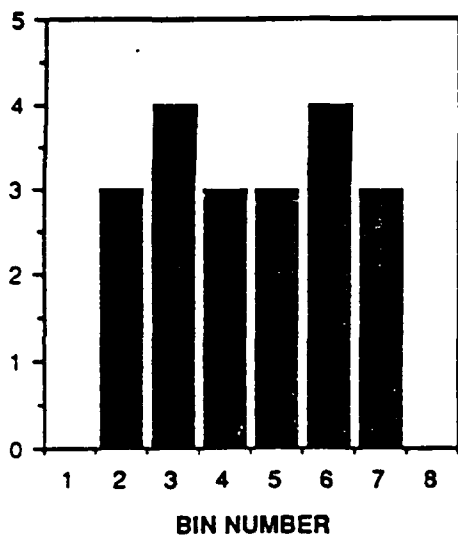
detections from the center of the search area (Figure 5.35). A neural net was trained with these features for a minefield with zero meters standard deviation and for false alarms. Simulated test data (i.e. mine detections) was then run against the trained neural net as a function of deployment standard distribution (0 meters to 10 meters). The results, presented in Figure 5.36 show that a mine field was correctly identified 100 % of the time with a a zero meters standard deviation (i.e. along a straight line). With three to five meters standard deviation, correct identification of a minefield dropped to 80%. and with a standard deviation of ten meters, correct identification was 60 %. In all cases there were no false alarms in the minefield (i.e. only valid detections). One concern in using the range histogram as a feature set is that the histogram is a one dimensional representation and therefore two dimensional spatial relationship information is lost.

In order to address this concern, the two dimensional FFT representation with ring and wedge integrators, used for individual mine detection, was also applied to minefield detection. This representation is invariant and maintains the spatial relationships of the individual detections. Figure 5.36 shows a comparison of the performance of the neural net algorithm trained with the two dimensional FFT feature against the one dimensional histogram based features. The algorithm using the two dimensional FFT features maintained 100 % performance out to a standard deviation of 5 meters and still had 90% correct minefield identification out to a standard deviation of 10 meters.

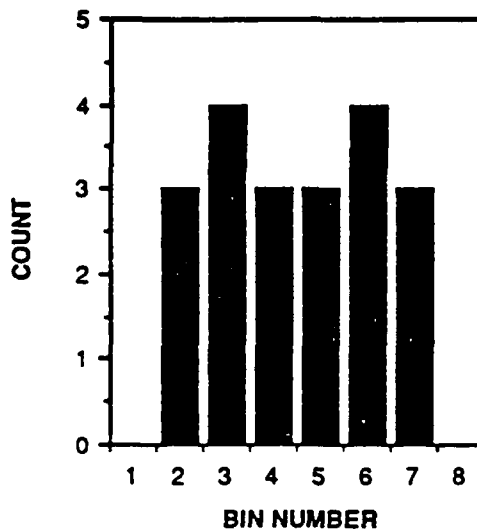
Given a feature set and an algorithm with reasonable performance in detecting a minefield without false alarms, the next issue was to determine minefield detection performance in the presence of false alarms and also the capability of the algorithm to correctly discriminate between minefield with false alarms and false alarms only (i.e. no minefield).

Using the same minefield deployment simulation, minefields of 20 detected mines each with deployment standard deviations of 0, 3, 5, 10, and 20 meters were generated. False alarms of 0, 10, 20, and 25 false alarms were added to each deployment case (Figures 5.37 - 5.40). In addition, simulated data was generated with false alarms only (figure 5.41). The performance results of the minefield detection algorithm using

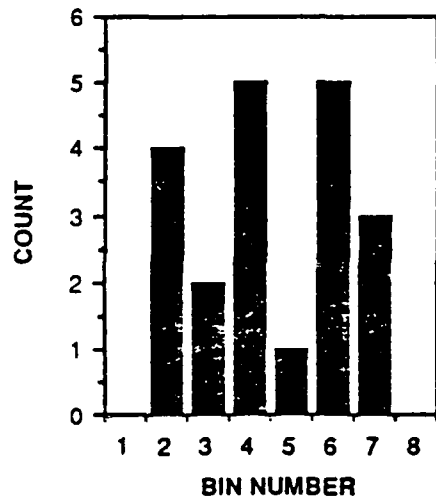
1-D / X- HISTOGRAM



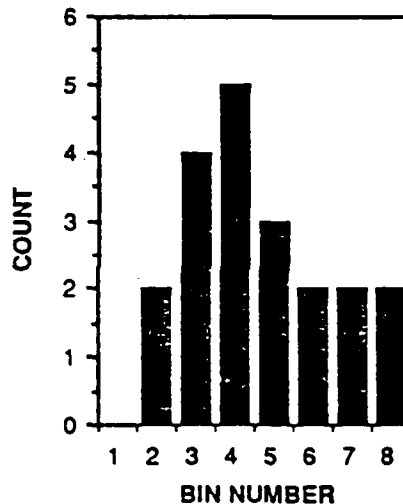
1-D / Y-HISTOGRAM



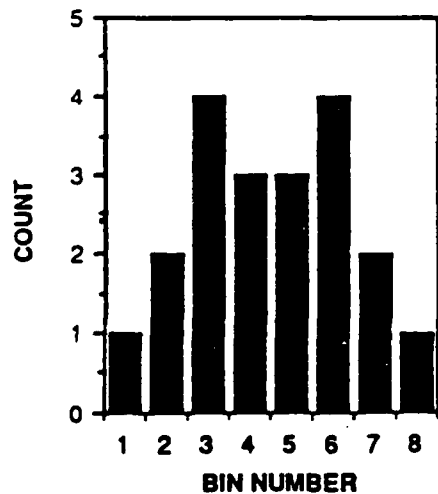
2-D / X-HISTOGRAM-SIG 10



2-D / Y-HISTOGRAM-SIG 10



FALSE ALARM/X-HISTOGRAM



FALSE ALARM / Y-HISTOGRAM

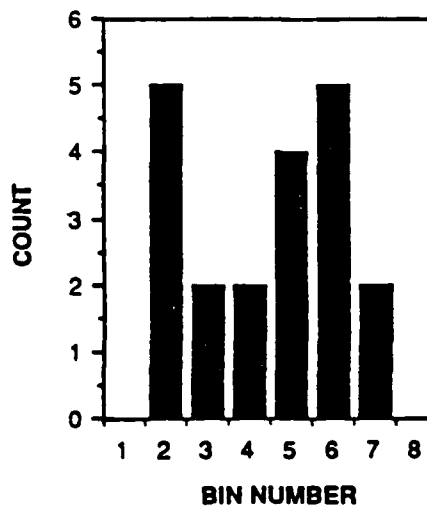


FIGURE 5.35
 Histograms of Spatial Distributions of Mine Like
 -95-

MINEFIELD DETECTION - NO FALSE ALARMS (2-D FFT FEATURES VS HISTOGRAM FEATURES)

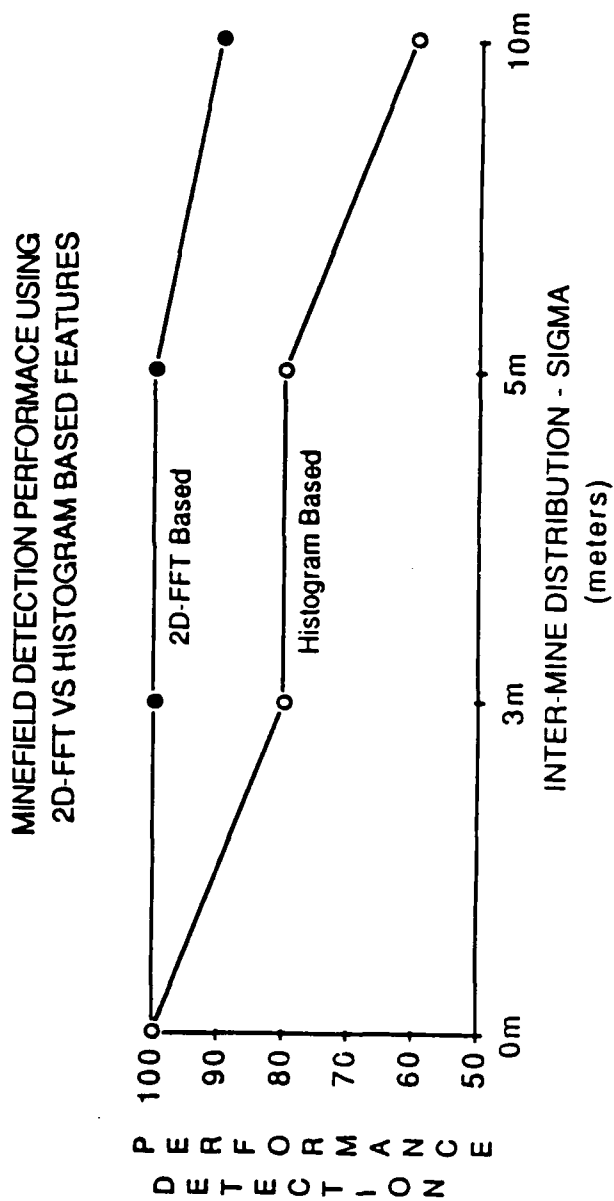


FIGURE 5.36
Minefield Detection Versus Mine Scattering

MINEFIELD DEPLOYMENT (20 MINES - 3 M SIGMA)

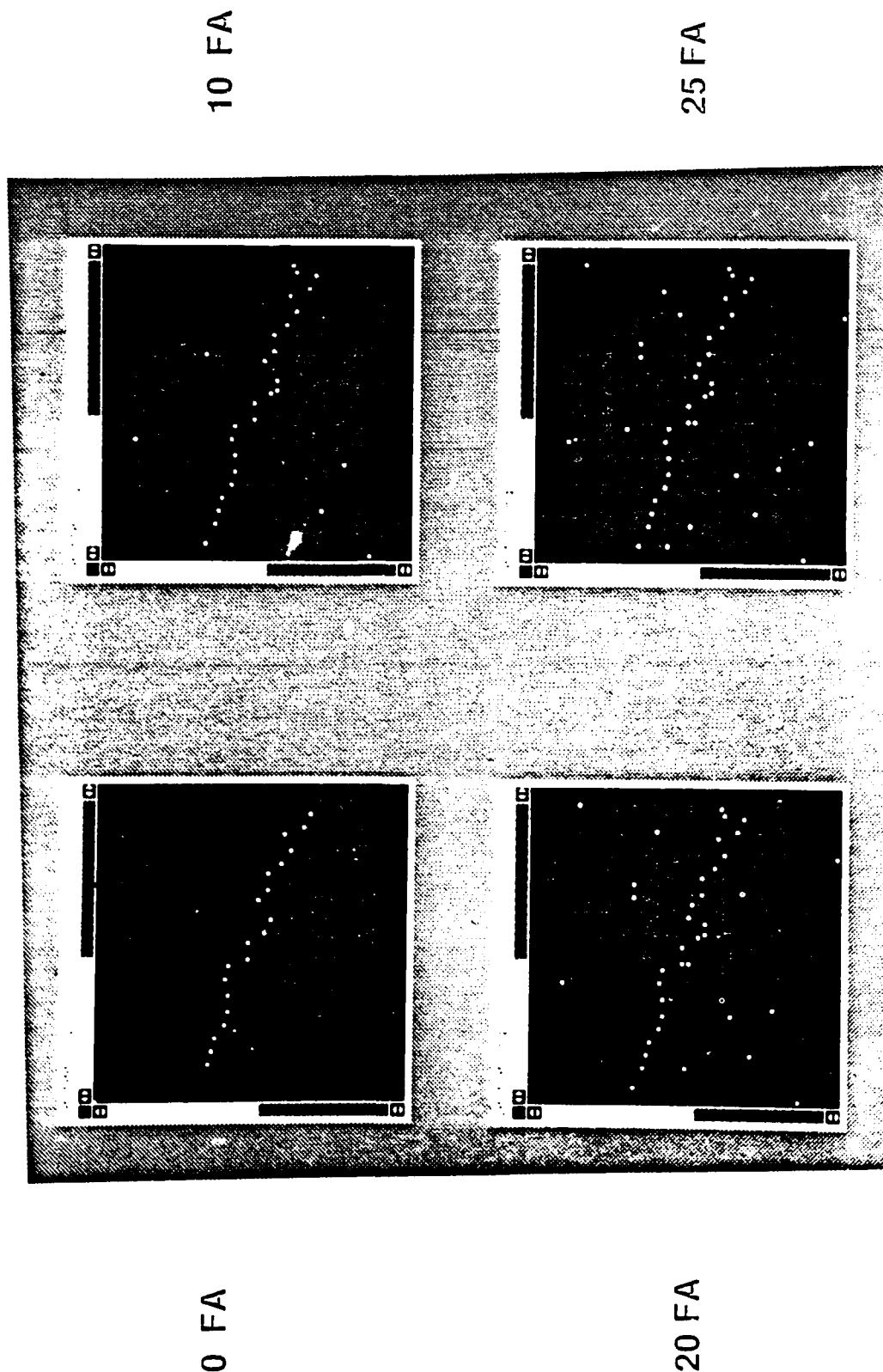


FIGURE 5.37 Synthetic Image
Composite Minefield/False Alarm (M-10)

MINIFIELD DEPLOYMENT (20 MINES - 5 M SIGMA)



FIGURE 5.38 Image (54-10)
Composite Minefield/False Alarm Synthetic

MINEFIELD DEPLOYMENT (20 MINES - 10 M SIGMA)

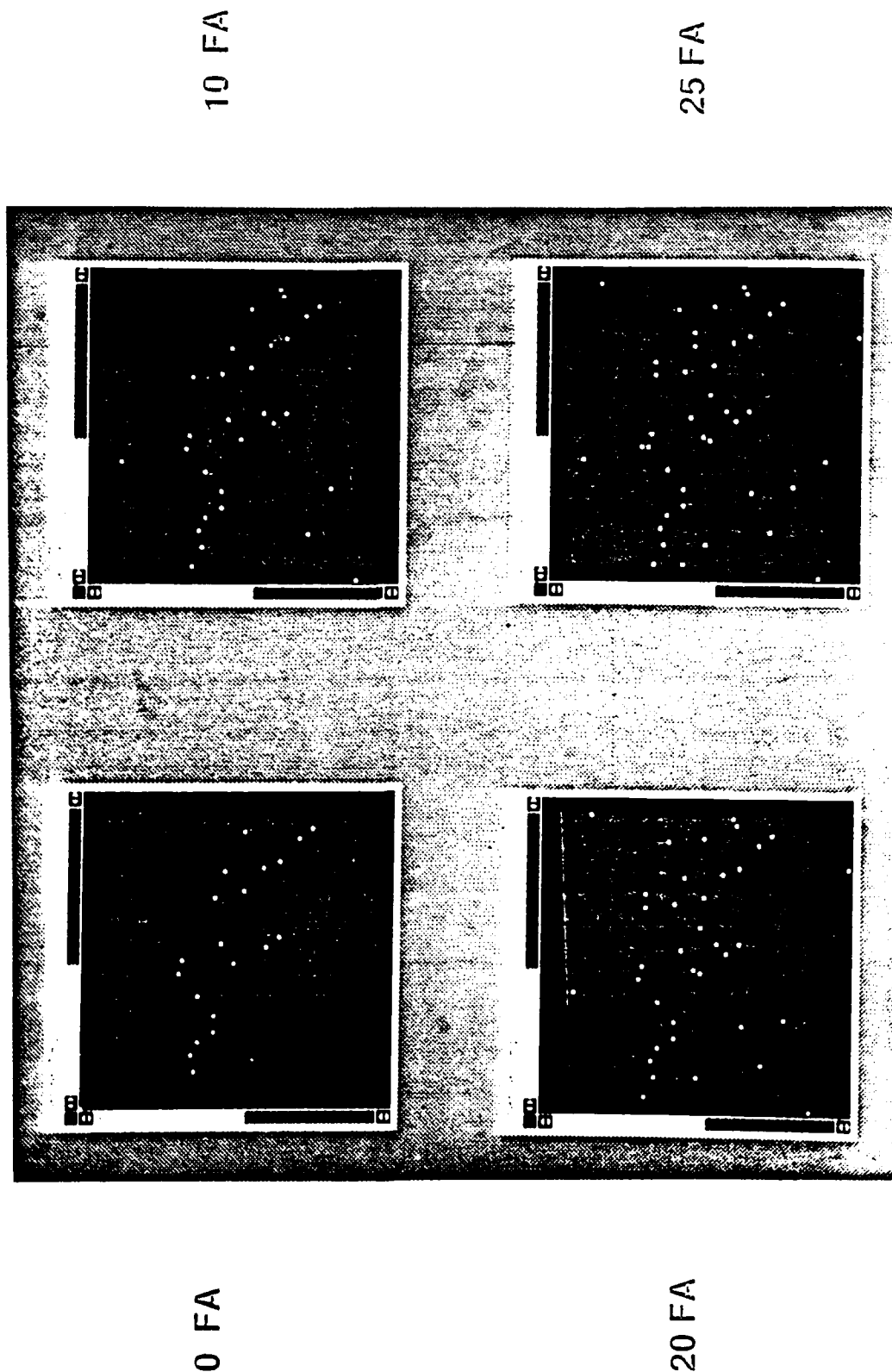


FIGURE 5.39 Image (10M-10)
Composite Minefield/Fals Alarm Synthetic

MINIFIELD DEPLOYMENT (20 MINES - 20 M SIGMA)

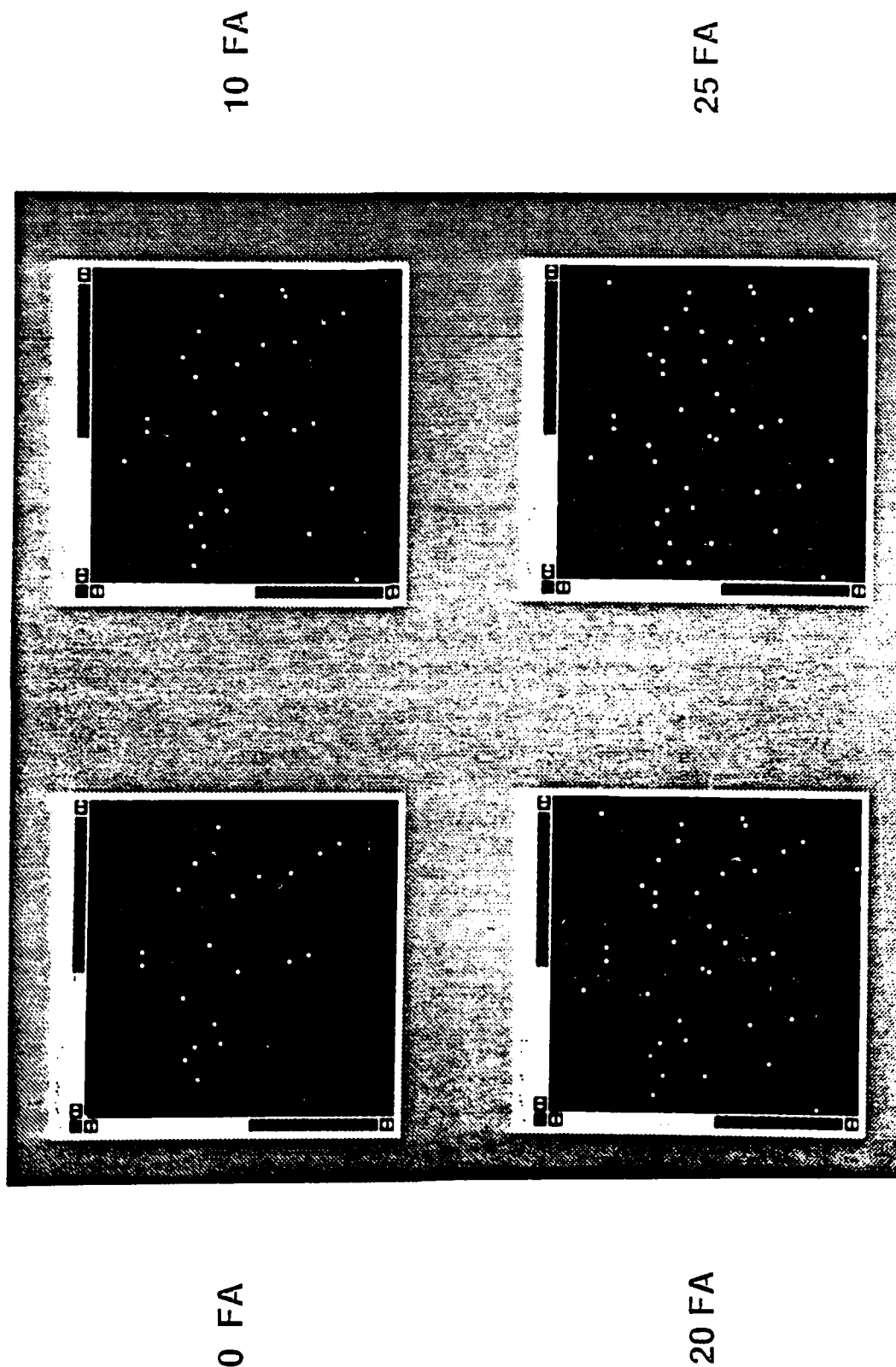


FIGURE 5.40
Image (20M-10)
Composite Minifield/Fals Alarm Synthetic

MINEFIELD DEPLOYMENT (FALSE ALARMS ONLY)

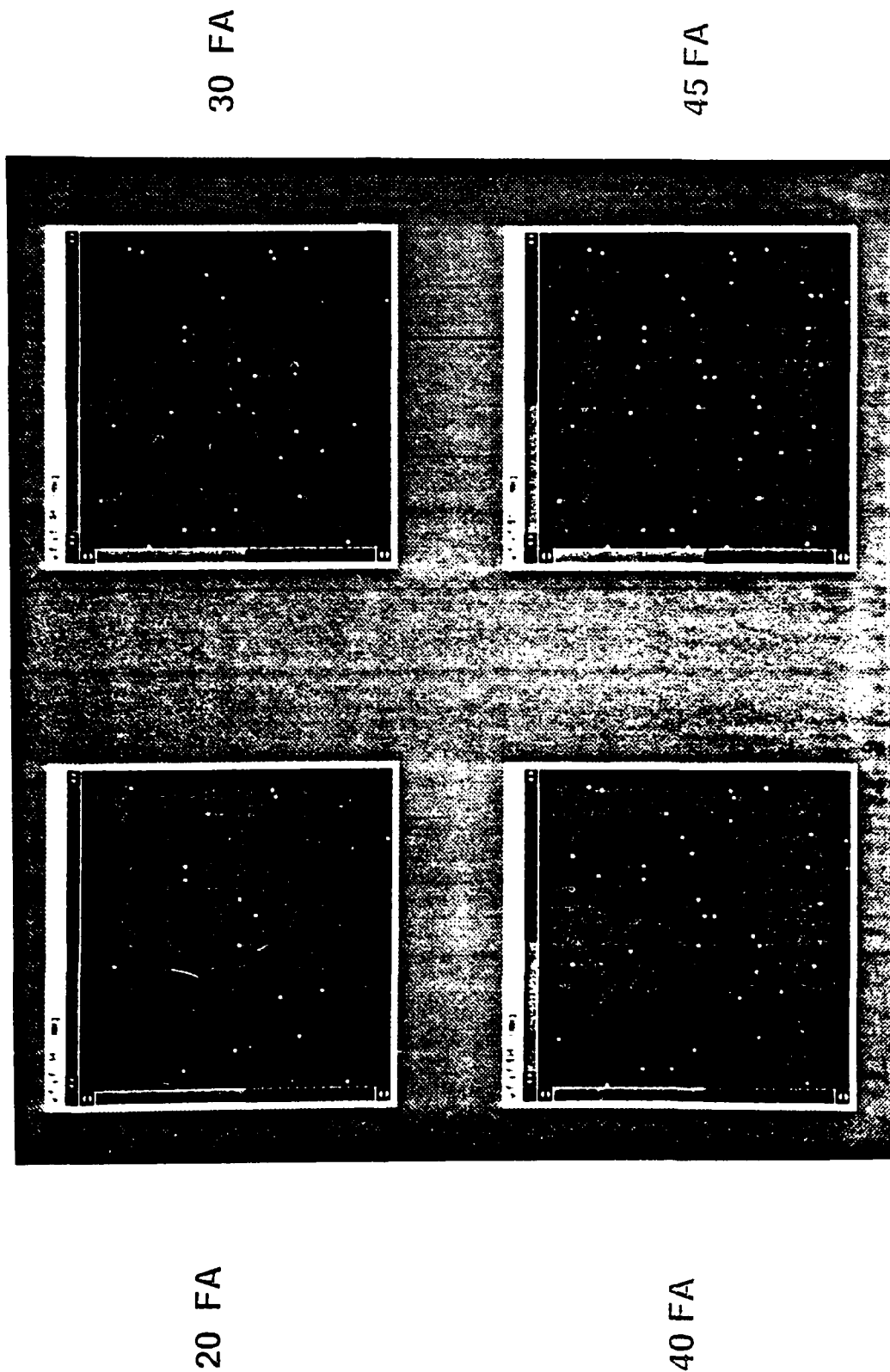


FIGURE 5.41
Sample False Alarm Spatial Distribution

MINEFIELD DEPLOYMENT (20 MINES - 20 M SIGMA)

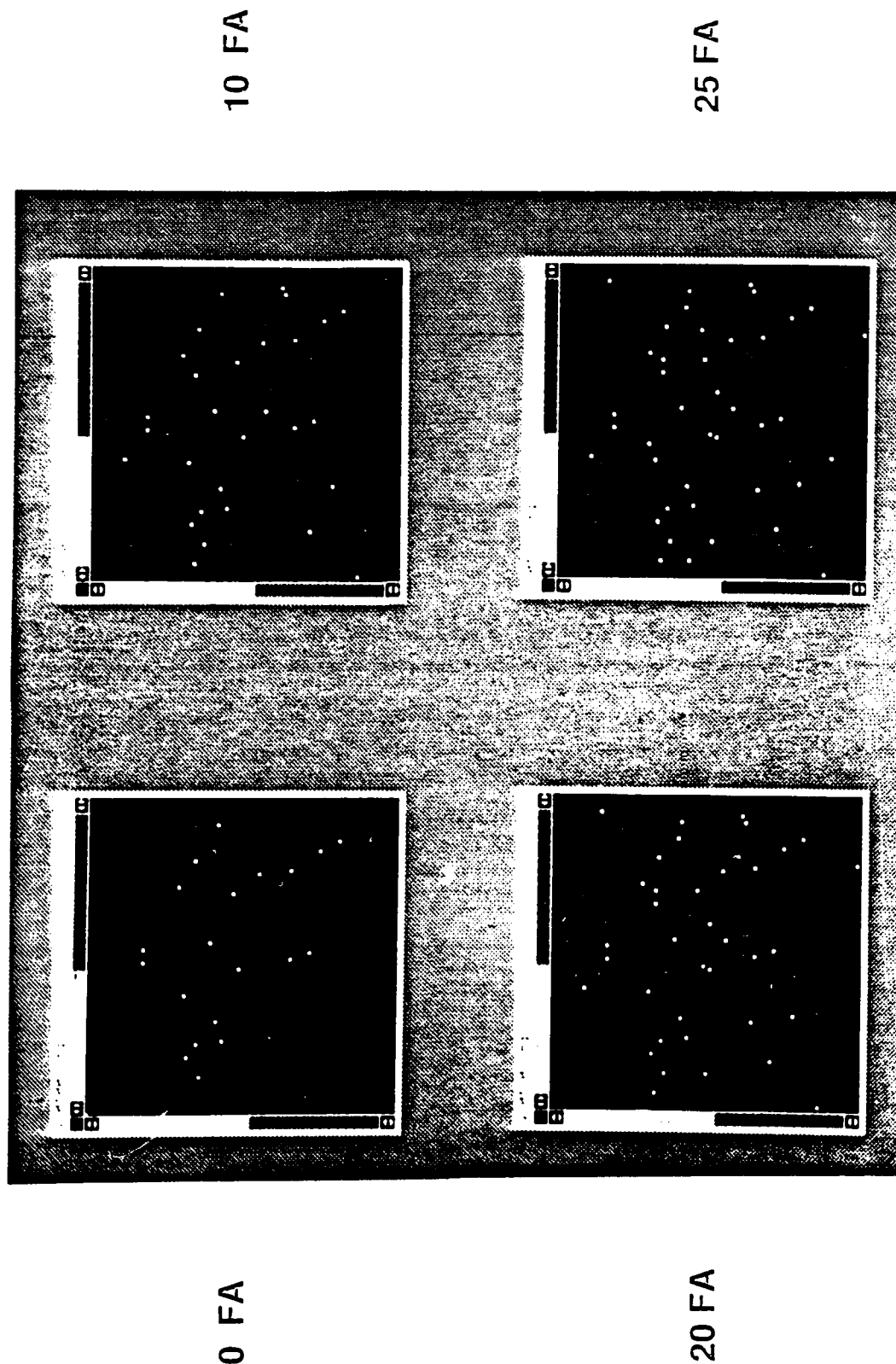


FIGURE 5.40
Image (20M-10)
Composite Minefield/Fals Alarm Synthetic

MINEFIELD DEPLOYMENT (FALSE ALARMS ONLY)

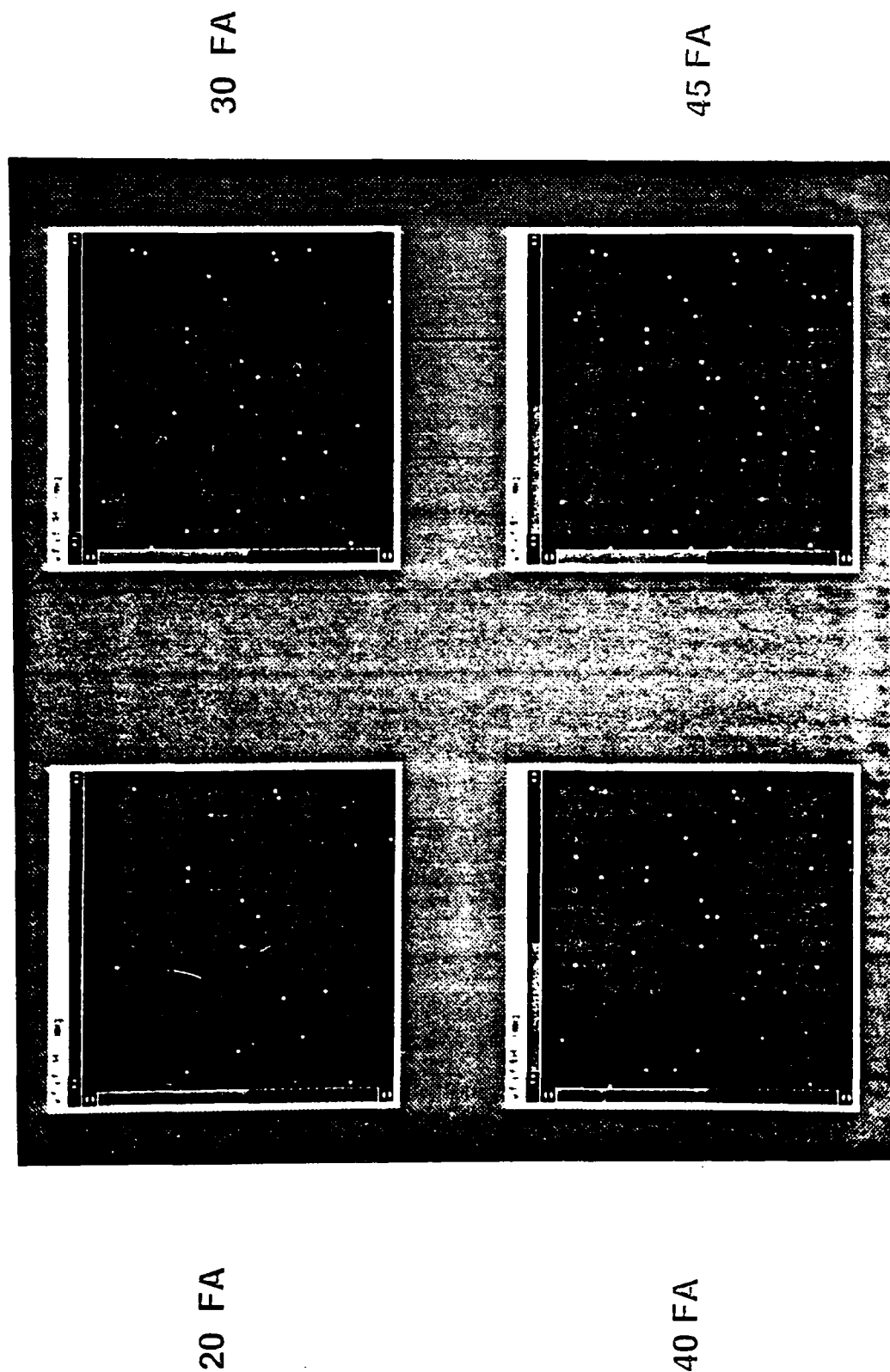


FIGURE 5.41
Sample False Alarm Spatial Distribution

a neural network trained with two dimensional FFT features are presented in Figures 5.42 and 5.43.

In Figure 5.42, the neural network was trained with a minefield of 20 detected mines with a standard deviation of zero meters and no false alarms, and with data sets of only false alarms. These represent the two classes of minefield and false alarms (i.e. no minefield) to the neural network. Ten trials were used for each test case. For zero and three meters standard deviation, 100 % minefield detection was achieved with up to 56 % false alarm density (i.e. 20 mines and 25 false alarms). With five meters standard deviation performance was maintained above 80 % correct minefield identification. The performance dropped off at ten meters and was poor at twenty meters. The ability of this algorithm to discriminate a minefield from false alarms was almost 100 %.

Using ten false alarms rather than the twenty false alarms previously used in training the neural network, the performance of the minefield detection algorithm improved substantially. Minefield detection was 100 % correct up to 56 % false alarm density with zero and three meters standard deviation in deployment. With five meters standard deviation, correct identification was maintained over 90 % out to 56 % false alarm density. With ten meters standard deviation, correct minefield identification was maintained at 90 % out to 33 % false alarm density. Even at twenty meters standard deviation, correct minefield identification was maintained at 60 % or better out to 33 % false alarm density (Figure 5.43) versus 0% correct identification in the previous case (Figure 5.42). The cost of this improved performance in minefield detection was a drop in the capability to discriminate a minefield from false alarms only from 100 % to approximately a worst case of 88% (Figure 5.43).

5.3.3.2 System Cues for Detecting the Location of Minefields

A number of cues to the existence of a mine and minefields were also analyzed. These cues do not require the direct observation of the mine or its associated signature but utilize environmental, doctrinal, and timing factors.

MINEFIELD DETECTION (TRAINING SET: 20 MINES / 20 FA)

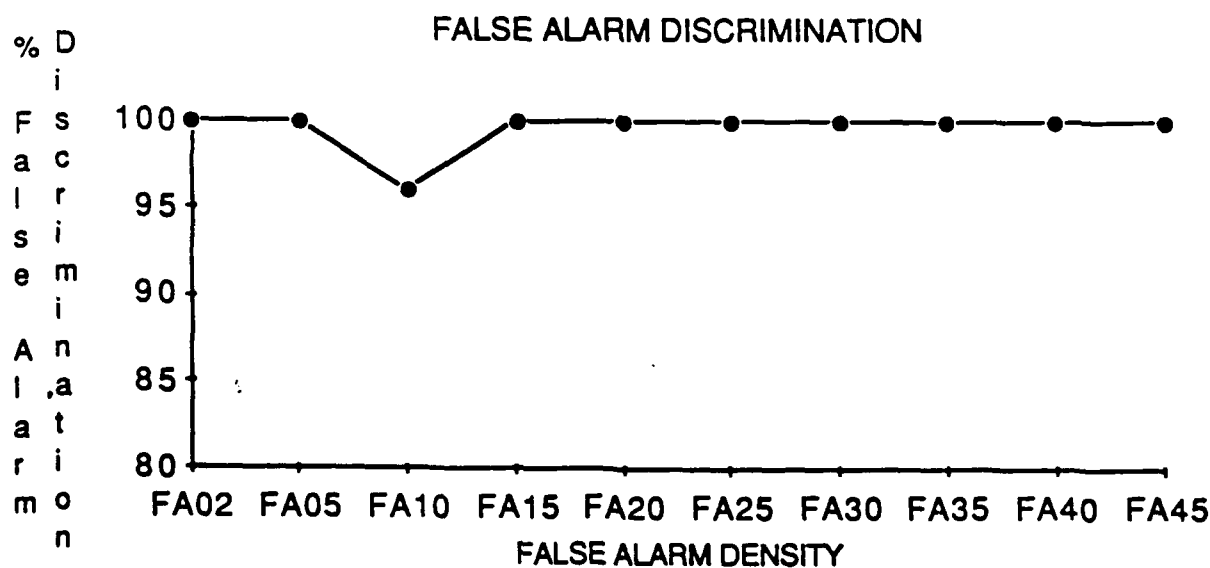
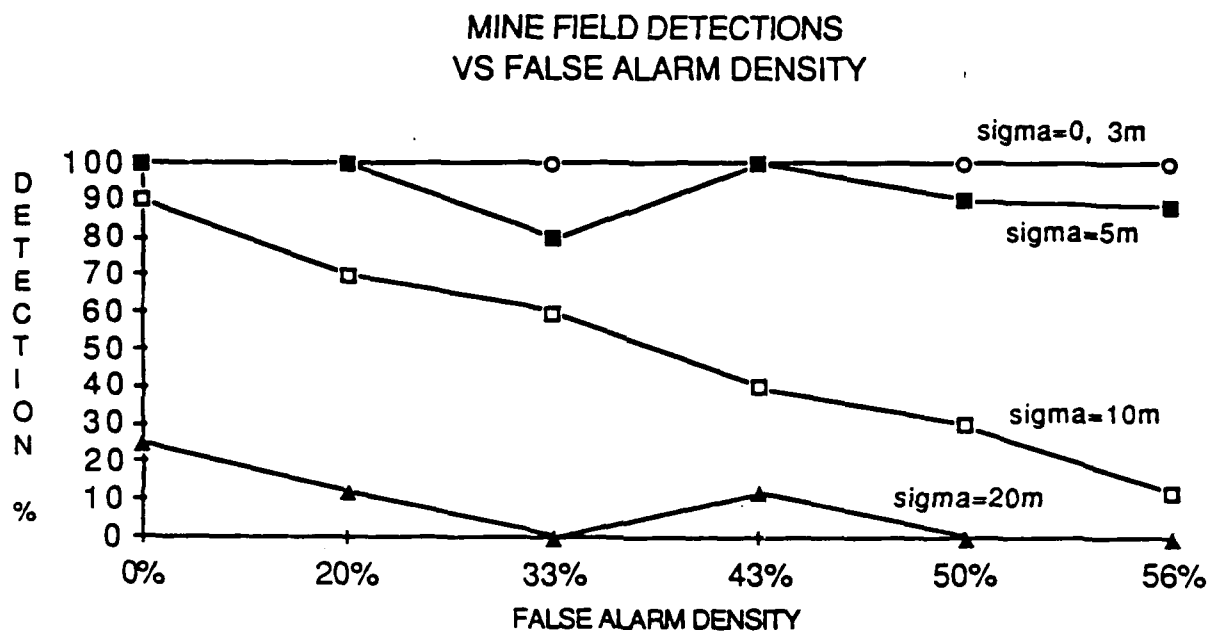


FIGURE 5.42 Alarm Rejection
Probability of Minefield Detection & False

MINEFIELD DETECTION (TRAINING SET: 20 MINES / 10 FA)

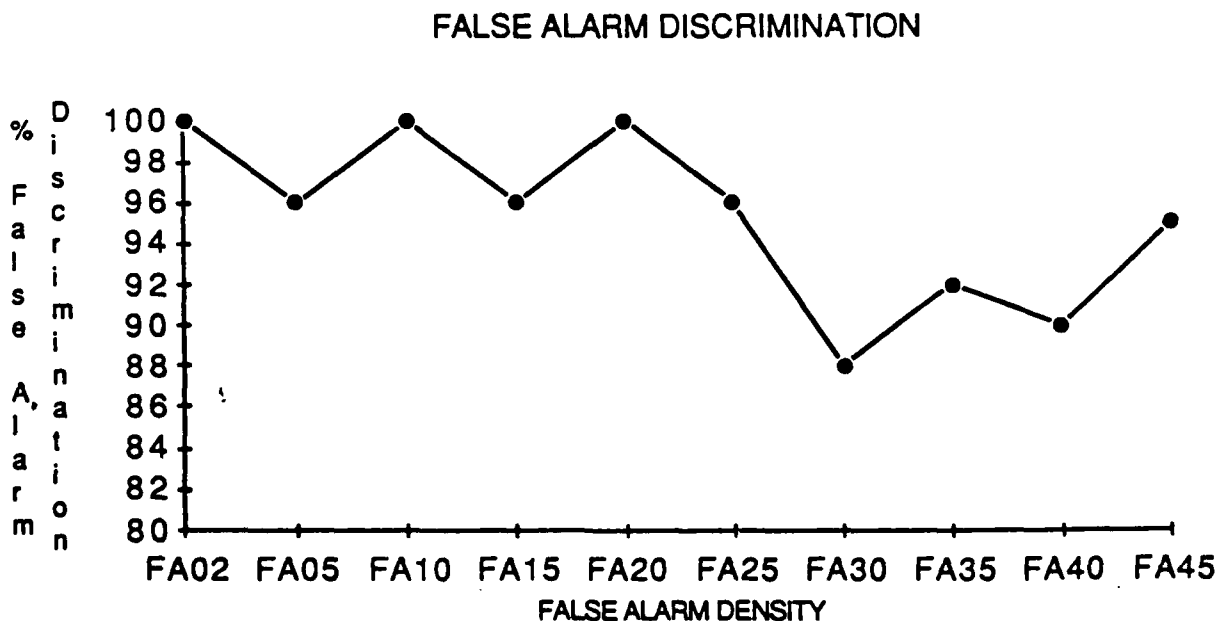
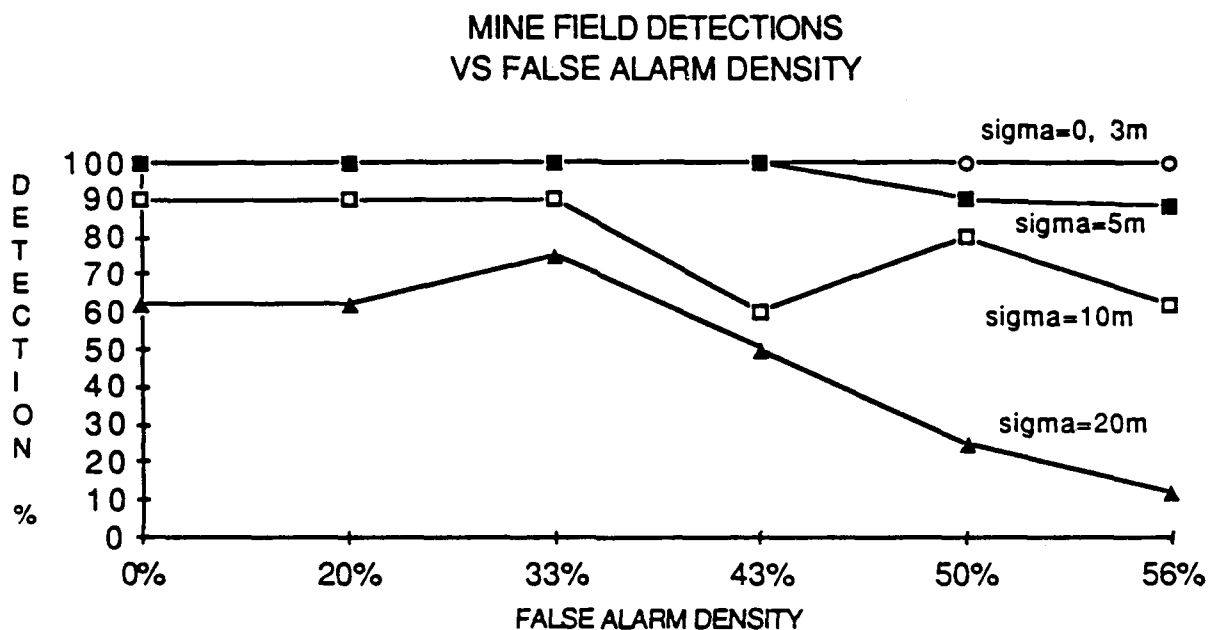


FIGURE 5.43
Minefield Detection

Figure 5.44 shows an example of scene classification. The top picture is a passive IR image of trees, a treeline, field and a vehicle in the treeline. The bottom picture displays the results of a neural network based algorithm trained to identify trees, treeline, field and vehicles. The vehicle is observed as two light blocks at the bottom center of this figure. The field is displayed as darker blocks and the trees and treelines are displayed as lighter blocks. This is an example of a type of cue that could aid the algorithms in detecting mines and minefields.

A table summarizing additional system cues for detecting or discovering enemy mines and minefields, for various antitank mines, antipersonnel mines, delivery systems and doctrine, is presented in Appendix D .

A major tool used in the processing of the mine data is the Knowledge Based Vision (KBVision) System. The KBVision system is a developer's environment for knowledge-based vision processing. Through the application of a wide variety of image processing and artificial intelligence techniques, users of this system are able to rapidly prototype and develop solutions to image understanding problems. It accommodates all processing levels from low level image processing through intermediate level feature manipulation to high level LISP based image understanding. A thorough description of the KBVision system is provided in Appendix E .

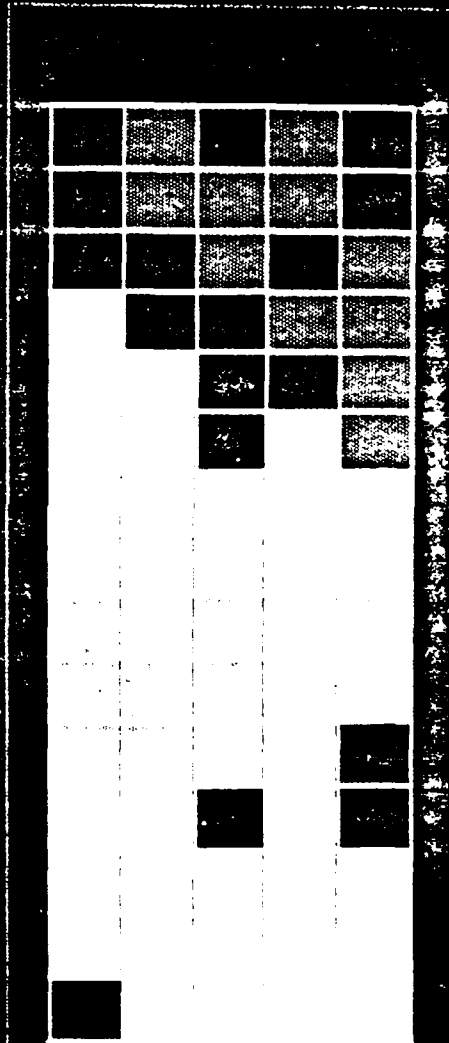
This workstation was used primarily to support the low level (Level1) individual mine detection algorithm development efforts during this phase of the program, however, its real power will manifest itself during the next phase, where additional emphasis will be put on the above Level 3 contextual image understanding and syntactic interferencing to estimate the likelihood of minefield presence.

5.4 Conclusions

5.4.1 Mine Detection

Based on the analysis and results presented in section 5.3.2, the following conclusions are made relative to mine detection:

- 1) Individual sensors with high level feature fusion are sensitive to dominant sensor features and to false alarms.



0/area1/data/dancft1/151/17481788/889.tab.raw.0

Figure 6.44

Figure 6.44: A high-contrast, black and white image showing a large, irregularly shaped object, possibly a rock or a piece of debris, against a dark background. The object has a rough, textured surface with many small, bright spots and a jagged edge. Above the object, there are several vertical white bars of varying heights, resembling a barcode or a scale.

2) Combining multiple individual sensors, using decision logic, reduces the number of false alarms. However, the detection capability remains sensitive to individual dominant sensor features.

3) Multi-sensor fusion using lower level features appear less sensitive to individual dominant sensor features and also reduces false alarms.

4) Of the low level features considered (histogram and two dimensional FFT) those features generated using the two dimensional FFT with ring and wedge integrators appear most robust.

5.4.2 Minefield Detection

Based on the analysis and results presented in section 5.3.3, the following conclusions are made relative to minefield detection:

- 1) A neural net based algorithm trained with features using a two dimensional FFT with ring and wedge integrators performs very well in both detecting minefields and in rejecting false alarm only conditions. This approach utilizes the spatial relationships and orientations unique to a minefield and allows substantial variability in intermine separation (20 meters standard deviation).
- 2) A number of cues to the existence of a mine and a minefield could also be used in minefield detection.

6.0 REAL TIME PROCESSOR HARDWARE/SOFTWARE DEVELOPMENT

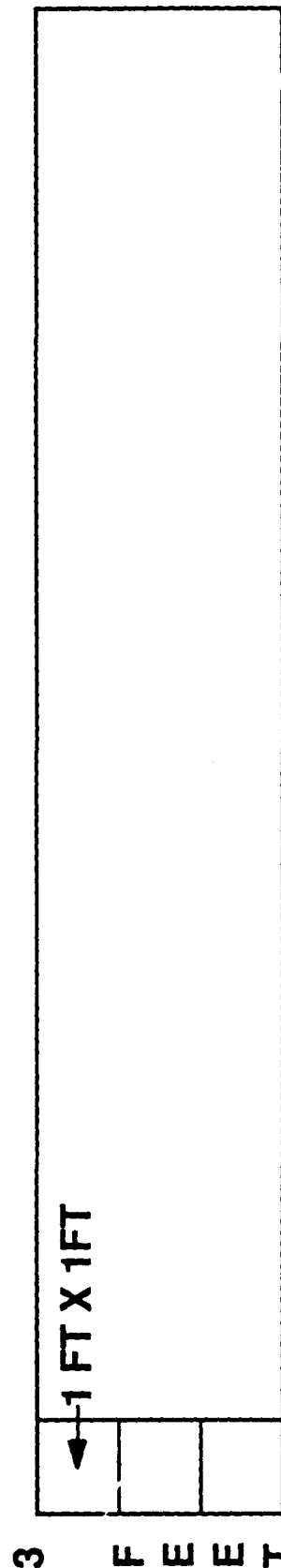
Since individual (Level 1) mine detection is considered to be the processing driver as compared to the processing requirements for minefield detection, a timing analysis was conducted to determine the processing performance required for real-time mine detection. A strawman system is described in Figure 6.1. This system consists of a multi-sensor suite scanning at a 30 Hz rate mounted on a vehicle with a maximum speed of 30 MPH. The interscan spacing is 1.5 ft. A three foot scan width is chosen in order to maintain a 50% overlap between scans. The cross range scan dimension is 100 feet and the window size is set at the size of the largest mine (one foot by one foot). With a 50 % overlap between windows, 600 windows are processed per scan. At 33.3 milliseconds per scan, this results in a required processing latency time, for a single pipeline architecture, of 56 microseconds per window. Assuming a single pipeline architecture with two processing chips, this allows 56 microseconds for feature extraction and 56 microseconds for neural transform processing.

The ability to achieve this level of processor performance was evaluated using a real time neural transform based mine detection algorithm with a scanning laser developed by TDS using available, off-the-shelf sensor and processing hardware. The testbed is an active pulsed GaAs IR laser range finder using a 0.9 micron laser at a 10 KHz sample rate with a maximum range of approximately 200 feet it can resolve range measurements to 6 inches with a field-of-view of 7 milliradians. The system consists of two counter-rotating mirrors which provide a linear scan across the field of view of ± 18.4 degrees (Figure 6.2 and 6.3). The processor is an IBM PC-AT (Intel 286) with a plug-in board containing a TI TMS C30 Digital Signal Processing chip running at 20 MHz . The system also contains a frame grabber with a video overlay board to see imagery on the PC screen, and an interface board to the laser scanner. (Figure 6.4).

The system was tested against the same set of 9 simulated mines (from data collection #2) at the TDS test facility on Cape Cod, Mass. The tests were run from an eighty foot tower with a 45 degree depression angle which resulted in a slant range of approximately 110 feet (Figure 6.5). The beam spot size was .77 feet which was over-sampled, resulting

SEARCH AREA / SCAN

100 FEET



VEHICLE SPEED = 44 FT / SEC @30 MPH

= 1.5 FT / SCAN @ 30 HZ

SCAN WIDTH = 3 FT (50 % OVERLAP)

SCAN LENGTH = 100 FT

PROCESSING TIME / SCAN = 33.3 MILLISECONDS@ 30 HZ

WINDOWS / SCAN = 600 (50 % OVERLAP)

POINTS / WINDOW = 144 @ 1 INCH RESOLUTION

PROCESSING TIME / WINDOW = 56 MICROSECONDS

FIGURE 6.1

Search System Timing/Throughput Sizing

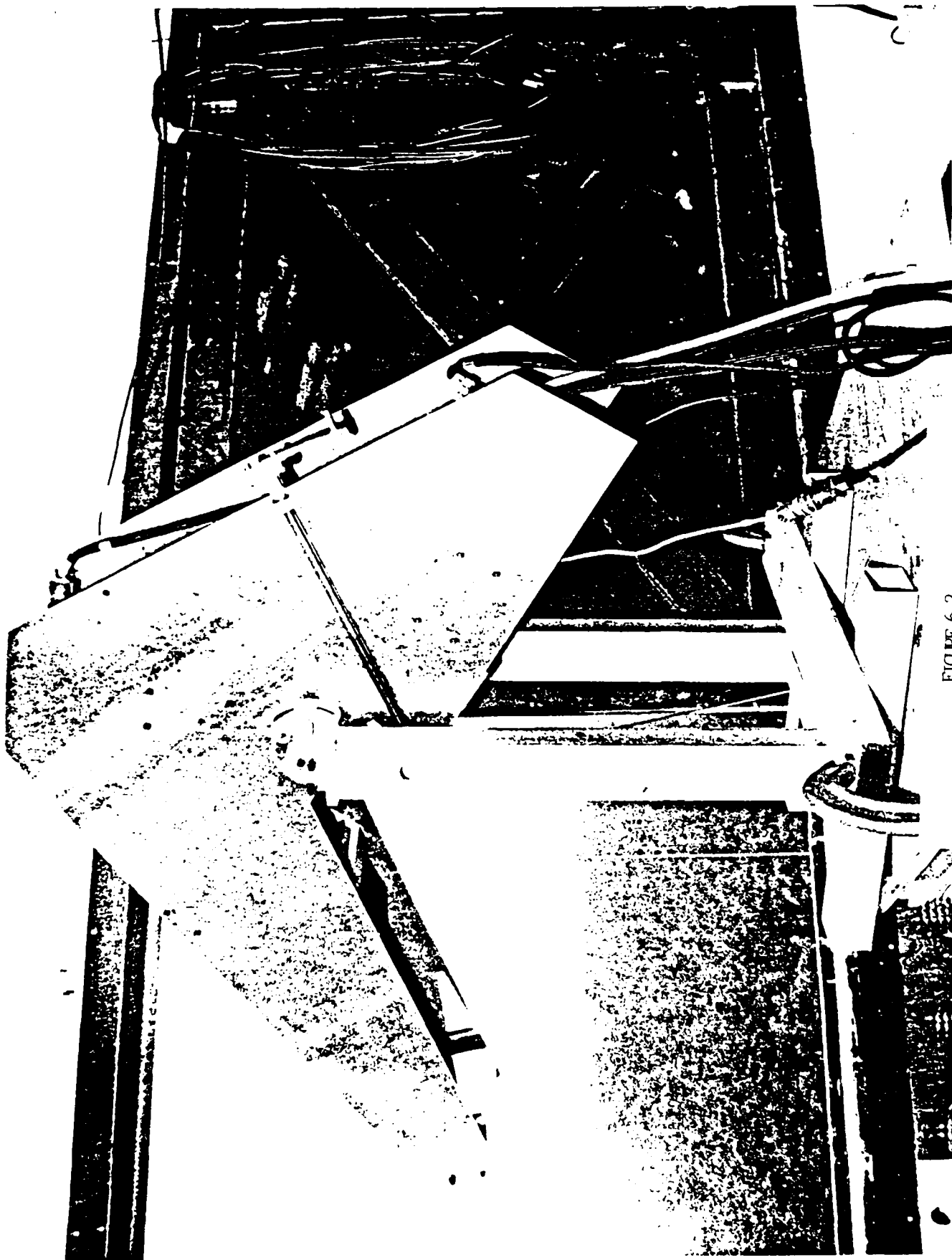


FIGURE 6.2

Scanning Laser Sensor Test Bed (Housing)



FIGURE 6.3
Scanning Laser Sensor Test Bed (Optics)



FIGURE 6.4

Real Time Processor/Display System

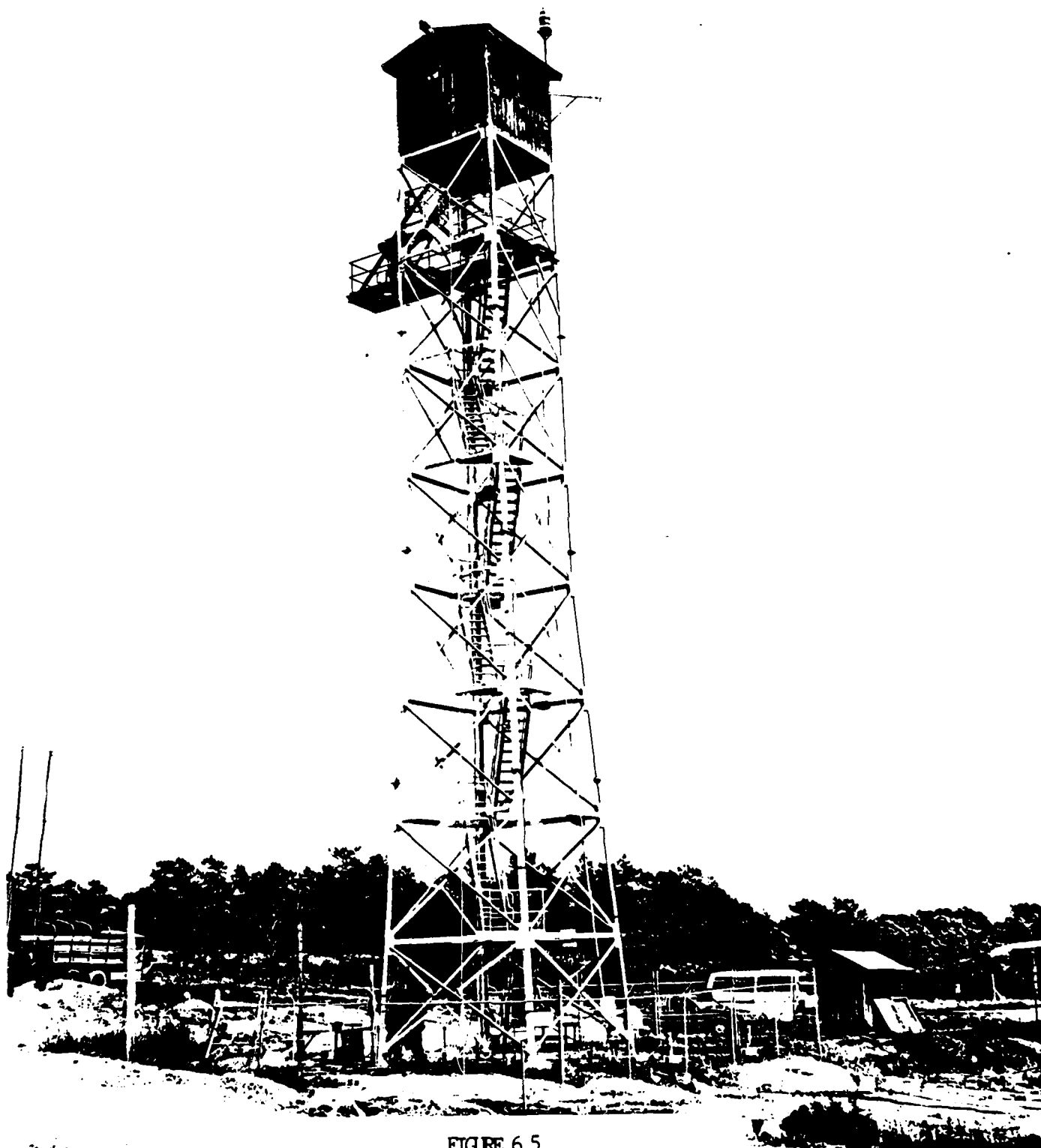


FIGURE 6.5
8S Fort Tower at Camp Edwards, MA

in a 0.4 foot sample spacing. The mines were laid out in the pattern shown in figure 6.6.

Figure 6.7 shows the PC screen. The field of view image from a TV camera, co-bore-sighted with the laser, is displayed in the upper right hand corner of the display along with a line indicating where the laser was scanning. In Figure 6.7, the laser is scanning across two mines in the field. The range to the center of the scan as well as other data is displayed in the upper left hand corner of the screen. Below this data, the actual range measurements are displayed with increasing range (profile) on the vertical scale and cross-range on the horizontal scale. The curvature in the range data is due to the range increasing as the laser sweeps across the ground.

Figure 6.7 displays two detections on the two scanned mines. They appear further in range rather than closer (which was expected) because of the absorption of the laser signal due to the color of the mines relative to the color of the background. This was confirmed by measuring return echo strength as a function of color and range (figure 6.8). This had an effect on range because of the way range was measured by this system. As illustrated in figure 6.9, as the echo return drops due to absorption, the range measurement taken at a threshold crossing increases. Therefore, the mines appear at a further range than the background .

The neural network was trained using a twelve component feature vector. For this design, the twelve components were 12 consecutive range samples obtained by placing a twelve point (one dimensional) window around sample mines and background. For the Strawman design, these twelve components could be any combination of multi-sensor features. The output of the neural transform indicates whether a mine or background was detected in each window, with each window/decision spaced one sample apart, across the range signal. In Figure 6.7 there were two mine detections plus two potential false alarms. The false alarms are eliminated by using logic to define a mine detection as having three consecutive values above a certain confidence level. The bottom trace on the screen shows the result of applying this rule to the output of the neural transform. In this case both mines were detected with no false alarms.

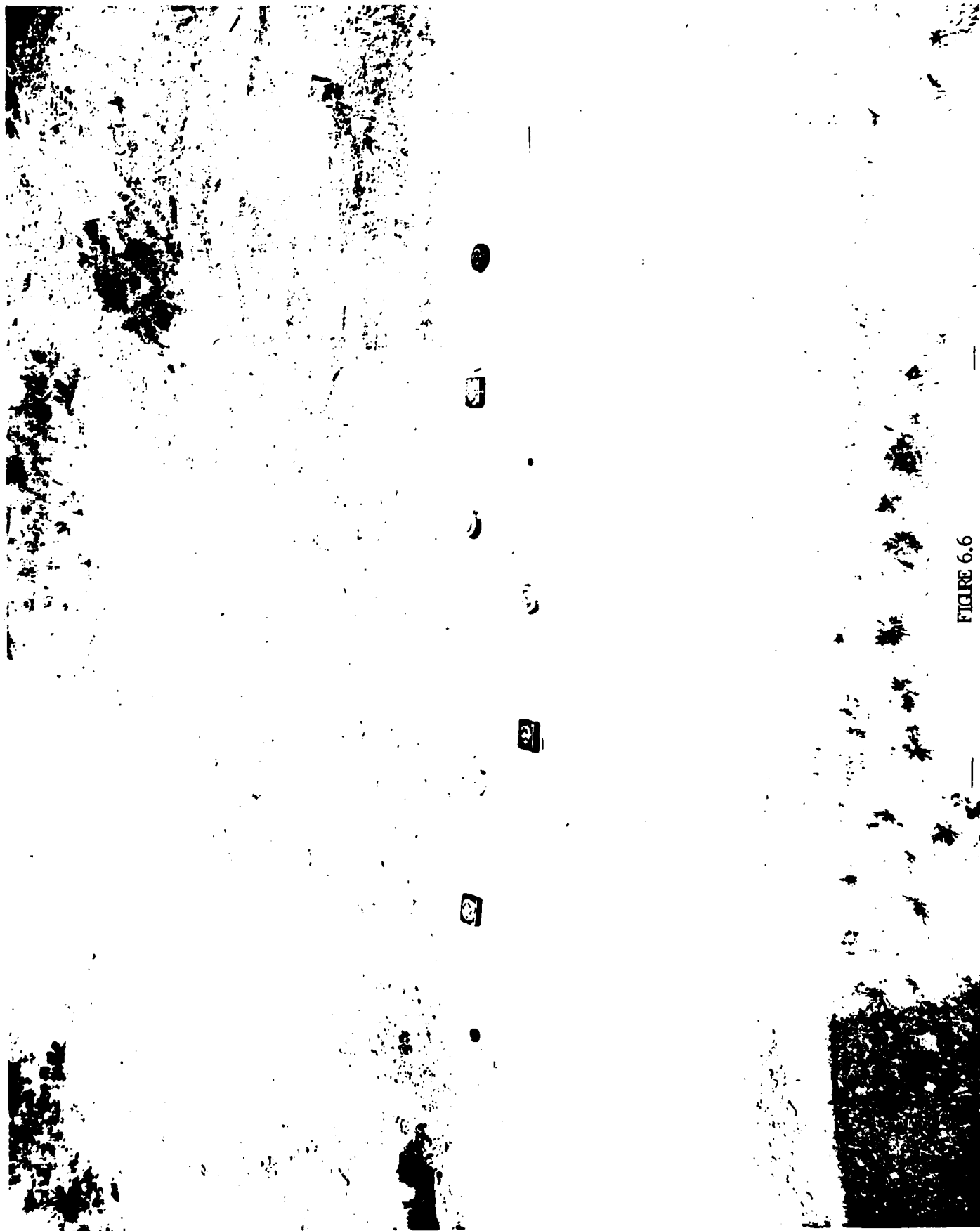


FIGURE 6.6
Laydown of Mine Simulants for Real Time Proc Demo

Tue Jan 27 11:49:11 1989
 Scan number = 4638
 Frames Stored = 13
 Total bytes = 17168
 Images (8165) = 188



C1 - HIDE

C2 - HIDE

INSTRUCTIONS

FIGURE 6.7

Real Time Display of Raw & Processed Data

RETURN ECHO VS RANGE (@ 20KC PRF)

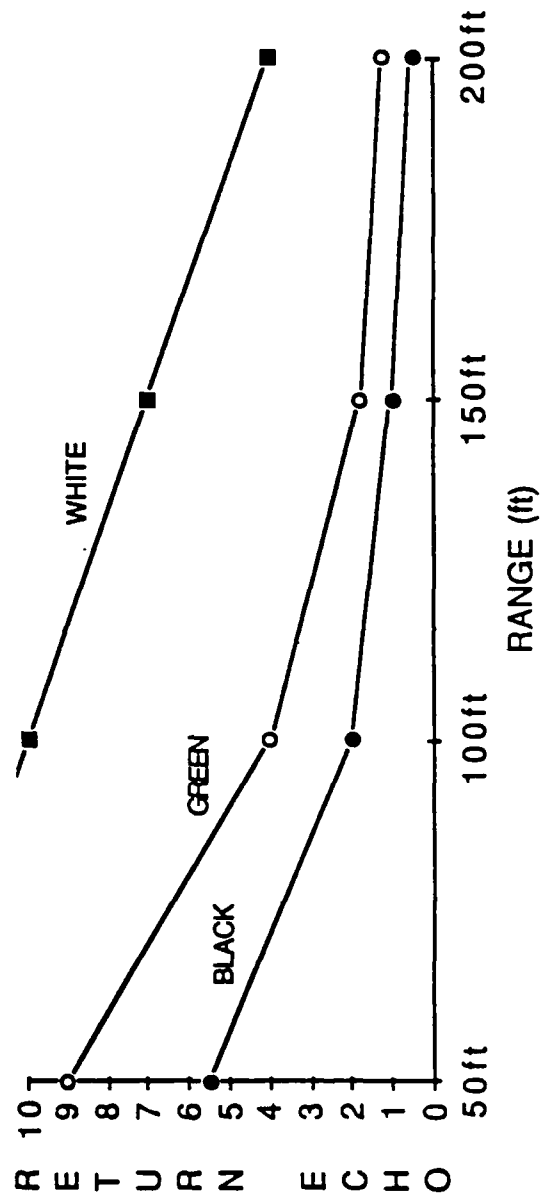


FIGURE 6.8
Echo Strength Versus Range as a Function

EFFECT OF ABSORPTION ON RANGE MEASUREMENT

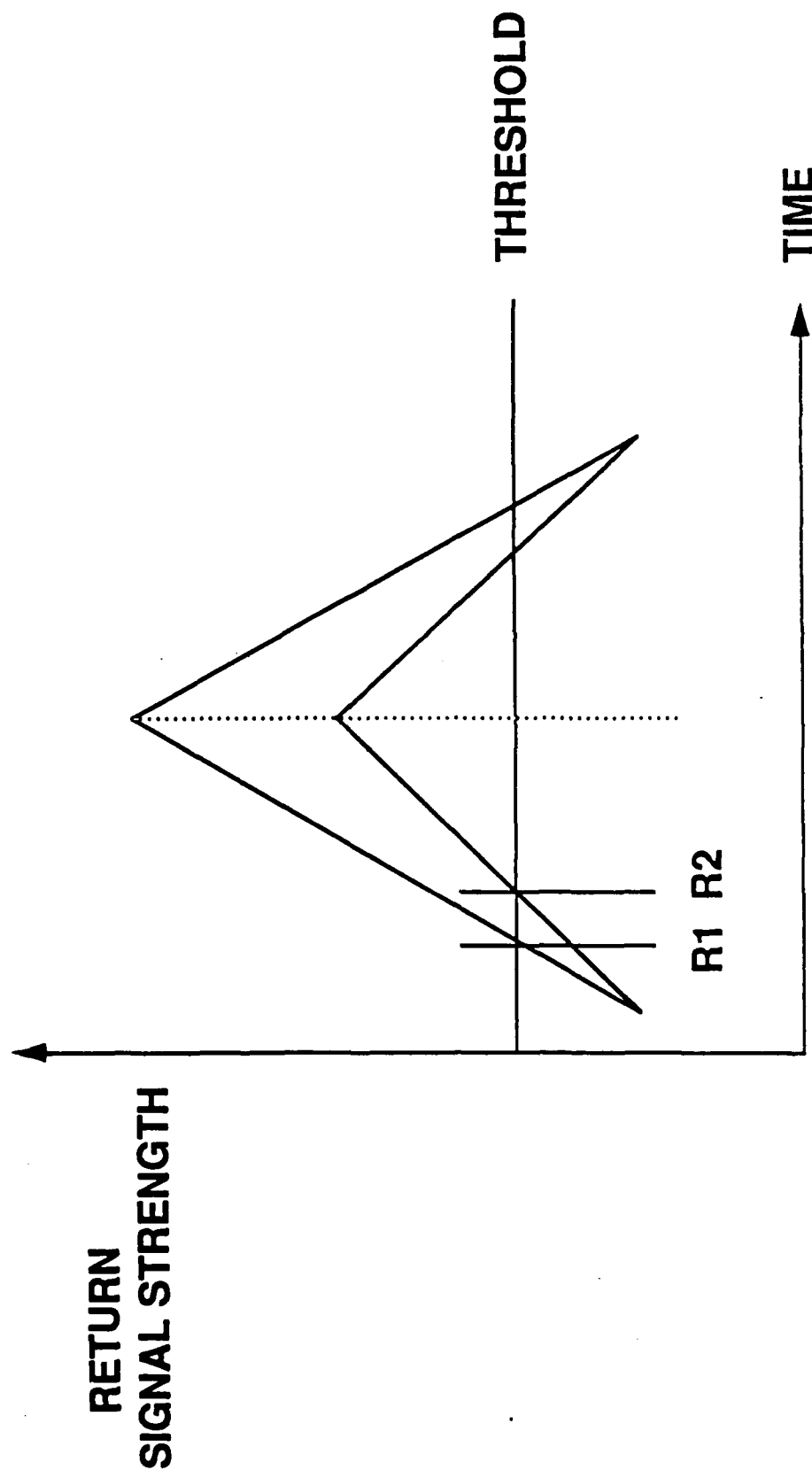


FIGURE 6.9

Effect of Absorption on Range Measurement

The fixed weight neural transform was coded based on the weights developed during training using a neural network development system. This code was loaded onto an off-the shelf IBM PC compatible TMS C30 Digital signal Processing board running at 20 MHz clock rate. The real time, laser based mine detection system resulted from the integration of the TMS C30 board with the Intel 386 based IBM PC. This system was then tested for individual mine detection against a laydown of simulated mines. Actual timing measurements taken in the laboratory and during these tests resulted in times of 150 microseconds per window (figure 6.10). This timing was a factor of three too slow for the required performance of the Strawman System.

The TMS C30 specified clock speed is actually 33 MHz. If the TMS C30 board is run this speed, the processing time per window would be reduced to 100 microseconds. These numbers are similar for the ATT 32C DSP chip which is also available off the shelf. However, this performance is still a factor of two too slow for the strawman system. A third chip evaluated was the Intel 860 processor chip. This chip can run at 50 MHz with an effective performance rate of 50 microseconds per window resulting in a per scan processing rate which meets the performance requirements of the strawman system (see figure 6.10) with a twelve component feature vector.

Given that the processing performance requirement could be satisfied for the strawman system, the actual memory required for the test system was determined to be 20 KBytes of which:

- 1) 15.8 KBytes were for storing the tables of weights, biases and the sigmoid function associated with the neural transform.
- 2) 312 Bytes were for the actual transform code.
- 3) 336 Bytes were for the executive shell and data scaling and,
- 4) 3.7 KBytes were for data buffers.

Therefore the processing requirements of the strawman mine detection system could be satisfied with a newly available, off-the-shelf processing chip (i860) and with very little memory required.

All these chips are CMOS technology. The TMS C30 and the ATT 32C chips both run at approximately 1 watt while the Intel 860 runs at 2-3 watts. Cost projections for the TMS family of DSP chips (C10, C25, C30) and the Intel 860 chip show substantial drops in cost over approximately a

PROCESSOR ANALYSIS

TMS C30 TMS C30 INTEL 860
(20 MHZ) (33 MHZ) (50 MHZ)

CLASSIFIER (TRANSFORM) / WINDOW

NO. SAMPLES IN TRANSFORM
PROCESSING TIME (MICROSEC)
MEMORY (BYTES)

- TABLES (WTS, BIAS, SIGMOID)
- CODE

- TRANSFORM

- SHELL / SCALE

- BUFFERS (RAW DATA,
PROCESSED SCAN,
NN INTERNAL LAYERS

12	12	12
150	100	50
15.8 K	15.8 K	15.8 K
312	312	312
336	336	336
3.7K	3.7K	3.7K

CLASSIFIER (TRANSFORM) / SCAN

NO. WINDOWS

PROCESSING TIME (MILLISEC)

TOTAL MEMORY (BYTES)

180	180	180
27	18	9
20K	20K	20K

three year period from introduction. Projected volume costs for the C30 and 860 are below \$200 at commercial rates (Figure 6.11). Military rates are typically a factor of four over commercial rates resulting in processor chips costs under \$1000. The memory required could be implemented in a couple of memory chips. The remaining hardware would be sensor interfacing and support chips.

The required sensor and processing power is presently becoming available to develop low cost, low power mine detection systems.

These capabilities address some of the constraints that may have limited system performance in the past. Of course, additional single chip processing power will become available over the next few years which will allow the more elaborate system architectures, as illustrated in Figure 6.12 , which may be needed to develop the full capability required for a successful mine and minefield detection system.

PROCESSOR CHIP COST TRENDS

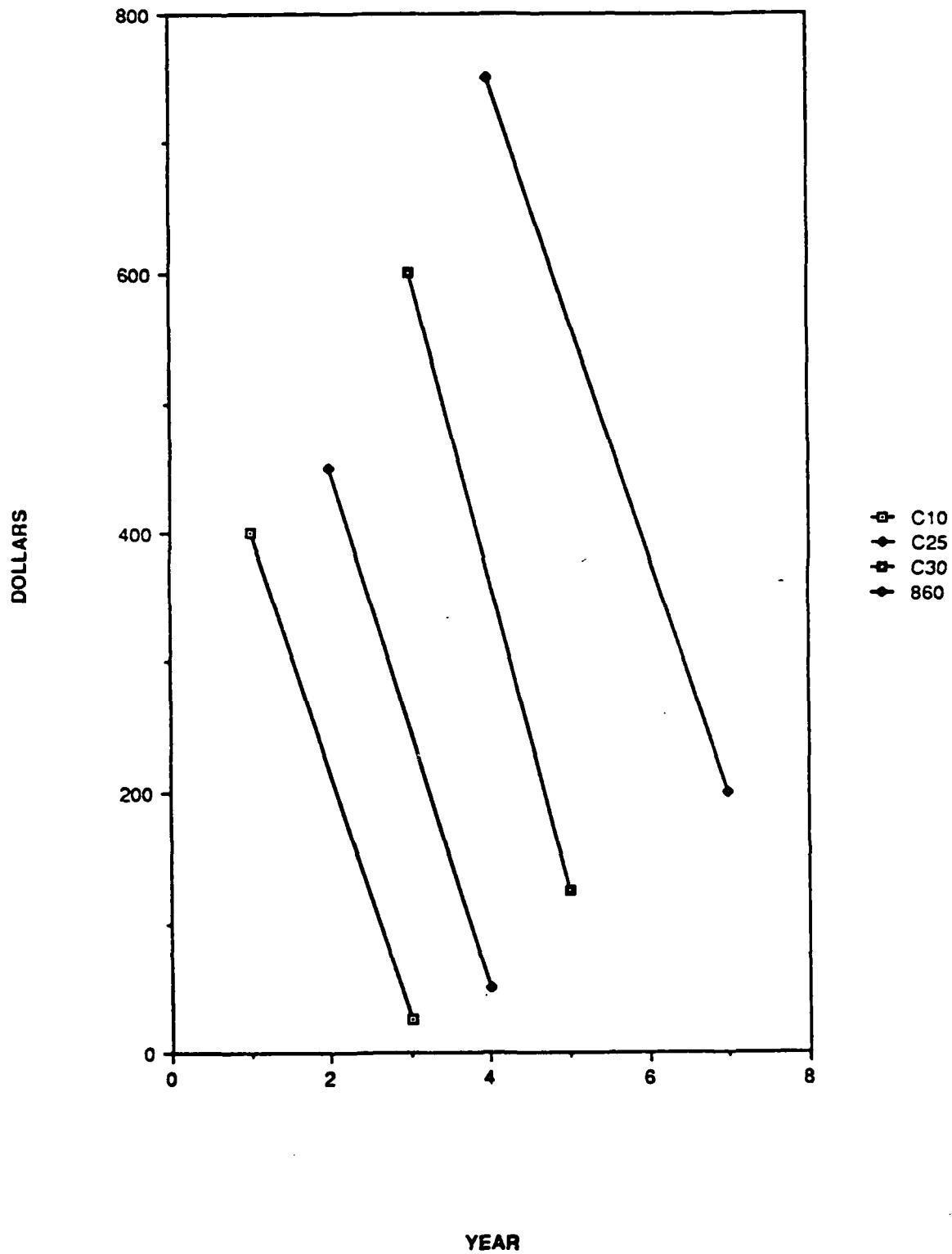


FIGURE 6.11
Processor Chip Cost Trends
-123-

PROCESSING SYSTEM ARCHITECTURE

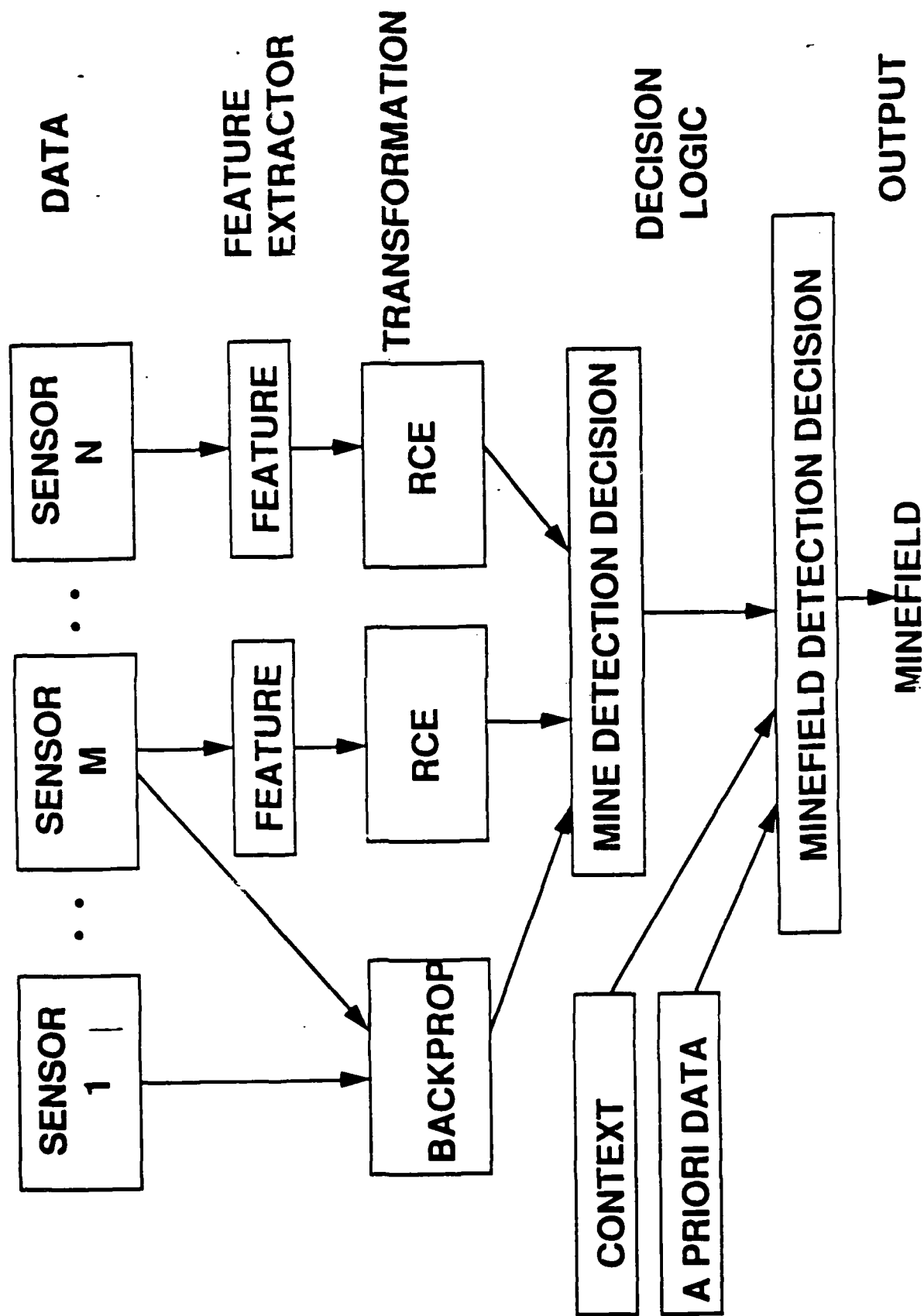


FIGURE 6.12
Processing System Architecture

APPENDIX A

BIBLIOGRAPHY

OF

REVELANT LITERATURE

Test Array #1 for Mine Detection Experiments

ERIM

1/80

AD-A086 142

DAAK70-78-C-0198

Describes Test Site:

- Vegetation: Type, Age, height,
- Stone Content
- Drainage

Describes Mines & Related equipment

- Surface
- Hand Buried
- Machine Buried
- Scatterable: N.B. Scarf Marks

Related Events

- Fence Posts
- Barbed Wire
- Lanes & Ruts
- Foxholes
- Dummy Mineholes
- Tophats & Corners
- Aluminum Angles
- Shell Casings

Weather Data Collected:

- Air Temperature
- Precipitation
- Wind Direction
- Wind Speed
- Cloud Cover: % cover, types, heights

Terrain Conditions

- Cover types
- Plant Height
- Plant Density

Sensors (non simultaneous)

- Minicam
- Photo
- FLIR & Photo
- AAD-5
- Spotlight Radar

Effects of Resolution, Field of View and Vegetation on Sensor Access

ERIM

7/80

AD A090 518

DAAK70-78-C-0198

For line scanners, photographic cameras, television cameras and FLIR's

Presumed need for 2 pixels covering a mine

Depression Angles < 45° required

An Assessment of Technical Factors Influencing the Potential Use of RPV's for Minefield Detection

ERIM

7/80

AD A092 682

DAAK70-78-C-0198

Soviet PM-60 and TM-46 give strong specular returns at 10.6 μm , lesser at 1.06 μm

Should fly under 1860 m

Near Nadir Viewing Angle Desirable

The MIDURA 1982-1983 Experimental Test Plan

ERIM

4/82

AD A172 410 (56602)

DAAK70-81-C-0205

To explore utility of existing assets to detect presence of surface and buried anti-tank mines and minefields.

Using AN/AAS-24 infrared scanner and KS-76 camera pair and AN/AAD-5 infrared scanner and KS-87 camera.

Covering snow conditions, semi-arid, and agricultural lands.

Scatterable mines need special consideration as may be dispersed either on their front or back with different reflectivity and emissivity characteristics.

Refers to BDM report BDM/W-79-231-TR "System Definition for the Detection of Remote Minefields (U) - Volume I" for defensive position protection minefield consisting of 545 TM46 mines installed by 3 cargo trucks with chutes. 3 Rows ~ 50 m apart and mines average 5.5 m apart. Mines 2.5 cm deep & camouflaged to match surrounding terrain. 181 mines per row, 990 m long rows. Minefields 100 m deep.

For snow: mines painted white; sometimes placed on top of compacted snow, some covered by 2" of loose snow. Scatterable mines in snow will create splash holes, perhaps even exposing a path on ground in shallow snow. In deep snow, mine may bury itself.

Record of First Meeting of expert Working Group on Minefield Detection Technology

ERIM

2/79

AD A088 670

DAAK70-78-C-0198

General notes on what was discussed

1 Soviet helicopter or truck can carry 200-400 mines

BDM possibly developed a Model of Minefield Detection Operations

Potential Limitations of Thermal Imagers for Minefield Detection

MERADCOM

4/76

AD B013 413 (56565)

Examined man portable & Vehicle mounted up to 4.6 m high: up to 24 km/h

Marginal Utility owing to environmental effects

Mine Detection by Thermal Imaging

MERADCOM

11/71

AD ? (56566)

Tested AN/PAS-7-() a.k.a. Handheld Thermal Viewer; AN/VAS-1-() Far IR Target Indicator;

AN/AQ-5 FLIR; AN/AAS-24 IR Detecting Set; An/AAS-29 FLIR & AN/PRS-7 Portable Mine Detecting Set

All buried Mines

Required NETD >0.3°C

Loads of data: Frequently no signature in Afternoon but daytime usually best, Hottest at 2 pm coldest at 6 am

Roadway Mine Detection by Airborne Infrared Scanner Imaging

HRB Singer Inc.

9/69

AD 505316 (56575)

N00019-69-C-0701

Buried Mines

Clear Dry Weather: 2°-4° C

Cloudy/Rainy: 0.25°-2.5° C

Greatest difference 15-60 minutes after implantation

Flew from 25-2000 foot altitudes

resolution ~ 3"-6" & $\Delta T < .5^\circ\text{C}$ best performance

No significant improvement with super-resolved disturbance areas

ΔT zero crossings ~ 2 hrs after sunrise/sunset (positive in daytime)

If implanted at night, initially positive, goes negative in minutes

Negligible effects from:

size of disturbance

depth of disturbance (2"-6" to top of mine)

Mine Type

Soil Type

Thermal Imaging of Road Mines

MERADC

3/70

AD 509 748 (56604)

Used AN/PAS-7 Infrared Detecting Set. Mines in roads observable from 1 hour after implantation to 2-1/2 hours after dawn. Thereafter, thermal clutter becomes a problem. Road should be relatively clear of vegetation. Canopy over road subdues thermal differences. Signatures disappear in saturated soil. Highly reflective material (e.g. crushed marine shells) produce clutter. Independence of mine type, time of burial during the night, and soil types.

Feasibility of Land Mine Detection by Infrared Thermal Imagery

ERDL

3/23/63

AD 342602 (56567)

Early capability concepts & anecdotal data

Array 1 Photo Imagery Analysis

ERIM

7/80

AD A090 518

DAAK70-78-C-0198

Mono & Stereo Analysis

Obscuration by vegetation a problem but not major negating factor

Analysis of Aerial Photography from Array II (1980)

ERIM

5/82

AD A172 337 (56603)

DAAK70-81-C-0205

Marginal results. Specular reflections off surface mines & shadows were important.

Radar Detection, Discrimination, and Classification of Buried Non-Metallic Mines
Georgia Institute of Technology
2/78

AD A054 427 (?)
DAAG53-76-C-0112

To analyze wideband CW radar to determine potential for detection, discrimination, and classification of buried objects and to determine the portion of the spectrum most useful for those capabilities.

Determined that 40 ms was required to detect, discriminate and classify each mine which was correctly processed. Spectrum from 0.5 - 1.5 GHz sufficed for anti-vehicular non-metallic mines in relatively dry soil

Report contains description of Data collection, data reduction, mathematical models (including wet soil effects), discrimination/classification algorithms (including CFAR, pattern recognition, & correlation processing), algorithm performance and comparisons, and hardware requirements.

Studies Concerning the Recognition of Subsoil Targets by Means of Microwaves
ERADL

9/21/62

AD 288 864 (56545)

Covers basic considerations, classification of techniques (matched, balanced, ground contact, cross polarized, shifted frequency, distance recognition, and surface sensing), target responses and an experimental system

Nonconventional Aspects of Radar Target Classification by Polarization Properties
MERADC

6/73

AD 763 155 (56543)

Reviews system requirements and examines role polarization phenomena can play in meeting requirements for detection of embedded objects in inhomogeneous media. Derives rigorous equations describing depolarized echo of radar reflectors as a function of physical shape and polarizational state of incident wave. Mie's scattering theory is extended to include dissipative media and to permit computation of RCS' of spheres for any combination of complex material constants.

Scattering of Electromagnetic Waves by Buried Dielectric Bodies
Mei, Morgan & Chang, UC Berkeley

6/77

AD A043 806 (56550)

DAAK02-75-C-0002

Theoretical solutions to scattering of electromagnetic fields by dielectric bodies of revolution using unimoment method and frequently applying finite element method.

Microwave Techniques for Imaging Objects Buried below the Surface of the Ground
General Dynamics

6/73

AD-771 988 (56553)

DAAK02-71-C-0264

0.21-3.9 GHz Bistatic .05 W CW detected objects down to 4" below surface in general conditions, inches above surface

Electromagnetic Soil Properties in the VHF/UHF range (Phase 1)
MERADCOM

5/72

AD 747 346 (56554)

General but not strict increase in attenuation with moisture content
windows occur above 500 MHz

2 - 20 db/m for dry (.10%); 40 - 60 db/m for medium (~ 15%); 60 - 100 db/m for wet (~ 25% +)

Automated Laboratory Short Pulse Microwave System for Mine Detection

SRI

10/71

AD 893495 (56552)

DAAK02-68-C-0160

Non-Metallic mines detectable at 400-3440 Mhz & 480-2000 Mhz bands by virtue of dielectric property differences between mine & soil. Metallic mines even better

Data on Signal strength versus height (1" to 24")

Some soil attenuation data

Research on a Vehicular-Mounted Mine-Detector Radar - Final Technical Report

CALSPAN

11/73

AD 528 796 (56546)

DAAK02-72-C-0444

Design & Fabricate 3 short pulse microwave radars and gather data from mines & assortment of false targets.

Five forms of discrimination were evaluated: Amplitude only, Amplitude plus Phase, Hybrid Processor (of first two), Discriminant Analysis, & Feature Vector. Concluded that Amplitude plus Phase using Eight spectral lines offers most promise.

Detailed Design for Amplitude plus Phase processor presented.

Microwave Mine Detector - Final Technical Report

Dalmo Victor

7/19/63

AD 349629 (56544)

DA 44-009-ENG-5165

Bistatic, 1" to 2-1/2" above ground

Description, Environmental Test Results, etc.

Antennas for Mine Detection Systems - Final Technical Report for Phase III

Ohio State University, ElectroScience Laboratory

5/71

AD 889410 (56540)

DAAK02-69-C-0693

Construction & test of 20 element phased array antenna for electromagnetic detection of dielectric buried mines operating in 100-1500 MHz emphasizing 500-1000 MHz..

Phase I was investigation of single loop 2 element arrays.

Phase II built & tested a search head using two six element arrays.

Scattering by Buried Obstacles

Mei et al, California University

11/74

AD A005 237 (56551)

DAAK02-71-C-0206

Theory, math & expected responses from mine shaped objects

Monostatic Microwave Imaging of Buried Objects Vol I

General Dynamics

10/74

AD A004 861 (56556)

DAAK02-71-C-0264

Developed images in damp (3-5%) smooth soil of objects buried 1" -5" from height of 4"

Microwave Radiometric Studies in Relation to Mine Detection

ERADL

11/66

AD 646 730 (56373)

for C band (4-6 Mhz) microwave detector against buried mines
found unsuitable for mine detection

The greatest effect of a buried mine on soil temperature distribution results from the moisture anomalies the mine produces in the soil

Contains good data & relevant equations for soil moisture, radiative heat transfer, and other theoretical/modeling concerns.

Measurement & Analysis of L- and X-Band Mine Cross Section

ERIM

8/79

AD A088 630

DAAK70-78-C-0198

Several anti-tank mines including Soviet TM-46 and East German PM-60
at 1.2 and 1.65 GHz

In free space, median Cross Sections ~-13 and -20 dBsm respectively

Concludes detection in typical East European clutter backgrounds not possible.

In X-Band: American M-15 a good substitute for TM-60: -3 to -4 dBsm at 10° depression. PM-60's -20 dBsm

Reason for frequency dependence not understood

Strong polarization dependence exhibited in L- but not X-Band

Fuze affected side view RCS'

Side views (low depression angles) preferred (<30°)

Survey of Microwave Attenuation Due to Atmospheric Gases and Precipitation

ERADL

2/14/63

AD 751 454 (56541)

Data & Curves for 3 to 300 GHz for those interested

Investigations of Soil Penetrating Radar with Emphasis on Short Pulse Mine Target Responses and the Development of System Components - Final Technical Report - Part B Development of System Components

Advanced Technology Corporation

3/31/68

AD 857 301

DAAK02-67-C-0512

Designed, fabricated & Tested two antennas: low frequency reflector backed magnetic dipole or loop antenna insertable into soil

Presents Dielectric constants and loss tangents for loam & clay; attenuation characteristics of soil versus frequency (70 - 110 Mhz); radiation patterns

Analysis of Oceanic Subsurface Features using Space Based Radar Imagery

Underwater Systems, Inc.

6/82

AD A118 411 (56558)

N00014-82-C-0114

Used SEASAT & SIR-A images to investigate limits to visibility of bathymetric features. Considered tidal levels, currents, wind, rain, radar incidence angle, radar aspect angle and radar processing.

Lack of ground truth severely limited results of study. Some dependence on current and independence of radar incidence angle was discovered.

2nd Annual Consultants Report on Mine Detection by Unique Nuclear Reactions

Texas Nuclear Corporation

11/28/60

AD 322791 (56555)

DA-44-009 ENG-4476

A few papers on techniques

Theory and Application of X-Ray and Gamma Ray Backscatter to Landmine Detection

MERADCOM

3/75

AD A015 541(56569)

Mostly Theory, Considers operation < 1' above ground

Analysis of Vapors Emitted from Military Mines

CRREL

9/73

AD 768 709 (56570)

Cyclohexanone positively identified from both metallic and nonmetallic mines. Compounds from nonmetallic mine casings also identified.

Detection of Cyclohexanone in the Atmosphere above Emplaced Antitank Mines

CRREL

4/74

AD 778 ? (56574)

Cyclohexanone detected 17 hours after emplacement. Collection over 7 hours to determine flux rate.

Seismic and Electromagnetic Tunnel Detection Investigation

7/75

MERADC

AD A018 984 (?)

Review of Tunnel Detection work from 12/66 through 12/69

Land Mine Detection System - Final Report

TRW

2/23/73

AD 008713? (56559)

DAAK02-72-C-0340

Acoustic Detection

Positive Results > 12" deep

3 KHz best

Actual results unreadable (apparently Oscilloscope Traces which didn't reproduce)

Geographical Analog Soils Survey -Final Report - Volume II

Southwest Research Institute

10/1/73

AD 784 283 (?)

DAAK01-72-C-0638

To locate CONUS land areas which are similar in all aspects to selected areas in other parts of the world. Analogous soil types were found for most cases. Analogous climates not always found with analogous soils.

Afghanistan, Austria, Belgium, Czechoslovakia, England, France, Germany (especially Flensburg, Koblenz, Meppen, Munsterlagen, Reichenhall & Bendsburg), Italy, Netherlands, Poland, Portugal, Soviet Union, Scotland, Spain, & Turkey.

**In Situ EM Soil Properties Measurement, Instrumentation, Theory, and Method -
Volume III**

Southwest Research Institute

6/7/74

AD 784 284 (?)

DAAK02-72-C-0638

Measure soil properties required for land mine detection applying rf measurement for frequency range 300-4000 MHz. Measurements limited to rock free fairly homogeneous soils owing to probe Kit developed which gave reliable

Soil Moisture Studies

ERADL

10/4/60

AD 247 265 (56568)

Data using microwave detector of soil including soil/mine

A Framework for Digital Airborne Reconnaissance Systems: Applications to Surface Minefield Detection using Passive Imagery Vol II

EWES

10/84

AD-C036 130 (38884)

Reporting on findings from other studies:

- buried mines under tall grass couldn't be detected

- mines buried in an unseeded wheatfield were identifiable but if reseeded PD reduced

- Exposed mines in daylight in wheatfield identifiable in both 4.5-5.5 μm and 8-14 μm

- less identifiable in grass in same conditions

- In one case exposed mine were more identifiable in grass than wheatfield in 1-3.3 μm band

- Different mine types produce similar ΔT

- Larger ΔT with buried mine than simply disturbed earth

- ΔT reduces with depth of burial

- Rain reduces ΔT

- Cloud cover reduces ΔT

- For IR sensors, overall PD = 45% & FAR = 70%

Developed thermal model for minefield signatures, results of model, and actual data collection

Appendix B: Soviet & Warsaw Pact Mine Warfare Doctrine & Equipment with Bibliography

Hasty Minefields:

- Intermittent Strips w/ small gaps;

- 500 /km

- Buried or surface

Deliberate Minefields:

- 3 rows per belt

- 40 - 100 m between rows

- 750 - 1000 AT mines / km

- 1 in 5 has shaped charge

AT & AP mines not mixed!

- a complete row of AP within a belt

- or on sides of a belt

AP mines 2000/km; 200-400 of these have tripwires

Numbers may vary by factor of 3 either way

depending on situation

Emplacement

- hand tracing tapes: 20 m long, varied spacing & offset

- Combination: rows 10-30 m sep, mines 4 or 5.5 m sep

- hand buried or camouflaged

- if double chute: 10-15 mines per minute

- Helicopter Dispensed: Parallel rows

- Minelayer: rows 10-30 m sep, mines 4 or 5.5 m sep

Up to 15 cm deep

List & Characteristics of Warsaw Mines

**A Characterization of West German Terrain and Land use in Connection with
Minefield Detection**

ERIM

8/80

AD-A092 681

DAAK70-78-C-0198

North German Plain: Ditches, some swamps & Bogs, farming on Loess

Fulda Gap: Plateau of Infertile Hard rock, brown forest soil over rock, silt

Hof Corridor: little soil over rock, alluvial soil

Soviet Minefields: .5 - 15 Hectares, up to 1 km long

PM-60 are plastic

TM-46 are metal

Scenarios:

- 1) protect flank in meeting engagement
345 PM-60 surface over 50 x 1000 m for 1 hr
- 2) Protect Shoulders during Breakthrough
750 TM-46 Surface over 150 x 1000 m for 20 hr
- 3) Block enemy Reinforcements
60 TM-46 surface over 50 x 100 m for 8 hr
7 PM-60 buried within 50 m radius for 8 hr
- 4) Support Prepared Defense
545 TM-46 or MV-5 over 150 x 100 m indefinite

Climatology of Selected areas of West Germany affecting Sensor Performance

ERIM

6/79

AD-A086 945

DAAK70-78-C-0198

North German Plain, Fulda Gap, and Hof Corridor

Predominance of surface Mines expected

Covers:

Temperature

Monthly Mean

Daily Minimum/Maximum

Diurnal & Day to Day variations

Precipitation

Monthly Mean Rain & Snow

Days precipitation per month (~ half of each month)

Thunderstorm Frequency (10% - 23% May through August)

Precipitation Rate

Water concentrations by region & altitude

Rainfall duration

Sky Cover

Fractional Sky Cover

Vertical Distribution

clear/partly cloudy/cloudy days (Cloudy 3 weeks per month)

Cloud Types

Cloud Obscuration vs Depression angle

Water content of Clouds

Sky Cover duration

Probability of ground fog

(33-37% fall & winter lasting 5-6 hours

12% Spring lasting 3.6 hours, negligible in Summer)

Visibility

Frequency of visibility by month

Ceiling/visibility duration

Other

Monthly precipitation-temperature relations

Air mass incidence & Statistics

Height of 500 mB Atmospheric Pressure surface

Representative Weather Sequences

Identification and Screening of Remote Mine Detection Techniques

ERIM

6/79

AD-A086 944 (56578)

DAAK70-78-C-0198

Includes mines, minefields, minelaying equipment, and minelaying operations

Spotlight SAR promising

E-O in order of preference: Active 10.6 μ m, multispectral scanners; Passive IR

IR lowest because of atmospheric attenuation & resolution! (assumes standoff)

Intensifiers, TV, SIGINT excluded for operational considerations

Also brief reviews of Acoustic (i.e. remote explosion detection and minelaying equipment), vapor, nuclear, animals, and SIGINT

May be gaps of 20 mine separations

For 1 algorithm presented PD individual leading to PD of minefield

Presents PD versus altitude & Clutter for human interpretation

Use of Texture Analysis Methods In the Characterization of Minefields and Background In High Resolution Multispectral Imagery

Harlow & Trivedi - Louisiana State University

10/85

AD B099 011 (56577)

DACA39-83-M-0399

Identification of mines by size shape and texture

Multi spectral: visible (0.55-0.90), near IR (0.92-1.10), thermal IR (8.5-12.5)

Various mine types and mine-like clutter

Recorded environmentals: vegetation density, type, surface topography, solar radiation, wind velocity, humidity

Fulda region & Aberdeen Proving Grounds

Refers to rule based logic presented in Vol I to AD-C036 130

Uses Gray Level Co-occurrence Method

Applied to both mines & minefields

Positive results

Detection of Remote Minefields - Project Plan 1

ERIM

15/12/78

AD-A172 476 (56578)

DAAK70-78-C-0198

Many Scenarios listed in Appendix

INDICATORS:

Offensive: look for main avenues of approach & assembly areas

Concentration/Assembly areas

Lane Clearing/marketing/obstacle removal

Divisions massed toward flanks

Echeloned columns moving forward

Blocking: look for critical terrain objectives (road, junctions, bridges, etc) in friendly rear areas

Airborne or Air Assault units introduced in rear areas

Defensive: look for obstacles, battle positions, likely channelizations & areas of avoidance ending, pockets, etc

Construction & occupation of successive defensive lines

preparation of battalion strongpoints on key terrain

PATTERNS

Row Mine Pattern:

4 rows

5 m mine separations over 100 m

10 to 25 m row separations over 50 m

Strip Pattern:

2 strips

5 m separation alternating offset \pm 3 m from strip line

20 - 40 m strip separation

APPENDIX B1

SENSOR SUITE DESCRIPTION FOR

DATA COLLECTION 1

Sensor Suite and Data Descriptions for Data Collection I

Following are the descriptions and specifications of the selected sensor suite for Data Collection I

B.1 Laser Range Finder

B.1.1 Description

The Model G150 (manufactured by Optech Incorporated) is a pulsed laser rangefinder for performing distance measurements to virtually any target.

The unit operates on the principle measuring the time of flight of an optical pulse generated by a Gas laser. By firing the laser at a high repetition rate and employing averaging reduce random errors, a resolution of 1 cm is achieved.

State-of-the-art microprocessor and surface mount technology has been used, resulting in a compact package suitable for hand-held operation or for mounting on a tripod. The unit will be interfaced to a computer via the standard RS232 output. This allows continuous unattended monitoring. The Model G150 is suitable for measurements to both fixed and moving targets and will operate in the day or night. A measurement can be initiated either by means of the push-button switch on the unit or by means of an external trigger provided by a computer or control circuit.

The unit will be mounted near the MMW radar to take advantage of the azimuth and elevation control capability of the testbed.

Detailed specifications for the rangefinder described in the previous paragraph are listed in the following paragraph.

B.1.2 Specifications

Range	0.1m to 100m (4" to 320')
Resolution	1cm (.4")
Accuracy	$\pm(5\text{cm} + 50 \times 10^{-6} \times \text{distance})$ from 10°C to +30°C $\pm(10\text{cm} + 50 \times 10^{-6} \times \text{distance})$ from -20°C to +50°C
Laser Wavelength:	904 nm
Beam Divergence:	5mRad
Measurement Time:	0.6 sec.
Display:	6 Digit LED
Digital Data Output:	Serial (RS 232 compatible)
Analog Output:	0-5V or 4-20mA corresponding to 0-100m; 2.5cm
(optional)	(1") res.
Operating Temp.:	-20°C to +50°C
Storage Temp.:	-40°C to +50°C
Humidity:	0-95% non-condensing
Input Power:	Internal battery pack or 12 VDC external supply
Operating Time From	
Internal Battery:	1 hr continuous operation (approx. 3,600 measurements)
Size:	Approx. 200 x 115 x 105 mm (7.9" x 4.5" x 4.1")
Weight:	Approx. 1.5kg. (3.3 lb.) (excluding battery)

B.2 Passive IR Cameras (Inframetrics)

B.2.1 Description

The following pages provide information on the passive IR cameras manufactured by Inframetrics Inc. to be utilized during this test sequence it includes a camera in the (3-5 μm) and the (8-12 μm) ranges detail specifications follow.

B.2.2 Specifications

Spectral Bandpass (Nominal) 8-12 μm , 3-5.5 μm or 3-12 μm
Detector Mercury/Cadmium/Telluride (HgCdTe); @ 77K
Detector Coolant Liquid Nitrogen
Dewar Hold Time More than 3 Hours
Typical Minimum Detectable Temperature Difference
 @ 30C (8-12 μm , 3-12 μm) 0.1C
 @ 30C (3-5 μm) 0.2C
Noise Equivalent Temperature Difference (typical)
 @ 30C (8-12, 3-12 μm) less than 0.2C
 @ 30C (3-5.5 μm) less than 0.4C
Scan Rate:
 USA 8 KHz Horizontal; 60 Hz Vertical
Output Rate:
 USA 15,750 Hz Horizontal; 60 Hz Vertical
 International 15,750 Hz Horizontal; 50 Hz Vertical
Field of View (FOV) 15 Deg Vertical x 20 Deg Horizontal
 8X Continuously Adjustable E-O Zoom
Horizontal Resolution at 50% Slit Contrast:
 USA and International (8-12 μm) 1.8 mRad, 197 IFOVs/Line
 256 Pixels/Line
 USA and International (3-5.5 μm) 3.5 mRad, 100 IFOVs/Line
 256 Pixels/Line

Output Format

USA RS-170, NTSC & RGB
Dynamic Range 7 Bit, 128 Levels, 42dB
8 Bit, 256 Levels, (48 dB) with Image Averager

Temperature Reference

USA Internal Reference Sampled @ 60 Hz
Temperature Spans5, 10, 20, 50, 100, 200 Normal Range
50, 100, 200, 500 Extended Range
Temperature Measurement Range -20 to +400 C Normal Range
(for 8-12 um, no filters) 0 to +1500 C Extended Range
Temperature Readout Resolution 3 Digits

Power Requirements:

System 11-17 VDC, 10 Watts
Monitor (5" Video Color) 11-15 VDC, 15 Watts
AC Power Supply
USA. 108-125 VAC, 60 Hz
Ambient Operating Temperature. -15 to +45 C
Dimensions (l x w x h)/Weights:

Scanner. 8.1 x 4.9 x 4.8 in./6.5 lb.
Control/Electronics Unit 9.3 x 5.4 x 10.3 in./7.5 lb.
5 in. Video Monitor
USA. 12.7 x 4.9 x 6.3 in./8.5 lb.

B.3 High Speed Video Camera

B.3.1 Specifications

The following pages provide the detail specifications of the video camera manufactured by Panasonic.

PANASONIC VIDEO CAMERA

WV-D5000

POWER SOURCE:	12 VDC
POWER CONSUMPTION:	0.48A (MIN). 1.5A (MAX.)
SCANNING:	525 LINES/60 FIELDS/30 FRAMES PER SECOND
PICK-UP SYSTEM:	INTEGRATED COLOR MOSIC FILTER SINGLE CHIP CCD SYSTEM
PICK-UP ELEMENTS:	2/3" 574(H) x 499(V) PIXELS, INTERLINE TRANSFER CCD WITH COLOR MOSIC FILTER
VIDEO OUTPUT LEVEL:	1.0VP-P NTSC COMPOSITE/75 OHMS
HORIZONTAL RESOLUTION (LUMINANCE):	380 LINES AT CENTER
SIGNAL TO NOISE RATIO (LUMINANCE):	46 dB
ILLUMINATION REQUIRED:	140 FOOTCANDLES (1400 LUX) AT F4.0
REQUIRED MINIMUM ILLUMINATION:	0.7 FOOTCANDLE (7 LUZ) AT F1.4 LENS WITH +18dB GAIN UP AT 30 IRE LUMINANCE SIGNAL 1 FOOTCANDLE (10 LUX) AT F1.6 LENS WITH +18dB GAIN UP AT 30 IRE LUMINACE SIGNAL

LENS:

(1) AUTO FOCUS:	NO
(2) ZOOM RATIO:	12X
(3) FOCAL LENGTH:	10.5 - 126mm
(4) MAXIMUM APERTURE RATIO:	1 : 1.6 (F1.6)
(5) FOCUSING RANGE:	1m
(6) MACRO RANGE:	5 cm - 1m
(7) IRIS RANGE OF AIC:	1.6 - 22.C
(8) FIELD ANGLE:	TELE WIDE
DIAGONAL:	4.9 57.4
HORIZONTAL:	4.1 44.3
VERTICAL	3.1 33.9
(9) FILTER DIAMETER:	72mm P = 0.75
(10) FLANGE FOCAL LENGTH:	17.526mm

(11) ZOOM SPEED:

FAST:

APPROX. 7 SECONDS

SLOW:

APPROX. 10 SECONDS

LENS MOUNTING:

BAYONET MOUNT

VIEWFINDER

BLACK AND WHITE 1" ELECTRONIC VIEWFINDER WITH
CHARACTER DISPLAY (OPTIONAL: WV-VF01)

WHITE BALANCE:

AUTO TRACING WHITE-BALANCE (ATW) OR MANUAL

SETTING (AWC)

OPERATIONAL AMBIENT TEMPERATURE:

32°F 104°F (0°C +40°C)

OPERATIONAL AMBIENT HUMIDITY:

LESS THAN 90%

CAMERA MOUNTING:

ONE 1/4" -20 THREADED STANDARD CAMERA TRIPUD

DIMENSIONS:

WV-D5000 ONLY

5-7/16" (W) x 4-1/2" (H) x 5-3/8" (D)

(138.5(w) x 114 (H) x 136 (D)mm)

WEIGHT:

WV-D5000 ONLY:

1.9 LBS (0.9kg)

WEIGHTS AND DIMENSIONS SHOWN ARE APPROXIMATE.

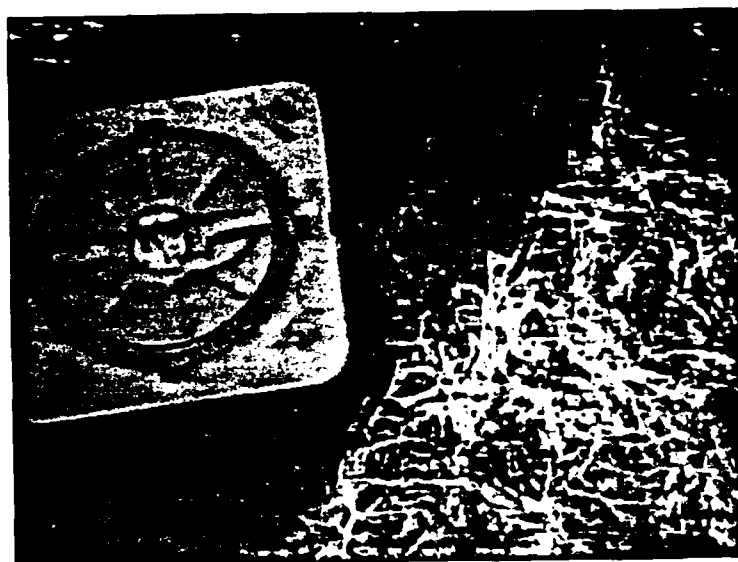
SPECIFICATIONS ARE SUBJECT TO CHANGE WITHOUT NOTICE.

APPENDIX B2

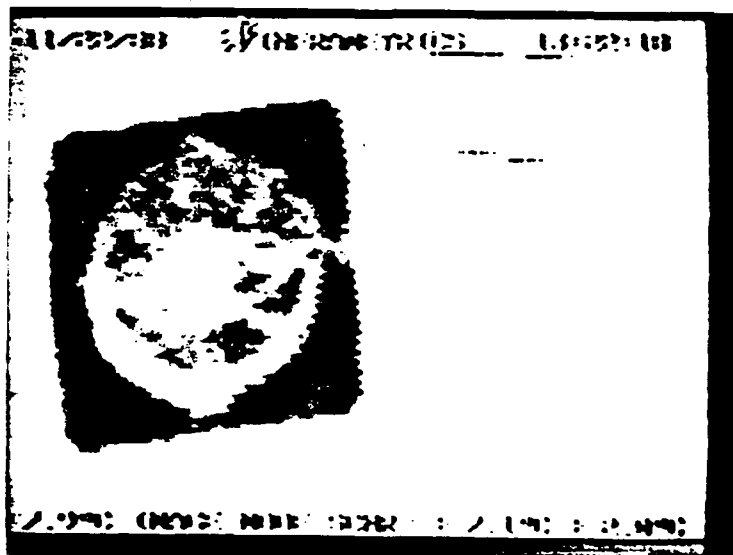
**COINCIDENT DATA FROM
DATA COLLECTION 1**

TARGET DESCRIPTION: PLASTIC SURFACE MINE
DATE: 11/22/88
TIME OF DAY: 13:26

VISIBLE
IMAGERY



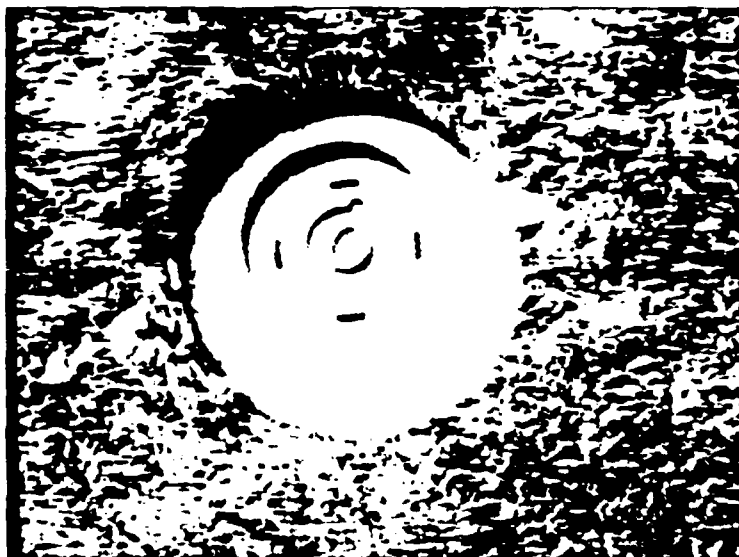
PASSIVE IR
IMAGERY (8-12UM)



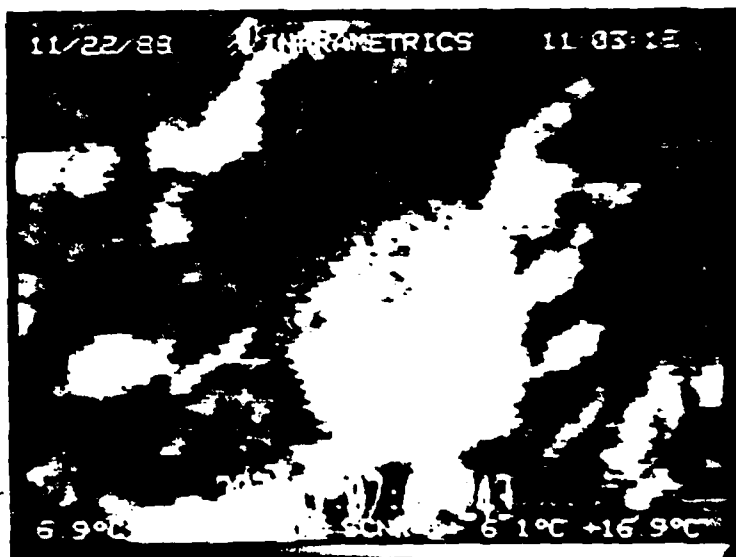
SLANT RANGE: 50 FEET
DEPRESSION ANGLE: 60 DEGREES

TARGET DESCRIPTION: METAL SURFACE MINE
MINE DATE: 11/22/88
TIME: 11:03

VISIBLE
IMAGERY



PASSIVE IR
IMAGERY (8-12UM)



SLANT RANGE: 50 FEET
DEPRESSION ANGLE: 60 DEGREES

TARGET DESCRIPTION: BARLEY COVERED PLASTIC MINE
DATE: 11/22/88
TIME OF DAY: 15:07

VISIBLE
IMAGERY



15 07 35

PASSIVE IR
IMAGERY (8-12UM)



15 07 35 890

SLANT RANGE: 50 FEET
DEPRESSION ANGLE: 60 DEGREES

TARGET DESCRIPTION: CLUTTER

DATE: 11/22/88

TIME OF DAY: 10:47

**VISIBLE
IMAGERY**



**PASSIVE IR
IMAGERY (8-12UM)**



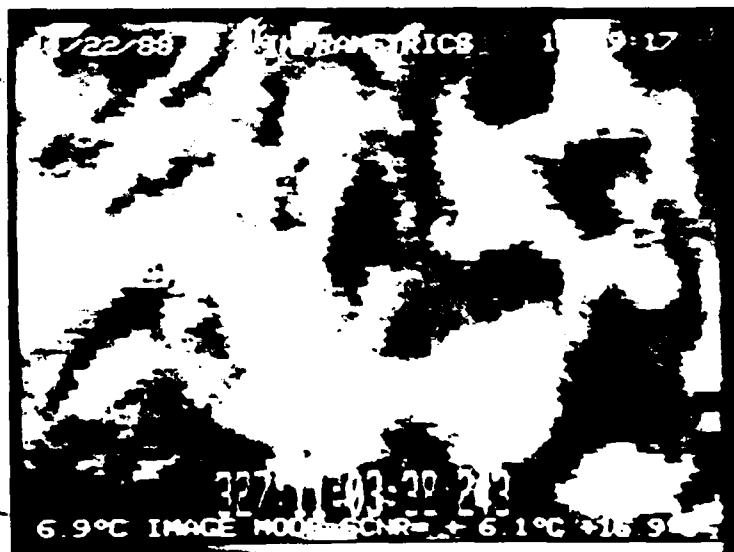
**SLANT RANGE: 50 FEET
DEPRESSION ANGLE: 60 DEGREES**

TARGET DESCRIPTION: CLUTTER
DATE: 11/22/88
TIME OF DAY: 10:59

VISIBLE
IMAGERY



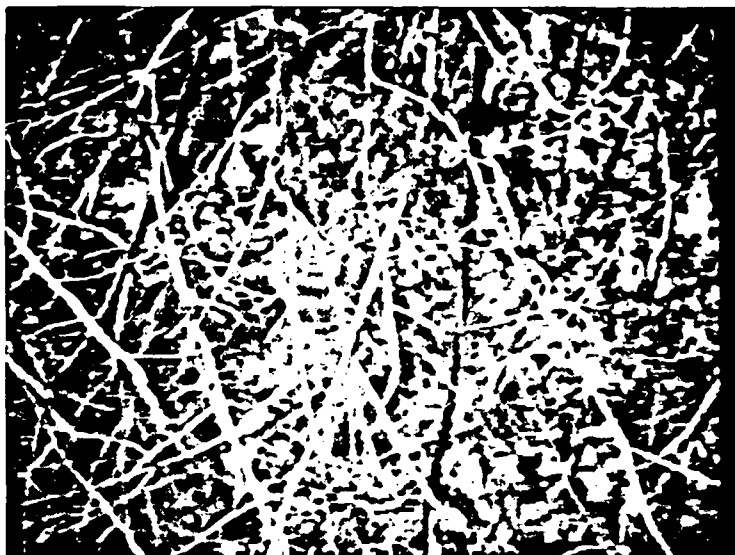
PASSIVE IR
IMAGERY (8-12UM)



SLANT RANGE: 50 FEET
DEPRESSION ANGLE: 60 DEGREES

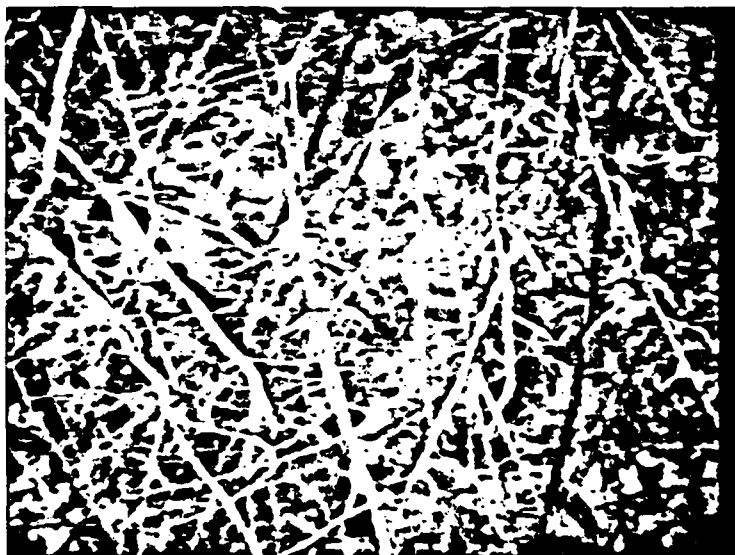
TARGET DESCRIPTION: METAL MINE IN HEAVY BRUSH
DATE: 12/19/88
TIME OF DAY: 13:17

VISIBLE
IMAGERY



13:17

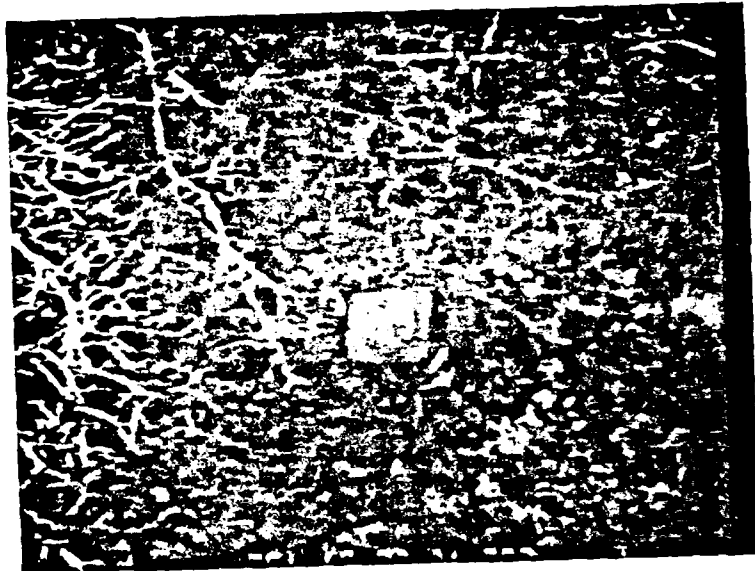
VISIBLE
IMAGERY



SLANT RANGE: 50 FEET
DEPRESSION ANGLE: 60 DEGREES

TARGET DESCRIPTION: PLASTIC MINE IN HEAVY BUSH
DATE: 12/19/88
TIME OF DAY: 13:26

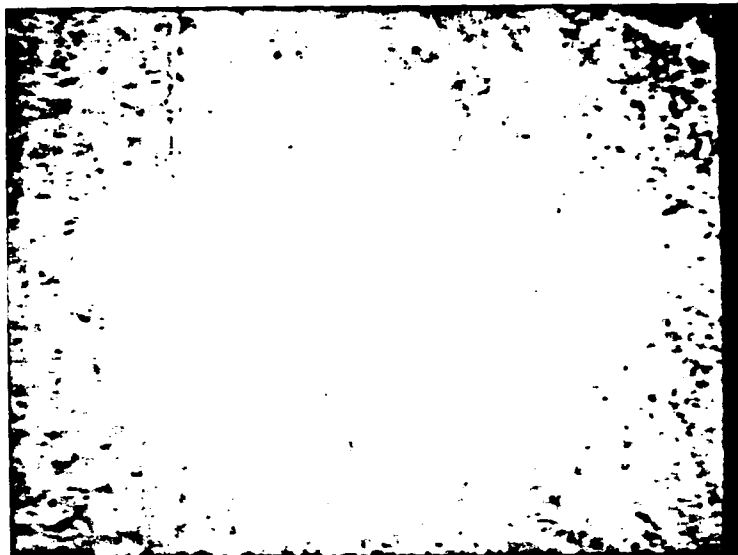
**VISIBLE
IMAGERY**



SLANT RANGE: 50 FEET
DEPRESSION ANGLE: 60 DEGREES

TARGET DESCRIPTION: METAL SURFACE
DATE: 12/20/88
TIME OF DAY: 13:37

VISIBLE
IMAGERY



PASSIVE IR
IMAGERY (8-12UM)

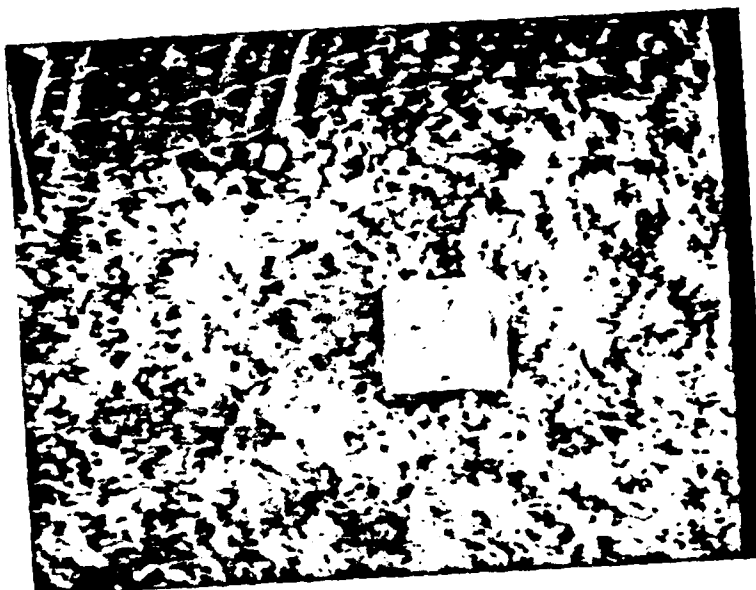


SLANT RANGE: 50 FEET
DEPRESSION ANGLE: 60 DEGREES

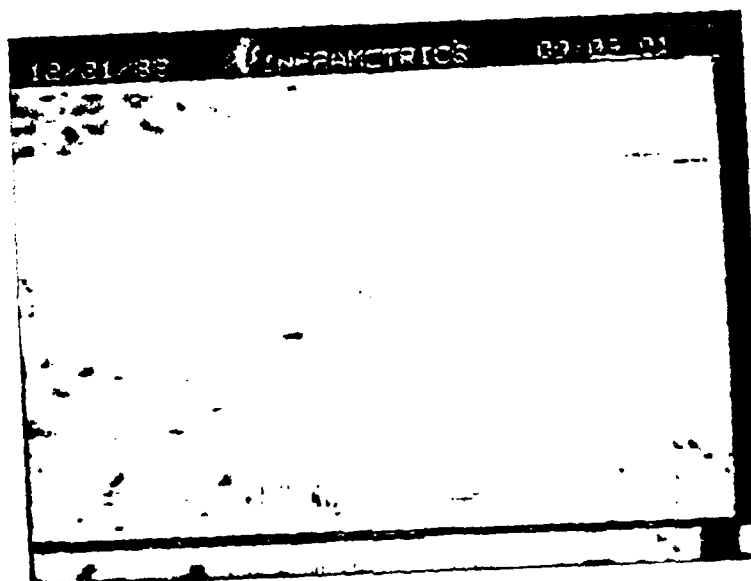
337 3013

TARGET DESCRIPTION: PLASTIC SURFACE MINE
DATE: 12/21/88
TIME OF DAY: 09.09

VISIBLE
IMAGERY



PASSIVE IR
IMAGERY (8-12UM)



SLANT RANGE: 50 FEET
DEPRESSION ANGLE: 60 DEGREES

TARGET DESCRIPTION: DISTURBED EARTH

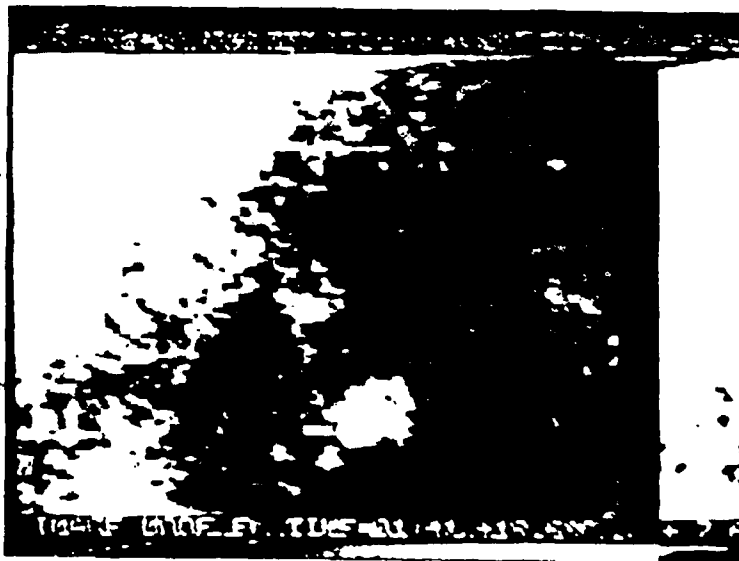
DATE: 12/21/88

TIME OF DAY: 10:15

VISIBLE



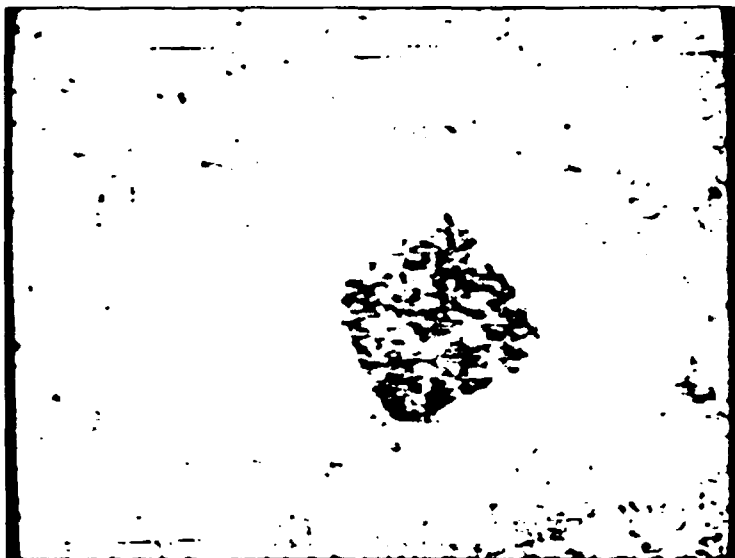
**PASSIVE IR
IMAGERY (8-12UM)**



SLANT RANGE: 50 FEET
DEPRESSION ANGLE: 60 DEGREES

TARGET DESCRIPTION: DISTURBED EARTH
DATE: 12/21/88
TIME OF DAY: 10:15

**VISIBLE
IMAGERY**



**PASSIVE IR
IMAGERY (8-12UM)**



SLANT RANGE: 50 FEET
DEPRESSION ANGLE: 60 DEGREES

TARGET DESCRIPTION: DISTURBED EARTH

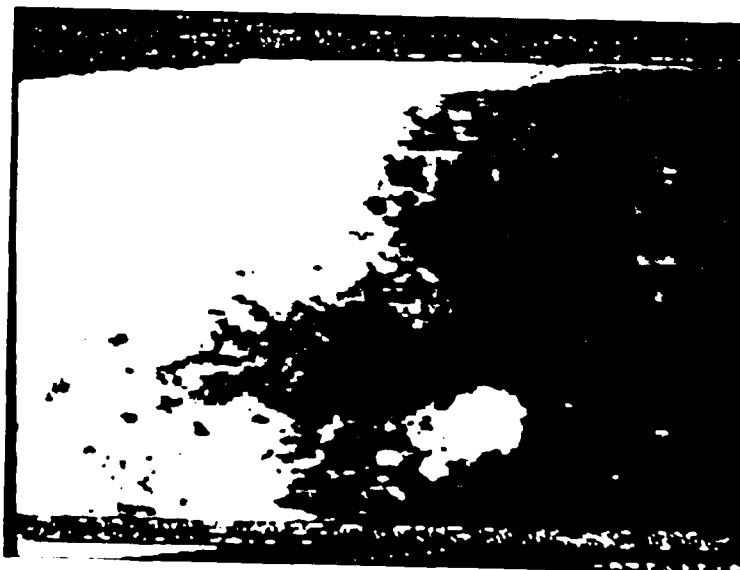
DATE: 12/21/88

TIME OF DAY: 10:15

**VISIBLE
IMAGERY**



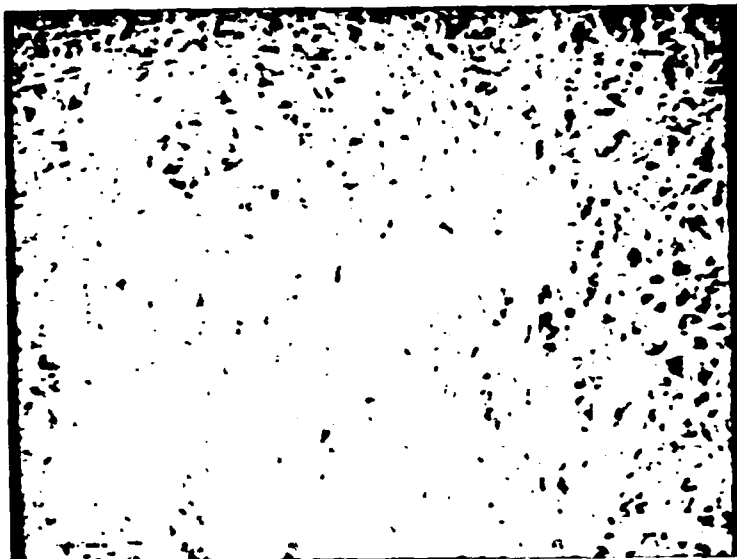
**PASSIVE IR
IMAGERY (8-12UM)**



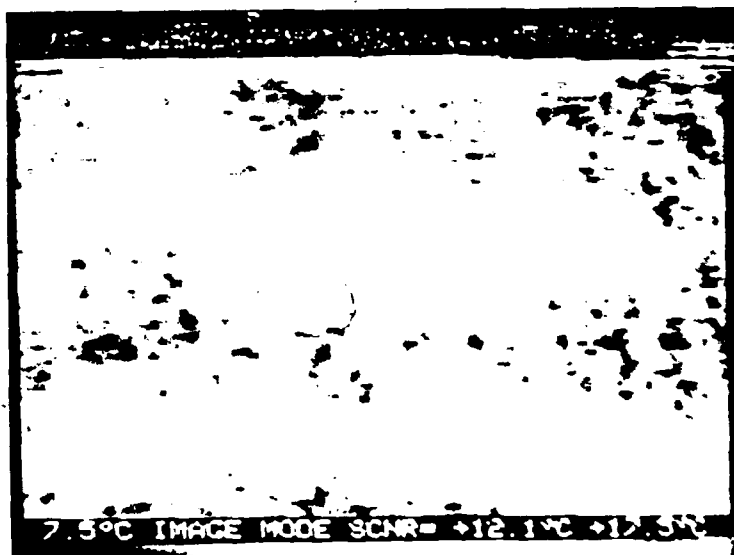
**SLANT RANGE: 50 FEET
DEPRESSION ANGLE: 60 DEGREES**

TARGET DESCRIPTION: METAL SURFACE MINE TALL GRASS
DATE: 12/21/88
TIME OF DAY: 11:20

VISIBLE
IMAGERY



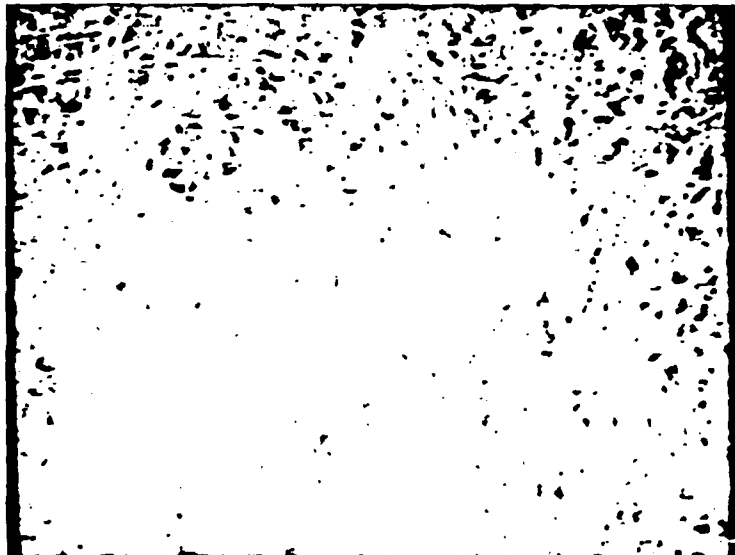
PASSIVE IR
IMAGERY (8-12UM)



SLANT RANGE: 50 FEET
DEPRESSION ANGLE: 60 DEGREES

TARGET DESCRIPTION: METAL SURFACE MINE TALL GRASS
DATE: 12/21/88
TIME OF DAY: 11:20

VISIBLE
IMAGERY



PASSIVE IR
IMAGERY (8-12UM)



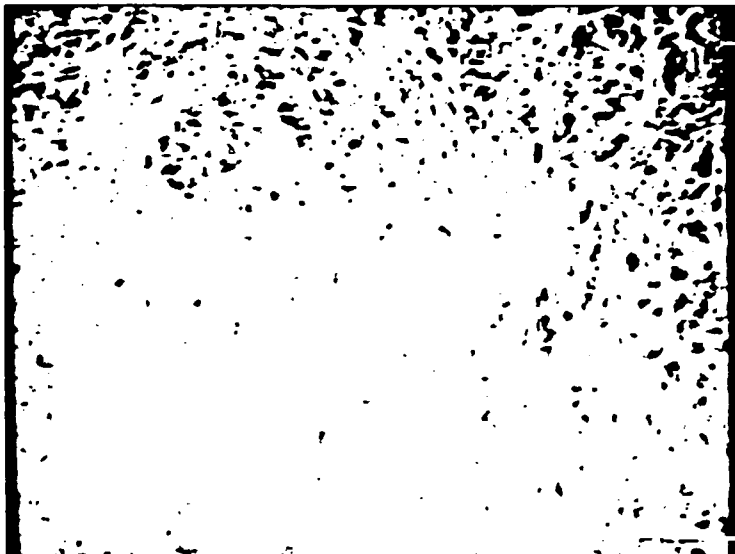
SLANT RANGE: 50 FEET
DEPRESSION ANGLE: 60 DEGREES

TARGET DESCRIPTION: METAL SURFACE MINE TALL GRASS

DATE: 12/21/88

TIME OF DAY: 11:20

**VISIBLE
IMAGERY**



**PASSIVE IR
IMAGERY (8-12UM)**



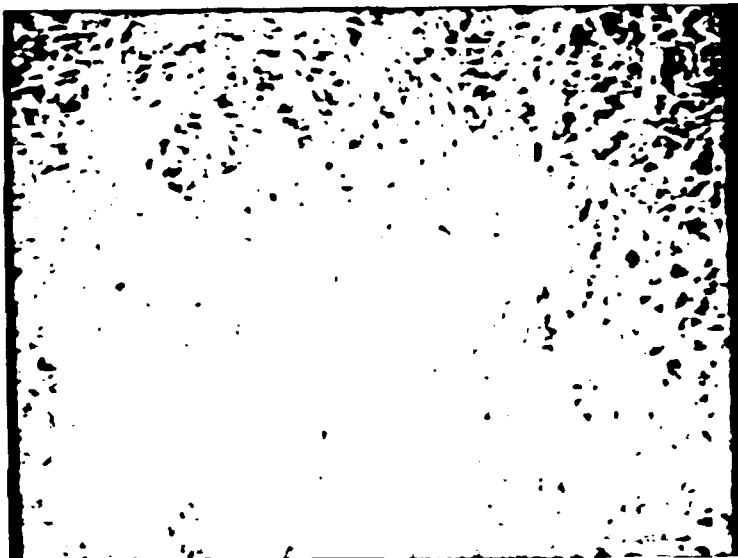
**SLANT RANGE: 50 FEET
DEPRESSION ANGLE: 60 DEGREES**

TARGET DESCRIPTION: METAL SURFACE MINE TALL GRASS

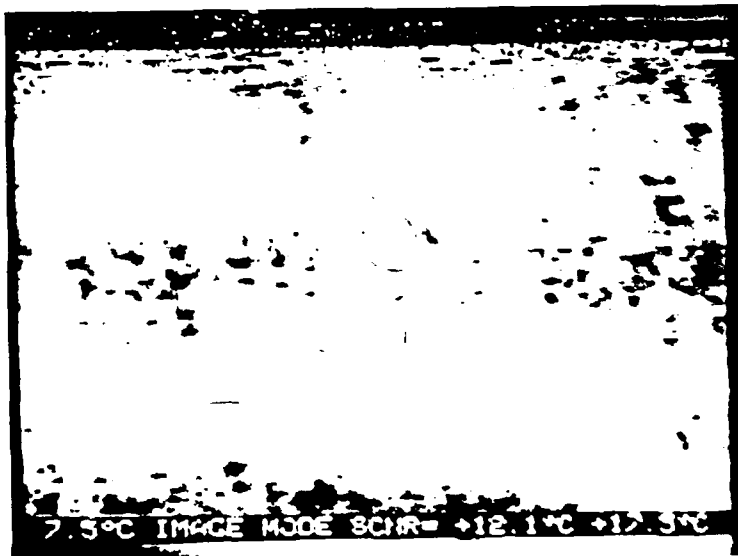
DATE: 12/21/88

TIME OF DAY: 11:20

**VISIBLE
IMAGERY**



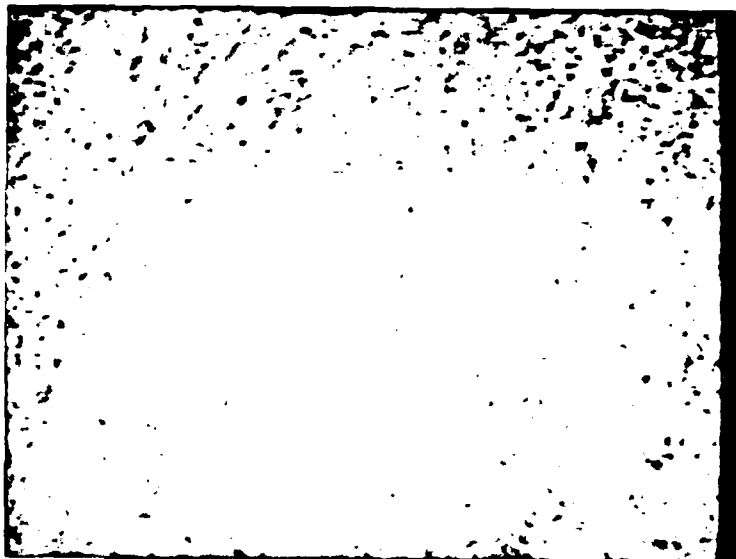
**PASSIVE IR
IMAGERY (8-12UM)**



**SLANT RANGE: 50 FEET
DEPRESSION ANGLE: 60 DEGREES**

TARGET DESCRIPTION: PLASTIC SURFACE MINE TALL GRASS
DATE: 12/21/88
TIME OF DAY: 13:08

VISIBLE
IMAGERY



PASSIVE IR
IMAGERY (8-12UM)

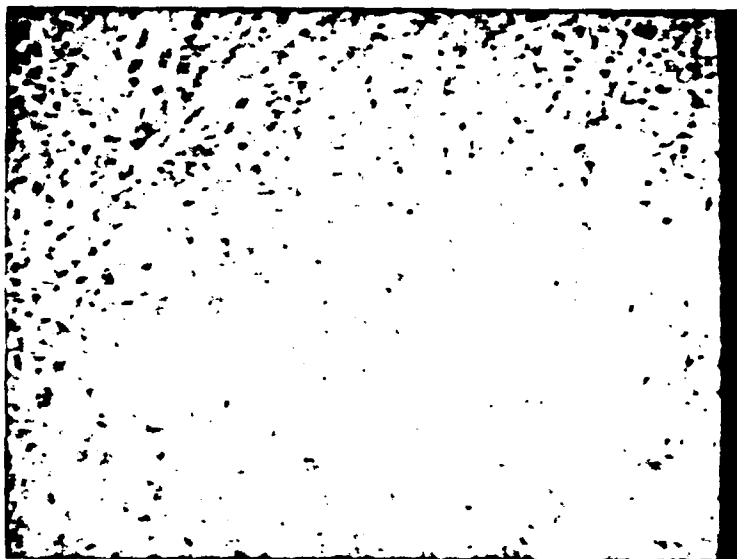


SLANT RANGE: 50 FEET
DEPRESSION ANGLE: 60 DEGREES

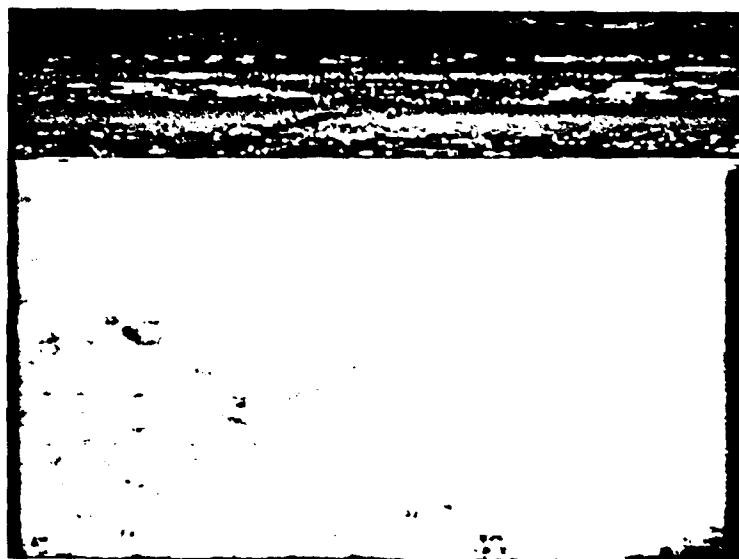
13082100

TARGET DESCRIPTION: PLASTIC SURFACE MINE TALL GRASS
DATE: 12/21/88
TIME OF DAY: 13:08

**VISIBLE
IMAGERY**



**PASSIVE IR
IMAGERY (8-12UM)**

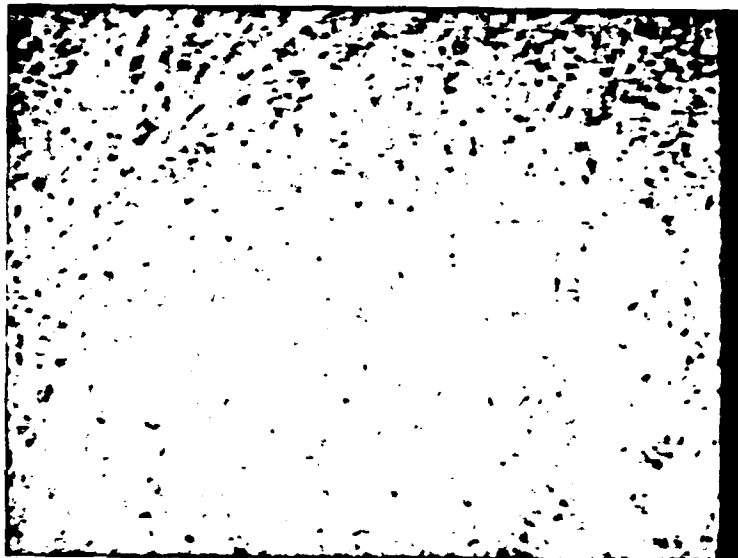


1308220Z

SLANT RANGE: 50 FEET
DEPRESSION ANGLE: 60 DEGREES

TARGET DESCRIPTION: PLASTIC SURFACE MINE TALL GRASS
DATE: 12/21/88
TIME OF DAY: 13:08

VISIBLE
IMAGERY



PASSIVE IR
IMAGERY (8-12UM)



SLANT RANGE: 50 FEET
DEPRESSION ANGLE: 60 DEGREES

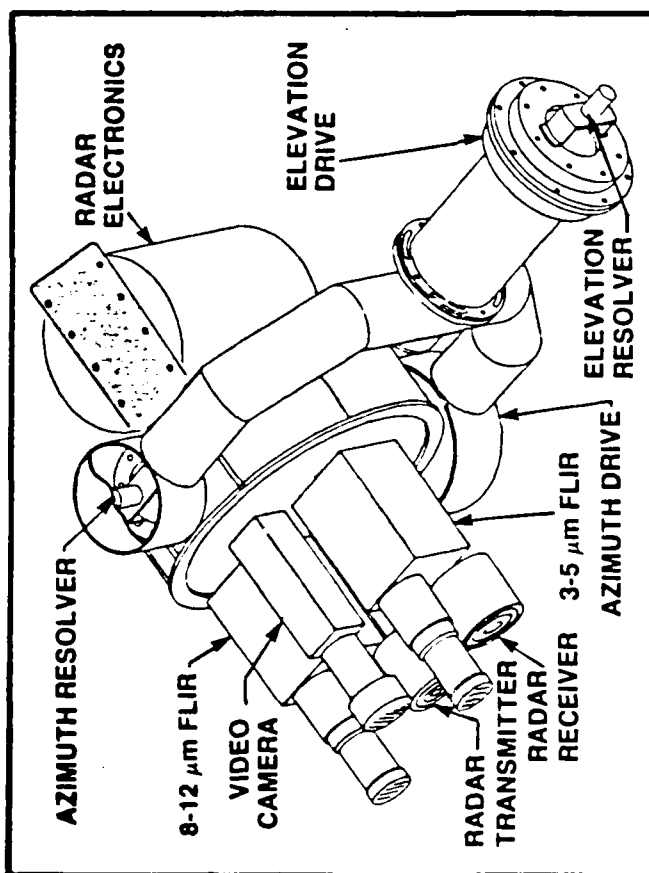
13082305

APPENDIX C

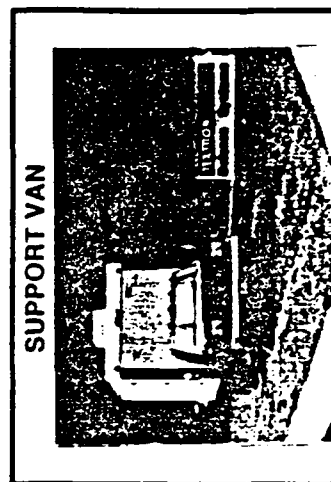
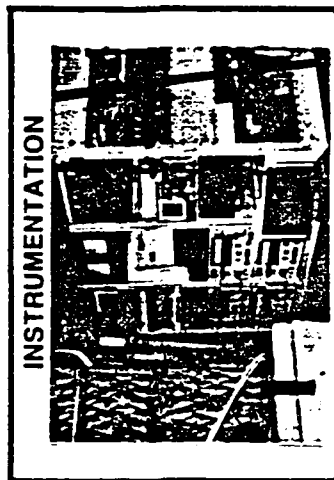
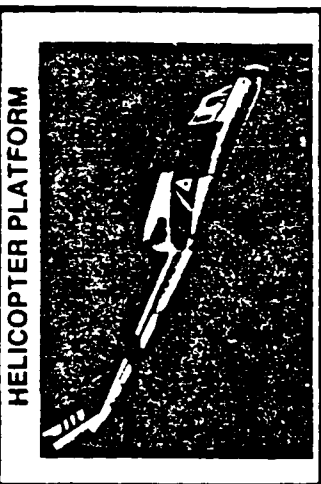
**AIRBORNE MULTISENSOR
TEST BED**

AIRBORNE MULTISENSOR TEST BED

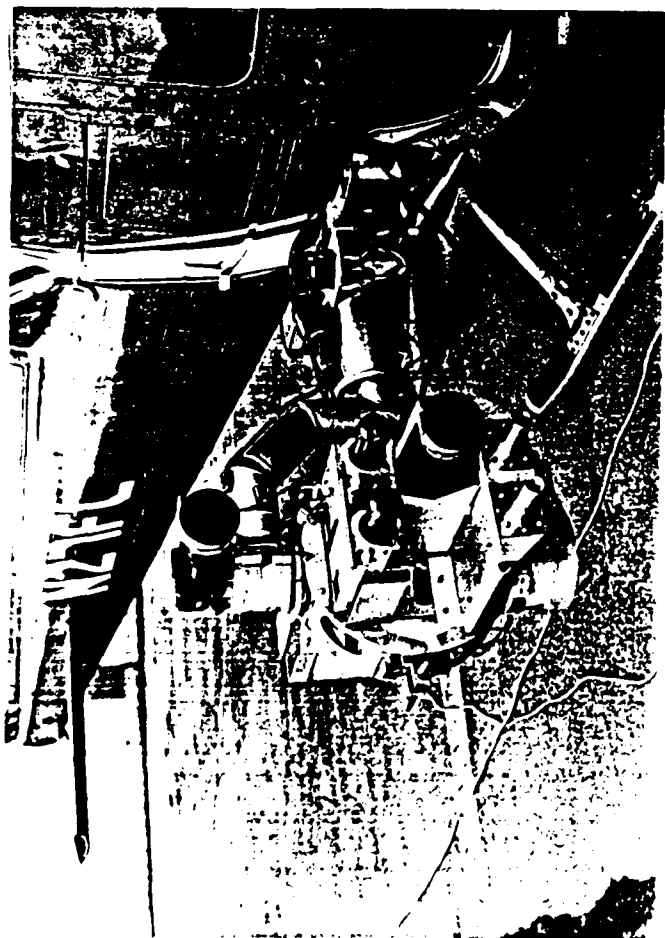
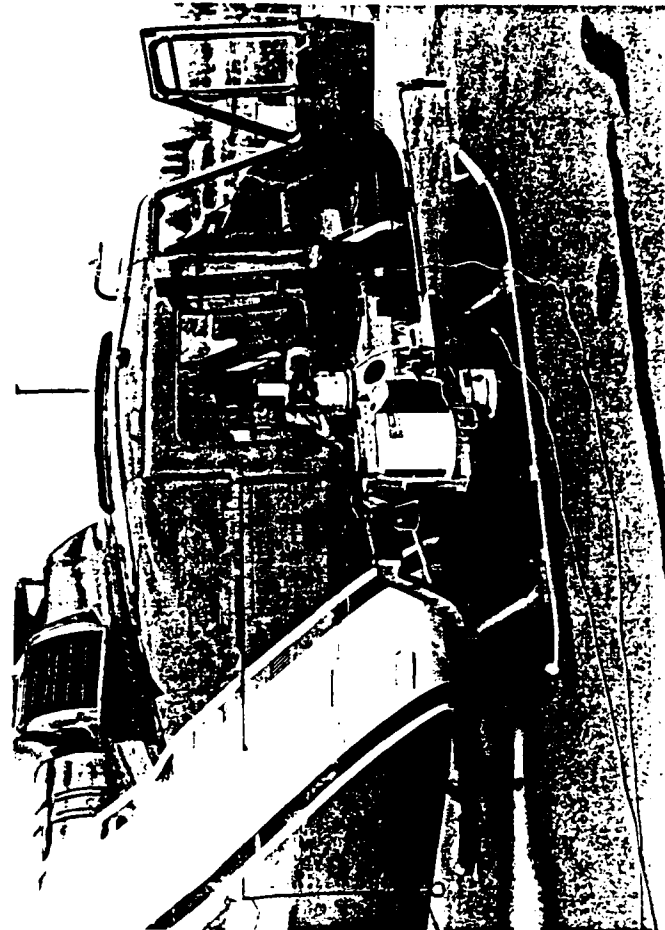
STABILIZED SENSOR SUITE



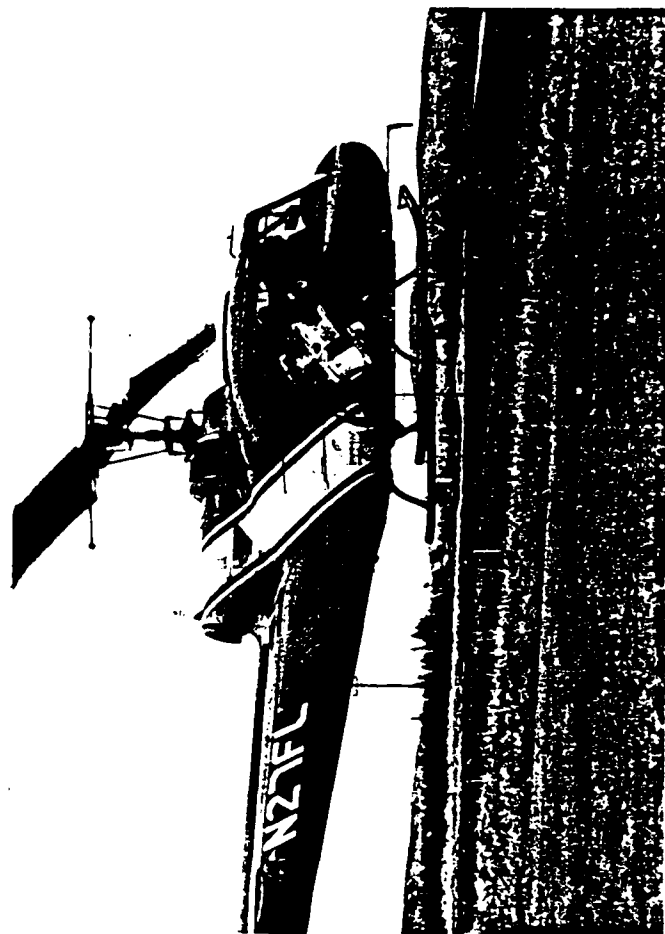
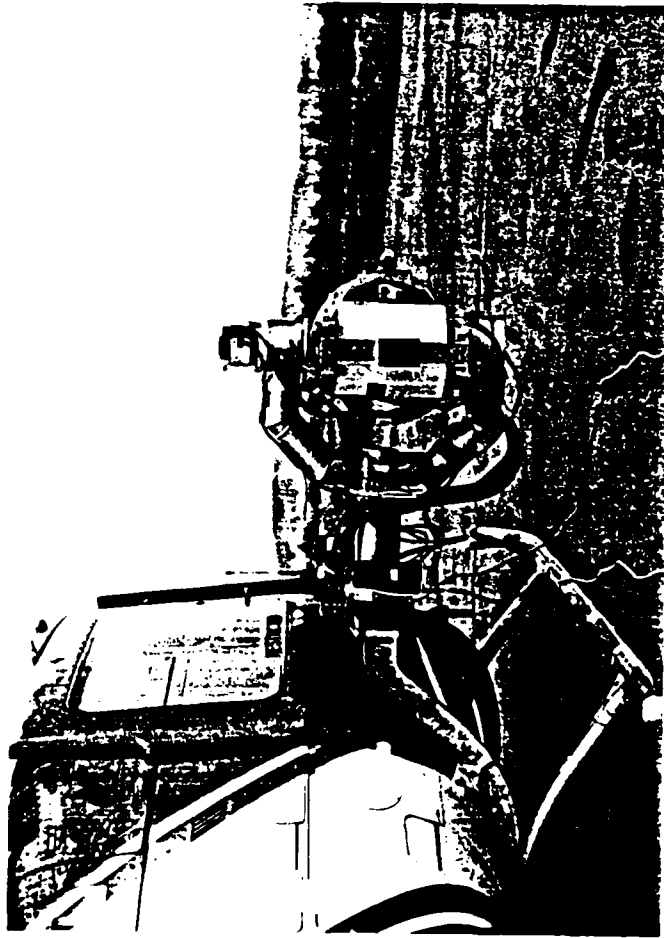
- 35 GHz MMW, FULLY COHERENT RADAR
- 3-5 μm , 8-12 μm IMAGING IR
- VISIBLE TV
- GROWTH TO INCLUDE:
 - 94 GHz MMW
 - ACTIVE IR



TEXTRON Defense Systems



TEXTRON DEFENSE SYSTEMS



TEXTRON DEFENSE SYSTEMS (TDS)

AIRBORNE TEST BED

INTRODUCTION

TEXTRON DEFENSE SYSTEMS AIRBORNE TEST BED IS MOUNTED ON A HELICOPTER TO PROVIDE CAPABILITY FOR MULTI-SPECTRAL COINCIDENT DATA COLLECTION FOR USE IN DEVELOPMENT AND EVALUATION OF ADVANCED SENSORS AND ALGORITHM CONCEPTS.

THE RESULTING COINCIDENT MULTI-SENSOR SIGNATURE DATA IS REQUIRED TO DEVELOP AND TEST BOTH SINGLE AND MULTI-SPECTRAL AIR TO GROUND SYSTEMS.

THE TDS AIRBORNE TEST BED CAN ECONOMICALLY COLLECT, REDUCE AND COMPILE COMPREHENSIVE COINCIDENT IR/MMW TARGET, COUNTERMEASURES AND BACKGROUND DATA FOR THE DEVELOPMENT OF ADVANCED "SMART MUNITIONS".

TEXTRON DEFENSE SYSTEMS (TDS) AIRBORNE TEST BED

CAPABILITY

- o UNIQUE CAPABILITY TO:
 - COLLECT MULTI-SENSOR COINCIDENT TARGET SIGNATURE & BACKGROUND CLUTTER DATA
 - COLLECT ANCILLARY GROUND TRUTH MISSION DATA
 - EVALUATE PROTOTYPE SENSORS

EQUIPMENT

- o AIRBORNE TEST BED (MODEL 1)
 - 3-5 μ M IMAGING RADIOMETER (1.2 mR RESOLUTION)
 - 8-12 μ M IMAGING RADIOMETER (0.6 mR RESOLUTION)
 - 35 GHz FMCW MILLIMETER WAVE RADAR (0.3 METER RESOLUTION)
 - WFOV & NFOV DIGITAL CCD VIDEO CAMERAS
 - MOTION COMPENSATED STABILIZED PLATFORM
 - INERTIAL REFERENCE
 - MINIRANGER POSITION DETERMINING SYSTEM

TEXTRON DEFENSE SYSTEMS (TDS) AIRBORNE TEST BED

EQUIPMENT (CONTINUED)

- o AIRBORNE TEST BED UPGRADE (MODEL 2)
 - ACTIVE IR
 - HIGHER RESOLUTION IR ARRAYS (0.25 mr)
 - 94 GHz RADAR OPTION
 - AIRBORNE HOST ALGORITHM TEST PROCESSOR
- o INSTRUMENTATION RACK
 - SENSOR & GIMBAL CONTROL ELECTRONICS
 - DATA DISPLAYS
 - DATA ACQUISITION & RECORDING HARDWARE
- o MOBILE GROUND STATION
 - QUICK LOOK PLAYBACK FACILITIES
 - ARCHIVE EQUIPMENT
 - FIELD GROUND POWER SYSTEM

TDS AIRBORNE TEST BED

DATA COLLECTION SYSTEM DESCRIPTION

EQUIPMENT SET & INSTALLATION

SENSOR SUITE AND GIMBAL PACKAGE MOUNTED ON THE UH-1H OR -1B HELICOPTER RIGHT FORWARD EXTERNAL STORES MOUNT (SEE FIGURE 1)

INSTRUMENTATION RACK AND RACAL RECORDER MOUNTED INTERNALLY ON UH-1H OR -1B HELICOPTER (SEE FIGURE 2)

OPERATIONAL USE

THE SENSOR SUITE IS MOUNTED LOOKING FORWARD ON A TWO AXIS (ELEVATION OVER AZIMUTH) INERTIALLY STABILIZED GIMBAL PLATFORM.

THE PLATFORM PROVIDES COMPENSATION FOR SENSOR LINE OF SIGHT (LOS) MOTION DUE TO AIRFRAME VIBRATION, PROVIDES AN INERTIAL REFERENCE FRAME (HEADING, ELEVATION AND ROLL) IN ORDER TO ISOLATE GIMBAL POINTING AND SCANNING FROM GROSS AIRFRAME MOTIONS IN YAW, PITCH AND ROLL, AND PROVIDES INERTIALLY REFERENCED READOUTS OF THE SENSOR LOS ANGLES.

- o ELEVATION ANGLE VARIABLE 0 TO 180 DEGREES
- o AZIMUTH ANGLE SCANNED +/- 30 DEGREES
- o AZ SCAN RATE VARIABLE 0 TO 60 DEG/SEC

TDS AIRBORNE TEST BED

DATA COLLECTION SYSTEM DESCRIPTION (CONT'D)

OPERATIONAL USE (CONTINUED)

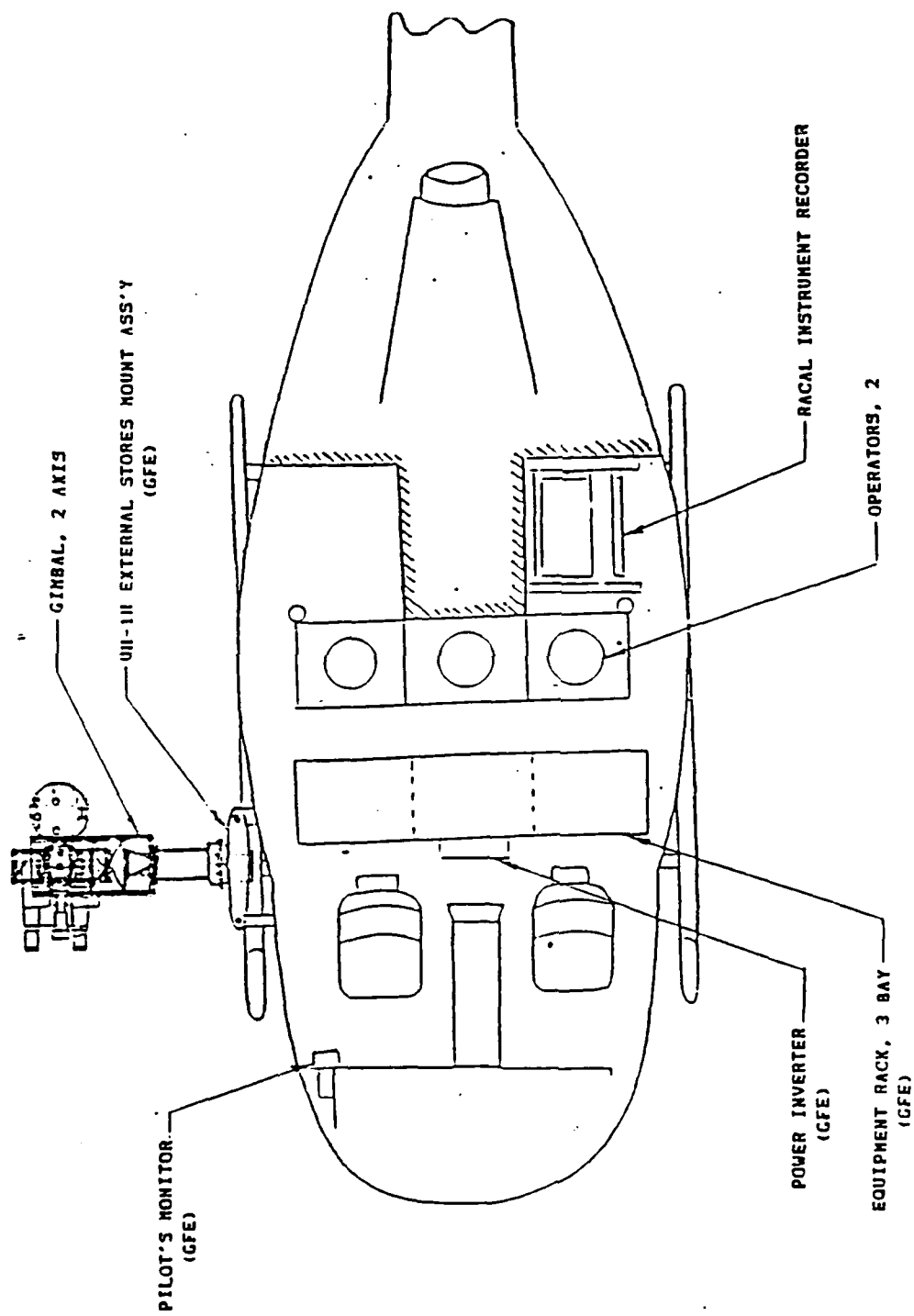
ALL SENSORS EXCEPT THE WIDE FIELD-OF-VIEW COLOR VIDEO ARE MOUNTED ON THE INNER (AZIMUTH) AXIS OF THE GIMBAL AND SCAN TOGETHER IN COMMON BORESIGHT. THE WIDE FIELD CAMERA IS MOUNTED ON THE OUTER (ELEVATION) AXIS OF THE GIMBAL. A RETICLE INDICATING SENSOR BORESIGHT IS INSERTED IN THE VIDEO OUTPUT FROM THE WIDE FIELD CAMERA. THE VIDEO CAMERAS ARE EQUIPPED WITH AUTO-IRIS, AUTO-FOCUS LENSES AND OPERATE WITH VERY SHORT SHUTTER TIMES TO PREVENT IMAGE BLURRING DUE TO LOS MOTIONS.

POSITION DETERMINATION & GROUND TRUTH DATA

THE PLATFORM HORIZONTAL TRANSLATIONAL POSITION IS DETERMINED BY AN ON BOARD MOTOROLA MINIRANGER FALCON 484 RADIO TRANSPONDER WORKING IN CONJUNCTION WITH SURVEYED GROUND BEACONS.

PLATFORM ALTITUDE IS DETERMINED FROM THE HELICOPTER'S BAROMETRIC OR RADAR ALTIMETER.

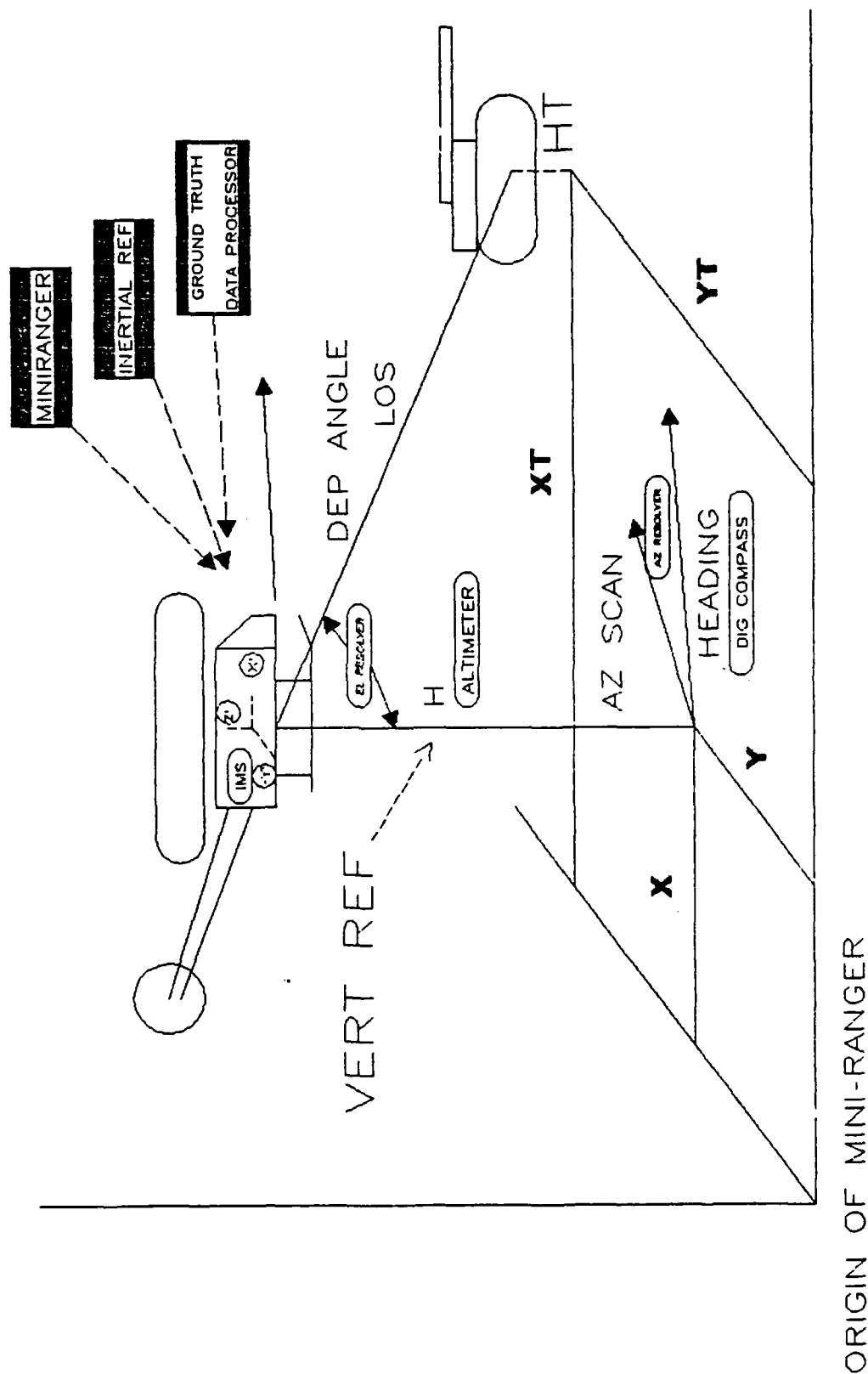
GIMBAL ANGLES, LOS ANGLES, HORIZONTAL POSITION AND ALTITUDE ARE AUTOMATICALLY TIME TAGGED, DIGITALLY ACQUIRED AND RECORDED SYNCHRONOUS WITH RADAR, IR AND VIDEO DATA.



UH-1 MODEL II HELICOPTER

FIGURE 2.3-3 TESTED HELICOPTER INSTALLATION

LINE OF SIGHT / GROUND TRACK MEASUREMENT EQUIPMENT



TDS AIRBORNE TEST BED

DATA COLLECTION SYSTEM DESCRIPTION (CONT'D)

RECORDED DATA

IR RADIOMETER AND COLOR VIDEO SIGNALS ARE RECORDED ON 3/4" VIDEO TAPE.

RADAR DATA IS RECORDED ON A 14 TRACK, 1" TAPE INSTRUMENTATION TAPE RECORDER.

PLATFORM AND GIMBAL SIGNALS ARE DIGITALLY ACQUIRED AND RECORDED ON FLOPPY DISK OR COMPUTER DIGITAL TAPE.

ALL DATA IS TAGGED AND ANNOTATED WITH A VIDEO FRAME BASED TIME CODE. AUDIO IS INSERTED AS REQUIRED.

DISPLAYS & MONITORS

ON BOARD DATA DISPLAYS CONSIST OF TV MONITORS, TO DISPLAY COLOR VIDEO AND/OR RADIOMETER IR VIDEO, AND AN OSCILLOSCOPE/SPECTRUM ANALYZER FOR VIEWING THE RADAR TIME AND FREQUENCY SIGNALS.

TO ASSIST THE HELICOPTER PILOT IN OVERFLYING THE TARGET AREA, A VIDEO MONITOR IS RECOMMENDED TO DISPLAY WIDE FIELD-OF-VIEW VIDEO.

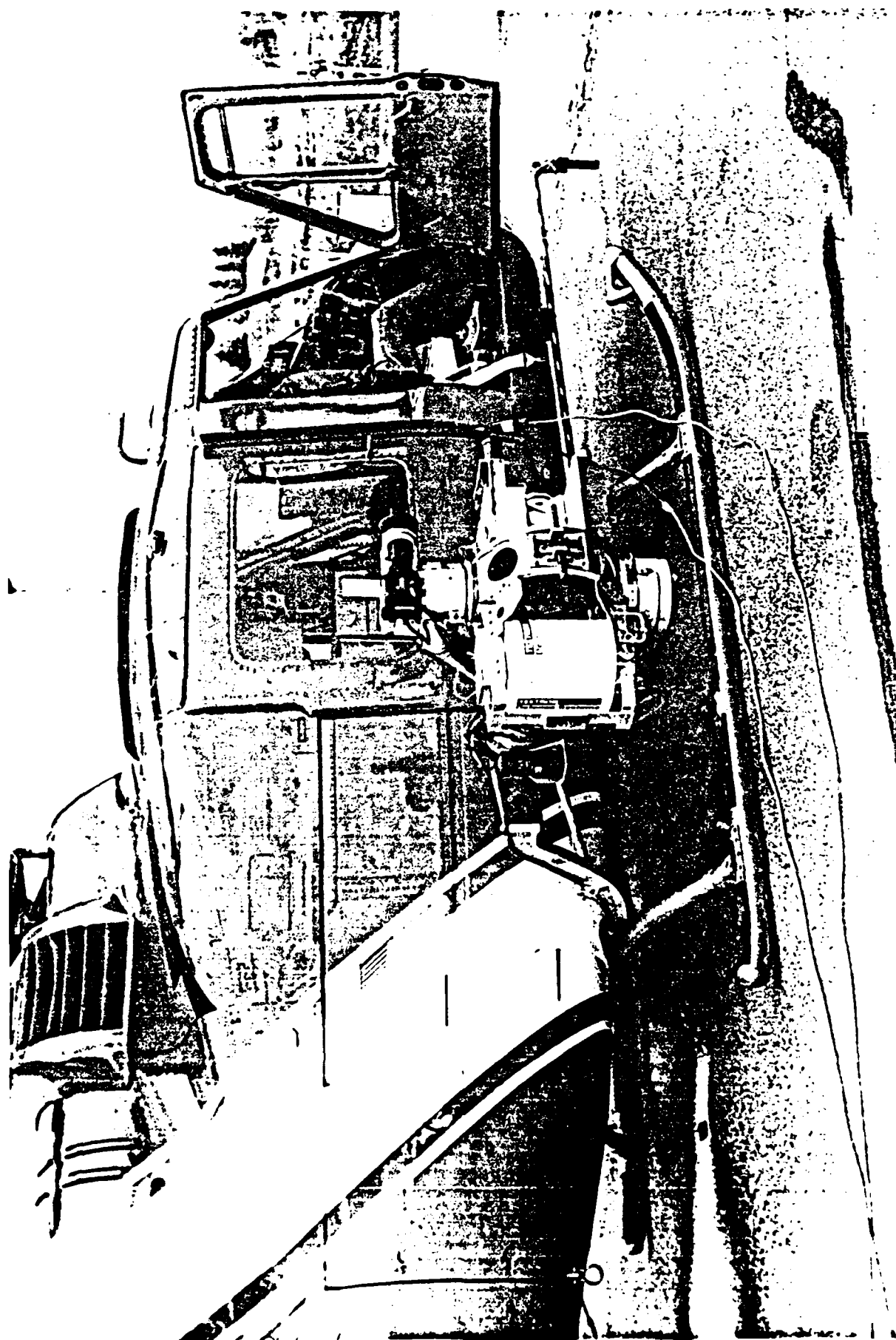


FIGURE 1B

AIRBORNE TEST BED EQUIPMENT RACK

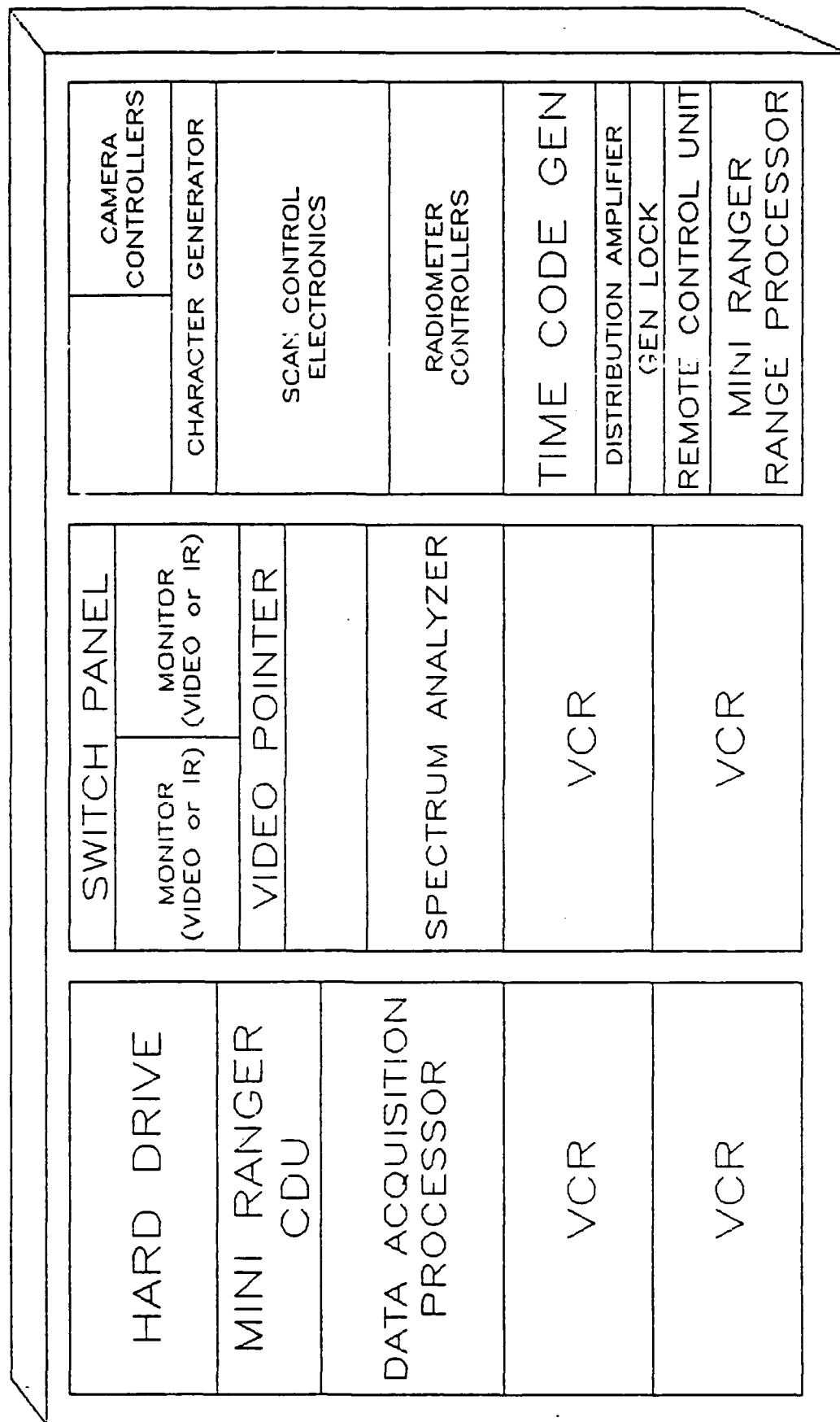
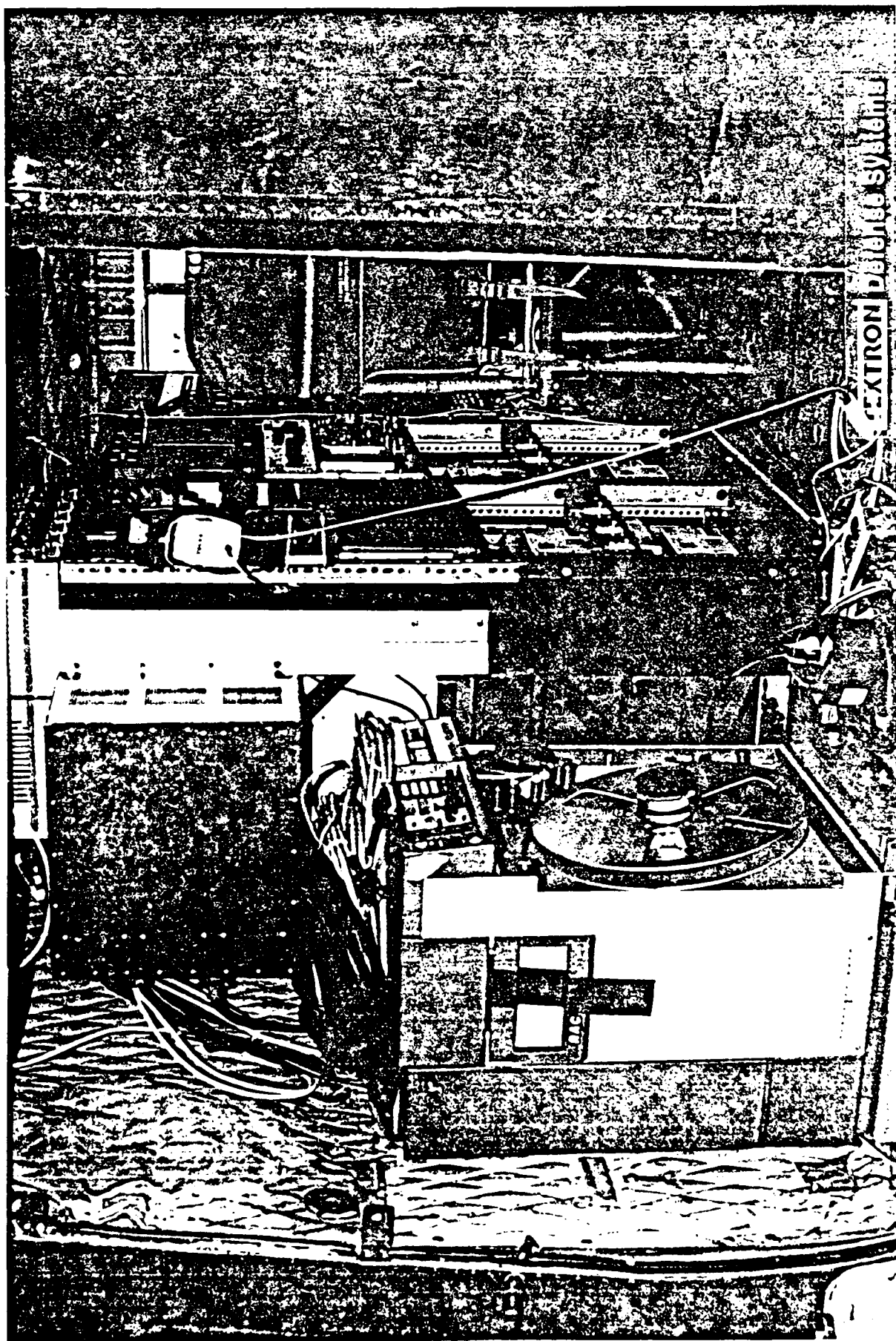


FIGURE 2A

RWD44



CESTRON PATENT SYSTEMS

TABLE 2.3-1 - IR RADIOMETER SPECS

PARAMETER	3 - 5 SPEC	8 - 12 SPEC
NOISE EQUIV DELTA T (AT 30 C)	0.4 DEG C	0.2 DEG C
FOV W/O TELESCOPE	15 DEG VERT X 20 DEG HORIZ	
WITH X3 TELESCOPE	5 DEG VERT X 6.7 DEG HORIZ	
IFOV W/O TELESCOPE	3.5 MRAD	1.8 MRAD
WITH X3 TELESCOPE	1.2 MRAD	0.6 MRAD
50% MTF W/O TELESCOPE	0.04 CYC/MR	0.08 CYC/MR
CUTOFF WITH X3 TELESCOPE	0.12 CYC/MR	0.24 CYC/MR
FRAME RATE (TV FIELD)	60 HZ	
FRAME SIZE	256 LINES X 512 PIXELS/LINE	
BLUR SPOT SIZE (50% MTF)	18 PIXELS	9 PIXELS
BLUR ANGLE W/O TELESCOPE	12.5 MRAD	6.3 MRAD
WITH X3 TELESCOPE	4.1 MRAD	2.1 MRAD
DYNAMIC RANGE	42 DB (7 BITS)	
TEMPERATURE RANGE	-20 C TO +400 C	
DETECTOR	HgCdTe	
COOLANT, HOLD TIME	LN2, 3 HOURS	
OUTPUT FORMAT	RS-170, NTSC	

TABLE 2.3-2 MMW RADAR SPECS (1 of 3)

MMW RADAR PARAMETER	REQUIREMENT	MEASUREMENT
<u>General Description</u>		
o Type Radar	COHERENT FM/CW, SEPARATE TRANSMIT AND RECEIVE ANTENNAS	
o Transmitted Frequency	35+/- .25 GHz	35.0-35.55 GHz
o Transmitted Polarization	RHCP	O.K. - by inspection
o Receive Polarization	LHC, RHC	O.K. - by inspection
o Input Power to Antenna	50 mW (MIN.)	16 mW
<u>Transmitter Characteristics</u>		
o Transmit, Receive Antenna Gains		
- Antenna Pair #1 (6" aperture dia.)	32.5 dBi	32.5 dBi (5)
- Antenna Pair #2 (3" aperture dia.)	26.5 dBi	26.5 dBi (5)
- Antenna Pair #3 (1.3" aperture dia.)	19.5 dBi	20 dBi (5)
o Transmit, Receive Antenna Beamwidths (Nom.)		
- Antenna Pair #1 (6" dia.)	3.9 DEG.	3.9°
- Antenna Pair #2 (3" dia.)	7.9 DEG.	8.6°
- Antenna Pair #3 (1.3" dia.)	17.5 DEG.	16.3°
o Transmit, Receive Antenna Sidelobes (Nom.)		
	<u>E-Plane</u> <u>H-Plane</u>	<u>E-Plane</u> <u>H-Plane</u>
- Antenna Pair #1 (6" dia.)	-17 dB -25 dB	-22.3 dB -29.0 dB
- Antenna Pair #2 (3" dia.)	-25 dB -25 dB	-24.9 dB -25.7 dB
- Antenna Pair #3 (1.3" dia.)	-17 dB -20 dB	-25.1 dB -25.0 dB

TABLE 2.3-2 MMW RADAR SPECS (2 of 3)

MMW RADAR PARAMETER	REQUIREMENT	MEASUREMENT
o Transmit, Receive Antenna VSWR		
- Antenna Pair #1 (6" dia.)	1.80:1	not tested
- Antenna Pair #2 (3" dia.)	1.80:1	not tested
- Antenna Pair #3 (1.3" dia.)	1.70:1	not tested
o Axial Ratio (Polarizer/ Antenna Assy)	< 1 DB	not tested
o Transmit/Receive Antenna Elec. Alignment	Adj. for Boresighting at 100 to 1000 Meters Range	O.K. - by inspection
o Frequency Modulation		
- Waveform Shape -	Triangle	O.K. - by inspection
- Up Ramp Duration (ms)	8 +/- 0.04	not tested (6)
- Down Ramp Duration (ms)	8 +/- 0.04	not tested (6)
- Ramp Non-linearity	0.025 % (MAX)	(1)
- Frequency Deviation (MHz)	500 +/- 10	550 MHz
- Settling Time, Ramp to Ramp	0.025 % MAX. Non-Linearity Within 50 us of Transition	Not measured

TABLE 2.3-2 MMW RADAR SPECS (3 of 3)

MMW RADAR PARAMETER	REQUIREMENT	MEASUREMENT
<u>Receiver Characteristics</u>		
o Receive Polarization	LHC, RHC	O.K. - by inspection
o Receiver Noise Figure (At Mixer Input)	10 dB SSB	16 dB SSB (2)
o Receive/Transmit Channel Isolation	> 30 dB	> 30 dB
o First IF Frequency	3.9 GHz (NOM.)	3.8 GHz (approx.)
o Second IF (Video) Frequency	20 KHz - 250 KHz	O.K.
o Outputs	Four Channels (LHC, RHC in Phase Quadrature)	O.K.
o Spurious	- 30 dBc	None observed
o Dynamic Range	60 dB (MIN.)	77 dB (3)
o RF/IF/Video Gain	43 dB (NOM) (Includes Mixer Losses)	25 dB (4)
<u>Physical Characteristics</u>		
o Size (Excluding Connectors)	10.6" dia X 12" length	
o Volume	1059 IN. 3	
o Weight	37 lbs. (NOM)	

Notes:

- (1) Radar has 1 foot resolution (measured in field); implies non-linearity in spec.
- (2) Calculated (equipment not available to perform measurement).
- (3) Calculated.
- (4) Not flat-range compensation built in.
- (5) Calculated from Beamwidth measurement.
- (6) Nominal duration of 8 mS measured; critical measurement not made.

TABLE 2.3-3 - GIMBAL SPECS

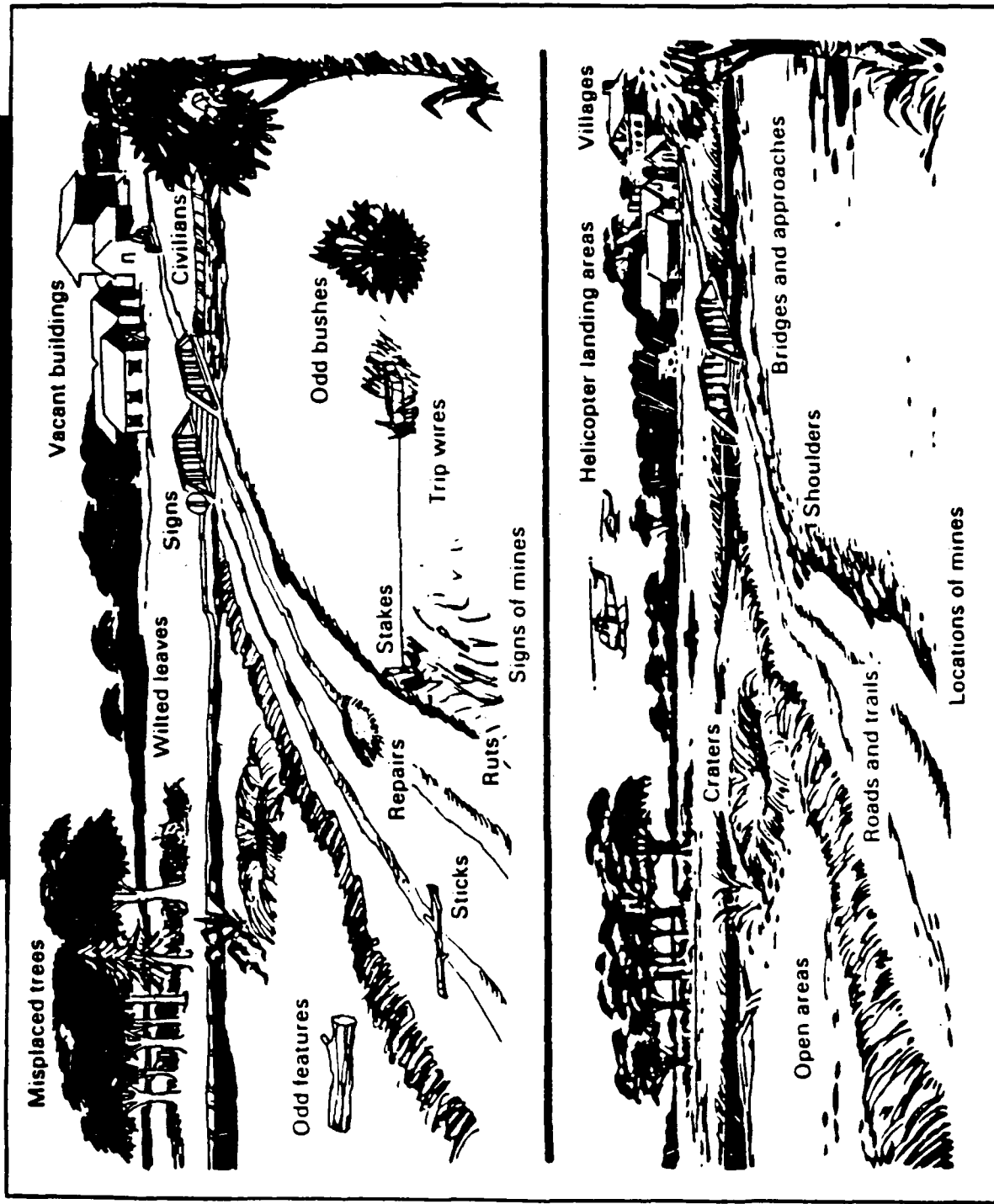
PARAMETER	AZIMUTH	ELEVATION
ANGULAR - RANGE	60 DEG	360 DEG
- SCAN ANGLE	+/- 30 DEG	+/-20 DEG
- SCAN RATE	15 - 60 DEG/SEC	<15 DEG/SEC
- ACCURACY	0.1 DEG	0.1 DEG
LOS JITTER	0.5 MRAD OVER 30 MSEC	
LOS DRIFT	15 MRAD OVER ONE HOUR	
TRANSIENT RESPONSE	<0.1 SEC, 15 DEG/S <0.4SEC, 60 DEG/S	
INERTIAL REFERENCES	3 AXIS GYRO FOR LOCAL VERTICAL GYRO-COMPASS FOR AZIMUTH	
AXIS CONFIGURATION	ELEVATION OVER AZIMUTH	
DATA OUTPUTS	GIMBAL POINTING ANGLES INERTIAL HEADING, ELEV, ROLL	

A vertical dashed line consisting of 20 rectangular segments is located on the left side of the page.

APPENDIX D

SYSTEM CUES FOR DETECTING THE LOCATION OF MINES


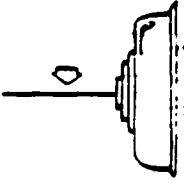


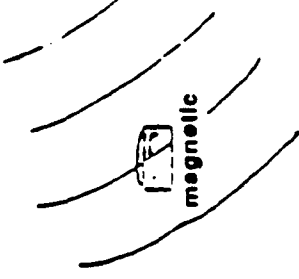

SIGNS AND POSSIBLE LOCATIONS OF MINES



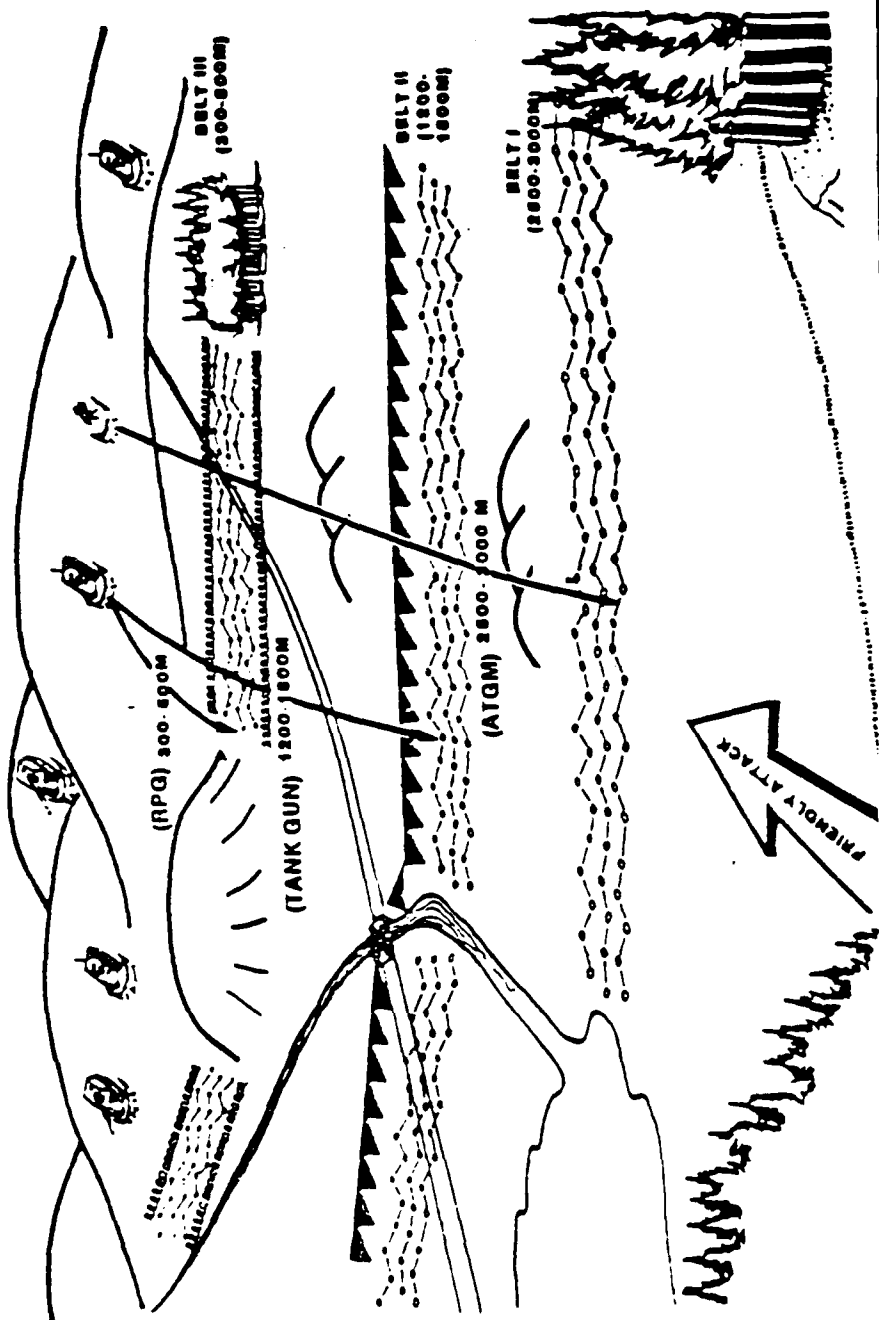
MINED HARD-SURFACE ROAD



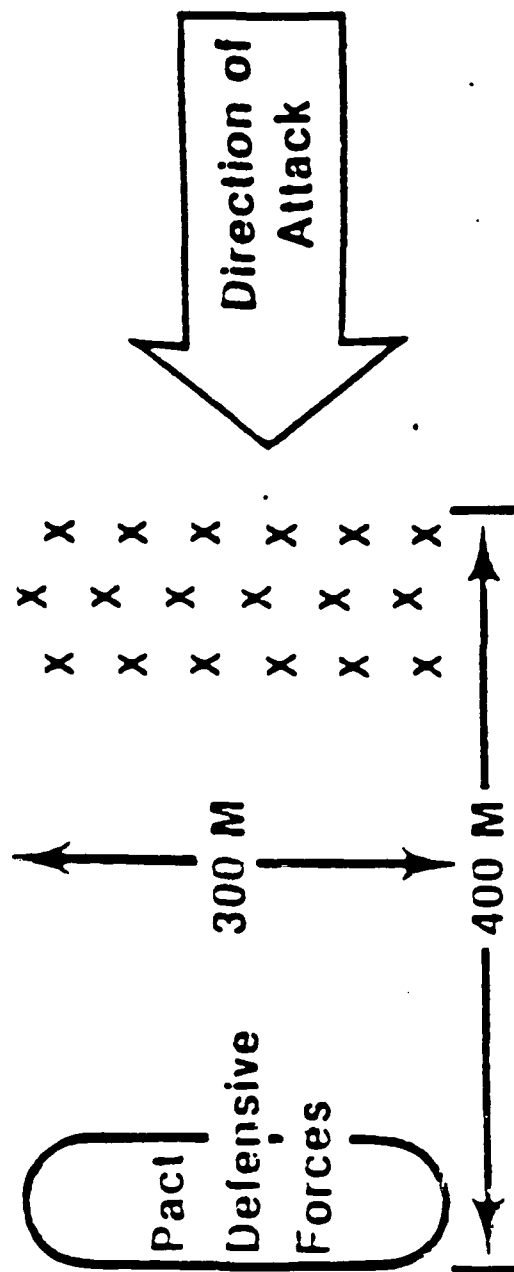
EFFECTIVENESS OF ANTITANK MINES

Mines and Fuzing	Fuze Sensing Width	System/Mobility Kills
Conventional	 <p>pressure</p>  <p>tilt rod</p>	Low/High
	 <p>M₁ Track width</p>  <p>K₁ Full width</p>	High/High
Scatterable	 <p>magnetic</p>	High/Low
	 <p>K₂ M₂ Full width</p>	

ENEMY DEFENSIVE POSITIONS AND FULLY-DEVELOPED MINE BELTS



THREAT HASTY MINEFIELD



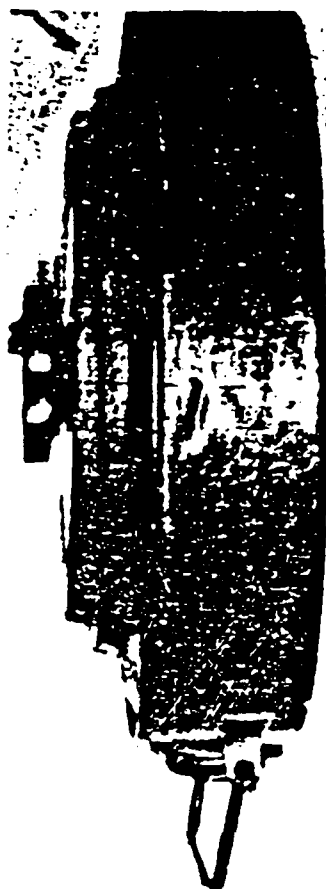
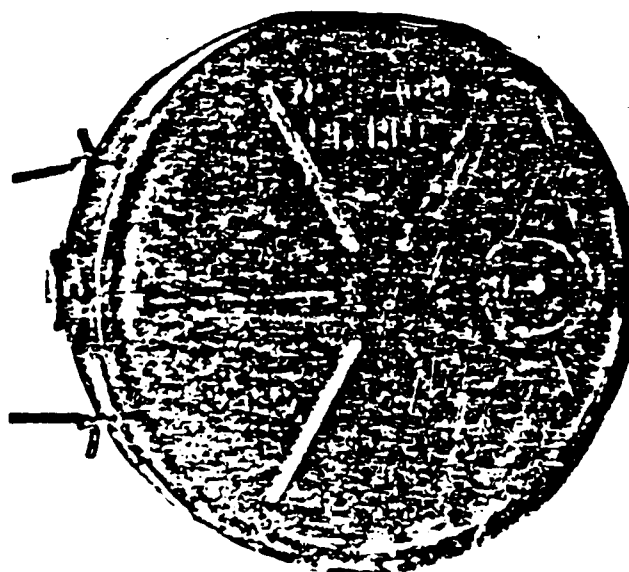
Antipersonnel Mines

CHARACTERISTICS	PMN	PMD-7	POMZ-2	OZM-3	MAF-1/MAF-2	PFM-1	MON-100
Type	antipersonnel	antipersonnel	antipersonnel	bounding antipersonnel	chemical bounding	antipersonnel	antipersonnel
Maximum diameter (mm)	blast	blast	fragmentation	bounding fragmentation	chemical (mustard)	scatterable blast	directional fragmentation
Height (mm)	110	length: 150 width: 75	61	75	150/185	INA	520
Weight (kg)	55	50	135 (not including stake)	120	350/286	INA	INA
Actuating force (kg)	0.5	0.3	2.0	3.0	8.7	0.074	5.0
Fuzing system	1.0 1.4 pressure plate	1.0 pull	1.0 trip wire pull	varies trip wire or electronic	varies electronic pressure delay	INA delay, pressure	2.0 tripwire or electronic
DOI	1960	1950	1942	1950	1940	INA	INA
Status	standard	obsolete	limited standard	standard	limited standard	standard	standard

Antitank Mines

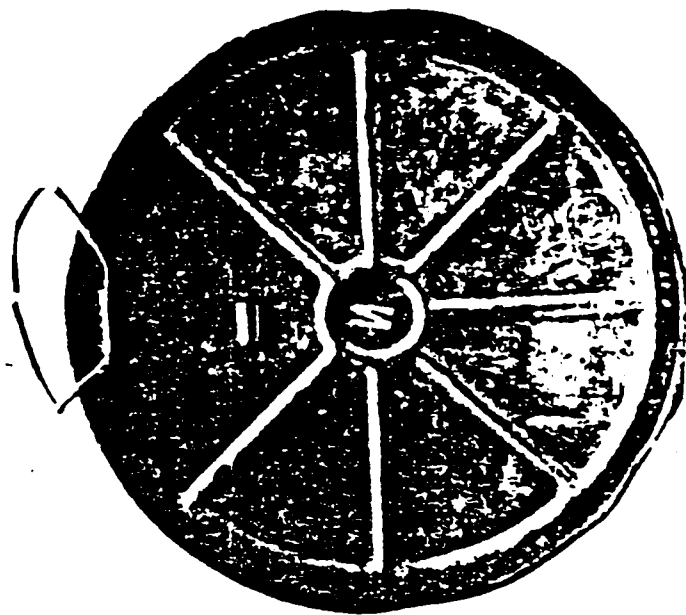
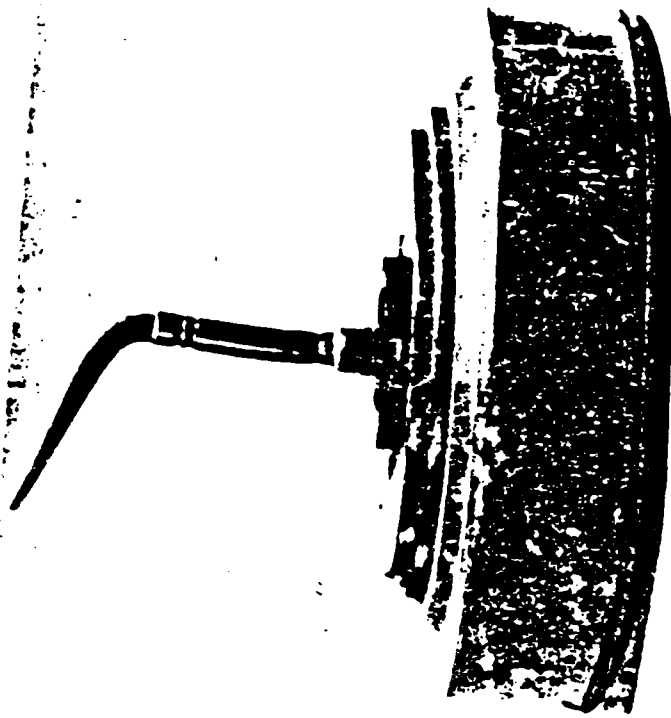
CHARACTERISTICS	TMN-48	TM-57	TMK-2
Type	antitank blast	antitank blast	antitank shaped-charge
Maximum diameter (mm)	310	300	80 (min) 300 (max)
Height (mm)	74	100	350
Weight (kg)	8.7	9.5	12.5
Actuating force (kg)	180	200 700	8-12
Fuzing system	pressure plate and antiskit device	pressure, tilt rod	tilt rod
DOI	1950	INA	INA
Status	standard	standard	standard

Antitank Mine IMN-46

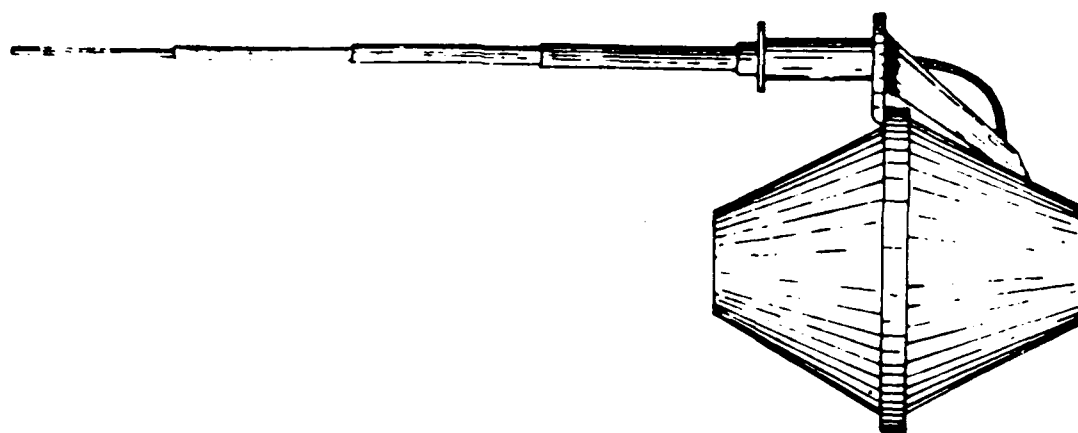


IMN-46

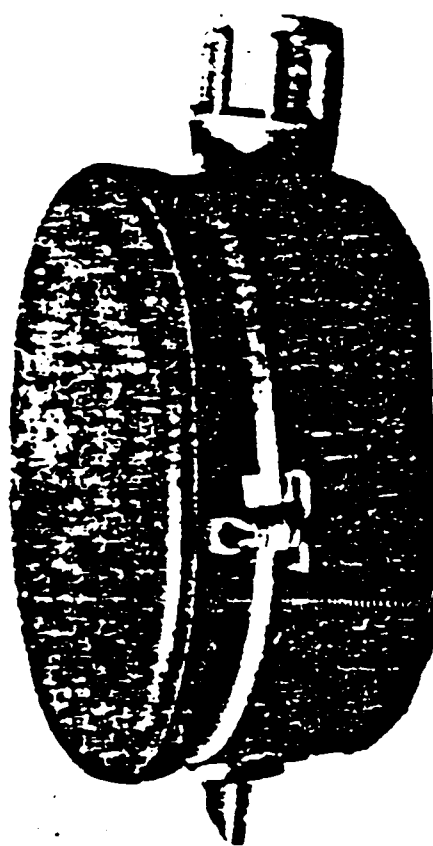
Antitank Mine TM-57



Mine TMK-2

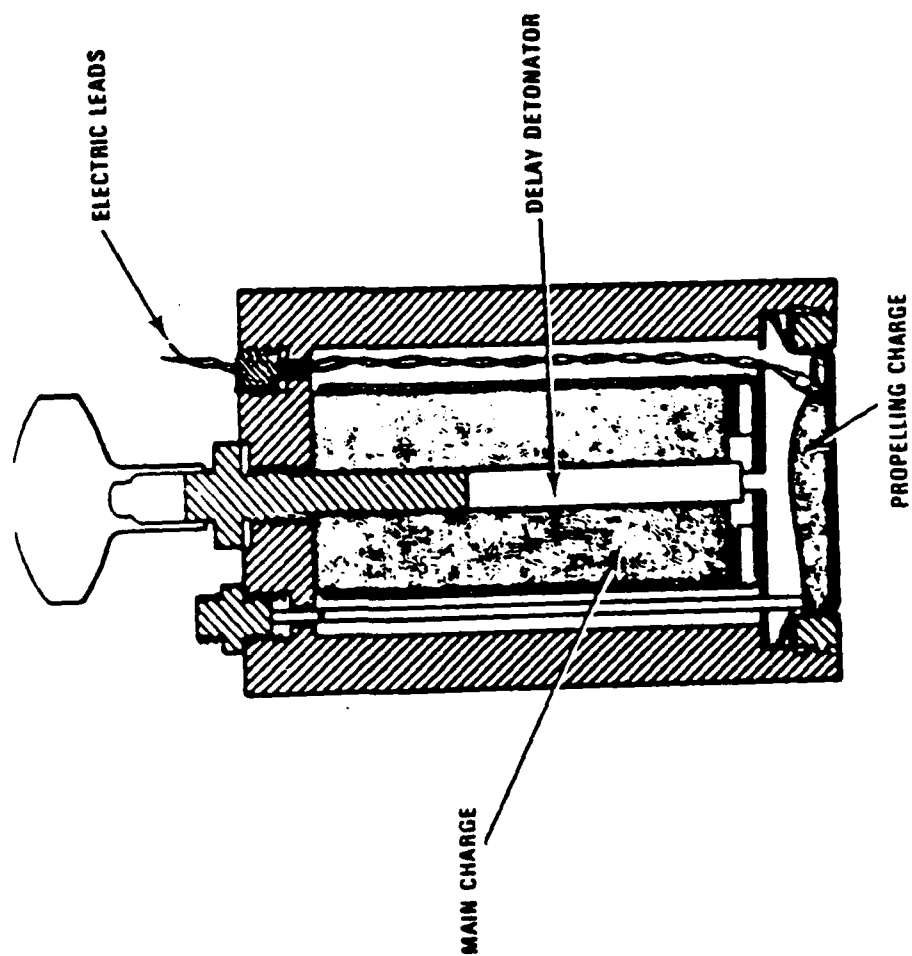


Antipersonnel Mine PMN



PMN

Bounding Antipersonnel Mine OZM-3



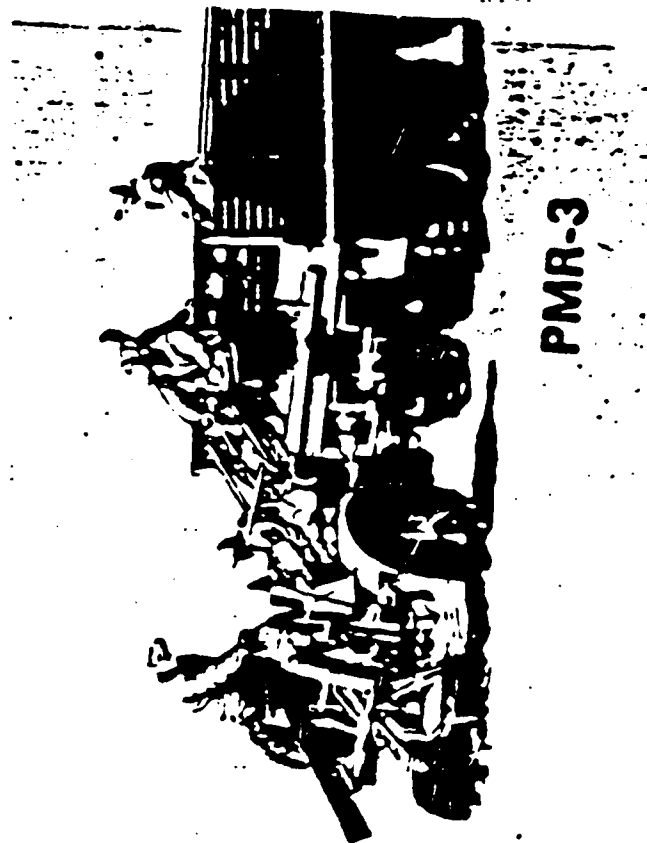
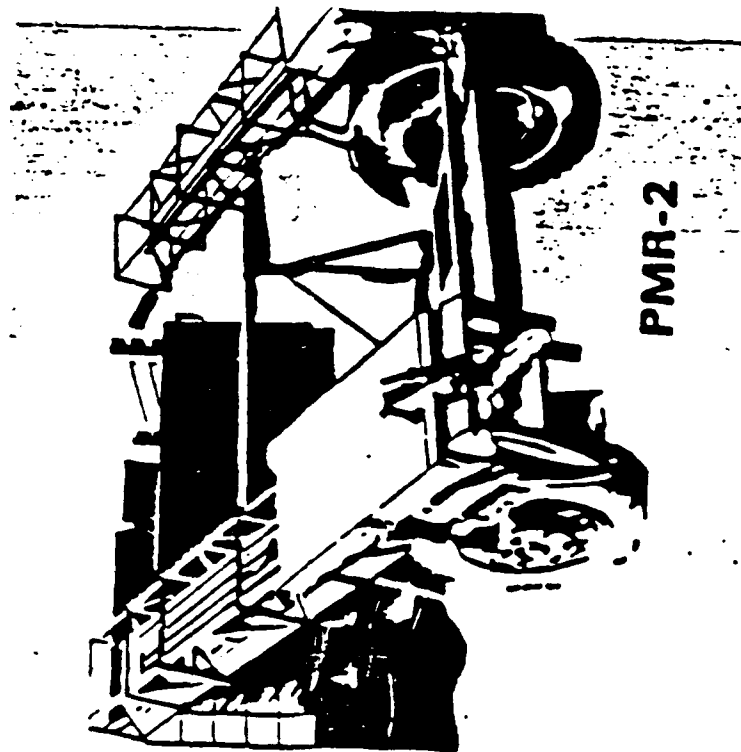
OZM-3

Scatterable Antipersonnel Mine PFM-1.

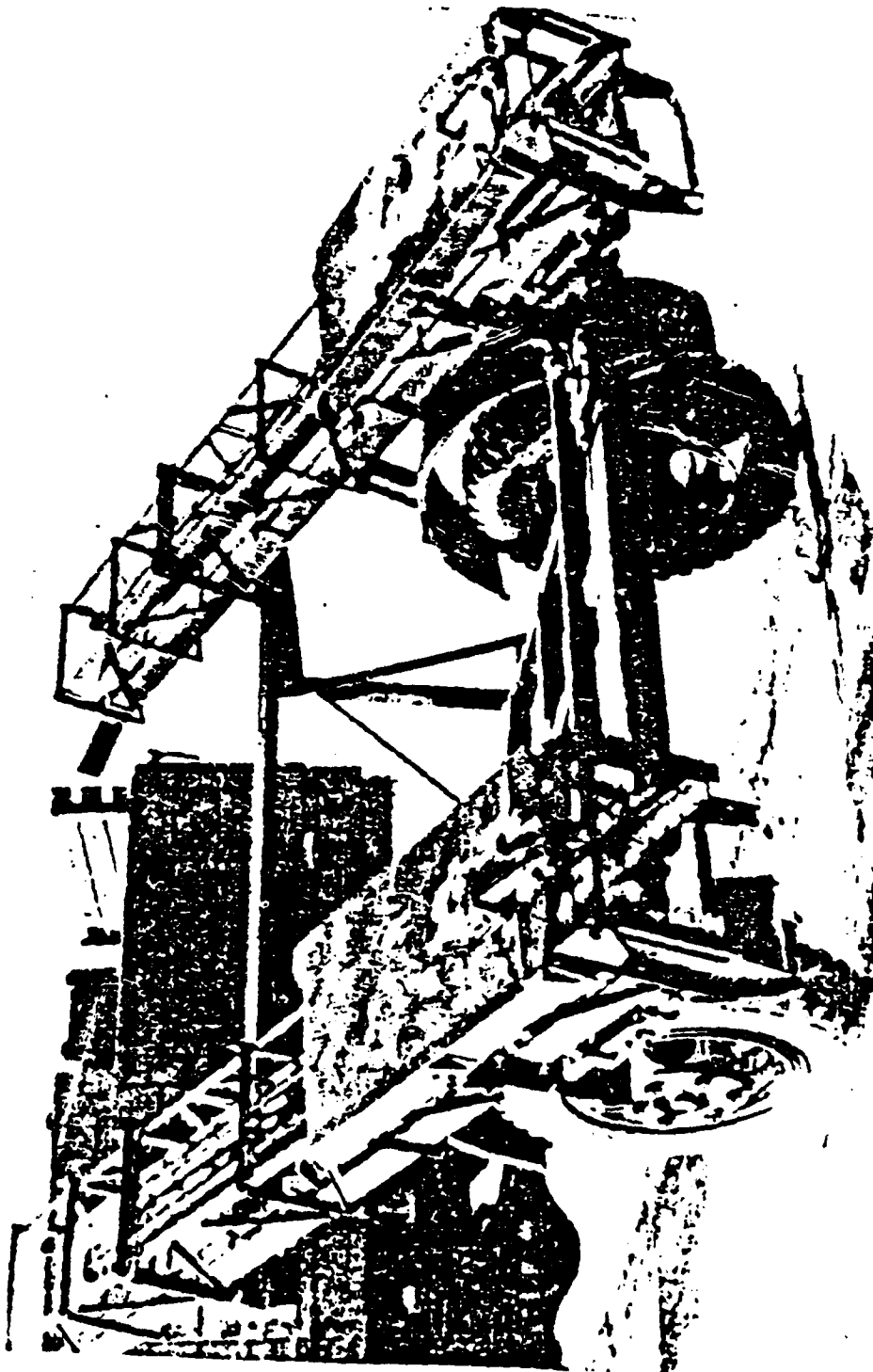


PFM-1

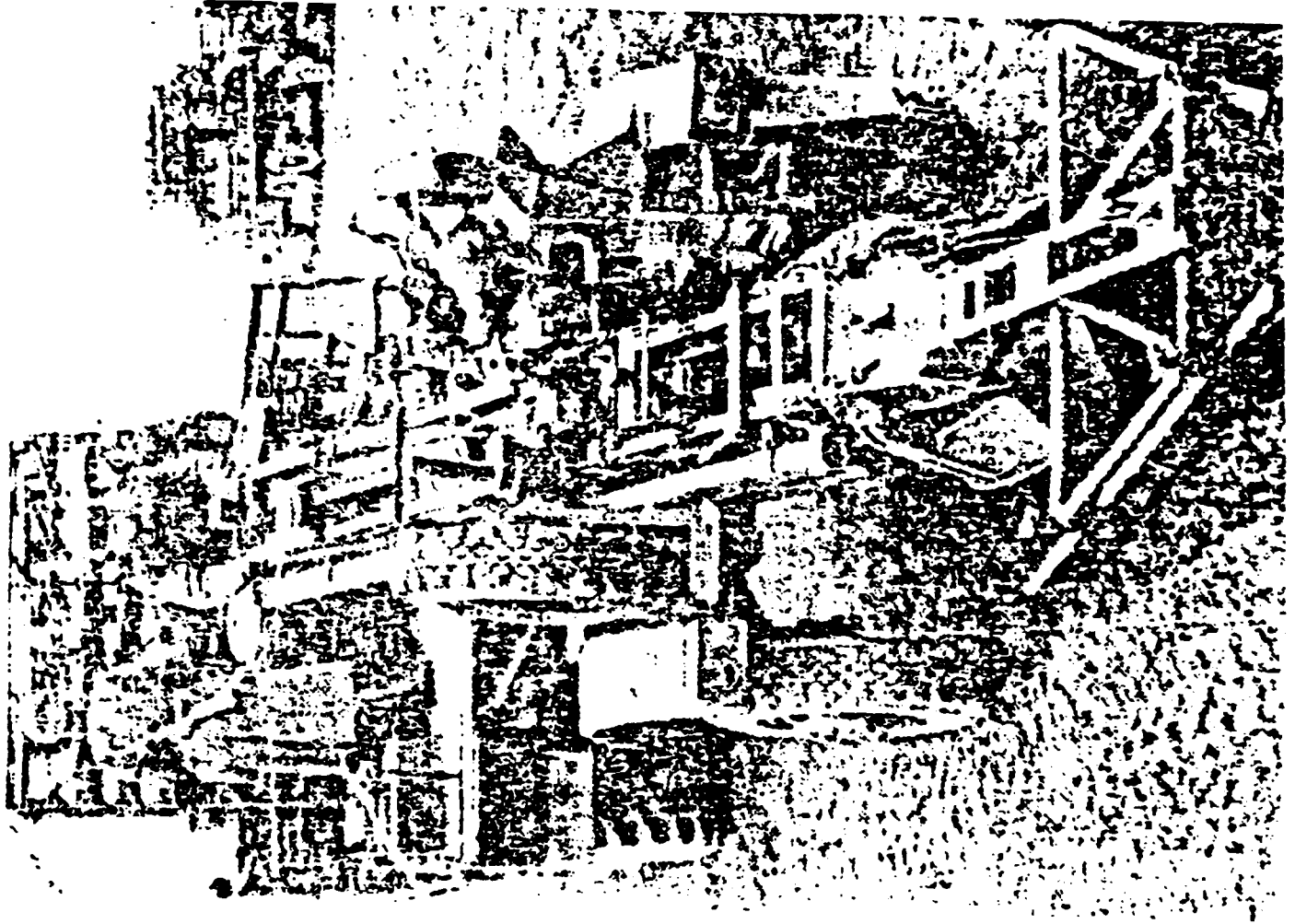
PMR-2 AND PMR-3 TOWED MINELAYERS



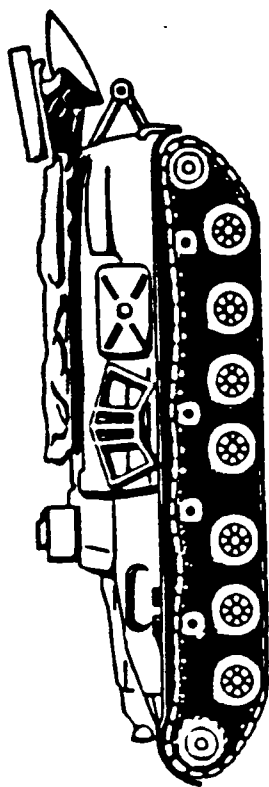
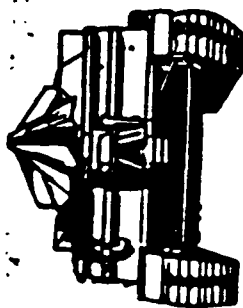
PMR-2 TOWED MINELAYERS



PMR-3 Mechanical Minelaying Trailer



GMZ TRACKED MINELAYER



Crew: 4

Weight: 25 tons

Width: 3.2 m (10.5 ft)

Length: (vehicle) 8.7 m (28.7 ft)

(plough lowered) 10.3 m (33.9 ft)

(plough raised) 9.1 m (30.0 ft)

Height: 2.7 m (8.5 ft)

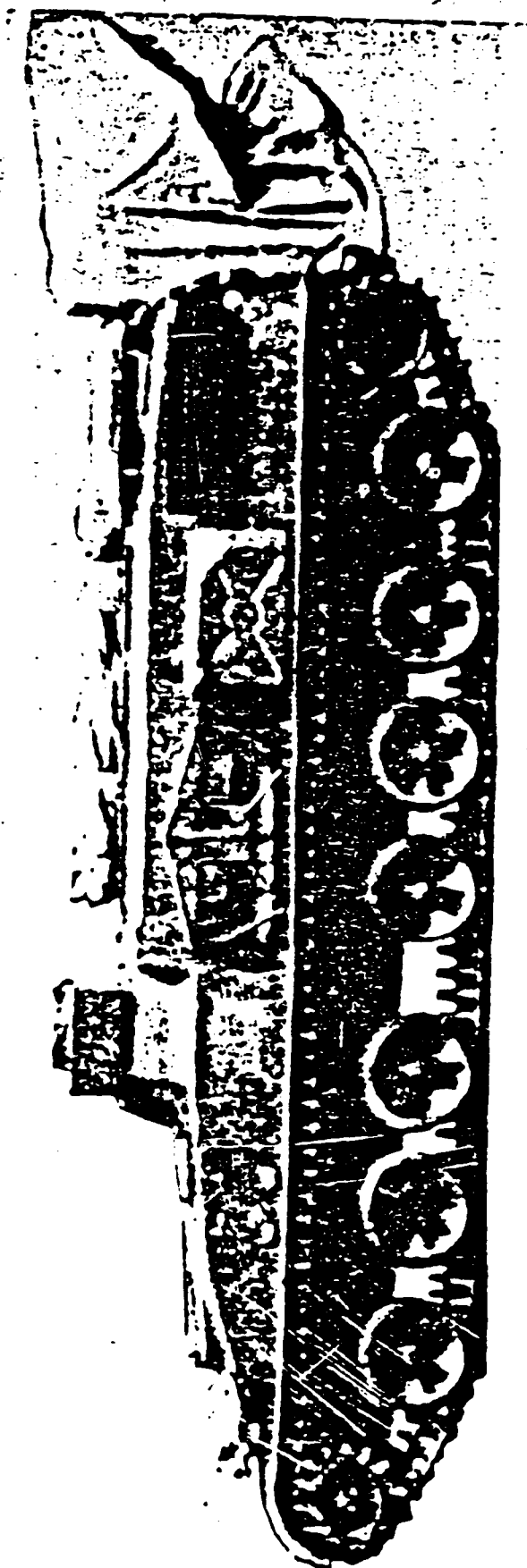
Max speed: (road) 50 km/h

Mine storage: 200

Burial depth: 4/min

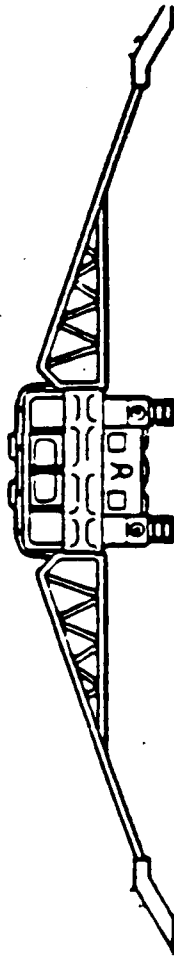
Minelaying rate, surface: 8/min

GMZ Armored Tracked Mechanical Minelayer

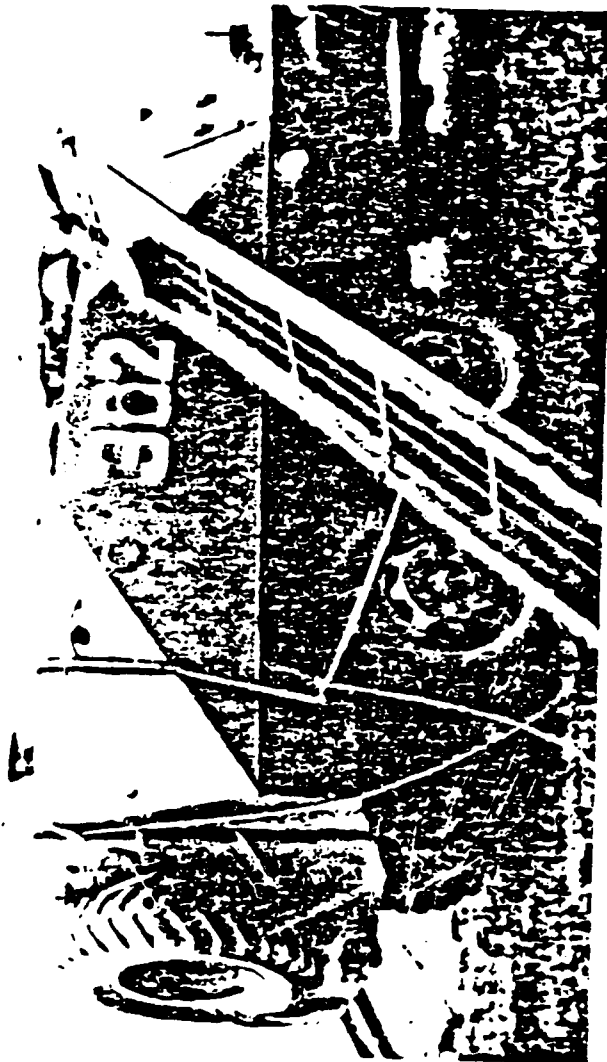


GMZ

MINELAYING CHUTES

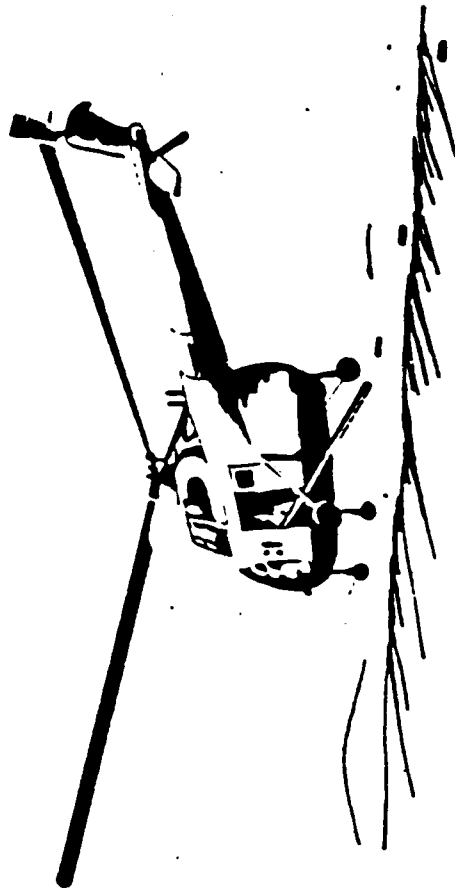


Minelaying Chutes



MINELAYING CHUTES WITH BTR-152

ANTI-TANK MINELAYING HELICOPTERS



SAITO KEISUKE

[illegible]

APPENDIX E

KBVISION SYSTEMS

KBVISION™ SYSTEM

E.1. DESCRIPTION.

The KBVision™ system is a developer's environment for Knowledge-based vision. Through the application of a wide variety of image processing and artificial intelligence techniques, users of this system are able to rapidly prototype and develop solutions to image understanding problems. The user interfaces of the system provide interactive menus which accommodate all processing levels from image processing through intermediate-level feature extraction to LISP based image understanding. A subroutine library enables programmers to incorporate new algorithms and knowledge bases into the system. Using the system utilities, new algorithms become accessible in the user interface indistinguishably from system supplied algorithms. Applying a mouse-driven Graphic Interface, complex image processing operations can be built and tested. These operations, called tasks, can be executed in parallel to shorten both development and processing time.

Application engineers augment the KBVision™ system with information concerning image characteristics, real world objects, and the relationships between objects that will be encountered in the real world domain. This knowledge, supplied to the system in the form of user written programs, is employed to create stand-alone applications which function independently from the system. Any application developed using the powers and resources of the system may be extracted and run independently on other processors.

KBVision™ users can access the optional Knowledge Level Interface (KLI) to build applications which combine real-world knowledge into image understanding strategies. Using a knowledge base of rules, recognition procedures, and object descriptions, these image understanding strategies can provide object oriented interpretation of image data. An application uses this knowledge of objects, their component relationships, and their meanings to intelligently process and analyze images. All image processing operations accessible through the Graphic Interface are also available at the Knowledge Level. Interpretation results are made available within the KLI through a KBVision-maintained blackboard. This blackboard provides synchronous and asynchronous communication between various interpretation processes.

E.2. ARCHITECTURE.

The KBVision™ system divides the Image Understanding task into two components: lower level Image Processing (such as , convolution, feature extraction, etc.) and higher-level Image Understanding (interpretation in terms of real-world objects). A graphic mouse-driven menu interface is used to simplify the application of system supplied image processing and understanding tools. This feature greatly facilitates the experimentation and development process. Several system supplied libraries enable programmers to extend the capabilities of the system to meet individual needs.

E.2.1. DATA LEVELS.

Three levels of data representation are used in the KBVision™ system. Data at each level is structured so as to facilitate access and to support the operations required by the various types of processes present in an image understanding system. The three levels are:

E.2.1.1. LOW LEVEL DATA.

Image data is derived from various sources, and may include data from visible, infrared, and millimeter sensors. Once imported into the system, this data is represented as one or more data arrays. The system supports bit, integer, float and double precision float Image data. Each Image can have data of only one data type. The term Image refers to a rectangular array of data with header information in a KBVision system defined format. The header may contain any amount of user defined data, and is most useful for storing a processing history. Pixels are the elements of these data arrays, and are the smallest image elements that can be manipulated.

E.2.1.2. INTERMEDIATE LEVEL DATA.

Images are composed of pixels. Various Image processing algorithms can extract Image features, such as lines, vertices and regions with common attributes. These features usually represent an area of more than one pixel and contain descriptive information. Image feature instances are called Tokens. Tokens of the same type are stored as Token lists, called Tokensets. For example, all lines found by a line-extraction algorithm are stored in one Tokenset, one Token representing one line. Tokens may be grouped into TokenSubSets, based upon a single or multiple feature attribute. These attributes are calculated when the token is created, or by other processes at a later time. Tokens, and sets of tokens may also have lexicons associated with them. A lexicon is a description assigned by the applications programmer.

E.2.1.3. HIGH LEVEL DATA.

.....

E.2.2. PROCESSING LEVELS.

The KBVision System contains a set of algorithms for processing Images, Tokens, and Hypotheses. Processing can occur at and between data levels as summarized in Table 2-1. The most common of these processes are described below.

- An Image-to-Image process, such as filtering or compression, is performed on Image data and produces an Image as output.
- An Image-to-Tokenset process, such as region extraction, takes an input Image and produces an intermediate level Tokenset as output.
- A Hypothesis-to-Tokenset process creates a new Token to describe a region that does not exist in the initial segmentation.
- A Hypothesis-to-Hypothesis process executes a particular interpretation strategy in response to an existing hypothesis.

<i>Process Input</i>	<i>Process Output</i>	<i>Example</i>
Image	Image	Filtering
Image	Tokenset	Segmentation
Image	Hypotheses	Pattern Recognition
Tokenset	Image	Pseudolmage Generation
Tokenset	Tokenset	Line Grouping
Tokenset	Hypotheses	Feature Const. Application
Hypotheses	Image	Interpretation Display
Hypotheses	Tokenset	Semantic Token Creation
Hypotheses	Hypotheses	Accumulation of evidence

Table 2-1: KBVision Processes

E3. APPLICATION SUPPORT.

The KBVision System

.3.1. ACCESS FUNCTIONS.

Level	Element	Group	Process	Representation	Access
Low	Pixel	Image	Task	Arrays	Image Access Functions
Intermediate	Token	Tokenset	Task	Intermediate Symbolic Representation	Token Access Functions
High	Hypothesis	Hypothesis	Schema or other Lisp Processes	Blackboard	Blackboard Access Functions

Table B-2. KBVision System Data Levels, Elements and processes

E3.1.1. IMAGE ACCESS FUNCTIONS.

The Image Access Functions provided by the KBVision™ system are divided into two categories: General Purpose and Pixel Access Functions. General Purpose Functions facilitate Image file reading and writing and the allocation of Image memory. Pixel Access Functions manipulate individual Image pixels and get (inquire) and set (modify) image values. Pixel Access Functions handle:

- Different Image pixel data types including integer, float, byte, and generic that is capable of handling any pixel data type.
- Boundary conditions (pixels referenced outside the actual Image can be handled in a number of ways including no bounds checking, ignore out-of-bounds condition, generate error, select nearest pixel, or reflect the image.
- Single pixel access or inquiry and Image windows.

Because of the combination of these capabilities, there are approximately 210 Pixel Access Functions. This presents a problem to the programmer who needs to be conversant with these functions in order to select the appropriate function. There is also a performance question associated with generic functions. A generic function will allow a programmer to avoid specifying whether an Image is composed of integer or float pixels. Instead, it will test the Image each time it is called, determine the data type and apply the appropriate operation. In a processing loop, this test exacts a fairly severe performance penalty.

To facilitate the use of Pixel Access Functions and avoid performance penalties, a system supplied set of Pixel Access Metafunctions is available. A programmer calls the Metafunction, specifies the pixel data type, boundary condition handling, get or set operations and pixel or window operation. The Metafunction then returns an appropriate Pixel Access Function to use in code, increasing execution speed considerably.

E.3.1.2. ISR ACCESS FUNCTIONS.

The ISR (Intermediate Symbolic Representation) is a set of tools for representing image events that are more abstract than pixels, such as lines, corners, surfaces, etc.. The ISR provides utilities for defining, storing, retrieving, displaying, manipulating, filtering, and organizing image events (Tokens).

The easiest way to understand how the ISR works is to look at the data structures which result from applying ISR functions to a sample Image event. Suppose that one has a digitized IR image of a military scene. The digitized data comprising the image is contained in a file which is known to the system as an Image. Initially, the Image level tasks perform some low level image processing of the Image to clean it up. It is then desired to locate features such as lines, regions, shapes, edges, etc. within the Image. Tasks process the Image to generate these features. Each symbol found by a Task is output as a structure which contains information about that particular symbol. For example, each line that is found is stored in a structure which contains the original location of the line, as well as various attributes of the line, such as its orientation, length, contrast, etc. This structure is called a Token by the ISR. As the Task discovers more lines, it stores them in a list of all line Tokens found in that Image. This list is called a Tokenset. At the end of processing, several Tokensets have been produced, each containing one kind of Token which has been extracted. These Tokensets are related because they derived from the same original Image (or specific set of Images). The group of related Tokensets is called an ISR Image.

An ISR Image is related to the original Image, but is composed of Tokens rather than pixels. While it corresponds in terms of pixel coordinates to a pixel image in KBVision™'s low level data representation, it may in fact be derived from several images (for example, from a multi-band Image, a stereo pair, or a time sequence) as well as from other non-image data from other sources (cartographic data, intelligence reports, etc.).

To complete the description, there are several additional structures provided by the ISR. Each Token has a number of constituent features. A line, for example, may have orientation, length, and contrast. A region, on the other hand, does not have an orientation, but it does have shape, size, brightness, and color. A need exists for some way to identify the various attributes in a Token. The Lexicon provides this identity. A Lexicon is a list of the attributes of the Tokens in a Tokenset. In addition, it may be desired to store the actual pixels that are used to calculate a Token. A Constellation is a two-dimensional array of bits that indicate the pixels associated with the Token.

In addition, suppose that it is desired to experiment with various parameters while processing the Image. It is useful to save these parameters with the experimental data since written notes or data files may become separated from the Image data. The ISR provides a property list which is a set of name-value pairs and which can be associated with a Tokenset, an Image or a Lexicon. The programmer is free to store any kind of data desired in a property list. It is possible to store documentation strings, parameter values, time stamps, or any other information one may want. Property lists are also useful to keep track of the relationship between intermediate level data and data at the other levels of representation.

Finally, one may want to process specific Tokens in a Tokenset. The ISR allows the creation of a TokenSubSet, which is a subset of the original Tokenset, containing a selection of the Tokens in the original Tokenset. A TokenSubSet is an ordered set of Token indices and as such lends itself to efficient manipulation.

During the creation of application specific routines to manipulate Token data, methods are needed to create, delete, modify, examine, store and retrieve these data structures. The KBVision™ contains the necessary utilities in a function library and consists of:

- General System Functions - print and clear the entire system
- ISR Image Functions - create, modify, delete, and query ISR Images
- Tokenset Functions - create, modify, delete, and query Tokensets
- Lexicon Functions - create, modify, delete, and query Lexicons
- Token Functions - create, modify, delete, and query individual Tokens
- Constellation Functions - create, modify, delete, and query Constellations
- TokenSubSet Functions - create, modify, delete, and query TokenSubSets

E.3.2. KLI FUNCTIONS.

To assist the programmer in creating and using the Knowledge Level Interface, a library of LISP functions is accessible through the KLI interface. However, LISP by itself provides a flexible, dynamic environment for rapid prototyping and development of object-based knowledge representations. It also allows the use of established artificial intelligence techniques for identifying objects.

The KBVision™ Schema Shell provides inter-process communication through a blackboard message-posting system. All inter-schema instance communication is accomplished with the blackboard. The blackboard can be divided into an arbitrary number of sections. Schemas can read, write, modify or erase blackboard messages.

Token display functions of the KLI enable the user to graphically display tokens and image data while the KLI is in the Graphic Display Configuration. The Task Interface functions of the KLI are designed to provide the developer with full capability to use those KBVision system tasks which have been developed within the Graphic Interface.

A user communicates with a schema by writing to the LISP Listener panes within the Schema Shell user interface. The Schema Shell accepts input from the LISP Listener as though it were a schema. Schema instances can be accessed directly by typing commands in the LISP Listener pane. This allows interactive development of image understanding strategies, as the user may act as a very complex schema, having total control over the execution of tasks, strategies, ISR access functions, graphics, and other schemas.

E.3.3. CONSTRAINT UTILITY.

A constraint on a Token attribute (or feature) provides a very simple representation of a unit of knowledge that can be used to generate object (recognition) hypotheses. For many objects there are natural semantics and simplistic descriptions which can be associated with a set of token attributes; for example, an object may be defined as large in size, rough in texture, green in color, etc. A range on each Token attribute, even if it is loosely constrained, captures some aspects of the objects semantics. Thus, a simple rule can be defined as a constraint on the range of a single Token attribute, and several rules may be combined to form a complex rule for a specific object class. Complex rules are defined as hierarchical combinations of simple rules and may be viewed as defining a volume in a multi-dimensional feature space which represents the set of joint constraints on a feature set.

In the KBVision™ system, simple rules are defined as piecewise-linear mapping functions on features. The Constraint System utility is an interactive environment for generating and testing such rules. A user may create a rule, display the results on a test data set, edit the rule, and construct complex rules. Rules developed in this interface may be stored and used by tasks running from the graphical task interface. They are most often used for calculating scores as to how well Token features fit a predefined model, storing these scores with the Tokens as new attributes, and

then filtering the Tokens on these scores to produce a TokenSubSet which contains only Tokens with the desired feature values.

E.3.4. DISPLAY UTILITY.

The KBVision™ Image Examiner is an extensive mouse and menu driven utility which allows a user to view Images, Tokensets, and their related attributes. An interactive histogramming function generates immediate histograms of Images and Tokensets, and allows user-definable false color mapping of this data. An alphanumeric display may also be selected to view Image z values or Token attribute values. In addition, complex yoking functions exist which allow the linking of data displays to give the user extensible control over the display of TokenSubSets, as well as Image and Token data. Finally, the state of the Image Examiner may be saved so that the user may re-enter the utility at a later point in time without losing any work previously done.

E.4. INTERFACES:

E.4.1. GRAPHIC INTERFACE.

The Graphic Interface provides a convenient means to process and manipulate Images and Tokensets. With the Graphic Interface, the user can perform a variety of Image analysis functions, called Tasks. It can be used independently or in conjunction with the high-level knowledge base.

E.4.1.1. DISPLAY AREAS.

The Graphic Interface contains seven display areas, each with a unique function. It can, when requested, temporarily pop-up alternate displays to acquire additional or more specific information about an item. This interface runs inside a system window and may invoke other Tasks which will operate in other system windows.

E.4.1.2. ICONS

In the Graphic Interface, icons are employed to visually represent Images, Tokensets and Tasks. A mouse is used to select icons and operations. It may be used to: move the cursor, issue commands, direct keyboard input, copy values and expressions, manipulate symbolic data files and process representations. Extensive use of these icons helps the user get his job done with a minimum of typing. The Graphic Interface uses colors to organize display items and denote process states. Using system supplied tools, user-developed algorithms are incorporated into the system and available to the user from this Interface.

E.4.1.3. TASKS.

System Image processing operations, called Tasks, process Low-level visual data into other Images or Tokens. Tasks can operate on and extract feature information from Tokens. They can also produce new Tokens. The Graphic Interface represents Tasks, Images and Tokensets graphically to simplify process and data links. Tasks can either be used independently or consolidated in Compound Tasks. A Compound Task is a collection of individual Tasks that effectively build a black box to accomplish an entire Image processing operation. Within the Graphic Interface, the user can experiment with Task combinations and sequences that accomplish specific operations. A full expression language permits Tasks that are nested within Compound Tasks to be conditionally executed in response to other Tasks. Compound Tasks can be called recursively, creating a looping mechanism.

KBVision™ system supplied Tasks are designed to be as general purpose as possible. For example, input and output Image names and Convolution kernels are not hard-coded into the system. This enables user specification for these and other parameters at runtime. The Graphic Interface enables user specification for Task limits, ranges, and conditions of execution. For example, to specify the input Image for a Task, a user would pick up the Image icon and drop it into the Task input Image box.

To edit a Task, the user selects the Task icon with the mouse and moves it into the Graphic Interface Edit Area. This area will display Task parameters that can either be copied to the expression window or modified in place. These parameters are expressed in terms of functions and variables so that parameters, default values and constraints on parameters can depend on other parameters. The system Expression Evaluator is an active part of the Graphical Interface. When editing a parameter, a spreadsheet-like mechanism evaluates expressions and updates all dependent parameter values.

In the Run Area, Tasks are run simultaneously, and colors (usually red and green) are used as indicators. Task status information is color coded to indicate whether a Task is: processing, finished, or waiting for another Task to complete. For example, when a Task is in the Edit Area, required parameter specifications are outlined in red. When the specification has been satisfied, the color changes to green to indicate an acceptable value. Whether Tasks are executed asynchronously or sequentially is determined by run mode selection. Asynchronous Tasks execute concurrently and , if the KBVision™ system is running on a system with a multiprocessor, Tasks are executed simultaneously. The History Box displays Task run status graphically to indicate whether a Task is ready to run, processing, or completed.

E 4.2. KNOWLEDGE INTERFACE.

The Knowledge Level Interface (KLI), provides a knowledge engineering environment for interactively developing, debugging, and testing knowledge structures and control strategies used in the Image interpretation process. A set of system supplied general purpose tools is provided to assist in examining and analyze interactions between knowledge-based process.

The Knowledge interface is a windowed environment which is used to:

- Isolate and view output streams for concurrent process sets.
- Interactively inspect individual process states.
- Examine the system global processing status, and
- Graphically display interpretation processing results with respect to Image Tokens.

As Common LISP is the knowledge processing environment, the core of the Knowledge Interface is provided through a LISP Listener window. This window enables a user to immediately create and modify LISP code in response to observed behavior. A set of pop-up menus allows user specification for display configurations, and inspection or modification of the overall system processing state. A second set of menus enables user inspection of specific process states to determine local variable values, the set of synchronization locks, or to process stack information. A third menu set provides tools for examining global system blackboard messages.

The Knowledge Interface contains multiple output windows than may be assigned to specific process instances, enabling the user to view behavior. A simplified system/user message facility is consistent with the concurrent nature of one of the powerful techniques for Image understanding called Schemas. A Graphics window display is enabled by a set of display functions that interface with LISP. These functions provide high-level Image Token display capability and standard low-level graphic functions (e.g. polygons or lines) for user defined displays.

The KLI provides an object-oriented environment for knowledge based Image understanding. It provides the mechanisms through which real-world semantic knowledge can be applied to the symbolic events that have been abstracted from the Image. This is accomplished through the use of tools that can attach meaning to the intermediate level symbols. (Tokens and Tokensets) that

represent pixel level image information. In the Knowledge-Level Interface, the applications developer can use LISP as a control language to direct the variety of processes that are used in image understanding. Within the interactive LISP environment the developer is able to:

- Direct low and intermediate level tasks of the KBVision system
- Access and/or modify Tokens and Token features
- Apply constraints to Tokens
- Graphically display hypotheses and,
- Record interpretation data on a general purpose blackboard.

The Knowledge-Level Interface also provides the developer with the Schema Shell, a set of tools for the use of concurrent, parallel, and object-oriented processes that perform object recognition. The Schema Shell is modular, enabling complex image-understanding applications to be built using proven routines. It removes the need to build each application from the "ground up".

The Knowledge-Level of the KBVision System has been designed so that an individual developer may choose whether or not to use the Schema Shell to control knowledge-based processing. If an alternate Common LISP based control or inference mechanism is used to direct the image interpretation process, the Knowledge-Level Interface still provides the necessary communication between the various levels of the KBVision System.

E.5. HARDWARE SUPPORT

The KBVision System is designed to operate on Masscomp Computers using a GA-1000 graphics board with 12 or 28 bit-planes and SUN Microsystems 3 and 4 series with Color displays. 10 Mb of disk storage is required for object code storage and at least 10 Mb of memory is recommended for efficiency. The system swap space should be adjusted for use with large application programs. In particular, the KBVision System runs well in systems with over 30 Mb of swap space. Use of the optional "Knowledge Module" (KLI) requires a Franz Common LISP license.